Imaging reward signals in the *Drosophila* brain

Kristijan Jovanoski
Magdalen College

Supervisor:
Professor Scott Waddell

A thesis submitted for the degree of
Doctor of Philosophy

Centre for Neural Circuits and Behaviour
Department of Physiology, Anatomy, and Genetics
The University of Oxford

Trinity 2018

Abstract

In the brain of the fruit fly *Drosophila melanogaster*, dopaminergic neurons are thought to convey teaching signals to synapses of the mushroom body during associative olfactory learning. Although rewarding dopaminergic neurons in mammals appear to encode prediction error, whether the equivalent neurons in *Drosophila* have a similar function remains unknown. Anatomically distinct subsets of dopaminergic neurons reinforce water and separate properties of sugars: sweet taste reinforces short-term memories while nutrient input is usually required for long-term memories. This thesis investigates dopaminergic reinforcement at the physiological level using two-photon *in vivo* calcium imaging of tethered flies during feeding, odour presentation, and appetitive conditioning.

One subset of dopaminergic neurons reinforces short-term sugar memory in starved flies and short-term water memory in dehydrated flies. During sugar-water droplet feeding, dopaminergic neurons show a calcium response that reflects salience and whose magnitude increases with sweetness of the droplet. In starved flies, dopaminergic neurons show differential responses to water and sugar, whereas in dehydrated flies, the neurons show uniform feeding responses. Moreover, sucrose-evoked responses in satiated flies are substantially lower than in either deprivation state. Such findings suggest a deprivation state-dependent valuation of reward not explained by current models of reward prediction error.

Feeding responses in the same dopaminergic neurons or other rewarding subsets involved in sugar reinforcement do not increase with the nutritious content of the droplet. However, feeding rapidly inhibits aversively reinforcing dopaminergic neurons that also control the state-dependent expression of sugar memories. Spontaneous calcium oscillations in the aversive reinforcing neurons become more frequent after feeding on sugars specifically, and their amplitude after feeding appears to be diminished by a possible rapid nutrient signal. Intriguingly, rewarding dopaminergic neurons also show substantial odour-evoked calcium responses that reflect both general and specific odour novelty; such activity is not yet accounted for in existing models of associative learning in *Drosophila*.

Rewarding dopaminergic neurons recorded during appetitive conditioning do not show acquired predictive capacity after training as expected from current models of reward prediction error. Although it remains unclear whether *Drosophila* dopaminergic neurons are inhibited by the unexpected omission of reward, one subset in particular appears to be excited by the unexpected presentation of reward. Taken together, these findings show that rewarding dopaminergic neurons in *Drosophila* may encode value, salience, novelty, and positive prediction error during associative learning.

Acknowledgements

First, I thank my supervisor Scott Waddell for his advice, patience, and support throughout the past four years. I am incredibly grateful for the freedom to pursue my research interests independently in his lab. Under his guidance, I have learnt much about how to think about fundamental problems in neuroscience and how to ask the right questions.

I am also grateful to Gaurav Das, with whom I started to read the scientific literature critically yet constructively. It is incredible to think that many experiments in this thesis were inspired by a single supplementary figure. Special thanks must go to Johannes Felsenberg, whose enthusiasm for science is contagious and from whom I have learnt a great deal about rigorous experimental design.

It is an incredible privilege to have undertaken this research at the Centre for Neural Circuits and Behaviour, and to have had such unrestricted access to a two-photon microscope throughout my candidature. The final version of this thesis owes much to the helpful feedback from Scott, Johannes, Nils Otto, Pedro Jacob, and Lu Li. I also thank Oliver Barnstedt, Emmanuel Perisse, and Paola Cognigni for their invaluable suggestions that influenced key experiments.

Finally, I am grateful to my family for their unwavering love and support. To my parents Vase and Dragan, thank you for encouraging me to learn for myself and follow my varied interests. To my brothers Slavco and Samoil, thank you for the many memorable adventures we have had over the years. But most of all, to Lu, my wonderful wife, thank you for inspiring me to take the road less travelled. Nothing comes close to the joy of seeing you at the start and end of each day.

Table of Contents

Abstract iii

Acknowledgements v

Table of Contents vii

List of Figures ix

List of Tables xi

1 Introduction 1
- 1.1 Research motivation . . . 1
- 1.2 Evolutionary importance . . . 2
- 1.3 Associative learning . . . 3
- 1.4 Reward prediction error . . . 8
- 1.5 The role of dopamine . . . 10
- 1.6 *Drosophila* olfactory memory circuits . . . 14
- 1.7 Two-photon calcium imaging . . . 18
- 1.8 Thesis overview . . . 19

2 Experimental methods 21
- 2.1 Fly husbandry . . . 21
- 2.2 Fly deprivation . . . 21
- 2.3 T-maze conditioning . . . 22
- 2.4 Feeding assay . . . 23
- 2.5 Imaging sample preparation . . . 25
- 2.6 Two-photon calcium imaging . . . 26
- 2.7 Image processing and analysis . . . 28
- 2.8 Proboscis extension reflex (PER) detection . . . 30
- 2.9 Oscillation analysis . . . 31
- 2.10 Statistical analysis . . . 32

3 State-dependent reinforcement 35
- 3.1 Background . . . 35
  - 3.1.1 Deprivation provides motivational drive . . . 35
  - 3.1.2 Flies express specific appetitive memories . . . 36
  - 3.1.3 Rewarding neurons reinforce sugar and water . . . 38
- 3.2 Results . . . 40
  - 3.2.1 Deprivation state affects sucrose reinforcement . . . 40
  - 3.2.2 Flies rapidly discriminate between sugars . . . 41
  - 3.2.3 PAM feeding responses change with deprivation state . . . 43
  - 3.2.4 PAM odour responses may reflect deprivation state . . . 45
- 3.3 Discussion . . . 51

3.3.1 Results summary . . . 51
3.3.2 State-dependent valuation . . . 52
3.3.3 Comparing and manipulating deprivation state . . . 55
3.3.4 Comparing different droplets . . . 57
3.3.5 Odour responses in different states . . . 59
3.3.6 Controlling for movement signals and artefacts . . . 60
3.3.7 Interpreting feeding bouts . . . 62
3.4 Conclusion . . . 63

4 Nutrient reinforcement **65**
4.1 Background . . . 65
4.1.1 Nutrient information is rapidly processed . . . 65
4.1.2 Fast and slow sugar reinforcement . . . 66
4.1.3 Possible nutrient reinforcer candidates . . . 69
4.2 Results . . . 74
4.2.1 R48B04 feeding responses may reflect palatability . . . 74
4.2.2 Blocking octopamine signalling to R48B04 neurons . . . 76
4.2.3 Different sugars evoke similar PAM-α1 responses . . . 83
4.2.4 Feeding evokes similar PAM-γ5b (broad) responses . . . 86
4.2.5 Feeding inhibits and reshapes MP1 oscillations . . . 90
4.3 Discussion . . . 91
4.3.1 Results summary . . . 91
4.3.2 Comparing and supplementing sugars . . . 93
4.3.3 Reward signals in PAM neurons . . . 96
4.3.4 Phasic inhibition of MP1 oscillations . . . 98
4.4 Conclusion . . . 101

5 Appetitive conditioning **103**
5.1 Background . . . 103
5.1.1 The role of dopamine in associative learning . . . 103
5.1.2 Previously attempted conditioning protocols . . . 105
5.2 Results . . . 107
5.2.1 Feeding responses encode salience and value . . . 107
5.2.2 PAM-γ5 neurons respond to prolonged odours . . . 111
5.2.3 Odours differentially evoke proboscis extension reflexes . . . 111
5.2.4 A multi-round appetitive conditioning protocol . . . 114
5.2.5 R48B04 neurons primarily signal reward salience . . . 117
5.2.6 R48B04 odour responses reflect novelty . . . 123
5.2.7 PAM-γ4 neurons may encode prediction error . . . 127
5.2.8 Optogenetic stimulation in the T-maze . . . 128
5.3 Discussion . . . 132
5.3.1 Results summary . . . 132
5.3.2 The origin of PAM responses in different contexts . . . 133
5.3.3 PAM responses during appetitive conditioning . . . 136
5.3.4 Designing an appetitive conditioning protocol . . . 137
5.3.5 Linking physiology with behaviour . . . 141
5.4 Conclusion . . . 142

6 Discussion and conclusion **145**
6.1 Experimental limitations . . . 145
6.2 Future experiments . . . 147
6.3 Thesis summary . . . 148

Bibliography **151**

List of Figures

1.1 The T-maze assay for classical olfactory conditioning. 5
1.2 The olfactory processing pathway in *Drosophila*. 14
1.3 Associative olfactory memories are formed in the mushroom body. 16

2.1 The feeding assay workflow. 24
2.2 The sample preparation and two-photon calcium imaging workflow. 25
2.3 The two-photon imaging setup based on a customized Slicescope. . 27
2.4 Anatomical regions of interest demarcated for each driver line. . . . 29
2.5 Detection of proboscis extension reflexes during two-photon imaging. 31

3.1 R48B04 neurons reinforce short-term sugar and water memories. . 39
3.2 Different PAM neurons reinforce long-term sugar memory in starved and dehydrated flies. 42
3.3 Tethered flies discriminate between different sugars in a state-dependent manner. 43
3.4 Feeding starved flies evokes differential PAM-γ5 responses. 46
3.5 Feeding dehydrated flies evokes uniform R48B04 responses. 47
3.6 Satiated flies have diminished sucrose responses in R48B04 neurons. 48
3.7 Odours evoke responses of different sizes in each R48B04 PAM subset. 50
3.8 Odour-evoked R48B04 responses decrease further in satiated flies. . 51

4.1 Nutrient information guides sugar memory preference immediately after training. 66
4.2 A possible model for immediate and delayed sugar reinforcement. 74
4.3 Supplementing arabinose with nutritious sugars does not increase R48B04 feeding responses. 75
4.4 Sugars that reinforce long-term memory do not evoke larger R48B04 feeding responses than sugars that reinforce only short-term memory. 77
4.5 Fucose and sucrose evoke similar R48B04 feeding responses. 78
4.6 Fucose evokes smaller responses than sucrose in PAM-γ4 neurons of TβH mutant flies. 80
4.7 Fucose evokes similar responses to sucrose in R48B04 neurons with knocked down OAMB receptors. 81
4.8 Supplementing fucose with nutritious sugars does not lead to larger responses in R48B04 neurons with knocked down OAMB receptors. 82
4.9 Feeding evokes differing responses in the three PAM subsets labelled by R15A04-GAL4. 85
4.10 Odours evoke different responses in each R15A04 PAM subset. . . 87
4.11 Feeding evokes similar responses in PAM neurons implicated in long-term memory reinforcement. 88
4.12 Odours evoke larger responses in PAM-β'2 neurons. 89
4.13 Sugar ingestion inhibits MP1 neurons in starved flies and modifies its oscillations. 92

5.1 Feeding evokes responses primarily upon onset in R48B04 neurons. 108
5.2 Feeding every 10 min evokes R48B04 responses of similar size. . . . 109
5.3 Feeding for 20 s every 3 min evokes diminishing R48B04 responses. 110
5.4 120 s odour presentations evoke prolonged PAM-γ5 responses. . . . 112
5.5 Different odour sequences can evoke different PER frequencies. . . 113
5.6 The multi-round appetitive conditioning protocol during imaging. 114
5.7 The components of a schematic odour response analysed during appetitive conditioning. 116
5.8 The largest difference during the initial forward pairing is the calcium response evoked by sucrose. 118
5.9 Repeated forward pairing induces a relative depression in the ongoing PAM-γ5 response to the CS^+ odour. 120
5.10 The largest difference evoked by backward training is the calcium response evoked by sucrose. 121
5.11 Repeated backward pairing induces a relative depression in the ongoing PAM-γ5 response to the CS^- odour. 122
5.12 Summary of the key differences between calcium signals evoked by the odour control and paired protocols. 124
5.13 R48B04 neurons do not show acquired predictive capacity after appetitive conditioning. 125
5.14 R48B04 odour responses reflect novelty. 126
5.15 PAM-γ4 neurons display positive prediction error during the presentation of unexpected reward. 129
5.16 T-maze conditioning with optogenetic substitution of reward. . . . 131

List of Tables

1.1 Sugars and their known roles in *Drosophila* appetitive memory. . . . 7

2.1 Fly strains used for experiments in this thesis. 22

4.1 Summary of nutrient reinforcement candidate requirements during the reinforcement of short-term and long-term appetitive memory. 73

Chapter 1

Introduction

1.1 Research motivation

Dopamine is a neurotransmitter that modulates movement [1], learning [2], and motivation [3]. Prevailing models suggest that dopamine provides a fast (phasic) teaching signal that encodes reward prediction error [2] and a slow (tonic) signal that can drive purposeful behaviour [4]. However, the mechanisms by which dopamine conveys distinct signals for learning and motivation remains unclear [5].

Most research into dopamine has concentrated on mammals, whose brains are numerically complex [6, 7]: there are an estimated 20,000 to 30,000 midbrain dopaminergic neurons in the mouse brain alone [8–10]. In contrast, there are fewer than 280 dopaminergic neurons in the brain of the fruit fly *Drosophila melanogaster* [11, 12]. Since the fruit fly can display learning and motivated behaviours similar to those of mammals but with fewer dopaminergic neurons, it is a tractable candidate for investigation.

Early research into insects, however, suggested that another neurotransmitter, octopamine, signalled reward whereas dopamine signalled punishment [13–16]. This model has since been overturned by findings in *Drosophila* that dopamine can indeed convey reward downstream of octopamine [17]. The resulting convergence in our understanding of dopamine for flies and mammals suggests that

dopamine signalling could be a conserved adaptation that helps animals survive their changing environments.

The case for studying the numerically less complex but functionally sophisticated *Drosophila* nervous system is made more compelling by the numerous genetic tools that can record and manipulate the activity of specific neuronal subsets [18]. Such tools present the opportunity not only to test existing hypotheses about dopamine in fruit flies, but also to provide new insights into dopamine function. This thesis investigates the physiology of *Drosophila* dopaminergic neurons that convey reward during associative learning.

1.2 Evolutionary importance

If dopamine signalling is indeed part of the shared evolutionary history of animals, then it is presumably important for the ultimate reproductive success of each individual [19]. *Drosophila* have a short life cycle of around 10 days and a single mated female can lay up to 100 eggs per day [20]. Such high numbers of offspring in a short time imply that *Drosophila* inhabit unstable environments with selective pressures that favour fertility over longevity [21].

Individual fruit flies with favourable adaptations may achieve reproductive success by reaching sexual maturity earlier, mating earlier, and investing resources into more offspring instead of prolonging their own existence. Given the unpredictable nature of their environment, however, *Drosophila* must obtain resources quickly while avoiding predation. Female flies in particular must identify nutritious substrates in which they can deposit their eggs after fertilization [22, 23].

Drosophila are attracted to decaying fruits rich in protein (from yeast) [24] and nutritious simple sugars such as fructose, glucose, and sucrose [22]. The evolutionary importance of sugars in the *Drosophila* diet is reflected by the rapidity with which fruit flies remember nutritious sugars and use their energy. Starved adult flies form a robust long-term memory (one that lasts for days) after a single

two-minute pairing of sucrose with an odour [25, 26]. Moreover, starved flies whose muscle glycogen has been depleted by flying to exhaustion can resume flight merely 30 s to 120 s after consuming a nutritious sugar [27]. *Drosophila* can survive solely on a nutritious sugar in solution for several days [28–32], underlining its dietary importance even without other essential macronutrients.

As individual fruit flies navigate an unknown environment, those that can rapidly recall which fruits contain nutritious sugars will be more efficient in their future foraging, can devote more time towards mating, and lay fertilized eggs in the best sites. Such flies first need to associate external stimuli with nutritious sugars efficiently and then remember this association for a sufficient period of time. Moreover, this recall needs to be expressed during appropriate times to address a current dietary deficit. In *Drosophila*, dopaminergic neurons are involved in both the formation and behavioural expression of such memories [17, 33–36].

1.3 Associative learning

An emergent property of dopamine signalling and other adaptations in the nervous system is that animals across diverse phyla have the ability to learn about their environment. Such learning may be associative or not depending on the number of environmental elements involved [37, 38].

Non-associative learning modifies the response of an individual to a single stimulus due to repeated exposure [37]. Habituation occurs when a repeated stimulus progressively diminishes the strength or probability of a response, whereas sensitization occurs when a repeated stimulus progressively amplifies a response instead [37]. In either case, an animal learns whether the characteristics or frequency of a single stimulus are biologically relevant.

Associative learning is the process by which an individual learns that one component in its environment is connected with another [38]. Such connections can be formed with stimuli or events that an individual perceives to be rewarding

(appetitive) or punishing (aversive). Different types of conditioning can give rise to associative learning depending on the components that are connected [38].

An unconditioned stimulus (US) is one whose intrinsic properties (e.g., food or electric shock) evoke a reflexive response (e.g., salivation or withdrawal) in an animal. During classical (Pavlovian) conditioning [39], an unrelated neutral stimulus (e.g., a sound) precedes the US and the animal learns that this stimulus can predict future occurrences of the US [40–43]. The neutral stimulus becomes a conditioned stimulus (CS) because it can now evoke the reflexive response alone, but only due to conditions that associated it with the US [13, 39, 44, 45].

During operant (or instrumental) conditioning, an animal receives reward or punishment after it displays a particular behaviour (e.g., lever pressing) [46–49]. Once the animal learns that its voluntary behaviour controls occurrences of the reward or punishment, it increases or decreases the frequency of that behaviour respectively [46, 47]. Through both types of conditioning, animals learn associations that help them to predict elements in their environment more reliably.

Since associative olfactory learning in *Drosophila* was first experimentally demonstrated over half a century ago [50], there has been substantial progress towards uncovering the mechanistic basis of learning-induced changes, or plasticity, in the *Drosophila* nervous system [51–65]. The development of the binary T-maze choice behavioural assay in particular [66–69] has played a key role in linking the genes and neurons involved in classical olfactory conditioning with behaviours expressed by populations of trained fruit flies.

The T-maze protocol trains a population of ~100 fruit flies to associate an odour with an aversive stimulus such as electric shock [67, 68] or a rewarding stimulus such as sugar [66, 69] (Figure 1.1). During training, flies are presented with two separate odours: one paired with the US (denoted CS^+) and one that is not paired (denoted CS^-). Flies are tested minutes or hours later by being lowered into a T-junction with the CS^+ emanating from one end and the CS^- from the other.

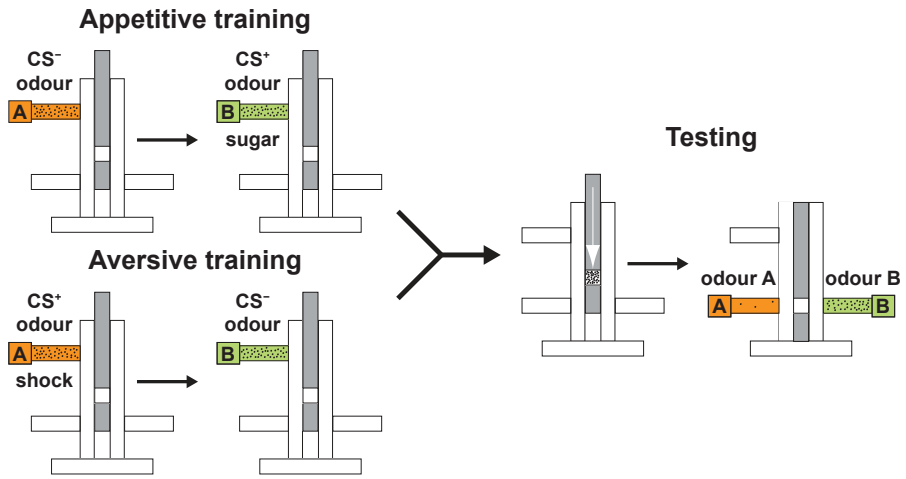

Figure 1.1: The T-maze assay for appetitive and aversive classical olfactory conditioning. In this protocol, ~100 flies are presented with two odours. Appetitive training (top left) pairs one of these odours with a reward such as sugar, whereas aversive training (bottom left) pairs this odour with a punishment such as electric shock. The odour paired with the US is termed the CS^+, whereas the unpaired odour is termed the CS^-. After a specified period of time (minutes to hours) post-training, the flies are tested (right) with a binary choice between the CS^- and CS^+. If appetitive or aversive training was successful, the majority of flies will approach or avoid the CS^+ respectively. T-maze diagram adapted from Vosshall (2007) [70].

Presented with a binary choice, flies express their aversive or appetitive memory by choosing to approach or avoid the tube from which the CS^+ odour emanates. Approach in the T-maze refers to any movement (typically walking) towards and then lingering in the preferred tube, whereas avoidance refers to the opposite behaviour. The first study of fly learning [50] demonstrated that flies typically express approach or avoidance independently of other flies, although social interactions have since been found to influence certain types of learning [71, 72].

After training, memories are either soon forgotten or stabilized for the long-term in a process called consolidation [73]. Training *Drosophila* in the T-maze with electric shock or sugar has revealed that these stimuli can reinforce different types of memory [25, 26, 29, 30, 74–76]. If electric shock is delivered in multiple trials with intervening breaks (spaced training), it can lead to a long-term memory (LTM) that requires protein synthesis during consolidation after training [75]. However, if electric shock is delivered in sequential trials without intervening breaks (massed training), it can lead to an anaesthesia-resistant memory (ARM) [74] whose consol-

idation is less dependent on protein synthesis [75]. Despite their names, both ARM and LTM are resistant to anaesthesia induced by cold shock after training [74, 76].

Appetitive conditioning with sucrose leads to an LTM whose consolidation depends on protein synthesis, irrespective of whether the training was a single session, massed, or spaced [25, 26]. Training with other sugars can lead to LTM or a short-term memory (STM) that lasts up to around 30 min [29, 30]. Sugars that are sweet but not nutritious are thought to reinforce STM whereas those that are both sweet and nutritious appear to reinforce LTM [29, 30, 35, 36]. However, some non-nutritious sugars can also reinforce LTM [32] and it therefore remains unclear whether LTM arises from an intrinsic property of certain sugars or from the neural circuits that only certain sugars engage upon ingestion [32, 77, 78]. Table 1.1 summarizes the properties of different sugars and their known roles in *Drosophila* appetitive memory.

Shock and sugar reinforced training paradigms each have inherent limitations. Electric shock has considerable advantages in that the same dosage can be delivered reproducibly and involuntarily, but it is not an ecologically relevant stimulus encountered by fruit flies [82]. In contrast, sugars are physiologically relevant stimuli that are important for metabolism and survival [27, 28]. The neural pathways that convey sugar taste in *Drosophila* are also much better understood than the circuits that convey electric shock sensation [82]. However, each fly consumes a different amount of sugar during training and must be sufficiently starved to form and retrieve appetitive memories [25, 26, 33, 66]. Such dependence on a nutritional deprivation state may be a limitation, but it also suggests that neurons signalling deprivation state could be integrated with neurons that form and retrieve appetitive memories.

Table 1.1: The properties of sugars and their known roles in *Drosophila* appetitive memory. Sweet: whether flies exhibit appetitive behaviour to the sugar. Nutritious: whether flies can survive on the sugar alone for longer than on water. STM: whether flies express short-term appetitive memory up to 30 min after training with the sugar. LTM: whether flies express long-term appetitive memory 24 h after training with the sugar. Y (yes); N (no); blank (unknown/not attempted); non-exhaustive list of references provided where applicable. *D-sorbitol is more accurately described as a polyhydric (sugar) alcohol that can be derived from monosaccharides.

Sugar	Sweet	Nutritious	STM	LTM
Monosaccharides				
D-arabinose	Y [29–32]	N [27–31]	Y [17, 29, 35, 36, 79]	N [29, 30]
L-arabinose	Y [32]	N [32]	Y [32]	Y [32]
D-fructose	Y [29, 31, 80]	Y [27–29, 31]	Y [29]	Y [29]
L-fructose	Y [80]	–	–	–
L-fucose	Y [31, 32]	N [28, 31, 32]	Y [32]	Y [32]
D-galactose	–	Y [27, 28]	–	–
D-glucose	Y [30, 31, 80]	Y [27, 28, 30, 31]	Y [79]	Y [30, 79, 81]
L-glucose	Y [31, 80] N [30]	N [30, 31]	Y [79]	N [79, 81]
D-mannose	N [31]	Y [27, 28, 31]	–	–
L-rhamnose	–	N [27, 28, 32]	–	–
D-sorbitol*	N [29, 31]	Y [27–31]	N [29]	Y [30] N [29]
L-sorbose	Y [32]	N [27, 28, 32]	Y [32]	N [32]
D-ribose	N [31]	Y [28] N [31]	–	–
D-xylose	N [29]	Y [27, 28] N [29]	N [29]	N [29]
Combined monosaccharides				
D-arabinose + D-sorbitol	–	–	Y [17]	Y [29, 30, 35]
D-xylose + D-sorbitol	–	–	–	Y [29]
Disaccharides				
lactose	–	N [27, 28]	–	–
maltose	Y [31]	Y [27, 28, 31]	–	–
sucrose	Y [29–31]	Y [27–31]	Y [17, 34–36]	Y [17, 34–36]
trehalose	–	Y [27, 28]	–	–
Trisaccharides and polysaccharides				
maltodextrin	Y [29]	Y [29]	–	–
raffinose	–	Y [28]	–	–

1.4 Reward prediction error

The learning that underlies classical reward conditioning is thought to arise from a comparison between two values, or estimates of rewards, upon observing a stimulus [83, 84]. The first is the reward value an animal expects based on previous experience of that stimulus (V), while the second is the value the individual actually receives when the stimulus is next observed (V^*) [83, 84].

A reward prediction error (RPE) arises when there is a difference between these two quantities ($RPE = V^* - V$) [83–85]. Prediction error is positive when the animal receives more reward than expected ($V^* > V$), negative when it receives less ($V^* < V$), or zero when the reward received is exactly what was expected ($V^* = V$) [83–86].

The prediction V is then updated to reflect what was learnt from the current trial ($V_{new} = V_{old} + \alpha \cdot RPE$) to predict future rewards more accurately [83–86]. The learning rate α, which varies between 0 and 1, weights the prediction error and helps revise V towards V^* immediately ($\alpha = 1$) or incrementally (e.g., $\alpha = 0.1$) [83–86]. This iterative error-based update process first described by Bush and Mosteller [83, 84] is a key part of reinforcement learning, the process by which individuals use previous experiences to make better decisions that increase reward and reduce punishment [87].

The Bush-Mosteller model [83, 84] has since had two key conceptual revisions. First, Rescorla and Wagner (1972) [40] modified the Bush-Mosteller model to account for multiple stimuli. Each stimulus observed by an animal provides it with different predictions of reward. When multiple stimuli are observed at a time instead of just one, the animal makes a single prediction V_{net} that is the sum of predictions for all stimuli present [40, 86]. The net prediction error is then calculated ($RPE_{net} = V^* - V_{net}$) and used to update the reward value of each stimulus as before [40, 86].

The Rescorla-Wagner model [40] helps to explain the phenomenon of blocking, in which associative learning about one CS-US pairing can impair future asso-

ciations between other stimuli with the US [88]. If one stimulus (CS1) is paired with the US until it becomes a reliable predictor, and then a new stimulus (CS2) is presented together with CS1 before the US, animals do not learn the CS2-US association as effectively [88]. In effect, prior learning about CS1 has 'blocked' learning about CS2 because the added CS2 predicts nothing initially in addition to what CS1 already predicts [86, 88]. Since there is no prediction error, nothing is learnt about CS2 despite its pairing with the US [86]. With this explanation for blocking, the Rescorla-Wagner model suggests that learning is primarily driven by prediction errors [86].

Sutton and Barto [87, 89] extended the Rescorla-Wagner model from predicting each learning trial to all points in time [85, 87, 89]. Each trial can be thought of as a series of n discrete time points [85]. An animal has a different expectation of reward at each time point (V_t). The total prediction for a particular trial, V, is therefore the sum of the predictions for each of these time points ($V = V_{t=1} + V_{t=2} + V_{t=3} + \cdots V_{t=n}$) [85, 87, 89]. Hence, the prediction at each time point encodes not only the reward value expected at that time point, but also the theoretical sum of values at subsequent time points (i.e., $V_{t=1} = V - V_{t=2} - V_{t=3} - \cdots V_{t=n}$) [85, 87, 89]. Time points more distant in the future are weighted less because earlier rewards have more value [85, 87, 89].

The Sutton and Barto model, also known as the temporal difference model [87, 89], better explains how a CS comes to predict a US. When the CS is presented at the very first time, it conveys no information about the US because the latter has not yet occurred [85, 87, 89]. At that moment, there is no prediction error and hence no learning. In contrast, when the rewarding US is presented at a later time point, such an unexpected event increases the value of that later moment. The resulting positive prediction error then drives learning [85, 87, 89].

Since the expected value at each time point also includes the sum of future time points, the next CS presentation has greater value because it now also includes the

value of the previously unexpected US [85, 87, 89]. However, the next presentation of the US is less surprising, and results in less positive prediction error.

With repeated pairings, the expected value of the CS increases while that of the subsequent US decreases [2, 85, 87, 89]. When the US occurs exactly as expected, it no longer evokes prediction error alone. If the US does not occur when expected, it evokes a negative prediction error, which in turn reduces the value of the next CS [2, 85, 87, 89]. The temporal difference model therefore shows how classical conditioning can shift prediction error from the US to the CS [2, 85, 87, 89].

1.5 The role of dopamine

In the mammalian nervous system, phasic dopamine activity is thought to guide learning by encoding reward prediction error (RPE) [2, 90, 91]. Despite the impressive evidence in support of the reward prediction error hypothesis, the role of dopamine is now increasingly being reconsidered [5, 92].

When a mammal receives a reward that is unexpected or better than expected, dopaminergic neurons in its midbrain display an excitatory response whose magnitude is correlated with the size of the unexpected reward [93–97]. These neurons show an increasing response to the CS as it becomes more predictive [94, 96, 97], often stop responding when the US becomes expected [94], and show a phasic decrease in activity when the expected US fails to occur [2, 94, 98].

Although mammalian dopaminergic neurons encode RPE [99, 100] and modulate learning [101, 102], it remains unclear how exactly they themselves calculate RPE [103]. To complicate matters further, dopamine is also implicated in ongoing processes of motivation and movement that can be separated from those of learning [102, 104–107].

One possible explanation is that dopamine may be involved in learning and motivation on different time scales [4]. Motivation would be reflected by the slow and continuous (tonic) activity of dopaminergic neurons firing a few spikes (action

potentials) per second, and learning by brief (phasic) bursts of many spikes or paused activity. What is less clear is how phasic and tonic activity each influence the forebrain, a key target of midbrain dopaminergic neurons. While phasic bursts evoke rapid increases in forebrain dopamine concentrations that last less than a second [108, 109], it is thought that tonic activity makes a very small separate contribution [110].

Much of the evidence for tonic dopamine activity has been collected using microdialysis, a technique that can directly measure levels of dopamine but with low temporal resolution averaging from 1 min to 10 min [5]. Microdialysis of forebrain dopamine shows that forebrain dopamine is correlated with movement [1] and motivation [3]. However, tonic firing rates of dopaminergic neurons do not appear to change with different motivational states [111, 112]. Moreover, the slow measurement of dopamine by microdialysis does not mean that dopamine dynamics are themselves slow. One study [102] found that tonic dopamine appeared to fluctuate as fast as it was sampled using microdialysis.

Fast-scan cyclic voltammetry can measure electroactive molecules such as dopamine with better (sub-second) temporal resolution than microdialysis [5]. Studies using voltammetry have detected, over seconds or sub-seconds, rapidly increasing dopamine levels as an animal comes closer to receiving reward, peaking upon obtaining reward, and dropping rapidly upon consuming it [102, 113–115]. Such rapid dopamine fluctuations linked with motivation suggest that it has a fast (phasic) role in both motivation and learning [5].

Given that rapid dopamine fluctuations appear to reflect motivation whereas dopaminergic neuron firing reflects RPE, distinguishing between motivational value and RPE is non-trivial [5, 102]. Since the temporal difference model defines RPE as the change in value from one moment to another [87, 89], RPE and value signals are intrinsically correlated [5]. Techniques such as calcium imaging, functional MRI, and voltammetry measure relative changes in neuronal activity and compare the changes with a baseline period earlier in each recording. However,

if motivational value changes in the lead-up to reward, then normalization with the baseline can unwittingly derive an RPE signal from what is actually a signal change reflecting motivational value [5, 102].

Dopaminergic neurons that project to the forebrain from the ventral tegmental area (VTA) of the midbrain have similar RPE-like responses in both monkeys and mice [100, 116]. However, even within the VTA alone, dopaminergic neurons have considerable functional and molecular diversity [117–119]. Instead of encoding RPE, some of these neurons phasically increase their firing in response to punishing stimuli instead [120, 121]. Moreover, dopaminergic neurons in other parts of the midbrain show phasic dopamine activity in response to alerting sensory events [122–124] or spontaneous movements [125]. Some recent attempts to find a common thread between all of these roles suggest that dopamine estimates whether a limited internal resource is worth expending [5] or signals violations of expectancies to drive associations between events [92].

Although volume transmission is thought to be the primary mode of intercellular communication by dopamine in mammals [126], whether local or volume dopamine transmission predominates in *Drosophila* remains unclear [62]. While both phasic and tonic dopamine activity have been well characterized for mammals [4], most dopamine activity observed in *Drosophila* to date has been phasic [34, 35, 127, 128]. Tonic dopamine activity in *Drosophila* has primarily been observed in a single pair of dopaminergic neurons that are thought to signal satiety [129].

Dopaminergic neurons in *Drosophila* are thought to convey the US signal during olfactory associative learning [17, 34, 127, 130]. However, the only two studies recording adult *Drosophila* dopaminergic neurons during conditioning [127, 128] have used aversive rather than appetitive training. Both studies concluded that the dopaminergic neurons recorded do not encode prediction error for the punishing US but may encode the predictive power of the CS [127, 128].

Although such an investigation of rewarding dopaminergic neurons has not yet been attempted, dopaminergic neurons in *Drosophila* have been implicated in

aggression [131], arousal [132], courtship learning [133], ethanol-induced locomotion [134], protein hunger [135], sucrose feeding behaviour [136], and wakefulness [137]. The diversity of roles in behaviour may reflect modulation by different dopaminergic neurons in different regions of the brain, or a common component of dopamine signalling that has not yet been identified.

It remains unclear whether prediction error drives classical conditioning in insects [128]. Most studies to date have investigated whether insects also show the blocking phenomenon demonstrated in mammals. There is disagreement about whether the honeybee *Apis mellifera* exhibits blocking [138–141], while one study [142] has provided evidence for blocking in the cricket *Gryllus bimaculatus*. The only such study in *Drosophila* [143] concluded that it does not exhibit blocking, albeit for aversive rather than appetitive conditioning.

The same study demonstrated that *Drosophila* show a simple learning phenomenon [143] also observed in mammals [144, 145] that the RPE hypothesis does not adequately explain. In a learning paradigm called sensory preconditioning [144, 145], an animal first experiences two neutral stimuli paired together before any experience of the US. Only one of these stimuli is subsequently paired with the US. However, the animal learns that both stimuli are cues predicting the US, even though one was never directly paired with the US [92, 144, 145].

The temporal difference model [87, 89] does not adequately explain the associative relationship formed between the two cues before any value could be transferred to the cue that was directly paired with the reward [92]. Since the model also does not appear to predict the responses of *Drosophila* dopaminergic neurons during aversive conditioning [127, 128], it would be illuminating to reveal the physiological responses of rewarding dopaminergic neurons in *Drosophila* during classical appetitive conditioning.

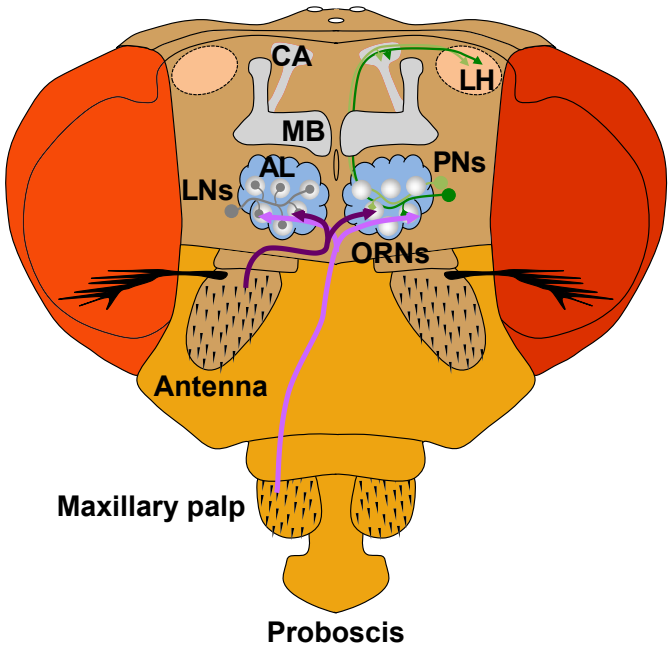

Figure 1.2: The olfactory processing pathway in *Drosophila*. Odours are detected by olfactory receptor neurons (ORNs) found in sensillae on the antennae and maxillary palps. ORNs bilaterally project their axons into two symmetrical glomeruli in the antennal lobe (AL). Excitatory and inhibitory local interneurons (LNs) that span multiple glomeruli process ORN input. Projection neurons (PNs) then deliver odour information from each glomerulus to the mushroom body (MB) calyx (CA) and the lateral horn (LH). Diagram adapted from Perisse et al. (2013) [82].

1.6 *Drosophila* olfactory memory circuits

In the *Drosophila* brain, the centre for associative olfactory learning consists of two paired mushroom bodies (or corpora pedunculata), named after their morphology [51]. The mushroom body in each hemisphere consists of a neuropil formed by the axons of ~2000 intrinsic cholinergic neurons called Kenyon cells (KCs) [146–148].

Odours are detected by olfactory receptor neurons (ORNs) found in hair-like sensillae on the antennae and maxillary palps of fruit flies [82] (Figure 1.2). ORNs that express genes for the same olfactory receptor bilaterally project their axons into two symmetrical glomeruli, distinct globular structures in the antennal lobes [149]. In each antennal lobe glomerulus, ORN inputs are processed by local excitatory and inhibitory interneurons that span multiple glomeruli [150–153]. This processing helps to maintain consistent representations of odours across a range of concentrations [153–156].

The axons of ORNs also form synapses with the dendrites of projection neurons (PNs) confined to a single glomerulus [157]. PNs then deliver odour information to the mushroom body calyx, a cup-like structure where PN axons synapse with KC dendrites [51], and the lateral horn, a less defined area in the lateral protocerebrum demarcated by the branching ends of PNs [158]. The lateral horn appears to be segregated between PNs conveying fruit odours and PNs conveying pheromones [159].

In general, the lateral horn is thought to encode innate responses [158] while the mushroom body encodes learned odour responses [160] (Figure 1.3A), although emerging evidence is starting to blur this distinction [161–163]. PNs appear to be randomly connected to mushroom body KCs [164–166] and each odour they convey is thought to activate only sparse populations of KCs [164, 167, 168]. Each KC subtype, $\alpha\beta$, $\alpha'\beta'$, and γ (Figure 1.3B), receives PN inputs from a distinct combination of antennal lobe glomeruli [166]. However, PN-to-KC connectivity may not be completely random in light of recent findings that PNs cluster more tightly in the MB calyx than expected [64].

The axons of the 2000 KCs in turn form *en passant* synapses with their downstream targets, just 34 mushroom body output neurons (MBONs) [170]. These output neurons project to the rest of the brain [51] and promote either odour-evoked approach or avoidance [58, 59, 171, 172]. Each MBON belongs to one of 21 different anatomical classes and uses either acetylcholine, GABA (γ-aminobutyric acid), or glutamate as a neurotransmitter [170].

Dopaminergic neurons (DANs) project to 15 distinct non-overlapping compartments of the mushroom body that are precisely matched by the dendritic fields of particular MBONs [170]. Most DANs project from two separate anatomical clusters named after their location [11, 12] (Figure 1.3C): the protocerebral posterior lateral 1 (PPL1) cluster, whose DANs convey punishment [173–175], and the protocerebral anterior medial (PAM) cluster, whose DANs mostly convey reward [17, 34–36], although a minority convey punishment [174].

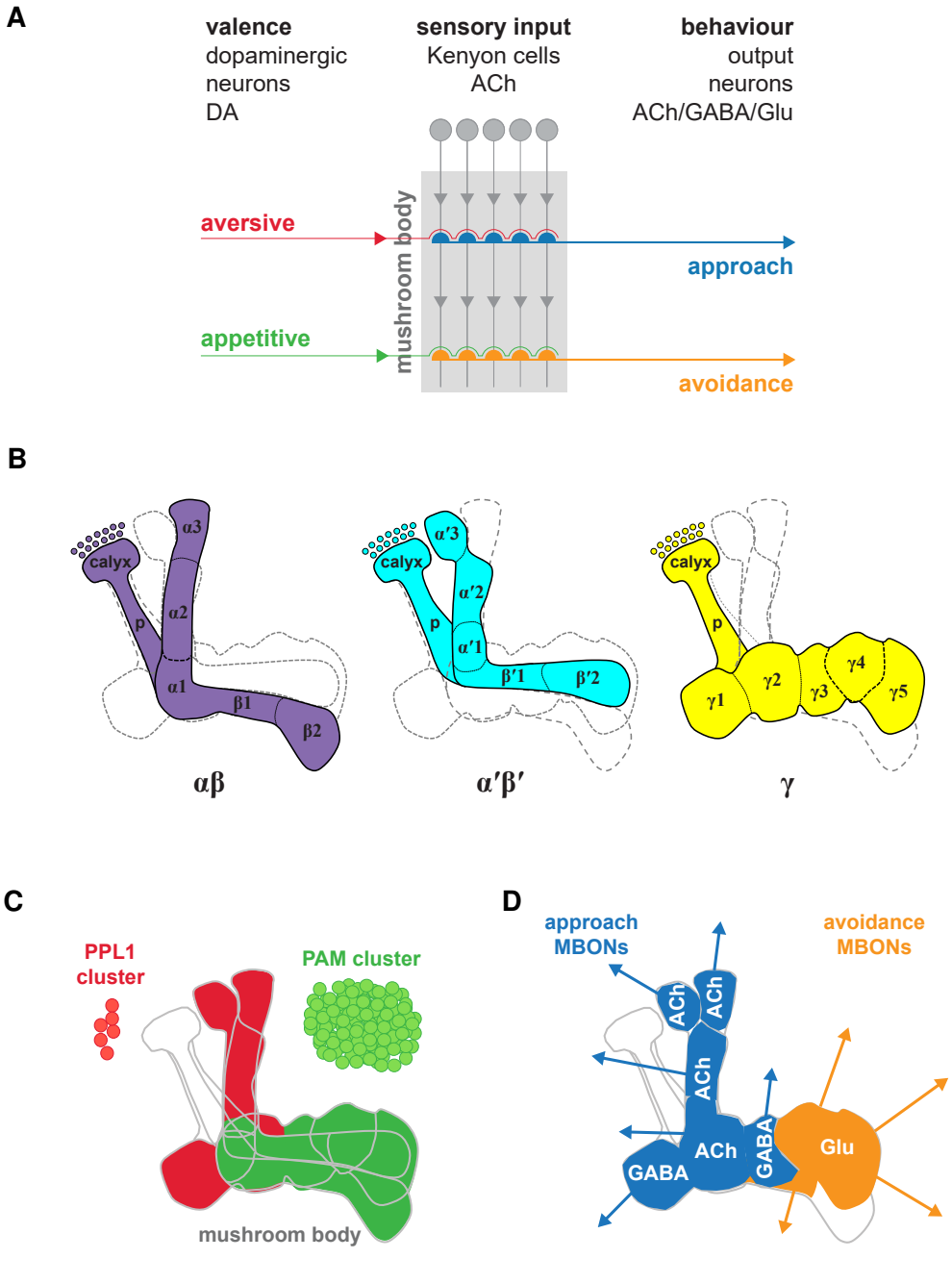

Figure 1.3: Associative olfactory memories are formed in the mushroom body. A) Odour cues are conveyed through the sparse activation of Kenyon cells (KCs). KCs project into the mushroom body lobes, where they form synapses with mushroom body output neurons (MBONs). Dopaminergic neurons (DANs) that innervate the mushroom body convey the teaching signal during olfactory associative learning. **B)** Three subtypes of KCs (αβ, α′β′, and γ) make up the lobes of the mushroom body neuropil. Each KC has dendrites in the calyx and an axon that projects through the peduncle (p) and into the lobes. At least 15 non-overlapping compartments (zones) have been identified along the mushroom body lobes based on the innervation of DANs and MBONs. **C)** The axon terminals of different DAN subsets project to non-overlapping mushroom body compartments. **D)** The dendritic fields of distinct MBONs correspond to the DAN terminals. Aversively reinforcing DANs from the protocerebral posterior lateral 1 (PPL1) cluster (red) overlap with approach-promoting MBONs (blue), whereas DANs from the protocerebral anterior medial (PAM) cluster that are mostly appetitively reinforcing (green) overlap with avoidance-promoting MBONs (orange). Neurotransmitters used by each neuronal type: ACh (acetylcholine), DA (dopamine), GABA (γ-aminobutyric acid), Glu (glutamate). Adapted from Perisse et al. (2013) [82] and Cognigni et al. (2018) [169].

Dopamine released by specific subsets of these neurons encoding positive or negative valence is thought to induce synaptic plasticity between odour-activated KCs and MBONs during learning [58, 59, 148, 176, 177]. By altering the strength of particular KC-MBON synapses, dopaminergic input appears to skew the balance between the different MBONs and hence that of behavioural output towards approach or avoidance [172] (Figure 1.3D).

DANs, KCs, and MBONs are thought to form microcircuits within a mushroom body compartment [60, 62]. DANs and KCs are connected in both directions: DAN axons synapse onto the axons of KCs, and KC axons form synapses with the axons of DANs [60, 62]. Both DAN and KC axons form synapses with the dendrites of MBONs [60, 62]. KC to DAN synapses seem to be excitatory and are thought to modulate the dopaminergic signal within a compartment during learning [178].

Outside specific compartments, some MBON axons also project to regions containing DAN dendrites [179]. These DAN targets sometimes project to the same mushroom body compartment as the MBON concerned [58, 61, 179] or other compartments [60, 61]. In contrast, no MBON axons have been observed to project back to the KCs; only the KC to MBON connection is thought to be unidirectional [169]. Nonetheless, DAN activation during learning could slowly activate MBONs directly, leading to possible local excitatory feedback loops between DANs, KCs, and MBONs in specific compartments [62].

The specific inputs to DANs that make different subsets convey positive and negative valence are not well characterized despite progress towards identifying some inputs [17, 33, 35, 180]. The two most significant known inputs are *Drosophila* neuropeptide F (dNPF) neurons that control the expression of appetitive memory through a DAN subset in the PPL1 cluster [33], and octopaminergic neurons that appear to convey short-term sugar reinforcement to subsets in the PAM cluster [17]. DANs have also been implicated in memory consolidation through feedback loops with MBONs innervating the same compartment [179] and memory reconsolidation through such feedback across different compartments [61].

1.7 Two-photon calcium imaging

Calcium is a universal intracellular second messenger whose versatility determines the functions of many different cell types [181]. The diverse roles of calcium are particularly apparent in the morphologically distinct parts of each neuron [182]. In axon (presynaptic) terminals, calcium influx triggers exocytosis of vesicles that contain neurotransmitters [183], whereas in dendritic (postsynaptic) spines, increased calcium induces activity-dependent synaptic plasticity [184]. Although neurotransmitter release happens in microseconds, calcium signals also regulate gene transcription in the nucleus over minutes and hours [185, 186].

Based on these observations and others, calcium signal changes have been used as a correlate of neuronal activity in experiments where the temporal resolution and sensitivity of electrophysiology are not essential. Genetically encoded calcium indicator (GECI) proteins [187] provide a readout of calcium activity in specific neurons over long time periods with high signal sensitivity and high spatiotemporal resolution [188]. GECIs emit fluorescence after Förster resonance energy transfer (FRET) between two fluorophores [187, 189] or after the excitation of single fluorophores [188, 190]. Currently, single fluorophore GECIs are more commonly used, particularly those from the GCaMP family [188]. The latest generation of GCaMP reporters (GCaMP6) can reliably detect the calcium transients resulting from a single action potential [188].

Calcium imaging is usually performed using either confocal or two-photon microscopy [182]. Confocal microscopy typically uses visible light one-photon excitation, which illuminates the specimen above and below the desired focal (imaging) plane, but can cause photodamage in other parts of the sample [182]. Confocal microscopes also use an aperture, or pinhole, that blocks any out-of-focus fluorescence from reaching the photomultiplier tube (PMT) detector [191]. However, the aperture also blocks photons that are generated in the focal plane but then scattered by tissue on their way to the PMT [182]. One way to compensate

is to increase the power of the excitation laser, at the cost of increasing tissue photodamage in both the imaging plane and elsewhere [182].

Two-photon microscopy [192, 193] is typically more expensive than confocal microscopy due to its need for a laser that can supply two low-energy near-infrared photons within femtoseconds to excite a transition in a fluorescent molecule [182]. However, infrared excitation wavelengths can penetrate tissue further because they are scattered less than visible light [194]. Moreover, since the requirement of two such coincident photons localizes excitation almost exclusively to the focal plane [195], there is no need for a pinhole to block out-of-focus fluorescence. Therefore, all emitted fluorescence, scattered or not, can be transmitted to the PMT with much less photodamage [182].

For these reasons, two-photon microscopy is widely used to record calcium activity in deeper brain regions [194]. Moreover, since its imaging depth can be up to 1 mm, no part of the whole adult fly brain measuring roughly 590 µm × 340 µm × 120 µm [196] is therefore off limits to two-photon calcium imaging.

1.8 Thesis overview

This thesis investigates the role of rewarding dopaminergic neurons in the *Drosophila* brain during associative olfactory learning, in particular classical appetitive conditioning. Two-photon calcium imaging is used to record the physiological responses of these neurons during the presentation of sugar-water droplets, odours, or both during appetitive conditioning. These experiments, whose methods are described further in Chapter 2, together provide a more nuanced understanding of the many functions of dopamine during feeding, odour detection, and learning.

Chapter 3 investigates the important role of deprivation state in gating the dopaminergic reinforcement and behavioural expression of appetitive memories. This is followed by two-photon calcium imaging of a specific subset of dopamin-

ergic neurons that reinforce sugar or water memories in different deprivation states. In particular, calcium responses evoked by single presentations of sugar-water droplets or repeated presentations of odours to tethered flies are compared between different deprivation states.

Chapter 4 explores the rapid processing of nutrient information after feeding in *Drosophila* and the different dopaminergic neurons that may be responsible for the rapid and delayed nutrient-guided reinforcement of appetitive olfactory memory. This is followed by a systematic experimental investigation of calcium responses evoked by feeding and odours in most of these dopaminergic subsets. The dopaminergic subset that was the focus of Chapter 3 is also investigated further concerning its responses to other sugar-water droplets and while impairing upstream octopaminergic signalling.

Chapter 5 investigates the same subset during appetitive conditioning protocols that present both odours and sugars together to tethered flies under the microscope. First, responses to sucrose reward and odour cues are characterized further under conditions that more closely approximate those during typical *Drosophila* appetitive conditioning protocols. Next, two different appetitive conditioning protocols under the microscope record how dopaminergic neurons respond to the unexpected omission or presentation of reward. Attempts to link the training protocols with behaviour that could reflect olfactory learning are also explored.

Chapter 2

Experimental methods

2.1 Fly husbandry

Drosophila melanogaster were maintained at 25 °C and 60% humidity with a light/-dark cycle of 12 h each with light provided between 8 A.M. and 8 P.M. For all experiments, flies were maintained on cornmeal-agar food that contained water, D-glucose, tegosept, and ethanol. For physiological experiments, flies were crossed and eclosed on cornmeal-agar food that contained molasses, propionic acid, and active yeast instead of D-glucose before being transferred to the food containing D-glucose. The wild-type *Drosophila* strain Canton-S was used for behavioural experiments. Table 2.1 lists all of the other fly strains used throughout this thesis.

2.2 Fly deprivation

For starvation, groups of ~10 flies were food deprived for 20 h to 24 h in a 25 ml vial containing a 2 cm × 3 cm piece of filter paper with 1% agar at the base. Starvation vials were stored in a 23 °C incubator throughout the deprivation period.

For dehydration, groups of ~10 flies were kept in a 25 ml vial without water for 4 h to 6 h. Throughout the dehydration period, flies had access to a sheet of dry sucrose-coated filter paper (2 cm × 3 cm) resting on top of a layer of cotton wool, which separated the flies from a thick layer of the dessicant Drierite (Sigma-

Table 2.1: Fly strains used for experiments in this thesis. Source refers to the first published reference detailing strain generation or characterization. Where applicable, stock identifiers refer to the Bloomington *Drosophila* Stock Centre (BDSC) or the Vienna *Drosophila* Resource Centre (VDRC).

Strain	Source	Stock Identifier
0104-GAL4	Gohl et al. (2011) [197]	BDSC 62639
c061-GAL4	Krashes et al. (2009) [33]	BDSC 30845
MB-GAL80	Krashes et al. (2007) [198]	BDSC 64306
MB320C-GAL4	Aso et al. (2014) [170, 171]	BDSC 68253
R15A04-GAL4	Jenett et al. (2012) [199]	BDSC 48671
R48B04-GAL4	Jenett et al. (2012) [199]	BDSC 50347
R48B04-GAL80	Huetteroth et al. (2015) [36]	–
Tbh^{M18}	Monastirioti et al. (1996) [200]	–
UAS-CsChrimson::mVenus	Klapoetke et al. (2014) [201]	BDSC 55135
UAS-GCaMP6f	Chen et al. (2013) [188]	BDSC 42747
UAS-GCaMP6s	Chen et al. (2013) [188]	BDSC 42746
UAS-$oamb^{RNAi}$	Dietzl et al. (2007) [202]	VDRC 2861GD
UAS-$shibire^{ts1}$	Kitamoto (2001) [203]	BDSC 44222
UAS-myr-tdTomato	Shaner et al. (2004) [204]	BDSC 32221

Aldrich) at the base. Vials were stored in a sealed polystyrene box containing a thin layer of Drierite and cotton wool throughout the deprivation period.

2.3 T-maze conditioning

Male flies from GAL4 lines were crossed to UAS-CsChrimson::mVenus or UAS-$shibire^{ts1}$ female flies and their mixed sex offspring 4 days to 8 days old were tested together in all T-maze conditioning experiments. Approximately ~100 flies were food or water deprived as described in Section 2.2. The odours used in all experiments were 4-methylcyclohexanol (MCH) [50] and 3-octanol (OCT) [50] (Sigma-Aldrich); each odour was diluted ~1:10^3, specifically, 10 µl MCH or 7 µl OCT in 8 ml mineral oil (Sigma-Aldrich). All experiments were performed at 23 °C and 55% to 65% relative humidity; temperature was raised to the restrictive 30 °C to 33 °C when specified during the training phase of $shibire^{ts1}$ experiments.

For training with sugar-water reward, flies were transferred to a tube that was then attached to a T-maze. They were exposed to the CS^- odour for 2 min and then to a clean air stream for 30 s. The flies were then transferred to a tube lined with an agar layer containing either 2 M sucrose or water in 1% agar. The tube was immediately reattached to the T-maze and flies were then exposed to the CS^+ odour for 2 min.

For each training round with optogenetic stimulation, each odour was presented for either 1 min or 2 min depending on the protocol with 30 s of clean air between each odour. Neither tube had any lining for these experiments. Stimulation was provided by a 630 nm LED activated at 500 Hz for 20 s or 120 s under the control of an S48 square pulse stimulator (Grass Technologies).

During the final testing phase of all T-maze protocols, flies were loaded into the elevator of the T-maze and lowered into the choice section, in which they were given 2 min to run into one of two tubes from which either the CS^- or CS^+ emanated. The flies that entered each tube were transferred into separate vials and then frozen to allow counting. Performance index (PI) was calculated as the number of flies in the CS^+ tube minus those in the CS^- tube, divided by the total:

$$PI = \frac{n(\text{flies in } CS^+ \text{ tube}) - n(\text{flies in } CS^- \text{ tube})}{n(\text{flies in both tubes})}$$

To account for any odour bias, a single PI was calculated from the mean of two experiments in which separate groups of identical genotype flies were trained with reciprocal CS^+/CS^- odour combinations of MCH and OCT.

2.4 Feeding assay

The feeding assay was adapted from that described by Qi et al. (2015) [80] with modifications to focus on feeding bout duration (Figure 2.1). Groups of ~100 flies were first food or water deprived as described in Section 2.2. Each fly was briefly anaesthetized for <10 s on ice and then stuck on its back and wings using nail

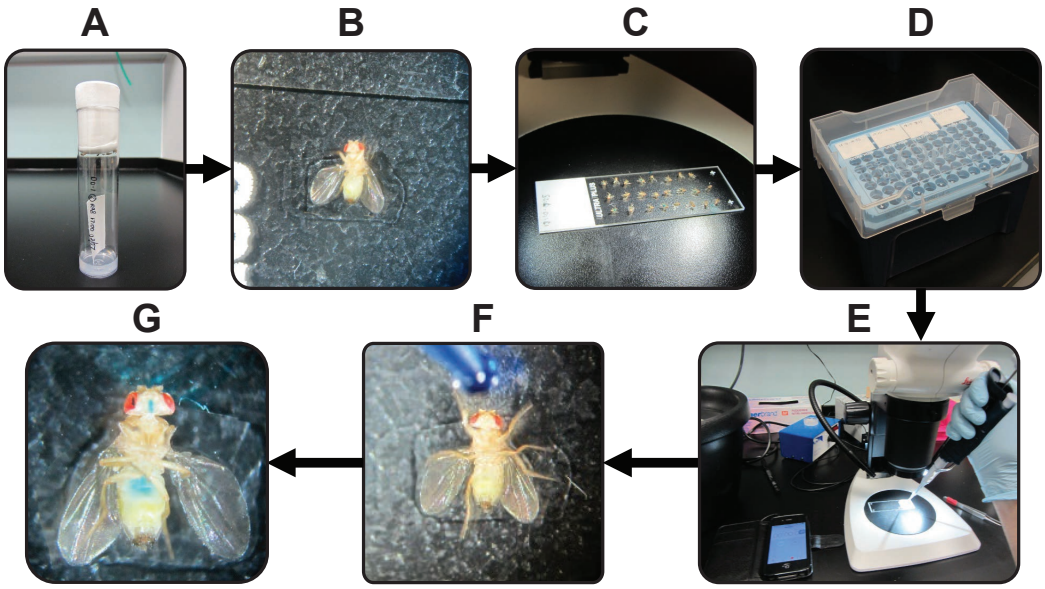

Figure 2.1: The feeding assay workflow. A) Flies were either starved or dehydrated as described in Section 2.2. **B)** Each fly was immobilized on a glass slide using nail varnish. **C)** Between 12 and 20 flies were immobilized to each slide. **D)** Slides were then placed in a moist or dehydrating container and allowed to rest for > 20 min. **E)** A 1 M sugar-water droplet was delivered to each fly under a dissection microscope while the start and end of each feeding bout was recorded with a stopwatch. **F)** The sugar-water droplet was delivered directly to the proboscis of each fly. **G)** Flies were checked for visible blue dye uptake of sugar-water after the experiment. Flies without any dye visible in their digestive tract were excluded from the analysis.

varnish on a glass slide. Between 12 and 20 flies were prepared on each slide. Food-deprived flies were then allowed to rest for >20 min in a moist container, whereas slides with water-deprived flies were rested in a container with Drierite.

Each droplet was prepared with 1 M concentration of sugar with tap water and Brilliant Blue FCF dye (Wako Chemicals). One hand was used to track the time of feeding bouts for each fly with a stopwatch. The other hand was used to carefully guide a pipette tip under a dissection microscope towards the back of the head of each fly to avoid contact with its untethered legs. The droplet was then presented directly to the proboscis and visible uptake of the blue droplet was taken to be the start of feeding. The start and end of each feeding bout was noted and the pipette was presented continuously to the proboscis until the fly no longer attempted to consume the droplet for at least 10 s.

For the analysis, the duration of all feeding bouts was first determined by subtracting the duration of all inter-bout intervals from the total duration of

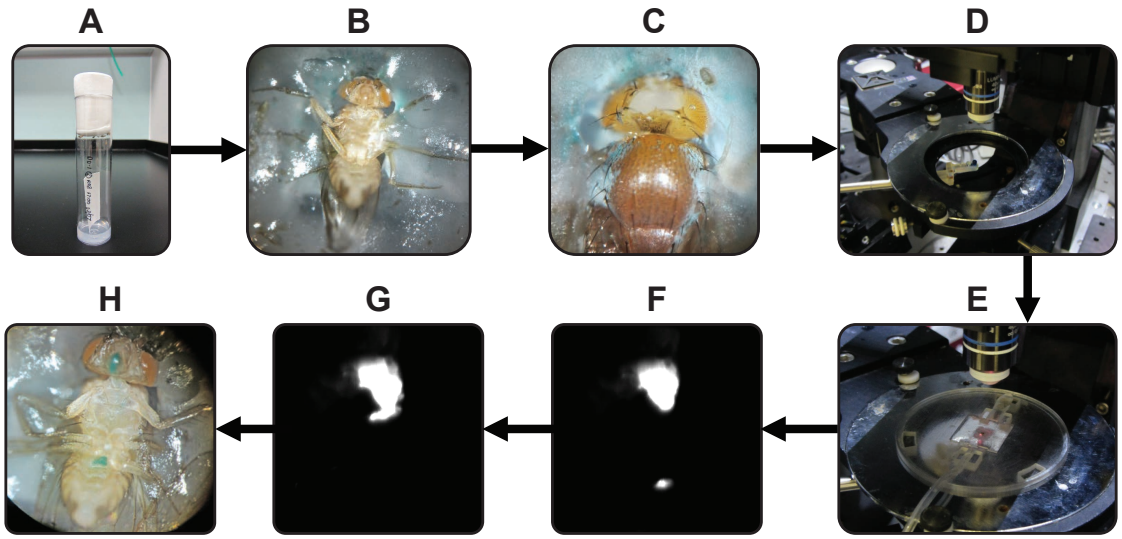

Figure 2.2: The sample preparation and two-photon calcium imaging workflow. A) Flies were either starved or dehydrated as described in Section 2.2 when applicable. **B)** Each fly was immobilized with wax along its thorax, legs, and eyes on a plastic sample dish. **C)** Sugar-free saline was applied to the posterior head capsule and opened at room temperature. **D)** A 1 M sugar-water droplet containing blue dye was loaded onto the feeding stage (centre). **E)** The sample dish with the tethered fly facing down was loaded onto the holder before the objective was lowered. For odour delivery experiments, a tube protruding from the sample dish was also connected to tubing from the odour delivery system (not shown). **F)** The head and proboscis of the fly (top) were illuminated by the laser, as was the edge of the droplet (bottom). **G)** The droplet was directed towards the proboscis at the desired time point and feeding was observed. The droplet stage was not loaded or brought to the proboscis for experiments involving only odour delivery. **H)** After experiments that involved feeding, each fly was inspected for visible dye. Flies without dye visible in their digestive tract were excluded from the analysis.

droplet presentation. The length of the first feeding bout was compared, as was the first bout length as a proportion of all feeding bouts. Flies that did not consume the presented droplet (29 out of 175 flies in total) were excluded from the analysis.

2.5 Imaging sample preparation

Groups of ~10 flies up to 10 days old were first food or water deprived as described in Section 2.2. Satiated flies were maintained on the cornmeal-agar food containing D-glucose described in Section 2.1. Each fly was briefly anaesthetized for <10 s on ice and then mounted onto a custom-made chamber [205] (Figure 2.2). The fly was tethered by immobilizing the thorax, legs, and then eyes with wax, whereas the proboscis, maxillary palps, and antennae were left unwaxed.

The posterior head capsule was then immersed in 1 ml sugar-free HL3-like saline solution (140 mM NaCl, 2 mM KCl, 4.5 mM $MgCl_2$, 1.5 mM $CaCl_2$, 5 mM HEPES-NaOH, pH 7.1, 275 mOsm kg^{-1}) [206] and opened at room temperature. After surgery, the brain was covered with a 15 µl droplet of the same solution supplemented with 1% agarose and then re-immersed in sugar-free saline. Each fly was then allowed to rest for > 20 min before imaging.

2.6 Two-photon calcium imaging

A Ti:sapphire laser (Chameleon Ultra II, Coherent) excited fluorescence using 70 fs pulses (80 MHz repetition rate) centred on 910 nm. A customized Scientifica Slicescope (Figure 2.3) acquired images of 256×256 pixels at 5.74 Hz using two-photon microscopy with a 40×, 0.8 NA water-immersion objective (Olympus). For dual colour imaging, green (GCaMP6) and red (tdTomato) detection channels were used (500/15 nm and 578/21 nm filters respectively, Semrock). Only the first filter was used for single colour (GCaMP6) imaging.

Dual colour imaging was used for all experiments with R15A04-GAL4 and 0104-GAL4; R48B04-GAL80, and all experiments with R48B04-GAL4 from Figure 5.3 onwards. Single colour recording was used for all other imaging experiments. Data acquisition and scanning control were performed by ScanImage 3.8 software [207] via MATLAB (MathWorks, release 2012a). Before imaging, the presence of the fluorophore in the expected neurons was briefly verified via wide-field imaging with an Andor Zyla 4.2 sCMOS camera and Andor SOLIS software.

Odours were delivered on a clean air carrier stream using a custom-designed system [151], which synchronized odour delivery timing with two-photon image acquisition via LabVIEW (National Instruments). The odours used were 4-methylcyclohexanol (MCH) [50], 3-octanol (OCT) [50], and isoamyl acetate (IAA) [15]; each odour (Sigma-Aldrich) was diluted 100× in mineral oil (Sigma-

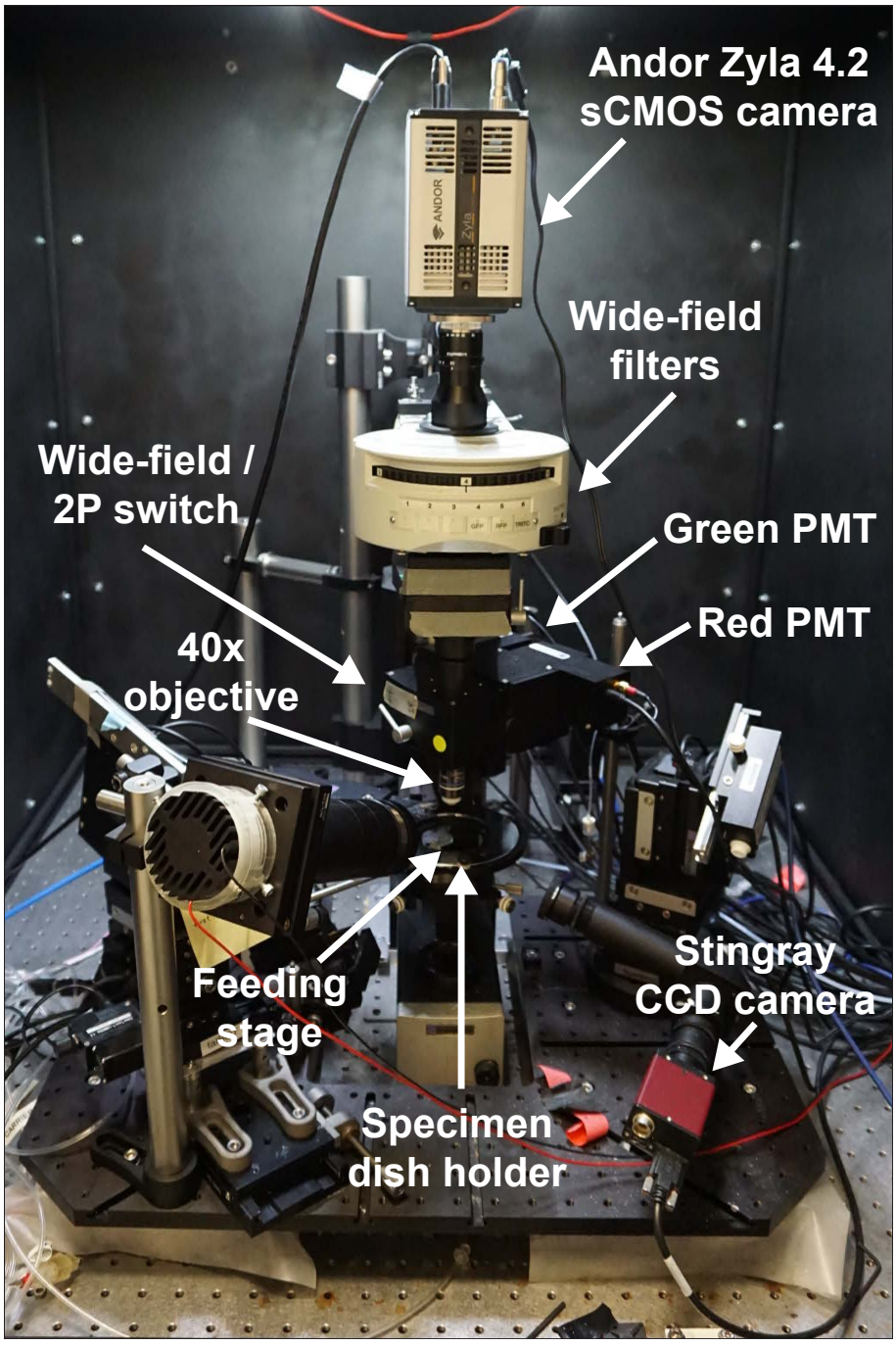

Figure 2.3: The two-photon imaging setup based on a customized Scientifica Slicescope. Sample fluorescence was first verified using an Andor Zyla 4.2 sCMOS camera (top) with a fluorescent filter set. Dual colour two-photon images were acquired using one GaAsP PMT through a green filter and another GaAsP PMT through a red filter. A switch allowed the light path to change between two-photon and wide-field imaging. Each fly tethered to a custom-made sample dish was loaded onto a sample holder and imaged through a 40× water-immersion objective. Flies were presented with droplets presented by the feeding stage or odours presented by a delivery system not visible here. Illumination during imaging was provided by a Ti:sapphire laser behind the setup. A Stingray CCD camera recorded the behaviour of the fly throughout imaging.

Aldrich) and then further blended 1:9 with the clean air stream before being delivered to each tethered fly.

A custom-built feeding stage [205] delivered a 15 µl to 20 µl droplet towards the freely-moving proboscis of a tethered fly. Each droplet was prepared with 1 M concentration of sugar with tap water and Brilliant Blue FCF dye (Wako Chemicals). A custom-written LabVIEW subroutine [205] controlled the feeding stage position by specifying its horizontal and vertical coordinates. Since feeding was voluntary and proboscis position varied between tethered flies, the feeding stage was manually directed by remote control towards the appropriate coordinates at the desired times. Each fly was photographed before surgery and after imaging to confirm whether feeding was successful. Flies without visible dye in their digestive tract post-imaging were excluded from the analysis.

A Stingray CCD camera (Allied Vision Technologies) recorded fly feeding and proboscis extension reflex behaviour at 15 Hz during two-photon imaging. The recording was then used to determine the exact timing of feeding and of each proboscis extension reflex. To determine this time accurately, the CCD camera started recording ~ 1 s before two-photon imaging and stopped recording ~ 1 s after two-photon imaging ended. MATLAB (release 2016a) was then used to discard frames that did not capture the laser light intensity before and after recording (described further in Section 2.8).

2.7 Image processing and analysis

Fiji (ImageJ) [208, 209] was used to demarcate anatomically distinct regions of interest manually for each driver line investigated (Figure 2.4). MATLAB (release 2016a) was used for all subsequent processing of the fluorescence signal. For each region of interest, the mean intensity of each frame was extracted for each channel recorded. For dual colour imaging, the mean intensity of each GCaMP6f frame

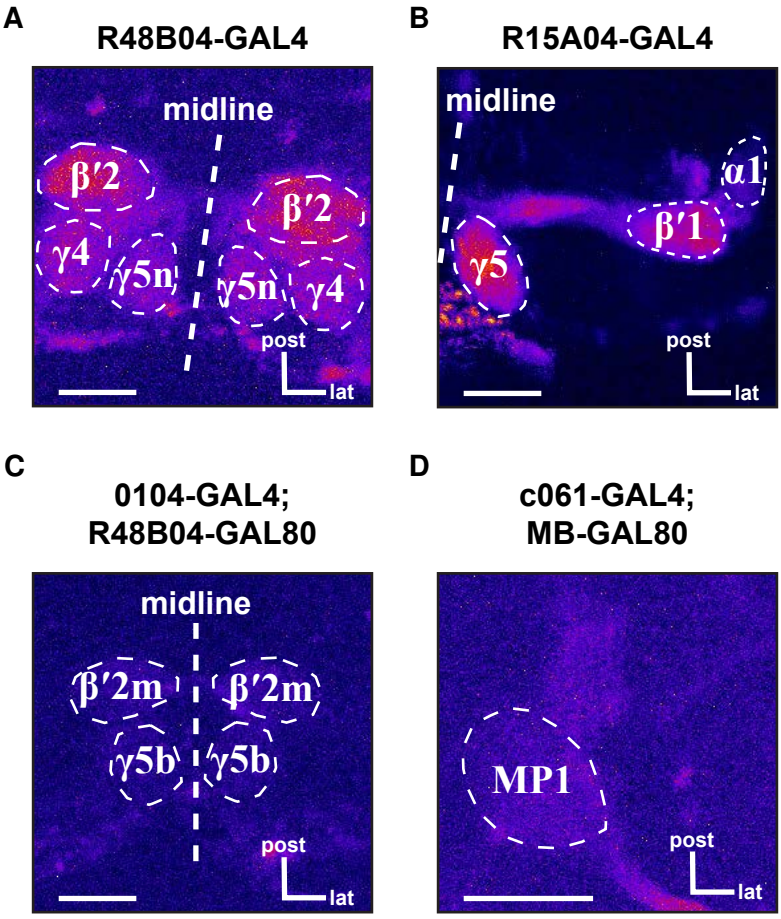

Figure 2.4: The anatomical regions of interest demarcated for each driver line investigated. Each driver line displayed is a pseudocoloured maximum projection of a two-photon imaging stack for GCaMP6f (or GCaMP6s for MP1) recorded from a representative sample viewed dorsally. Orientation: lateral (lat); posterior (post). Scale bar: 10 µm. **A)** The projections of PAM-β′2, PAM-γ4, and PAM-γ5n (narrow) to the mushroom body were demarcated in both hemispheres. **B)** The projections of PAM-α1, PAM-β′1, and all of PAM-γ5 (broad and narrow) to the mushroom body were demarcated in one hemisphere. **C)** The projections of PAM-β′2m (middle), and PAM-γ5b (broad) to the mushroom body were demarcated in both hemispheres. **D)** The projection of a single MP1 neuron was demarcated in one hemisphere (in this case, the left).

was divided by the mean intensity of the corresponding tdTomato frame to reduce motion-related artefacts.

The resulting fluorescence trace was normalized by calculating $(F - F_0)/F_0$, where F is the trace and F_0 is the arithmetic mean of the trace for a designated time period. For all imaging experiments in Chapter 3 and Chapter 4, and Figures 5.1 and 5.3, F_0 was defined as the mean of the 5 s before the onset of each stimulus. For all other imaging experiments in Chapter 5, F_0 was defined as the mean of the 20 s before the onset of each stimulus. The only exception was the CS^+ odour

responses in Figure 5.10, for which F_0 was defined to be the 20 s before the onset of the US. For all summary response curves, the central line was the arithmetic mean of each frame for all samples in a treatment group, and the standard error of the mean (SEM) was displayed as a shaded error bar above and below the central line.

The components of each response to be analysed were planned before each experiment and are specified in corresponding experimental data figures throughout this thesis. In brief, the peak of a response for a selected time period was defined to be its maximum value during that period. The overall magnitude of a response was defined to be the area under the curve for the time period concerned. Numerical trapezoidal integration was used to calculate the area. The post-response was defined to be the arithmetic mean of the response for a specific time period after the end of stimulus presentation.

2.8 Proboscis extension reflex (PER) detection

For each recording of fly behaviour captured by the CCD camera (introduced in Section 2.6) during two-photon imaging, the mean signal intensity of each frame was extracted using MATLAB (release 2016a). Abrupt signal changes in the resulting trace were then identified. These changes corresponded to the laser switching on and off; the frames outside these time points were then removed.

Fiji (ImageJ) was used to demarcate a backward L-shaped region of interest for the behavioural recording of each fly (Figure 2.5A). The region of interest was positioned such that the proboscis would only enter the region during a proboscis extension reflex (PER, Figure 2.5B). MATLAB was used to extract the intensity-time trace for the region of interest. Peak detection in MATLAB was then applied to identify sudden intensity changes in the trace; each detected peak corresponded to a single PER (Figure 2.5C).

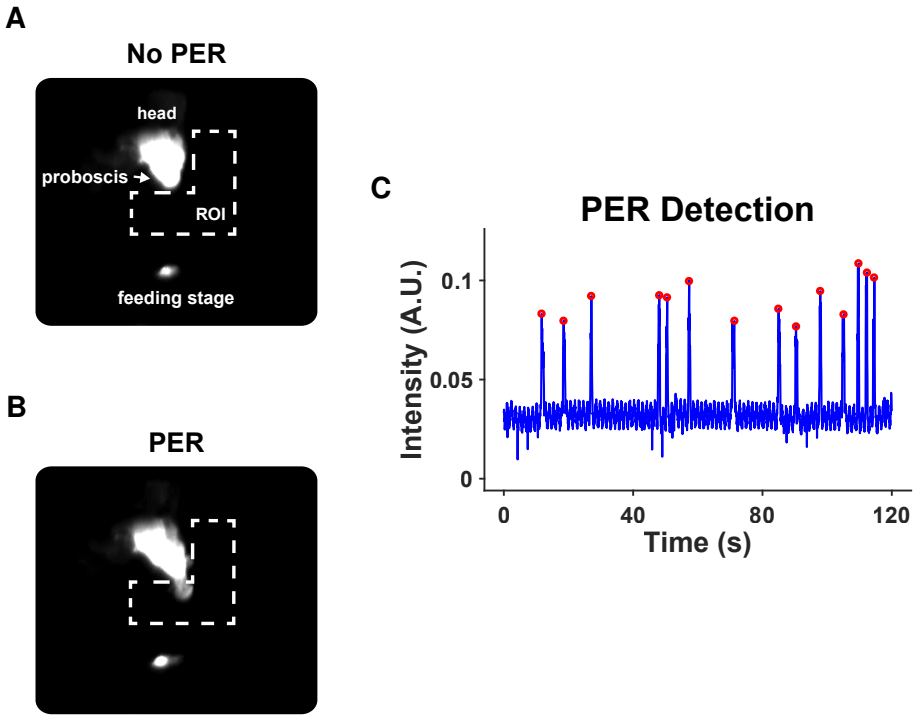

Figure 2.5: Detection of proboscis extension reflexes during two-photon imaging. A) A region of interest (ROI) was demarcated for CCD camera data such that the proboscis did not enter it during inactivity. **B)** During a proboscis extension reflex (PER), the proboscis enters the ROI and increases the mean ROI intensity for the corresponding frames. **C)** Sudden changes in mean intensity for the ROI (blue) between frames were detected as individual PER events (red circles).

2.9 Oscillation analysis

MATLAB (release 2016a) was used for all signal processing and oscillation analysis. The fluorescence-time trace for an MP1 region of interest was normalized using $(F - F_0)/F_0$, as described in Section 2.7. A fourth-order high-pass Butterworth filter with a 0.02 Hz passband, a 0.01 Hz stopband, a passband ripple no larger than 3 dB, and stopband attenuation no smaller than 20 dB was designed to remove low frequency noise (<0.01 Hz) arising from factors such as long-term drift.

The normalized fluorescence signal was first passed through the Butterworth filter. Next, the oscillation amplitude was derived by calculating the root-mean-squared value of the filtered time-domain signal. Similar results were obtained if the amplitude was instead calculated as the difference between the means of the 30% upper and lower quantiles of data points [210] (data not shown).

The power spectrum (frequency-domain) of the signal was then calculated by applying a fast Fourier transform to the time-domain signal using Welch's method (2 to 4 non-overlapping segments 25 s to 30 s in length; NFFT set to the next power of 2 larger than the total number of frames). Rhythmic spontaneous activity in the fluorescence time-domain resulted in a peak in the power spectrum (frequency-domain) that had a finite width. Peak width varied with noise from other frequencies and spectral leakage caused by windowing.

To estimate the characteristics of distinct rhythmic activity in a sample, a Lorentzian function was fitted to the power spectrum. The fit provided an estimate of the central frequency of the Lorentzian, f_0, and the full-width half maximum, Δf. The characteristic frequency of the oscillation was taken to be f_0. The regularity of the oscillation (i.e., its duration without further stimulatory input) was derived by the quality factor $Q = f_0/\Delta f$. A quality factor greater than 0.5 indicated that the peak corresponded to sustained (under-damped) oscillatory activity at that frequency. When the quality factor was 0.5 or less, then the peak did not correspond to oscillatory activity and both f_0 and Q were assigned zero values.

2.10 Statistical analysis

All feeding assay data and the behavioural experiments in Figure 3.2 were tabulated in Microsoft Excel and analysed in GraphPad Prism 6. All imaging experiments and all other behavioural experiments were analysed in MATLAB (release 2016a). All analytical comparisons in this thesis are presented as mean $\pm$ SEM bar plots; the sole exception is Figure 4.13, for which box-scatter plots are presented. Nonetheless, box-scatter plots were generated for each bar plot and the underlying distribution of the data was checked to determine appropriate statistical tests.

Sample sizes were not determined statistically before experiments, but sample sizes were similar to those reported in many previous publications [17, 34–36, 66, 205, 211]. All relevant information about the statistical comparisons used for each

experiment can be found in the legends of the corresponding data figures. The threshold for statistical significance was set to $p < 0.05$.

For Chapters 3 and 4, responses to sucrose, arabinose, and water for each PAM subset were compared first with one-way ANOVA. If a statistically significant difference was detected, then relevant groups would be compared using *post hoc* Tukey's honestly significant difference (HSD) multiple comparisons tests. When only two sugars were compared, two-sample t-tests would be conducted for each PAM subset imaged. For MP1 imaging (Figure 4.13), before and after non-parametric comparisons were conducted using Wilcoxon's signed-rank tests for each droplet.

For Chapter 5, odour responses during the first and last rounds of the multi-round appetitive conditioning protocol were analysed according to the parameters denoted in Figure 5.7. The forward pairing CS^- and CS^+ and the odour control CS^- and CS^+ were first compared using the non-parametric Kruskal-Wallis test. If a statistically significant difference was detected, then relevant groups would be compared using Wilcoxon's signed-rank test. For the experiment in Figure 5.15, two-sample t-tests were used to compare the sucrose response between the Predicted and Surprise groups for each PAM subset recorded.

Chapter 3

State-dependent reinforcement

3.1 Background

3.1.1 Deprivation provides motivational drive

Motivation is a process that drives an individual towards or away from a particular element in its environment. The most fundamental needs of any animal are physiological, in particular those relating to metabolism that are essential for survival. Food or water deprivation evokes motivational drive states of hunger or thirst in animals and can be readily manipulated. These states ultimately arise from metabolic deficit signals that increase the likelihood an individual seeks food.

For an individual to seek food effectively, it helps to recall stimuli in its environment that may not be nutritious themselves but are predictive of food. Such cues, once an individual learns to associate them with food, provide their own motivational drive and help specify possible food locations. Deprivation-driven motivation can be experimentally investigated in *Drosophila* since starved fruit flies can be rapidly trained to associate odours with sugars or water [25, 66, 205]. Critically, flies express their memory of these associations only when they are in the appropriate deprivation state [25, 33, 66, 205].

3.1.2 Flies express specific appetitive memories

Specific dietary deficits are thought to be signalled throughout the brain by neuromodulators, such as monoamines and neuropeptides, which can reconfigure essentially any component of a neural circuit to modify behaviour [212–214]. Neuromodulators have been extensively characterized in the crustacean stomatogastric ganglion [213], and many neuromodulators have important functions in *Aplysia*, *C. elegans*, and *Drosophila* [212, 214, 215].

Fruit flies form an appetitive olfactory memory for at least 24 h after a single pairing of an odour with sugar [25, 26, 66]. However, the memory is only expressed as learned food-seeking behaviour when flies are sufficiently starved [25, 33]. This state-dependent modulation may arise from four prominent neurons in the protocerebrum that branch extensively in the dorsal brain [33, 216, 217] and express *Drosophila* neuropeptide F (dNPF), an orthologue of mammalian neuropeptide Y (NPY) [218].

Both dNPF and NPY promote feeding behaviour by repressing inhibitory components of neural circuits [33, 219]. In fruit flies, dNPF inhibits a single pair of dopaminergic neurons in the PPL1 cluster called MP1 or PPL1-γ1pedc because they innervate the γ1 zone of the medial lobe and peduncle (MP) of the mushroom body [53]. The ongoing activity of MP1 neurons appears to signal satiety since it inhibits the behavioural expression of long-term appetitive memory [33]. Food deprivation triggers dNPF release and allows sugar memory to be expressed by inhibiting MP1 neurons [33]. MP1 has reduced tonic activity in starved flies [129] and directly blocking MP1 output also releases sugar memory expression [33].

Dopamine neurons in the PPL1 cluster signal punishment [15, 16, 127]. MP1 neurons could be termed 'multi-purpose' in that they also reinforce several aversive stimuli such as electric shock [175, 220], heat [220], and bitter taste [211]. Two-photon calcium imaging has revealed that MP1 neurons have sustained calcium oscillations that are enhanced during aversive LTM formation [210], weakened

during anaesthesia-resistant memory (ARM) formation [210], but also enhanced after conditioning with the nutritious sugar D-glucose [81].

MP1 neurons show an immediate increase in calcium signal during electric shock [12], cooling [221], and feeding on sugar or the insect repellent DEET [211]. Despite extensive physiological characterization, there has been no investigation to date into how MP1 oscillatory activity is immediately affected when a starved fly consumes food (this is addressed in Section 4.2.5).

The dendrites of the inhibitory GABAergic mushroom body output neuron MVP2 (or MBON-γ1pedc>α/β) [59] innervate the same regions of the mushroom body that receive MP1 inputs [53]. MVP2 projects its axons into the α/β and γ lobes but also outside the mushroom body [59, 170]. MP1 activity suppresses MVP2 [59, 222], and activating MVP2 during retrieval allows sugar memory expression even in satiated flies [59]. Activating MVP2 leads to odour-evoked approach behaviour [171] because it asymmetrically inhibits the MBON network outside the mushroom body [59]. In particular, MVP2 forms inhibitory synapses with the dendritic fields of the horizontal lobe MBONs M4 and M6 [59, 65].

Drosophila approach or avoidance behaviour is guided by the overall balance in odour-driven activity of the MBON network [172]. Blocking input to M4/M6 MBONs or their output skews the network from naive odour avoidance into approach [58, 148]. Therefore, MVP2 inhibits M4/M6 neurons when MP1 activity is inhibited by dNPF released after starvation, promoting approach towards an odour that predicts food.

Sugar memory expression can also be controlled by a subset of broadly projecting serotonergic neurons [223]. Artificially activating them induces satiated flies to eat more and promotes expression of appetitive memory, but activating all serotonergic neurons in the brain decreases feeding, even in starved flies [223]. Taken together, these results suggest that the serotonergic subset concerned could be upstream of dNPF neurons and that different cells releasing the same neuromodulator can have opposing behavioural effects.

3.1.3 Rewarding neurons reinforce sugar and water

Although the neural circuit just described controls the expression of appetitive memory in a starvation-dependent manner, MP1 and other dopamine neurons in the PPL1 cluster do not themselves process reward. Instead, dopaminergic neurons in the protocerebral anterior medial (PAM) cluster signal reward for sugar or water depending on deprivation state [17, 34–36, 205].

Octopamine was once thought to be the key signal of reward in insects [13–16], but it is now known to reinforce only short-term sugar memory [17]. Octopaminergic reinforcement requires signalling through the α-adrenergic-like OAMB receptor [224] on downstream PAM dopamine neurons [17] and also the β-adrenergic-like OCTβ2R receptor [225] on MP1 neurons [17].

When the budding yeast GAL4 transcription factor is driven by a promoter fragment from the *oamb* gene, it is expressed in an intriguing subset of PAM neurons in the fly brain. Known in the FlyLight GAL4 collection [199] by its identifier R48B04-GAL4, this driver line has been implicated in the formation of distinct short-term memories in different deprivation states [35, 36, 205].

An estimated 55 dopaminergic PAM neurons in R48B04 project to the β′2, γ4, and γ5 zones of the horizontal lobes in the mushroom body (Figure 3.1A) [36, 53]. R48B04 does not label all dopaminergic neurons projecting to these zones; it labels more neurons innervating γ4 than other GAL4 lines [205] and only a so-called 'narrow' subset of dopaminergic neurons innervating γ5 [36].

The dominant-negative and temperature-sensitive dynamin mutant *shibire*^{ts1} leads to rapid synaptic fatigue after 20 ms of repetitive stimulation [226]. Placing it under UAS_{GAL4} control transiently blocks neurotransmission of particular neurons at a temperature above 29 °C [203]. Blocking R48B04 output with *shibire*^{ts1} impairs reinforcement of short-term sugar memory in starved flies (Figure 3.1B) [35, 36] and that of water in dehydrated flies (Figure 3.1C) [205, 227].

The GAL4 inhibitor GAL80 [228] can be ectopically coexpressed using a different promoter fragment in the fly [229]. Partial overlap between the expression

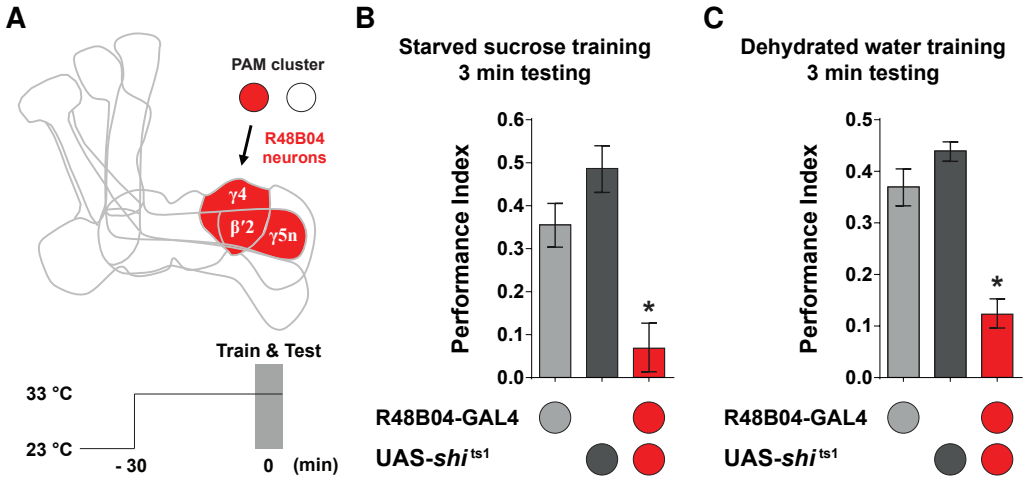

Figure 3.1: R48B04 neurons reinforce short-term sugar and water memories in different deprivation states. A) Top: R48B04 neurons project to the β′2, γ4, and γ5n (narrow) zones of the horizontal lobes in the mushroom body [36, 53]. Bottom: the training protocol and temperature used in these experiments. **B)** Thermogenetically blocking R48B04 output in starved flies using the dynamin mutant *shibire*^{ts1} (UAS-*shi*^{ts1}) impairs short-term sucrose memory ($p < 0.0001, N = 8$; ANOVA). Adapted from Huetteroth et al. (2015) [36] but similar results were published by Yamagata et al. (2015) [35]. **C)** Blocking R48B04 output in dehydrated flies impairs short-term water memory ($p < 0.0001$; ANOVA followed by *post hoc* Tukey's HSD test). Adapted from Lin et al. (2014) [205]; similar results were published later by Shyu et al. (2017) [227]. $N = 8$ for each group except UAS-*shi*^{ts1} control $N = 36$ due to other experiments also conducted by Lin et al.). All data plotted are mean ± SEM.

domains of GAL4 and GAL80 in the same fly limits GAL4 activity to cells that only express the former [229]. The GAL4-GAL80 subtractional approach has been used to identify which zones receive PAM inputs that specifically convey water or sweet reward [36, 205].

Subtractional experiments suggest that PAM-β′2 neurons promote naive water-seeking behaviour in thirsty flies [205] while PAM-γ4 neurons assign water value in dehydrated flies during olfactory learning [205]. Both of these PAM subsets are required to assign sweet taste during olfactory learning in starved flies [36]. No specific role in water or sugar reward learning has been assigned to PAM-γ5n (narrow) neurons [35, 36, 205].

Intersectional genetics works most effectively provided that GAL80 is driven with similar strength to GAL4 and that its inhibition in overlapping cells is indeed total. It also assumes that the same promoter fragment drives GAL80 and GAL4 in the same cells at a similar expression level, which may not always be the case due

to factors such as different insertion sites or expression constructs. For example, Huetteroth et al. (2015) [36] found that R48B04-GAL80 unexpectedly also blocks expression in unrelated PAM-β2 neurons.

From a gain-of-function perspective, only activating the entire R48B04 ensemble in starved flies leads to short-term sugar memory [35, 36]. Similarly, activating both γ4 and γ5n neurons in dehydrated flies leads to short-term water memory [205]. Subtractional experiments can remove β′2 or γ5n from R48B04, but it has not been possible to manipulate PAM-γ4 neurons exclusively [205]. Therefore, while it is likely that PAM-γ4 is the specific subset that reinforces water memory [205], at least PAM-γ5n cannot be conclusively ruled out yet.

The specific identity of neurons labelled by a GAL4/GAL80 combination poses fewer limitations for calcium imaging during feeding. The two experiments reported in the literature to date [35, 205] suggest that feeding evokes a response in all R48B04 neurons but to varying extents. Water feeding in dehydrated flies evokes a greater response in PAM-β′2 and PAM-γ4 [205], whereas sugar feeding in starved flies evokes a greater response in PAM-γ5n [35]. It is unknown whether water feeding evokes a calcium response in starved flies or whether sugar droplets evoke different responses in dehydrated flies.

Since rewarding R48B04 neurons are involved in the formation of olfactory memories relevant to specific deprivation states, the experiments in this chapter aim to characterize their physiology during feeding and odour presentation.

3.2 Results

3.2.1 Deprivation state affects sucrose reinforcement

The two studies that identified the role of R48B04 in short-term sugar memory [35, 36] also reported that another set of PAM neurons is required for long-term sugar memory formation in starved flies. This subset, identified as R15A04-GAL4 from the FlyLight collection [199], projects to the α1, β2, β′1, and γ5 zones of the

mushroom body (Figure 3.2A) [35, 36, 53, 205]. R15A04 labels a broader set of PAM-γ5 neurons including those labelled by R48B04; the additional neurons were designated as PAM-γ5b (broad) by Huetteroth et al. (2015) [36].

Since R48B04 neurons reinforce short-term sucrose or water memories in starved or dehydrated flies respectively (Figure 3.1) [35, 36, 205], whereas R15A04 neurons reinforce long-term sucrose memory in starved flies [35, 36], perhaps R15A04 neurons could reinforce a similar long-term memory in dehydrated flies.

Together with Gaurav Das, I starved or dehydrated flies that expressed UAS-*shibire*^{ts1} in either R15A04 or R48B04 neurons, whose output we then blocked by elevating the temperature during training with 2 M sucrose. After starving the flies for 24 h, we tested them for long-term memory at a permissive temperature (Figure 3.2A). As expected [35, 36], when these PAM subsets were blocked in starved flies (Figures 3.2B and 3.2C), long-term sucrose memory was impaired for R15A04 but not R48B04 neurons. After repeating the procedure for dehydrated flies (Figures 3.2D and 3.2E), we found to our surprise that long-term sucrose memory was impaired when only R48B04 neurons were blocked during training.

3.2.2 Flies rapidly discriminate between sugars

Since PAM-γ5n neurons are common to both R15A04 and R48B04, which reinforce appetitive memory in different deprivation states, I reasoned that perhaps PAM-γ5n responds differently to sugar or water reward depending on deprivation state. Therefore, I would need to perform a controlled comparison of feeding responses for different sugar-water droplets during two-photon calcium imaging. However, fruit flies prefer some sugars over others [29, 31, 32] and their preferences may change with deprivation state. I thus set out to determine the maximum period of time for which a tethered fruit fly (starved or dehydrated) would voluntarily consume any droplet in a single feeding bout.

I adapted a quantitative tethered feeding assay (Section 2.4) developed by Qi et al. (2015) [80] and presented individual flies with one of ten different 1 M

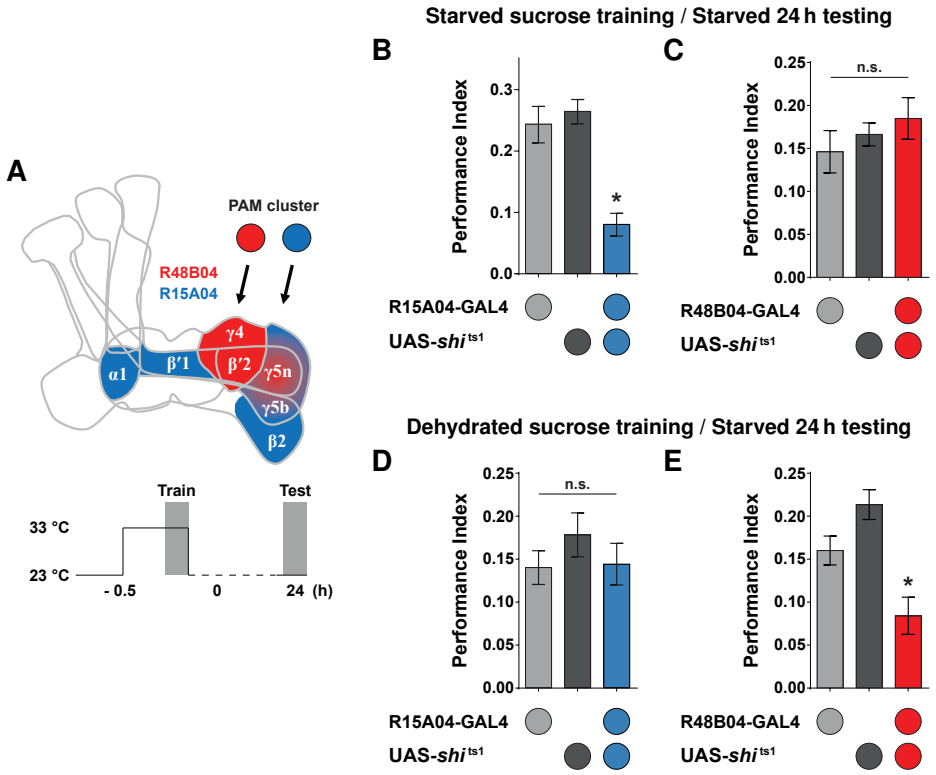

Figure 3.2: Different PAM neurons reinforce long-term sugar memory in starved and dehydrated flies. A) Top: R15A04 neurons project to the α1, β2, β′1, and γ5 zones of the horizontal lobes in the mushroom body [35, 36, 53, 205]. R15A04 includes all PAM-γ5n (narrow) neurons labelled by R48B04 plus others designated as PAM-γ5b (broad) [36]. Bottom: flies were thermogenetically blocked during training using *shibire*^{ts1} (UAS-*shi*^{ts1}) and tested for long-term sucrose memory at a permissive temperature 24 h later. These experiments were conducted together with Gaurav Das. **B)** In starved flies, blocking R15A04 output impairs long-term sucrose memory ($p < 0.01$ compared to controls, $N = 15$–19; ANOVA), whereas **C)** blocking R48B04 output does not ($p = 0.49$ compared to controls, $N = 6$–9; ANOVA). **D)** In dehydrated flies, blocking R15A04 output does not impair long-term sucrose memory ($p = 0.68$ compared to controls, $N = 11$–14; ANOVA), but **E)** blocking R48B04 impairs long-term memory ($p < 0.001$ compared to controls, $N = 22$–26; ANOVA). All data plotted are mean ± SEM.

sugar-water droplets. These were categorized by sweetness and nutrient content (Figure 3.3A) according to proboscis extension reflex (PER) and survival assays conducted by Burke and Waddell (2011) [29] and Stafford et al. (2012) [31]. Flies were either starved or dehydrated beforehand (Section 2.2).

While presenting a droplet to each fly, I recorded each feeding bout length until the droplet was rejected. I then compared the first bout length and its proportion of total feeding time (excluding inter-bout intervals) for each deprivation state and droplet type. Flies that did not consume the droplet presented were excluded from these comparisons. Irrespective of deprivation state, tethered flies consume any

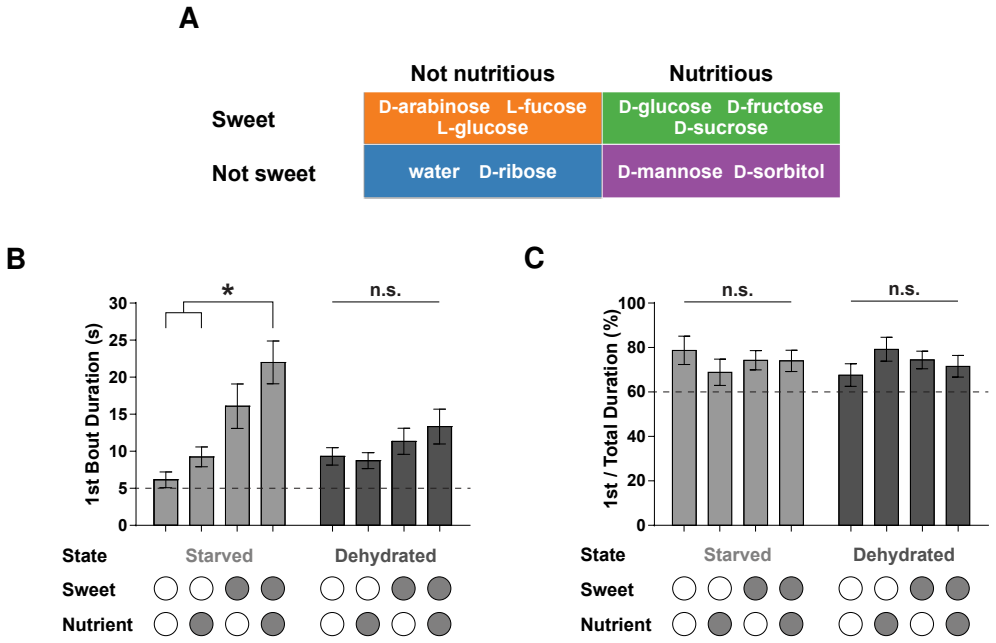

Figure 3.3: Tethered flies discriminate between different sugars in a state-dependent manner. **A)** Ten sugar-water droplets categorized according to their sweetness and nutrient content. In the tethered feeding assay, each fly was fed one of these different droplets with a concentration of 1 M. **B)** The first feeding bout length for starved or dehydrated flies on different types of sugar-water droplets. Shaded circles denote the presence of sweet or nutrient content in each droplet type. Flies in either deprivation state consume any droplet type for at least 5 s. Starved flies have a longer first feeding bout on droplets that are both sweet and nutritious than on any non-sweet droplets ($p < 0.005$ sweet and nutritious compared to each non-sweet group, ANOVA followed by *post hoc* Tukey's HSD test), while dehydrated flies have a similar first feeding bout on any droplet ($p = 0.29$, ANOVA). Two-way ANOVA revealed a possible but not significant interaction between deprivation state and droplet type on first bout consumption ($F(3, 234) = 2.58$, $p = 0.054$). **C)** The first feeding bout comprises at least 60% of the total feeding duration on any droplet type for both starved and dehydrated flies. The duration of all feeding bouts excludes inter-bout intervals. Two-way ANOVA revealed no significant interaction between deprivation state and droplet type on proportion of total meal ($F(3, 234) = 1.52$, $p = 0.21$) and no differences between each deprivation state ($p = 0.83$) or droplet type ($p = 0.98$). All data plotted are mean ± SEM, starved $N = 23$–35; dehydrated $N = 24$–40).

droplet presented to them for at least 5 s in their first feeding bout (Figure 3.3B). Starved and dehydrated flies also consume most of their meal (at least 60%) during the first feeding bout (Figure 3.3C). Therefore, a single 5 s feed should sufficiently represent a complete meal for any droplet presented during calcium imaging.

3.2.3 PAM feeding responses change with deprivation state

Having determined an appropriate way to compare sugar-water droplets in starved or dehydrated flies, I then used a tethered feeding preparation for two-

photon calcium imaging developed by Lin et al. (2014) [205]. I also tethered the legs of each fly because Cohn et al. (2015) [176] reported that tarsal movement causes calcium fluctuations in γ-lobe PAM neurons. Therefore, only the proboscis was left free to move and consume any droplet presented.

First, I presented starved flies with one of three droplets representative of the categories tested in Section 3.2.2: water (neither sweet nor nutritious), D-arabinose (sweet but not nutritious), and sucrose (both sweet and nutritious). These two sugars have been used to represent these categories in numerous studies [17, 29, 31, 35, 36]. The PAM neurons labelled by R48B04 project to anatomically distinct zones in the same plane of the mushroom body horizontal lobes. I could thus record the calcium responses of PAM-β′2, PAM-γ4, and PAM-γ5n neurons simultaneously for both hemispheres of the brain in each fly (Figure 2.4A).

I quickly came to appreciate that feeding is inherently voluntary and that verifying ingestion would be critical. I used an infrared camera to record feeding during calcium imaging, but the intensity of the two-photon laser at times introduced considerable ambiguity between flies that consumed a droplet and those that merely made contact. Since these differences could cause considerably diverse calcium responses, I resolved them by supplementing sugar-water droplets with blue dye and inspecting the thorax of each fly after imaging. Flies that did not have traces of dye visible in their digestive tract were excluded from my comparisons.

In starved flies that successfully consumed a droplet during imaging, a clear feeding response was observed in all R48B04 neurons (Figures 3.4A to 3.4C) but particularly in the PAM-γ5n subset. To compare the responses evoked by different droplets in each PAM subset, I compared the peak response in the first 10 s after feeding started, the overall magnitude by calculating the area under each response curve in the first 10 s, and any possible longer-term changes by calculating the mean signal in the final 25 s to 40 s, the time by which the calcium signal stabilized.

Each droplet evoked similar feeding responses in PAM-β′2 and PAM-γ4 neurons of starved flies (Figures 3.4A and 3.4B), although the overall magnitude (area)

of the PAM-β′2 response evoked by sucrose was greater than that for water but not arabinose (Figure 3.4E). In PAM-γ5 neurons, the droplets evoked quite divergent responses (Figure 3.4C): the immediate peak of the sugars was vastly greater than water (Figure 3.4D) and the overall magnitude of the sucrose response was greater than that of arabinose, which was in turn greater than that of water (Figure 3.4E). However, no longer-term differences between the droplets were observed for any of the regions (Figure 3.4F).

For dehydrated flies, I found that these differential responses collapse (Figures 3.5A to 3.5C). Although the largest responses were again observed in PAM-γ5n neurons (Figure 3.5C), water evoked a response with similar characteristics to those of the sugars in all three PAM subsets (Figures 3.5D to 3.5F).

Since hunger and thirst are both deprivation states and could in fact be competing with each other [230], during this experiment I also recorded sucrose responses in satiated flies with prior ad libitum access to food. Only sucrose was tested because satiated flies often rejected droplets during imaging. Feeding evoked substantially diminished responses in satiated flies compared to deprived flies in all PAM subsets, particularly in PAM-β′2 and PAM-γ5 (Figure 3.6). Therefore, deprivation can evoke larger feeding responses in R48B04 PAM neurons.

3.2.4 PAM odour responses may reflect deprivation state

Since sucrose feeding responses are larger in starved flies for each PAM subset, I reasoned that perhaps starvation increases PAM excitability and may also elevate odour-evoked responses in R48B04 PAM neurons.

After preparing starved or satiated flies for the same tethered imaging protocol, I delivered two different odours to each fly in alternating 5 s puffs every 20 s until each fly had been exposed to five presentations of each odour. Since odours can be received involuntarily and each presentation does not affect deprivation state as feeding might, I could easily compare how odour-evoked responses changed over time. I alternately presented the odours 4-methylcyclohexanol (MCH) then

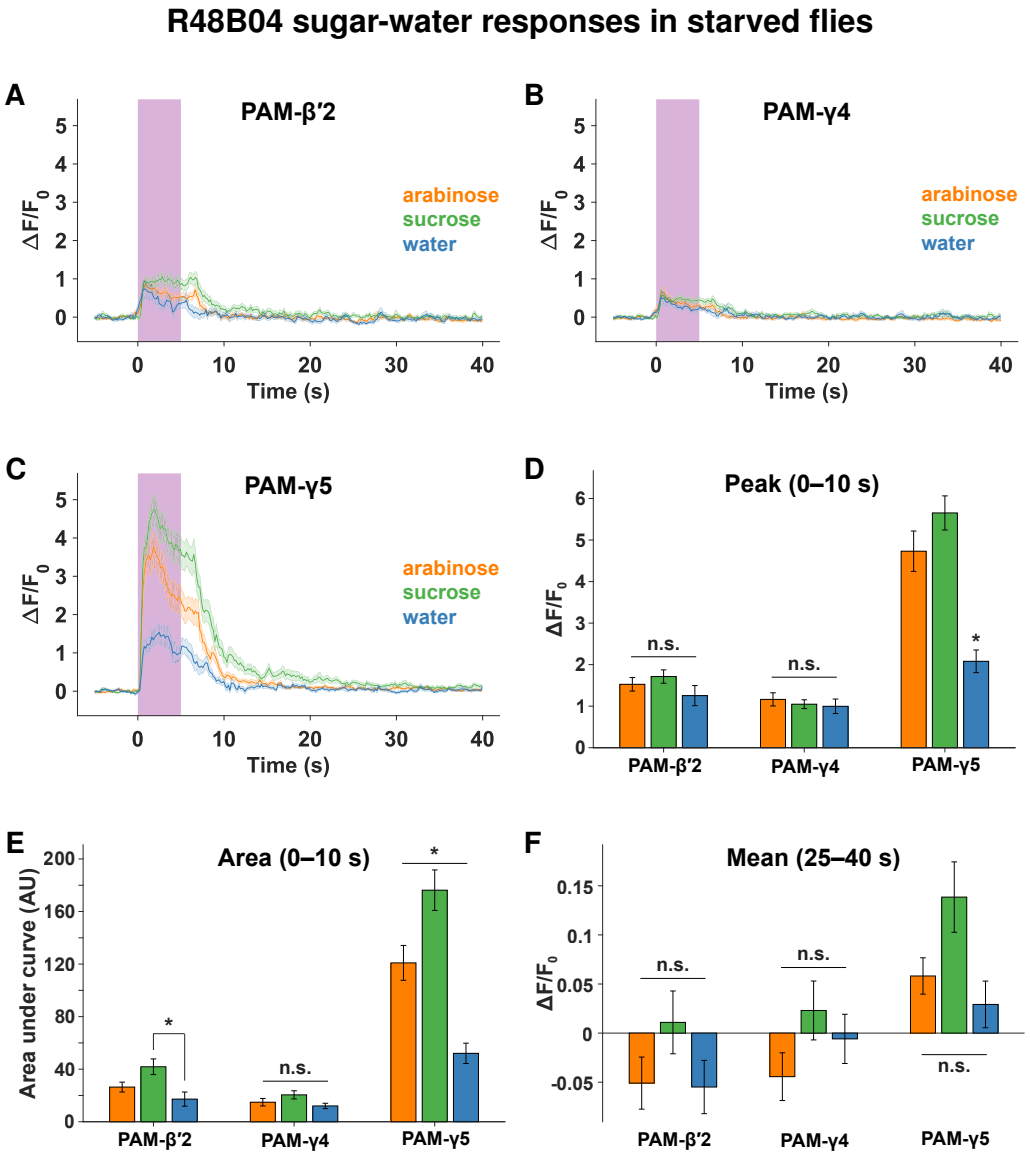

Figure 3.4: Feeding starved flies evokes differential PAM-γ5 responses. A–C) All R48B04 PAM neurons respond during feeding, but the largest and most diverse responses are evoked in PAM-γ5 neurons. **D)** Water evokes a PAM-γ5 response with a substantially lower peak than either sugar (first 10 s, $p < 0.0001$; ANOVA). No peak response differences between droplets were observed for PAM-β′2 ($p = 0.27$; ANOVA) or PAM-γ4 ($p = 0.73$; ANOVA). **E)** Consuming sucrose evokes PAM-γ5 responses with a greater area (first 10 s) than D-arabinose, which in turn is greater than water (all values significantly different from each other, $p < 0.05$; ANOVA with *post hoc* Tukey's HSD test). Differential responses may also be evoked in PAM-β′2 (sucrose versus water, $p < 0.05$; ANOVA with *post hoc* Tukey's HSD test), but not PAM-γ4 ($p = 0.17$; ANOVA). **F)** No differences were observed in the baseline post-response (last 15 s, $p > 0.05$ for each subset; ANOVA). All data plotted are mean ± SEM. Droplets compared: 1 M D-arabinose (orange, $N = 25$), 1 M sucrose (green, $N = 28$), water (blue, $N = 12$).

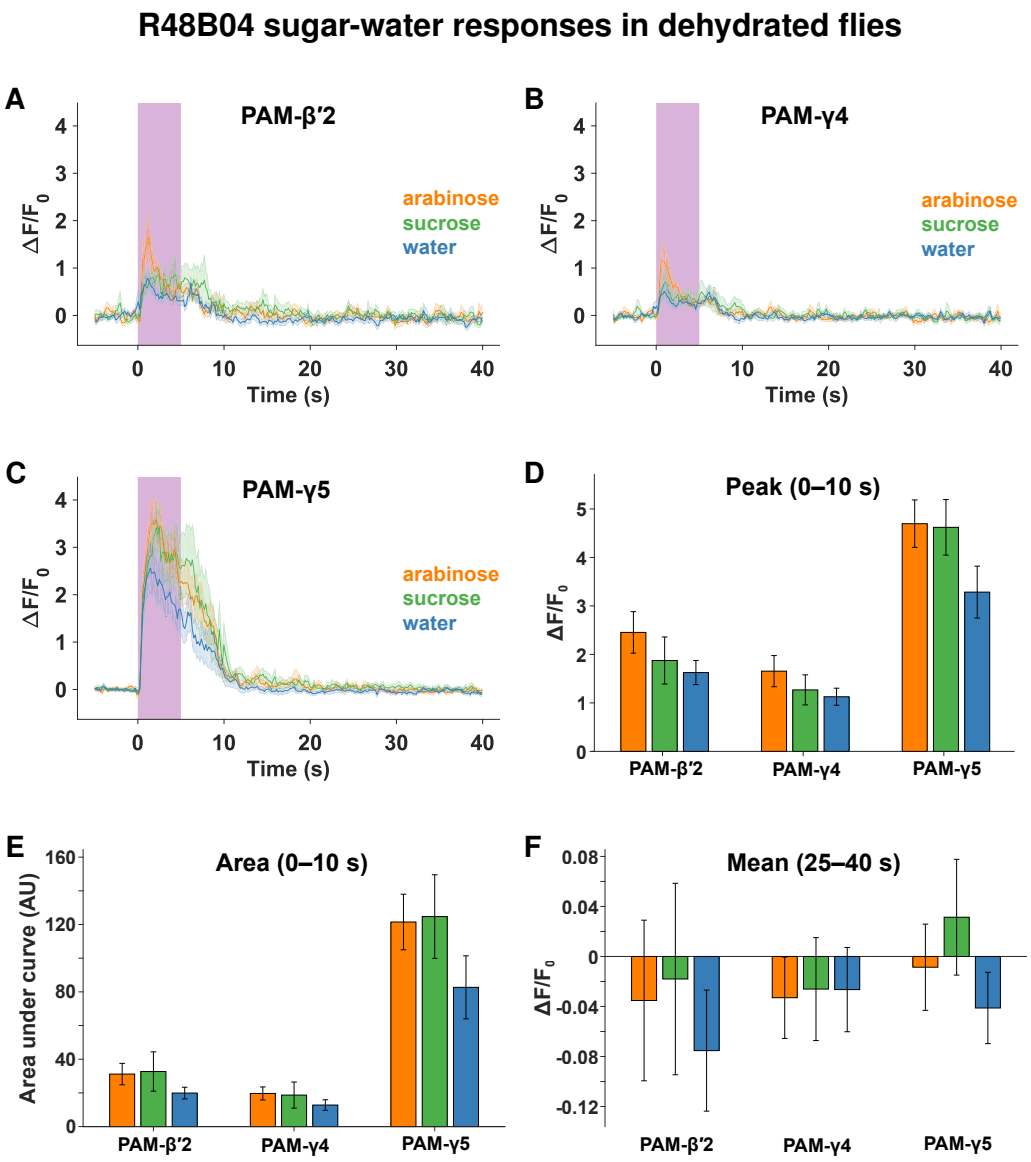

Figure 3.5: Feeding dehydrated flies evokes uniform R48B04 responses. A–C) All PAM subsets respond during feeding, but there are no differences between droplets in any region with respect to **D)** the peak response (first 10 s, $p > 0.11$ for each PAM subset; ANOVA), **E)** the overall magnitude (area, first 10 s, $p > 0.25$ for each PAM subset; ANOVA), or **F)** the baseline post-response (last 15 s, $p > 0.37$ for each PAM subset; ANOVA). All data plotted are mean ± SEM. Droplets compared: 1 M D-arabinose (orange, $N = 13$), 1 M sucrose (green, $N = 12$), water (blue, $N = 15$).

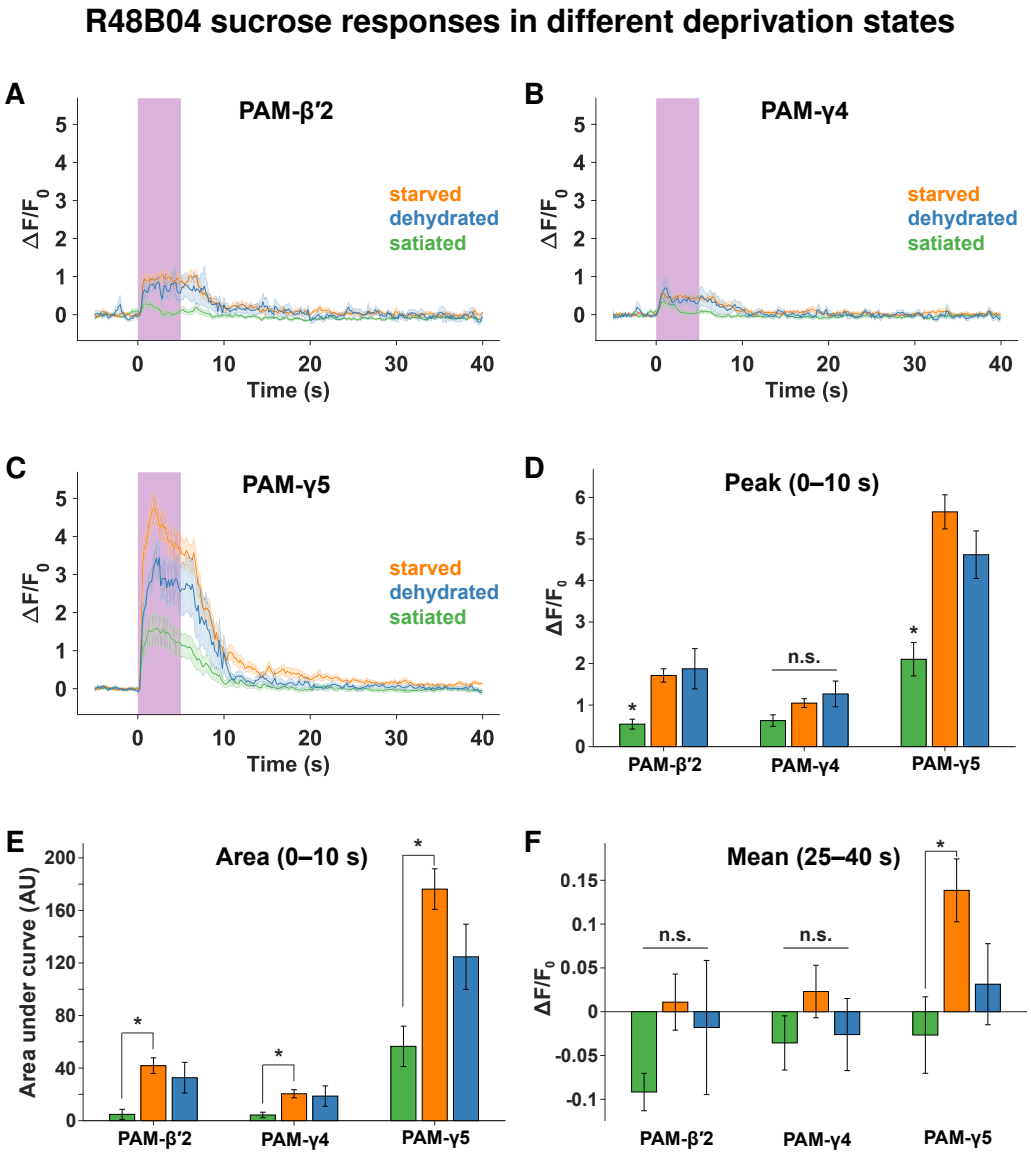

Figure 3.6: Satiated flies have diminished sucrose responses in R48B04 neurons. A–C) All PAM subsets in satiated flies respond to sucrose feeding, but with a diminished profile compared to either of the deprivation states. **D)** The peak response (first 10 s) to sucrose in satiated flies was substantially smaller than in either deprivation state for PAM-β′2 and PAM-γ5 ($p < 0.005$ for each subset; ANOVA). A similar but not statistically significant trend was also observed in PAM-γ4 ($p = 0.06$; ANOVA). **E)** The overall magnitude (area, first 10 s) of R48B04 responses to sucrose in satiated flies was substantially smaller compared to starved flies ($p < 0.05$ for each subset; ANOVA followed by *post hoc* Tukey's HSD test). A similar but not statistically significant trend was also observed for satiated flies compared to dehydrated flies ($0.10 > p > 0.05$ for each subset; ANOVA followed by *post hoc* Tukey's HSD test). **F)** The baseline post-response (last 15 s) in PAM-γ5 was lower for satiated flies than for starved flies ($p < 0.05$; ANOVA followed by *post hoc* Tukey's HSD test). No such difference was observed in PAM-γ5 between satiated and dehydrated flies ($p = 0.68$; *post hoc* Tukey's HSD test). No post-response differences between states was observed for PAM-β′2 ($p = 0.22$; ANOVA) or PAM-γ4 ($p = 0.39$; ANOVA). All data plotted are mean ± SEM. Deprivation states compared: starved (orange, $N = 28$), dehydrated (blue, $N = 12$), satiated (green, $N = 14$).

3-octanol (OCT), both of which have been used in *Drosophila* olfactory conditioning protocols for decades [50].

While feeding evoked the most prominent responses in PAM-γ5n neurons, odour presentation to starved flies yielded different results (Figure 3.7). Instead, PAM-β′2 neurons displayed the largest initial responses to both odours (Figures 3.7A and 3.7B); these were of similar magnitude to those in PAM-γ5n neurons evoked by feeding (Figures 3.4C and 3.5C). Odour presentation led to smaller but still prominent PAM-γ4 responses (Figures 3.7C and 3.7D), but the smallest by far were evoked in PAM-γ5n neurons (Figures 3.7E and 3.7F).

Odour response profile also varied with both odour and PAM subset identity. In PAM-β′2 and PAM-γ4 neurons, MCH also evoked a larger off-response than OCT, but both odours evoked a similar on-response (Figures 3.7A to 3.7D). In contrast, there were no observable response profile differences for PAM-γ5n neurons (Figures 3.7E and 3.7F). With repeated presentations, odour-evoked responses in PAM-β′2 and PAM-γ4 diminished most after the first presentation of each odour, and then diminished more slowly thereafter. For either subset, the response peak (first 5 s) was similar for both MCH and OCT in each presentation round (Figures 3.7G and 3.7H). In PAM-γ5n neurons, odours evoked a similar response that did not substantially diminish with repeated presentations (data not plotted).

With repeated presentations, PAM-β′2 and PAM-γ4 MCH responses in starved flies had a consistently higher peak than in satiated flies (Figures 3.8A and 3.8B), although the first odour evoked a similar peak in either state. This trend was also observed for OCT responses in both PAM subsets but to a lesser extent (Figures 3.8C and 3.8D). No such differences between starved and satiated flies were observed for PAM-γ5n odour responses (data not plotted). Therefore, starvation may elevate PAM-β′2 and PAM-γ4 excitability during repeated odour presentation.

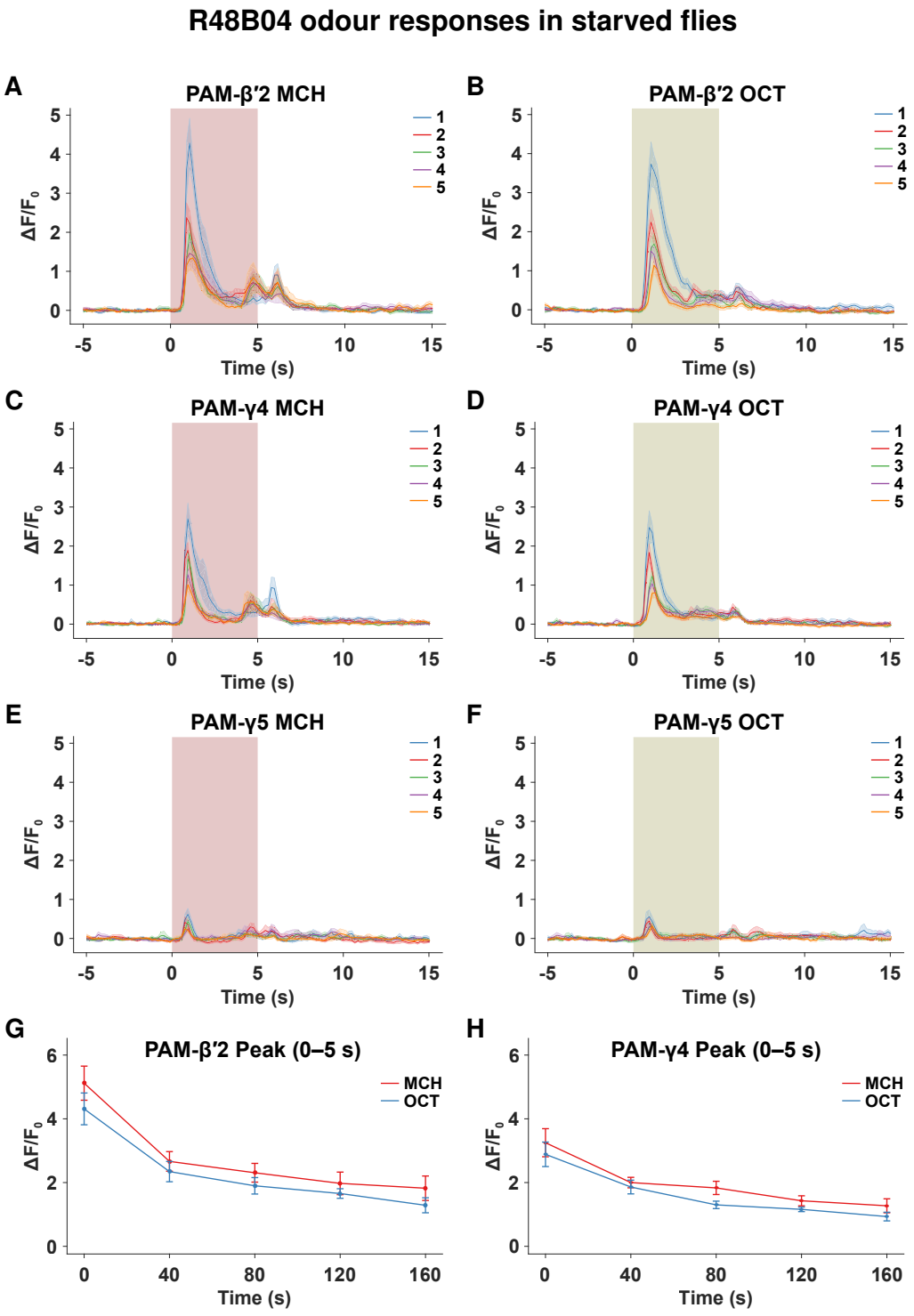

Figure 3.7: Odours evoke responses of different sizes in each R48B04 PAM subset. The odours MCH and OCT were alternately presented five times (increasing numbers in legend of each response plot) for 5 s every 20 s to starved flies. **A–B)** Both odours evoke the largest responses of all three subsets in PAM-β′2. Repeated presentations lead to decreasing but still prominent responses to each odour. MCH also evokes a larger off-response than OCT. **C–D)** The odours also evoke prominent responses in PAM-γ4, with similar decay after repeated presentations and the MCH off-response. **E–F)** The smallest responses are evoked in PAM-γ5, although a peak is still visible and the responses do not diminish with repeated presentations. **G–H)** Peak responses (first 5 s) to MCH and OCT diminish with repeated presentations in both PAM-β′2 and γ4. All data plotted are mean ± SEM, $N = 12$).

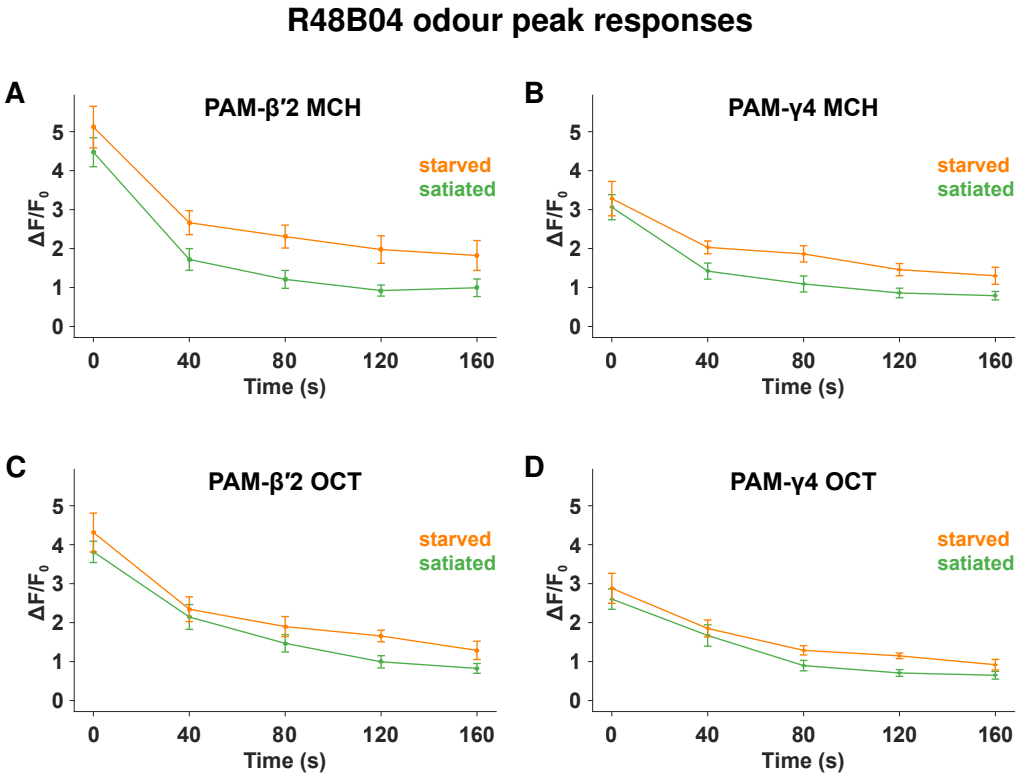

Figure 3.8: Odour-evoked responses decrease further in R48B04 PAM neurons of satiated flies. **A–B)** Repeated 5 s MCH presentations every 40 s evoke diminishing peak PAM-β′2 and PAM-γ4 responses, which decrease further in satiated flies (green) compared to responses in starved flies (orange). **C–D)** The same trend is observed for peak responses to repeated presentations of OCT (alternating with MCH every 20 s) in both PAM subsets but without a significant difference. All data plotted are mean ± SEM. Deprivation states: starved ($N = 12$), satiated ($N = 11$).

3.3 Discussion

3.3.1 Results summary

Different subsets of PAM neurons reinforce long-term sugar memory depending on whether flies are starved or dehydrated before training (Figure 3.2). There is a striking parallel between the droplet feeding behaviour of tethered flies (Figure 3.3) and the feeding-evoked calcium responses of R48B04 neurons (Figures 3.4 and 3.5): both differentiate between the content of droplets in starved flies but these differences collapse in dehydrated flies.

The most prominent R48B04 feeding-evoked responses are found in the PAM-γ5 subset, while those of the PAM-β′2 and PAM-γ4 are smaller and of similar magnitude to each other (Figure 3.4). In contrast, the most prominent R48B04

odour-evoked responses are found in the PAM-β′2 subset, followed closely by PAM-γ4, and much more distantly by PAM-γ5 (Figure 3.7).

Whereas a state of general deprivation substantially elevates sucrose feeding responses in all PAM subsets (Figure 3.6), it may possibly also elevate calcium responses evoked by repeated odours in the PAM-β′2 and PAM-γ4 subsets (Figure 3.8). Taken together, these results suggest that deprivation state modulates feeding behaviour, appetitive memory, and R48B04 PAM calcium responses.

3.3.2 State-dependent valuation

The results in this chapter and those previously published suggest that flies remember rewards based on their value during training, but their ultimate expression of such memory is gated by deprivation state. Reward value increases the more an individual fly gains from acquiring it during a certain deprivation state, but the fly must be motivated enough to express this memory so that it can satisfy its current deprivation state [25, 33].

Such a system ensures that flies form salient memories with the greatest value that later direct behaviour when flies experience particular deprivation states. It is therefore expected that starved flies form sucrose memory and dehydrated flies form water memory (Figure 3.1) [35, 36], but less expected that dehydrated flies, which presumably value all rewards containing water equally (Figures 3.3B and 3.5), can recall a sucrose memory when starved afterwards (Figure 3.2E).

One possible explanation for such recall is that flies form parallel memories of sucrose and water that each have different lifetimes. Parallel memories appear to be formed in flies that are conditioned with sucrose contaminated with the bitter insect repellent DEET [211] or with ethanol vapour [171, 231]. Immediate aversion later switches to approach in both cases, albeit reinforcing parallel appetitive and aversive memories rather than two parallel appetitive memories.

Parallel reward reinforcement fits nicely with a model whereby different PAM subsets reinforce specific reward components [36, 205]. In such a model, PAM-

γ4 neurons would presumably reinforce the short-term water memory component [205] (Figure 3.1C). However, R48B04-GAL4 labels neither of the PAM subsets thought to reinforce long-term sucrose memory, PAM-α1 [35, 232] or PAM-γ5b (broad) [36]. R48B04 PAM neurons instead appear to reinforce long-term sucrose memory in dehydrated flies (Figure 3.2E), whereas R15A04 PAM neurons, which include PAM-α1, do not (Figure 3.2D).

Since either R15A04 or R48B04 PAM neurons reinforce long-term sucrose memory depending on deprivation state (Figure 3.2), perhaps the PAM-γ5 neurons labelled by both drivers first gate reward in a state-dependent manner during training. Then, neurons labelled exclusively by R48B04 reinforce both short-term and long-term memories in dehydrated flies, while others labelled exclusively by R15A04 reinforce long-term memory in starved flies.

Therefore, it is possible that dehydrated flies may use R48B04 neurons during wet sucrose conditioning to reinforce a particularly potent water memory that can be recalled during starvation 24 h due to the value it was assigned during feeding. Whether the sugar-water memory can be recalled in dehydrated flies 24 h post-training is not known, but R48B04 neurons do not reinforce a long-term (24 h) water memory in dehydrated flies [227]. Instead, R48B04 neurons might reinforce a sugar memory parallel to that of water that can only be retrieved in starved flies, when MP1 neurons are inhibited (Section 3.1.2) [33].

Perhaps PAM-γ4 neurons indeed reinforce the water component, while a delayed post-ingestive nutrient signal from the sucrose component activates PAM-α1 or PAM-γ5b sometime after training to consolidate the water memory. Dopamine release by PAM-α1 one hour immediately after conditioning starved flies is required for appetitive long-term sugar memory consolidation [179], but unexpectedly, blocking PAM-α1 after conditioning dehydrated flies with wet sucrose does not impair long-term sucrose memory (G. Das, personal communication).

The delayed post-ingestive nutrient signal from the sucrose component could activate PAM-β′1 neurons or α′β′ Kenyon cells (KCs) [227]. These neurons respec-

tively reinforce and consolidate long-term water memory that is separable from the short-term memory reinforced by R48B04 neurons [227]. However, blocking either set after training dehydrated flies with sucrose has not been attempted.

Since R48B04 block during training also effectively hinders the consolidation of a long-term sugar memory in dehydrated flies, R48B04 block could exclude consolidation happening in neurons other than direct targets of these PAM subsets due to a post-ingestive signal. Blocking either downstream KC (again possibly $\alpha'\beta'$) or MBON targets of these PAMs could therefore reveal their hitherto unknown role in consolidating such a memory. Such activity should only occur in dehydrated flies if it is to explain why R48B04 block during training does not hinder long-term sugar memory consolidation in starved flies (Figure 3.2C).

The significantly smaller sucrose responses in the R48B04 neurons of satiated flies (Figure 3.6) suggest that these PAM subsets may calculate value or prediction error in a state-dependent manner. Since sucrose was consumed by flies in all states, the differing responses evidently do not reflect the surprise of unexpected food alone. The reduced responses may instead represent the bare minimum of dopamine released as a consequence of feeding, and the devalued sucrose reinforcement signal would not be enough to reinforce an appetitive memory. Moreover, visual inspection of dye consumption after imaging suggests that sucrose responses do not scale with the amount of droplet consumed by flies in general. Spectrophotometry of the dye content of flies after imaging could confirm whether the value signalled by R48B04 neurons is indeed not correlated at all with the size of reward.

The experiments in this chapter have investigated how deprivation state affects feeding or odour responses separately, but not cues that have already been paired with reward. However, two studies on dopamine neurons in the nucleus accumbens of the rat suggest that their cue-evoked activity also changes with physiological state [233, 234]. Both studies used an instrumental learning task for rats in which a particular reward was devalued through satiety [233] or free prior

access [234]). The instrumental cue now evoked dopamine release differently, even though it should still predict the reward as it was before its devaluation [233, 234].

Reward prediction error based on the temporal difference model suggests that with repeated cue-reward pairings, value shifts over time from the reward to the cue [87, 89]. Such a model predicts that a reward devalued separately after many pairings should not affect that of the cue as it does in these studies [233, 234]. My results show that deprivation state affects the value of the reward itself, and from the two studies in rats, it could be the case for *Drosophila* that deprivation state devalues any associated cues as well. However, we still do not yet know if temporal difference reinforcement learning accurately models rewarding dopamine neurons in *Drosophila*; this is addressed in Chapter 5.

3.3.3 Comparing and manipulating deprivation state

Since there is more than one way to reach an equivalent deprivation state, it can be difficult to compare experiments conducted by different experimenters. We starved flies for 24 h by storing them with only 1% agar post-training, whereas Yamagata et al. (2015) [35], for example, re-fed flies for 1 h immediately after training (to reduce mortality) and then starved them for 23 h before testing. Such protocol differences could potentially confound comparisons of long-term memory for different sugars. However, our starvation method is consistent with that used by Huetteroth et al. (2015) [36], who reached similar conclusions as Yamagata et al. about the roles of R48B04 and R15A04 PAM neurons in starved flies.

We (and Lin et al. (2014) [205]) dehydrated flies quickly for 6 h by storing them together with a desiccant. In contrast, Shyu et al. (2017) [227], for example, dehydrated flies more slowly for 16 h by leaving them with only dry sugar paper before training. Nonetheless, both Lin et al. and Shyu et al. found that R48B04 training block in dehydrated flies impaired short-term water memory [205, 227]. Although the two approaches are not identical, they may be sufficiently equivalent.

Manipulating the diet of animals to induce deprivation is relatively straightforward, but it is not so trivial to compare results obtained in different deprivation states. Flies that are starved, though they have access to water in agar, may be more dehydrated than flies that are satiated because starvation could hinder their water consumption. Similarly, dehydrated flies may be more nutrient deprived than satiated flies as they find it increasingly difficult to consume the dry sugar that is available.

A change in one deprivation state could therefore cause another, resulting in a composite deprivation state that provides an alternative explanation for R48B04 short-term reinforcement of both sugar and water reward. Instead of being gated in a state-specific manner by upstream neurons, R48B04 neurons could become more excitable by inputs that signal a general state of dietary deprivation. During feeding, R48B04 responses could then be elevated by a state-relevant predictive property of the droplet consumed (e.g., sweet taste for hunger or liquid for thirst).

This explanation is consistent with the significantly lower sucrose responses evoked in the R48B04 neurons of satiated flies compared with starved or dehydrated flies (Figure 3.6). Moreover, feeding sucrose to some satiated flies evoked no clear R48B04 calcium responses, even though I verified droplet consumption and observed normal odour responses in the same flies. It might then logically follow that the length of deprivation could be correlated with feeding response magnitude to the same droplet, but I found no such correlation when comparing these two variables in starved or dehydrated flies (analysis not shown).

Even though I ensured that flies had access to food for a similar length of time before deprivation started, it is possible that some flies were already more deprived than others when deprivation began from my perspective. Such variation could be controlled by deliberately feeding individual flies to either food or water satiety and then depriving them for a specific time period before imaging. However, complete control over deprivation state would still not be possible because the subsequent rate of deprivation might vary among individuals.

The deprivation of a key metabolite presumably causes the regulatory neurons concerned to release a deprivation signal that is broadcast throughout the brain. The variation between flies fed the same droplet in the same deprivation state could therefore reflect variation in the extent that upstream inputs to PAM neurons had received such a signal instead of the extent of deprivation itself.

The difficulty in controlling deprivation is specifically why the groups compared here have been termed starved and dehydrated rather than hungry and thirsty; the former terms more accurately reflect the differences between groups than our expectations of motivational state. Since treatment within each deprivation group is consistent, perhaps within-group comparisons between droplets are more informative than comparisons between states for the same droplet.

Another way to address this problem would be to test the specificity of deprivation state for particular memories. Lin et al. (2014) [205] trained dehydrated flies with water or starved flies with sugar and then tested their retrieval of the corresponding associative memories in different deprivation states. For short-term water memory, Lin et al. found that dehydrated flies performed better than starved flies, whereas for long-term sugar memory, Lin et al. found that starved flies performed better than dehydrated flies. An illuminating follow-up study would be to train the same flies with water and sugar before testing whether water or sugar memory retrieval is specific to a particular deprivation state.

3.3.4 Comparing different droplets

The results in this chapter depend upon controlled comparisons between different droplets. The water consumed in any droplet will activate proboscis gustatory neurons expressing the osmosensitive ion channel Pickpocket 28 (PPK28) [235, 236]. Since PPK28 is required for water learning [205], it is possible that neurons connecting these gustatory neurons and R48B04 PAM neurons together comprise a water reinforcement circuit that is more active when flies are dehydrated.

While the possible pathway remains unknown, four interoceptive neurons (sensors of internal state) located in the suboeosphageal zone (SEZ) called ISNs (interoceptive SEZ neurons) have been shown to regulate sugar and water consumption oppositely [230]. When flies are starved, decreased extracellular osmolality and increased levels of the glucagon-like peptide adipokinetic hormone (AKH) both activate ISNs, promoting sugar consumption. In contrast, dehydrated flies have increased extracellular osmolality, which inactivates ISNs and consequently promotes an inverse effect of water consumption instead.

If there are neurons that ultimately connect the SEZ-confined ISNs to R48B04 neurons in the PAM cluster, then such connectivity could explain why both flies in the tethered feeding assay (Figure 3.3B) and R48B04 PAM neurons during imaging (Figures 3.4 and 3.5) differentially respond in favour of sweet droplets during starvation but similarly to all droplets during dehydration. Although ISN neurons have not been implicated in learning, PPK28 signals also limit AKH release [237], suggesting a possible functional link between these two sets of neurons.

Another possibility is that the principle of opposing signals from starvation and dehydration may apply more globally throughout the fly brain and could also gate the activity of neurons that provide direct input to R48B04 PAM neurons. Since octopamine is not required for water learning [205], identifying non-octopaminergic upstream neurons that are required for water and possibly also sugar learning might be a necessary first step. Nonetheless, the presence of water in all droplets and their corresponding feeding responses in all three R48B04 PAM subsets suggests that the dopamine released by these neurons may at least partly signal either the salience or motor action of feeding.

Although all feeding experiments in this chapter compared sugar-water droplets, it would also be informative to compare responses evoked by feeding on dry sugars. With minor modifications to the feeding stage in my setup, it would be possible to determine whether PAM sugar responses in starved flies decrease by the magnitude of the water responses observed in this chapter. Any

specific differences between the droplet and dry forms of sugar for a particular PAM subset could indicate a water-specific reinforcement signal.

3.3.5 Odour responses in different states

Odour-evoked responses have been characterized for some dopaminergic neurons [61, 127, 162, 178], but not for any of the PAM neurons labelled by R48B04. That odours evoke responses in PAM neurons (Figure 3.7) implies that odour signals must somehow reach these neurons.

The most likely candidates that convey the odour signals to R48B04 neurons are the Kenyon cells that they innervate, since there is evidence that dopaminergic neurons are both pre-synaptic and post-synaptic to Kenyon cells through reciprocal axo-axonic synapses [178]. However, lateral horn output neurons cannot be ruled out, with some emerging evidence suggesting that they may also connect to PAMs, or at least to PAM-$\beta'1$ and subsets of PAM-$\beta'2$ [163]. Optogenetically stimulating either Kenyon cells or lateral horn output neurons while recording from PAM neurons would provide illuminating insights into the extent of their contribution to PAM odour-evoked responses.

The differing sizes of odour responses in each R48B04 PAM subset could reflect either the respective numbers of active upstream connections (such as odour-activated Kenyon cells) directly conveying odour information to each subset or additional inputs that differentially excite or inhibit each subset to modulate odour-evoked responses. Starvation elevates MVP2 odour-evoked responses [59] and differentially modulates yeast odour-evoked responses in some PPL1 dopaminergic subsets [162]. However, no starvation-induced changes have been observed for odour responses in PAM-$\beta2$ or PAM-$\beta'2a$ (anterior) neurons [162].

Similarly, I observed no changes induced by starvation to the size of the initial odour response evoked in PAM-$\beta'2$ and PAM-$\gamma4$ (Figure 3.8). However, with subsequent odour presentations, I noticed a consistent trend whereby subsequent odour responses diminished more in satiated flies. These differences were probably

more pronounced for MCH than OCT since it was the first odour presented and thus evoked the larger initial response. Although the reason for the trend remains unclear, it could suggest that odours are perhaps more salient to starved flies that repeatedly encounter them while foraging for food.

3.3.6 Controlling for movement signals and artefacts

To compare feeding responses to different droplets or between deprivation states, controlling movement artefacts and movement-induced activity in the neurons of interest is critical. If the desired imaging plane moves substantially during feeding, then important information about the feeding response will be irretrievably lost. If movement-induced activity evokes signals similar to the feeding response, then identifying and differentiating the latter becomes much more difficult.

The first approach is to restrict the moving part by tethering with wax, glue, string, or hair. The proboscis is usually restrained during odour or shock presentation protocols but should be free to move when investigating feeding. I found the best compromise was to apply wax or glue to the eyes to restrict head movement but even this approach had limited effectiveness alone.

The second strategy is to remove a muscle that causes the movement of concern, typically muscle 16 of the frontal pulsatile organ for feeding preparations [176, 206]. Although removing muscle 16 reduces the pulsing movement of the brain, I considered the intervention to be unnecessarily invasive, especially since the key problematic movement is caused by the lunging proboscis during feeding.

The third approach is to coexpress a reference fluorescent protein (e.g., the bright red fluorescent protein tdTomato [204, 238, 239] to complement GCaMP) in either the same or neighbouring neurons. Multi-stack registration can be used to stabilize the reference channel and apply the generated transformations to the functional imaging channel [176], or the functional imaging channel fluorescence can be divided by that of the reference channel to help cancel out sample plane movements [240].

I found the ratio of the channel fluorescence identified prominent movement events more effectively but neither approach could adequately retrieve the information lost if the desired imaging plane moved substantially during feeding. Nonetheless, although coexpression is not used in this chapter, it is used extensively in subsequent chapters. I first used it primarily because it helped me locate neurons of interest with a low baseline GCaMP fluorescence, but it also reliably tracked sample drift with time as my recording lengths eventually expanded from 90 s to over 20 min per recording (Figure 5.6).

The final approach is to add a substance such as agarose to the dissection saline and thus form a porous matrix that immobilizes the brain [34, 210]. I discovered that using agarose was the most effective approach by far since even the most drastic feeding movements now led to only minor changes (if any) in sample plane position. There was no substantial decrease in fluorescence signal recorded while using agarose and it decreased my sample failure rate substantially.

Limiting movement-induced activity is less trivial because it is intrinsic to the activity of some R48B04 dopaminergic neurons. Motor patterns causing the legs (tarsi) to flail or stop flailing cause basal activity to fluctuate in γ-lobe PAM neurons [176], but in my experience tarsal movement led to unpredictable calcium signal peaks in all three R48B04 PAM subsets, including PAM-β'2. Movement-induced activity was substantially reduced when I tethered the tarsi before imaging, although proboscis extension itself could occasionally evoke prominent simultaneous responses in PAM-β'2 and PAM-γ4 neurons. I also sometimes observed a spontaneous peak in PAM-γ5 just before several consecutive proboscis extensions.

Nonetheless, after taking the above precautions, I could confidently identify feeding responses and distinguish them from other spontaneous or movement-induced signals. However, it would also be interesting to tether the proboscis instead and leave the tarsi unwaxed to determine how R48B04 neurons respond when tarsi come into contact with sugar-water droplets.

3.3.7 Interpreting feeding bouts

Within the first 5 s of feeding, tethered flies discriminate between different sugar-droplet types in a state-dependent manner (Figure 3.3B). Starved flies appear to favour sweet droplets that may be predictive of nutrient content, whereas dehydrated flies do not discriminate between different classes of droplets because they all contain water. Therefore, flies not only rapidly detect predictive properties of the droplet that they consume, but their specific deficit influences whether they continue feeding.

Although Qi et al. (2015) [80], from whom I adapted the assay, claim that flies can detect the nutritional value of D-glucose and D-fructose within 20 s to 30 s compared to their L-enantiomers, I did not observe such differences between those specific sugars or broader sugar-water categories in my tethered feeding assay. Rather, I found that flies fed on non-sweet but nutritious sugars for as long than they did on similar non-nutritious sugars (Figure 3.3B). My observations suggest that flies do not decide to continue feeding on a droplet within the first 5 s solely based on its caloric content.

The different findings could arise from important differences in our protocols. Qi et al. aspirated individual flies into a pipette tip and then satiated them with water before starting their assay. In contrast, I tethered individual flies by their wings to a microscope slide with nail varnish and included water as one of the droplets to be tested. Since the fly tarsi were not constricted in my assay, I had to avoid contact with the tarsi prior to presenting the droplet to the proboscis. Tethering flies with UV-cured glue could eliminate any possible aversive effects from the nail varnish odour, even though all flies were tethered similarly.

Qi et al. delivered 100 mM sugar-water droplets using a graduated capillary tube that allowed them to measure the total volume consumed afterwards. They found that although flies fed for roughly 30 s on either D-glucose and L-glucose, they consumed a greater volume of the former [80]. I used a pipette tip to deliver 1 M sugar-water droplets and could not record volume.

Nevertheless, the results of both investigations suggest it is unlikely that flies consume a greater volume of particular droplets within the first 5 s of feeding because they are nutritious. Therefore, 5 s forms a suitable basis of comparison between droplet types for my two-photon calcium imaging experiments in both this chapter and the next, which focuses on the potential immediate reinforcement of nutrient value.

3.4 Conclusion

Taken together, the findings in this chapter suggest that R48B04 PAM neurons show a deprivation state-dependent valuation of reward that is not explained by current models of reward prediction error. The neurons respond substantially more to the same unexpected sucrose reward when flies are deprived of food or water compared to when flies are satiated. Moreover, in starved flies, the neurons respond primarily to the sweet taste of sugar, whereas in dehydrated flies, the same dopaminergic neurons respond primarily to the presence of water.

Deprivation state also appears to modulate the feeding behaviour of tethered flies on different types of sugars, and the subsets of PAM neurons that can reinforce a long-term sucrose-water memory. Although the underlying causes of these observations are not known, they highlight the important role of deprivation state in both associative learning and rapid sugar discrimination.

R48B04 PAM neurons also substantially respond to the presentation of odours, an observation not yet accounted for in existing models of associative learning in *Drosophila*. Although the first odour presentation evokes similarly prominent responses in both starved and satiated flies, subsequent presentations appear to activate PAM responses in starved flies more. Together, these results suggest that the first odour response may convey novelty and that deprivation state may also increase the excitability of PAM neurons to odours.

Since R48B04 PAM neurons respond differentially to nutritious sucrose and non-nutritious arabinose in starved flies, the next chapter explores whether this difference arises from a rapid nutrient reinforcement signal. Other dopaminergic neurons implicated in sugar reinforcement are also investigated concerning their responses to both sugars and odours.

Chapter 4

Nutrient reinforcement

4.1 Background

4.1.1 Nutrient information is rapidly processed

Rewarding nutritious stimuli are thought to be more complicated than other stimuli that animals encounter because they can serve as conditioned reinforcers of themselves [241]. The initial taste can predict post-ingestive consequences, reinforcing associative food-related memories and causing otherwise neutral tastes to become rewarding [242]. The delayed nature of this reinforcement distinguishes nutrient learning from most other forms of associative learning, where close temporal contiguity between stimuli is usually the most reliable predictor [241].

The temporal dichotomy between sweet taste and nutrient value is challenged by observations that *Drosophila* can process nutrient content rapidly. Fruit flies can metabolize the energy content of nutritious sugars for flight within 2 min [27] and develop a preference for odours paired with such sugars in a similar period of time (Figure 4.1) [29]. These observations suggest that nutrient reinforcement may be almost as rapid as sweet taste reinforcement or only slightly delayed afterwards.

A key question concerns how quickly the fly nervous system accesses the nutrient content in food. The firefly enzyme luciferase emits photons when it binds its cofactor D-luciferin [243]. Luciferin can be consumed by *Drosophila* and is

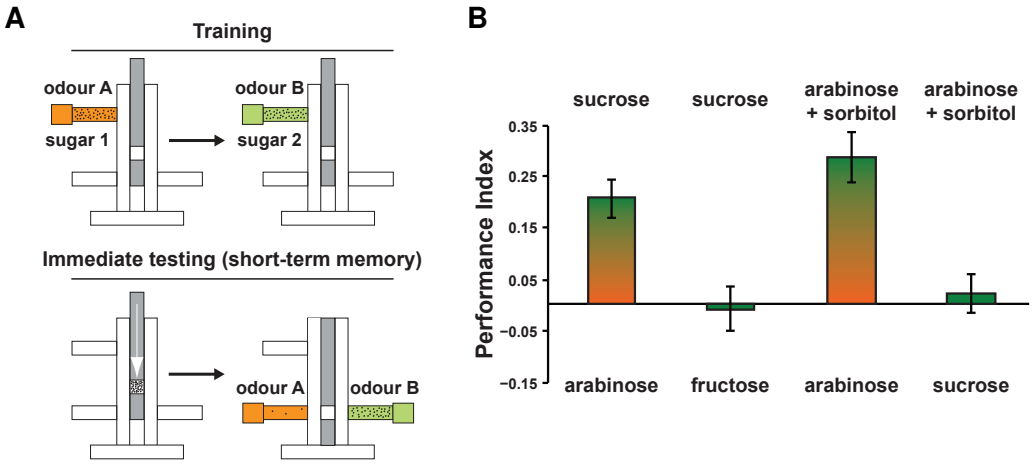

Figure 4.1: Nutrient information guides sugar memory preference immediately after training. **A)** The T-maze protocol was modified by Burke and Waddell (2011) [29] so that flies would experience one odour paired with one sugar for 2 min, a break for 30 s and then the other odour paired with another sugar for 2 min. The flies were then immediately tested for olfactory preference for 2 min. The sugars used were arabinose (non-nutritious but sweet); fructose, sucrose (both nutritious and sweet), or arabinose supplemented with sorbitol (also nutritious and sweet). T-maze diagram adapted from Vosshall (2007) [70]. **B)** Flies always prefer the odour previously paired with a nutritious substance, preferring sucrose or arabinose + sorbitol over arabinose alone. They show no preference when both odours are paired with nutritious substances. When two sugar types were compared, the nutritious substance was always presented second during training. The bar colour gradients indicate the sweet only (orange) option or that which is also nutritious (green). All data plotted are mean $\pm$ SEM, $N \geq 10$. Adapted from Burke and Waddell (2011) [29].

eventually absorbed by their nervous system [244]. When flies with neuronally-expressed luciferase consumed food mixed with luciferin, photons were detected on the timescale of just 10 s to 20 s [245], implying that sugars can reach the fly nervous system very rapidly.

Indeed, fructose-sensitive neurons have been identified in the superior posterior lateral protocerebrum [77] and glucose-sensitive neurons in the ellipsoid body [78], but whether these neurons can detect such nutritious sugars tens of seconds after their consumption remains unknown.

4.1.2 Fast and slow sugar reinforcement

For nutrient information to guide sugar memory preference rapidly, this sugar component must presumably be reinforced quickly. Rewarding dopaminergic neurons in the protocerebral anterior medial (PAM) cluster receive input from octopaminergic neurons that reinforce only short-term appetitive memory [17]. Oc-

topamine is synthesized from the amino acid tyrosine through a two-step process catalysed by the enzymes tyrosine decarboxylase (TDC) [246] and tyramine-β-hydroxylase (TBH) [200]. Investigations into octopamine signalling [15, 17, 36, 211] have provided different insights into immediate appetitive memory.

When GAL4 is driven by a promoter fragment of the *Tdc2* gene that encodes neuronal TDC [246], it is expressed in all octopaminergic neurons that innervate the mushroom body [17]. When Tdc2-GAL4 neurons are thermogenetically blocked at a restrictive temperature using the dynamin mutant *shibire*^{ts1} (UAS-*shi*^{ts1}) [203], flies cannot form immediate memories of the sweet but not nutritious sugar D-arabinose [17]. However, flies can form an immediate appetitive memory if arabinose is supplemented with the nutritious but not sweet sorbitol [17].

These results imply that Tdc2-GAL4 octopaminergic neurons reinforce only sweet taste and that nutrient value can reinforce immediate appetitive memory separately. Indeed, dopaminergic PAM neurons are required for immediate appetitive memory of both non-nutritious arabinose and nutritious sucrose [17]. Hence, a model has emerged in which some subsets of PAM neurons lie functionally downstream of Tdc2-GAL4 octopaminergic neurons and reinforce sweet taste, while others reinforce nutrient value separately [35, 36, 179, 247].

Experimental manipulations of TBH, the final enzyme in the octopamine biosynthesis pathway, introduce some subtlety overlooked by this model. Flies with a null mutation in both copies of the TβH gene that encodes TBH completely lack octopamine but survive to adulthood [200]. TβH mutant flies (TβH^{M18}) cannot form an immediate memory of nutritious sucrose around 3 min after training [15, 17, 36, 211] but eventually form a longer-term sucrose memory at least 30 min after training [36, 211].

Therefore, immediate nutrient reinforcement does not require the output of Tdc2-GAL4 octopaminergic neurons yet still requires octopaminergic signalling. However, flies with Tdc2-GAL4 output blocked during training or TβH mutant flies both eventually form a longer-term nutrient memory after sucrose training [17,

36, 211], suggesting that immediate and delayed nutrient reinforcement could be two separate processes. Alternatively, signalling from octopaminergic neurons not labelled by Tdc2-GAL4 could be required for immediate nutrient reinforcement.

Thermogenetically blocking the output of a set of PAM dopaminergic neurons labelled by the 0104-GAL4 line from the InSITE collection [197] with *shibire*^{ts1} impairs immediate memory of both arabinose and sucrose [17]. These observations implicate 0104-GAL4 PAM neurons in the immediate reinforcement of both sweet taste and nutrient value. Neurons can also be artificially stimulated using the temperature-sensitive transient receptor potential (TRP) channel dTrpA1, which can depolarize neurons at a temperature above 25 °C [248]. Thermogenetically stimulating 0104-GAL4 neurons that express dTrpA1 contingent with odour presentation induces immediate appetitive memory in both wild-type flies and TβH mutants [17].

These results suggest that 0104-GAL4 PAM neurons can reinforce immediate memory even in the absence of octopamine and are therefore functionally downstream of octopaminergic neurons [17]. Continuously blocking the output of all PAM dopaminergic neurons (not just those labelled by 0104-GAL4) after one-minute sucrose training does not impair appetitive memory 30 min post-training [34]. Therefore, any role that PAM neurons play in immediate or delayed sugar reinforcement presumably occurs within 60 s of feeding.

The functional connections between octopaminergic and dopaminergic neurons have also been verified anatomically in the anterior medial protocerebrum and the tip of the mushroom body β' and γ lobes [17]. However, identifying exactly which PAM neurons specifically reinforce nutrient value remains unclear, with inconsistent conclusions emerging from different studies [35, 36, 179]. The neuronal subsets that are possible candidates for immediate and long-term nutrient reinforcement are compared next.

4.1.3 Possible nutrient reinforcer candidates

In *Drosophila*, sweet taste and nutrient value reinforcement are thought to be separable components of sugar reward that can be reinforced by distinct subsets of dopaminergic neurons [36, 247]. In particular, the PAM-β′2 and PAM-γ4 subsets are thought to reinforce sweet taste in the short-term (2 min to 5 min after training) [36] whereas PAM-α1 [35, 179] or PAM-γ5b [36] are thought to reinforce nutrient value specifically in the long-term (up to 24 h after training).

Two other sets of findings contribute further to the lack of clarity regarding the specificity of long-term nutrient reinforcement. First, our findings in Section 3.2.1 suggest that R48B04 neurons, which label PAM-β′2, PAM-γ4, PAM-γ5n (narrow) neurons (Figure 3.1A), can also reinforce long-term sucrose memory, but only when flies are dehydrated during training. Second, consolidation of appetitive long-term memory also appears to depend on the activity of MP1 neurons (introduced in Section 3.1.2) up to 5 h post-training [81].

R15A04-GAL4 labels the PAM-α1, PAM-β2, PAM-β′1, and PAM-γ5 (both narrow and broad) subsets (Figure 3.2A) [35, 36, 53, 205]. Two independent studies [35, 36] found that if R15A04 output was blocked in starved flies during sucrose training, such an intervention would impair long-term but not short-term appetitive memory (also see Figure 3.2B). However, each study reached different conclusions as to which PAM subset was specifically responsible for the long-term defect.

PAM-α1

The split-GAL4 approach uses one enhancer to drive expression of the DNA-binding domain of GAL4 and another enhancer for its activation domain. Each enhancer drives expression in different cells, but the active GAL4 is reconstituted only in cells common to both enhancers, leading to more restricted and hence specific labelling [249]. One study [35] screened a library of split-GAL4 drivers [170] for PAM neurons. Candidate driver lines were thermogenetically activated in

starved flies with dTrpA1 [248] during training and then tested for long-term appetitive memory [35].

The study authors concluded that PAM-α1 was most likely to be the specific subset required for appetitive long-term memory [35]. However, the split-GAL4 line they used to manipulate PAM-α1 (MB299B-GAL4) also substantially labels PAM-β2 [35]. Blocking MB299B-GAL4 output during training impairs long-term but not short-term sucrose memory [35, 179]. Therefore, PAM-α1 or PAM-β2 may reinforce a nutritious memory that gradually develops after training, but not immediate sweet or nutritious memory.

PAM-γ5b

The other study [36] used a negative intersectional approach (Section 3.1.3) in which GAL80 blocked GAL4 labelling of particular PAM subsets. The authors used thermogenetic blocking with *shibire*^{ts1} to manipulate various GAL4/GAL80 combinations before testing them for long-term sucrose memory. The intersection between 0104-GAL4 and R48B04-GAL80 labelled the most specific set of neurons whose blocking impaired long-term memory: the PAM-β′2m (middle) and PAM-γ5b (broad) subsets [36].

Since blocking another GAL4 driver labelling only PAM-β′2m and PAM-γ5n (narrow) did not lead to such impairment, the authors concluded that long-term nutrient reinforcement requires PAM-γ5b [36]. However, blocking neurons labelled by 0104-GAL4 R48B04-GAL80 during arabinose training also impaired memory 3 min later [36], suggesting that either PAM-β′2m or PAM-γ5n could also reinforce sugars immediately. Therefore, PAM-γ5b may be required for short-term and long-term nutrient reinforcement, while PAM-β′2m may provide only short-term reinforcement.

PAM-γ4

During training in starved flies, R48B04 neurons reinforce immediate sucrose memory (Figure 3.1B) [35, 36] but not long-term memory (Figure 3.2C) [35, 36]. These results have been taken to suggest that R48B04 neurons therefore reinforce only the sweet component of sugars [35, 36]. It should therefore be possible to bypass their reinforcement immediately by supplementing arabinose with sorbitol as was demonstrated previously for Tdc2-GAL4 neurons [17].

Intriguingly, blocking R48B04 output impairs the immediate memory of all sugars tested, not just the sweet but non-nutritious arabinose [35, 36]. If any R48B04 PAM subset actually reinforces immediate nutrient memory in starved flies, it would most probably be PAM-γ4 because it can reinforce immediate water memory in dehydrated flies [205]. While perhaps still unlikely, R48B04 neurons therefore cannot be ruled out entirely and their upstream inputs should at least be investigated further.

MP1 (PPL1-γ1pedc)

MP1 neurons do not reinforce appetitive memory during training, but they are involved in its long-term consolidation [81] and expression (Section 3.1.2) [33]. When flies are satiated, the spontaneous calcium oscillations of MP1 neurons are larger in amplitude [129]. MP1 oscillation amplitude alone could be a signal that reflects deprivation state, but MP1 oscillation frequency can also be altered by particular sugars [81].

Flies conditioned with a sweet but non-nutritious sugar typically form a short-term but not a long-term appetitive memory [29] (although two sweet-only sugars appear to be exceptions [32]). One study [81] showed that flies could form a long-term memory of sweet but non-nutritious L-glucose only if it was followed by a nutritious meal (e.g., D-glucose) up to 5 h post-training. The study authors also found that MP1 output was required during the 5 h time period [81]. Moreover, they observed that MP1 oscillation frequency and regularity (a measure

for how long oscillations are sustained) both increased 30 min after training with D-glucose compared to L-glucose [81]. MP1 oscillation frequency also increased 30 min after flies were fed D-glucose (compared to L-glucose) 3 h after L-glucose conditioning [81].

Although the authors took these results to suggest that MP1 oscillatory activity is therefore enhanced during appetitive LTM formation [81], they could also reflect a temporary change in MP1 activity to a particular sugar post-feeding. Furthermore, since the authors previously reported that MP1 oscillatory frequency and regularity also increase 30 min after aversive spaced training [210], what these oscillations actually encode remains unclear.

DPM

Dorsal paired medial (DPM) neurons are a pair of GABAergic (and possibly serotonergic) neurons that innervate all lobes of the mushroom body, to which they are both afferent and efferent [52, 250, 251]. DPM neurons are required for both long-term appetitive and aversive memory [25, 52, 198, 250–254]. Blocking DPM output during sucrose training does not impair 3 h appetitive memory but blocking it for 30 min immediately after training does [252]. DPM neurons are therefore involved in consolidation but not the acquisition of such memory.

One study reported that appetitive conditioning with sucrose or arabinose supplemented with sorbitol caused the DPM calcium response evoked by the conditioned odour to last twice as long compared to conditioning with arabinose alone [254]. Although the study also claimed that DPM neurons did not respond to sucrose alone [254], a more recent investigation has revealed that DPM neurons do indeed respond to feeding, but with similar response profiles to both nutritious D-glucose and non-nutritious L-glucose [79].

Summary

For all of the possible nutrient reinforcement candidates just discussed, Table 4.1 summarizes whether short-term or long-term memory is impaired by blocking each subset during or after training with non-nutritious or nutritious sugars. Figure 4.2 summarizes a possible model for immediate and delayed sugar reinforcement. Since all of the aforementioned dopaminergic subsets are somehow involved in the reinforcement of short-term or long-term appetitive olfactory memories, this chapter characterizes all of their immediate calcium responses evoked by feeding or odour presentation.

Table 4.1: Summary of when each nutrient reinforcement candidate is required during the reinforcement of short-term and long-term appetitive memory. Each entry specifies whether blocking the neuronal subset (in the leftmost column) during training or after training (consolidation) impairs the memory tested when the sugar reinforcer is sweet only (Sweet) or both sweet and nutritious (Nutritious). Y (yes), N (no), blank (unknown/not attempted); references provided where applicable. If yes, then the neuronal subset is required during the stage of learning for that particular type of reinforcer. Although not dopaminergic, DPM and Tdc2 neurons are also included for comparison.

Timing of block	**Training**	**Training**	**Training**	**Consolidation**
Memory tested	**2–5 min**	**2–5 min**	**3–24 h**	**24 h**
Subset / Sugar	**Sweet**	**Nutritious**	**Nutritious**	**Nutritious**
0104	Y [17]	Y [17]	Y [17]	–
DPM	–	–	N [252]	Y [252]
MP1	–	–	N [33, 81]	Y [81]
PAM-α1	N [35]	N [35, 179]	Y [35, 36, 179]	Y [179]
PAM-β2	N [35]	N [35, 179]	Y [35, 36, 179]	Y [179]
PAM-β′1	Y [35, 36]	Y [35, 36]	N [35, 36]	–
PAM-β′2(m)	Y [35, 36]	Y [35, 36]	N [35, 36]	–
PAM-γ4	Y [35, 36]	Y [35, 36]	N [35, 36]	–
PAM-γ5b	Y [35, 36]	Y [35, 36]	Y [35, 36]	–
PAM-γ5n	Y [35, 36]	Y [35, 36]	N [35, 36]	–
R15A04	N [35, 36]	N [35, 36]	Y [35, 36]	–
R48B04	Y [35, 36]	Y [35, 36]	N [35, 36]	–
Tdc2	Y [17]	N [17]	N [17]	–

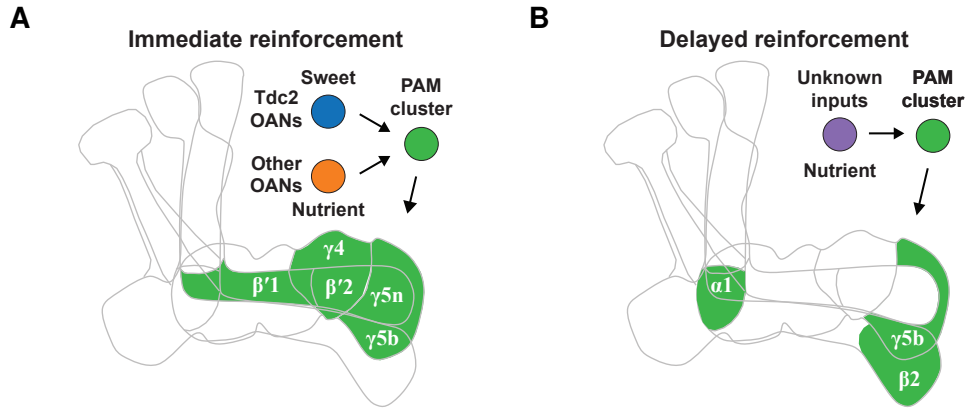

Figure 4.2: A possible model for immediate and delayed sugar reinforcement. A) Sweet taste is immediately conveyed to dopaminergic neurons (DANs) in the PAM cluster (green) via octopaminergic neurons (OANs) that are labelled by Tdc2-GAL4 (blue). Unidentified OANs (orange) not labelled by Tdc2-GAL4 may also immediately convey nutrient value to the PAM cluster. DANs projecting to the β′1, β′2, γ4, and γ5 zones of the mushroom body are implicated in both cases. **B)** Unknown upstream inputs (violet) convey nutrient information to DANs in the PAM cluster (green) projecting to the α1, β2, and γ5b (broad) zones in the mushroom body.

4.2 Results

4.2.1 R48B04 feeding responses may reflect palatability

Having observed that the sugars tested in Chapter 3 (D-arabinose and sucrose) evoked differential PAM-γ5 feeding responses in starved flies (Figure 3.4), I reasoned that perhaps this gap could be bridged by supplementing arabinose with nutritious sugars [17, 29–31, 35, 254].

First, I repeated the experiment in Figure 3.4, only this time for three different compound sugars. Since there is some evidence that haemolymph osmolarity could influence satiety [230, 255], I ensured that all droplets compared were equal in their osmolarity. Each droplet tested contained the sweet but non-nutritious D-arabinose: one was supplemented with D-ribose (neither sweet nor nutritious) [31], another with D-sorbitol (nutritious but not sweet) [29–31], and the last with D-mannose (more nutritious than sorbitol but not sweet) [28, 31]. All three droplets evoked similar responses in the R48B04 PAM subsets (Figure 4.3), suggesting that nutrient supplements do not increase feeding responses in these neurons.

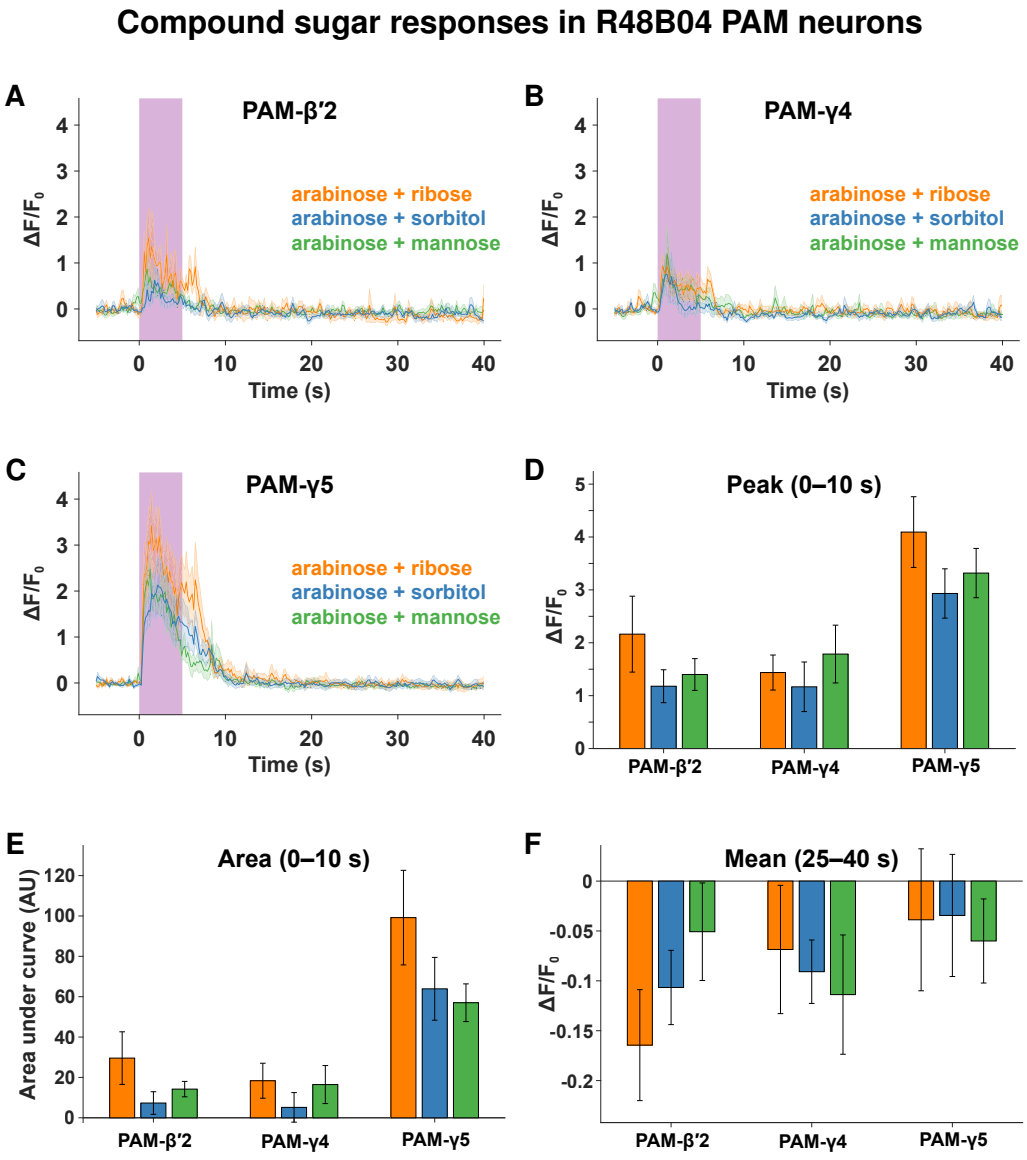

Figure 4.3: Supplementing arabinose with nutritious sugars does not increase R48B04 feeding responses. Starved flies were fed one of three droplet combinations: D-arabinose plus ribose (neither sweet nor nutritious), sorbitol (nutritious but not sweet), or mannose (more nutritious than sorbitol but not sweet). **A–C)** All PAM subsets have similar feeding response profiles to any of the three droplet combinations. No differences between the droplets were observed for any PAM subset with respect to **D)** the peak feeding response (first 10 s, $p > 0.32$ for each subset; ANOVA), **E)** the overall magnitude (area, first 10 s) of the response ($p > 0.18$ for each subset; ANOVA), or **F)** the baseline post-response (last 15 s, $p > 0.26$ for each subset; ANOVA). All data plotted are mean ± SEM. All compound sugars presented at 1 M concentration ($N = 8$ each).

Supplementing arabinose with sorbitol during appetitive training leads to long-term sugar memory whereas arabinose alone does not [29]. However, the sorbitol nutrient signal could very well be conveyed through another unknown reinforcement pathway that does not include R48B04 PAM neurons. Next, I reasoned that perhaps an intrinsic property of individual sugars reinforces long-term memory, leading to elevated PAM-γ5 responses during feeding.

I compared D-arabinose with its similarly sweet enantiomer L-arabinose, which reinforces long-term memory despite lacking nutrient value [32]. Again, both sugars evoked similar responses in all three PAM subsets (Figure 4.4), suggesting that sugars intrinsically reinforcing long-term memory do not in and of themselves cause larger R48B04 feeding responses.

Although both D-arabinose and sucrose are sweet, it is possible that flies perceive the latter to be sweeter and such a perception leads to greater PAM-γ5 responses in starved but not dehydrated flies. I decided to compare sucrose with the similarly sweet but non-nutritious L-fucose [31], which also reinforces long-term memory [32]. Therefore, these sugars should be similar in most key respects except their nutrient content.

Indeed, feeding starved flies fucose evokes similar responses to sucrose in R48B04 neurons (Figure 4.5), although there was an observable trend towards a higher peak and post-feeding response for sucrose in PAM-γ5 neurons (Figure 4.5C). Nonetheless, the differences observed between sucrose and arabinose in Chapter 3 are more likely to reflect immediate palatability at 1 M concentrations rather than fast reinforcement of nutrient value.

4.2.2 Blocking octopamine signalling to R48B04 neurons

Although droplet palatability probably best explains the results reported in Chapter 3 and so far in this chapter, it does not adequately explain R48B04 reinforcement of long-term sucrose memory in dehydrated flies (Figure 3.2E). Having found a sugar without nutrient content that evokes a similar feeding response to sucrose,

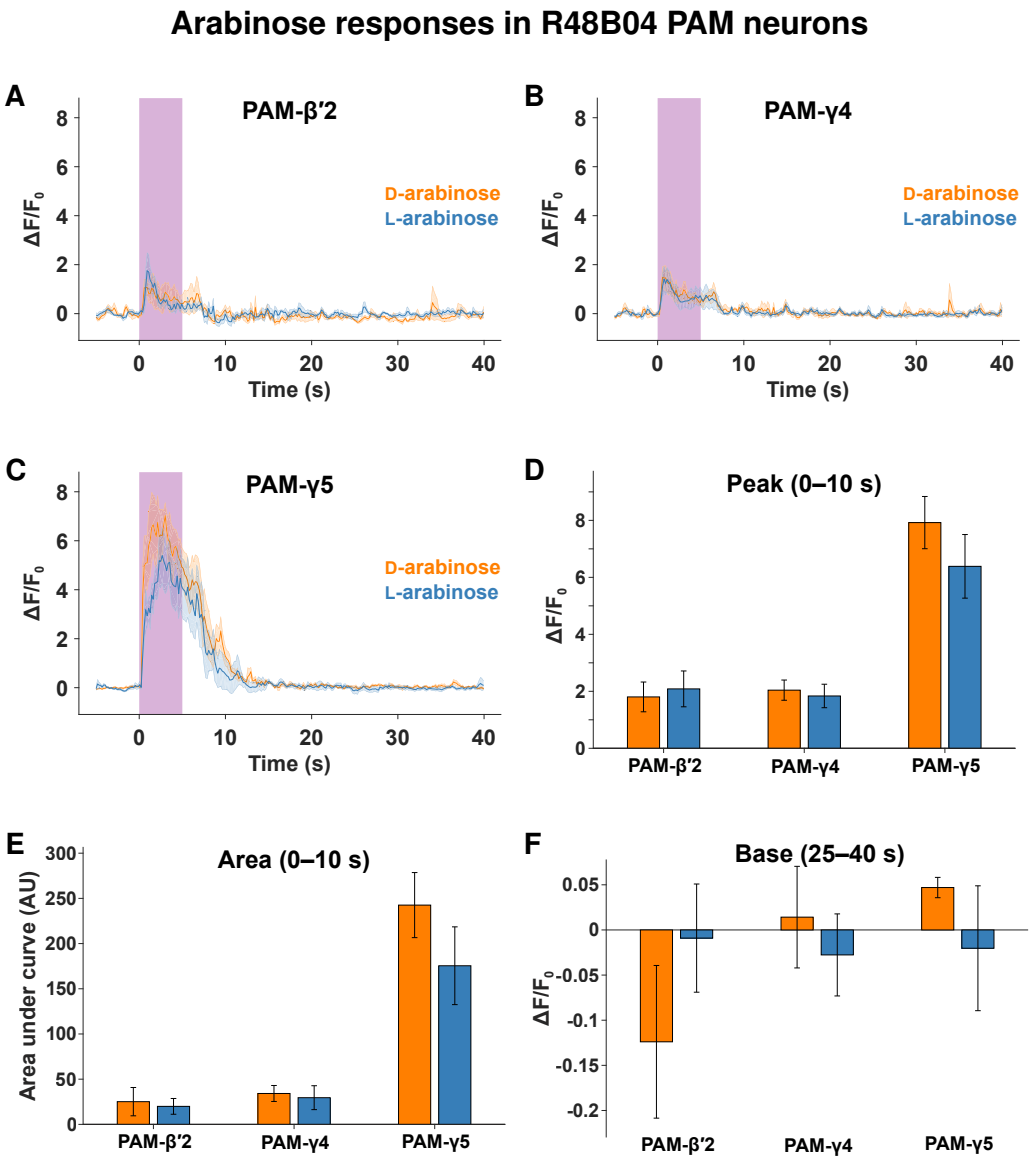

Figure 4.4: Sugars that reinforce long-term memory do not evoke larger R48B04 feeding responses than sugars that reinforce only short-term memory. Starved flies were fed either D-arabinose, which reinforces short-term appetitive memory, or its enantiomer L-arabinose, which reinforces long-term appetitive memory [32]. **A–C)** All PAM subsets have similar feeding response profiles to either arabinose enantiomer. No differences between the droplets were observed for any PAM subset with respect to **D)** the peak feeding response (first 10 s, $p > 0.31$ for each subset; two-sample t-test), **E)** the overall magnitude (area, first 10 s) of the response ($p > 0.26$ for each subset; two-sample t-test), or **F)** the baseline post-response (last 15 s, $p > 0.29$ for each subset; two-sample t-test). All data plotted are mean ± SEM. Sugars presented at 1 M ($N = 5$ each).

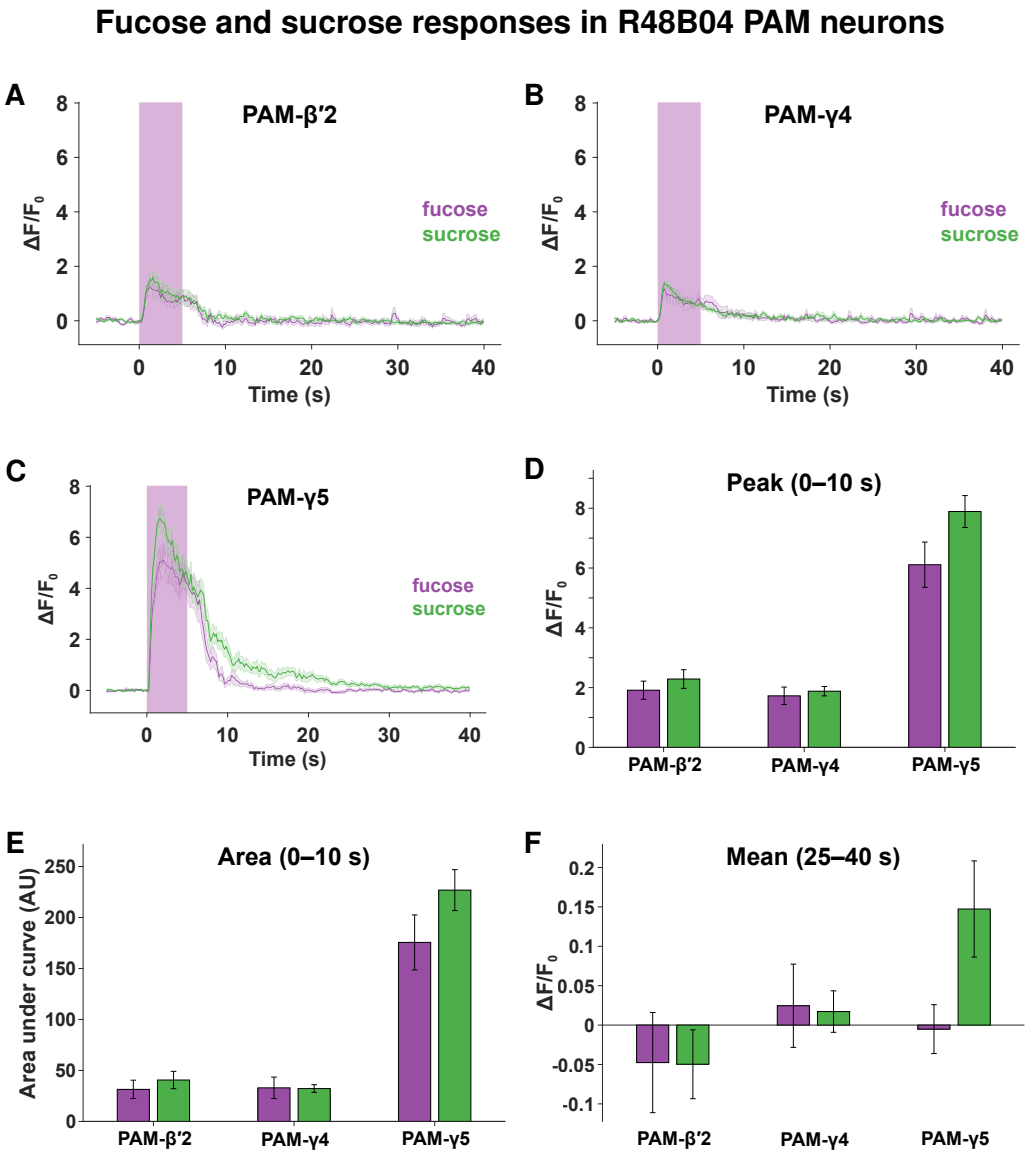

Figure 4.5: Fucose and sucrose evoke similar R48B04 feeding responses. Starved flies were fed either non-nutritious L-fucose or nutritious sucrose, both sweet sugars that reinforce long-term appetitive memory. **A–C)** All PAM subsets have similar feeding response profiles to fucose (violet) and sucrose (green), although the PAM-γ5 response evoked by sucrose decays more slowly. No significant differences were observed between fucose and sucrose for any PAM subset with respect to **D)** the peak feeding response (first 10 s, $p > 0.05$ for each subset; two-sample t-test), **E)** the overall magnitude (area, first 10 s) of the response ($p > 0.13$ for each subset; two-sample t-test), or **F)** the baseline post-response (last 15 s, $p > 0.05$ for each subset; two-sample t-test), even though there was an observable trend towards a higher sucrose peak ($p = 0.056$ for PAM-γ5; two-sample t-test) and an elevated sucrose post-response ($p = 0.06$ for PAM-γ5; two-sample t-test). All data plotted are mean ± SEM. Sugars presented at 1 M (fucose $N = 14$, sucrose $N = 21$).

I could now manipulate input to R48B04 neurons and investigate how this affects feeding responses evoked by each sugar.

Rewarding PAM neurons receive input from octopaminergic neurons that reinforce only short-term appetitive memory [17]. In particular, R48B04 neurons are thought to express the octopamine receptor OAMB because its knock-down in these PAM neurons causes a defect in short-term sugar memory [36]. Octopamine is also known to trigger an intracellular calcium increase in PAM neurons [17]. Hence, I reasoned that manipulating octopamine could perhaps reveal calcium signals in R48B04 neurons that have another source.

I first repeated my comparison of fucose and sucrose in starved TβH flies (Figure 4.6), even though it was more difficult to feed them due to their presumably diminished perception of sweet taste. Unexpectedly, there was a clear reduction in the overall magnitude of PAM-γ4 feeding responses (area, first 10 s) to fucose but not sucrose (Figures 4.6B and 4.6E). The reduction observed could suggest that a prolonged PAM-γ4 signal conveying nutrient value is for some reason obscured by octopamine signalling in wild-type flies. Alternatively, octopamine allows PAM-γ4 neurons to convey the sweet taste of fucose but is not required for PAM-γ4 to convey that of sucrose.

Since the TβH mutation is present in all cells and could have several unforeseen consequences for reward signalling, I then attempted to rule out octopamine more specifically by expressing RNAi against the mRNA of the OAMB receptor solely in R48B04 neurons. These wild-type flies would have octopamine present in the brain but it presumably would not activate R48B04 neurons during feeding.

I compared fucose with sucrose again, this time in flies with *oamb*-RNAi expressed specifically in R48B04 neurons, but did not observe any differences between the sugars for any PAM subset (Figure 4.7). I confirmed this result separately by supplementing fucose with either non-nutritious ribose or nutritious sorbitol and observed similar responses for both compound sugars in all three PAM subsets (Figure 4.8). Therefore, the PAM-γ4 difference I observed in TβH flies could

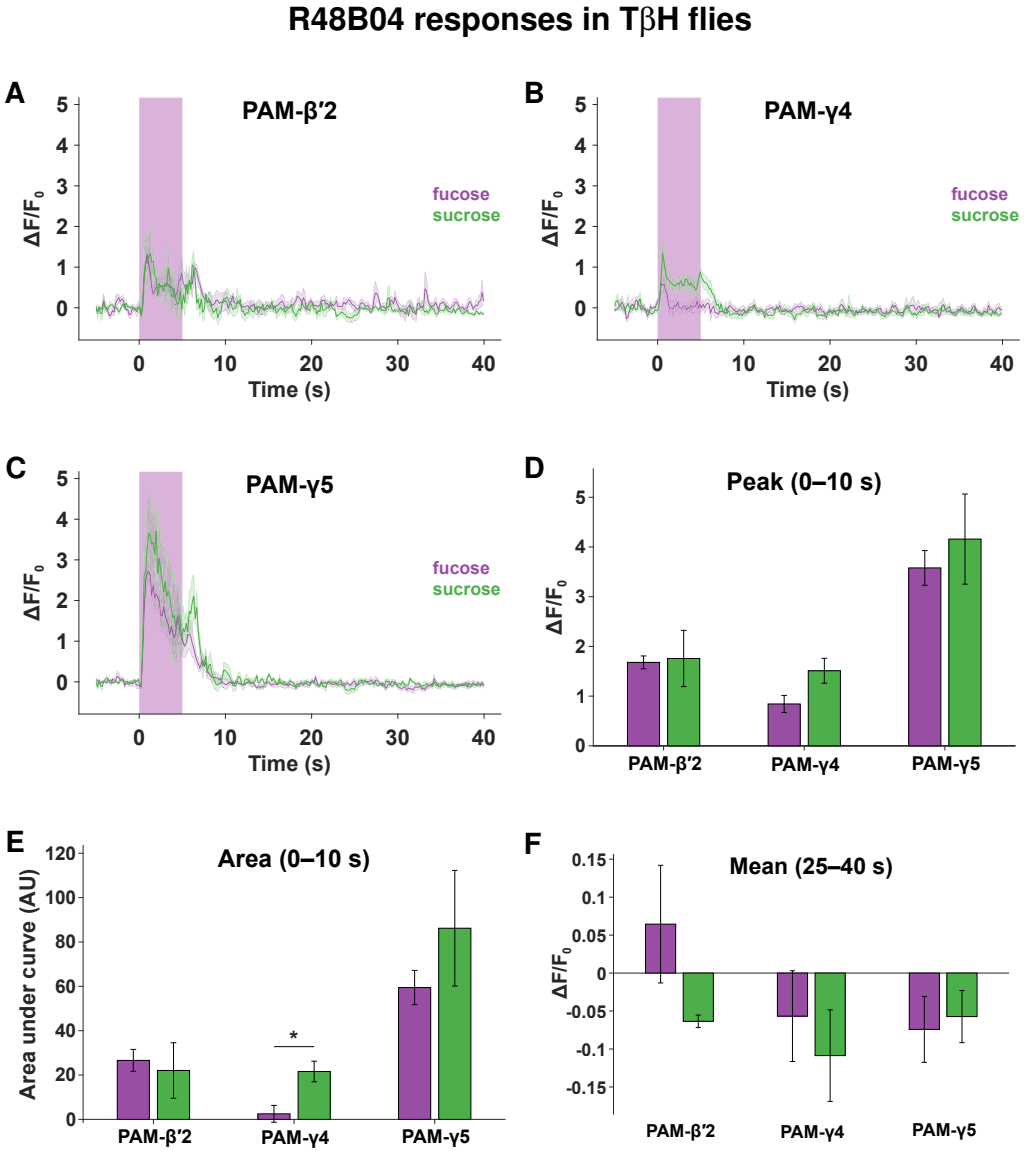

Figure 4.6: Fucose evokes smaller responses than sucrose in PAM-γ4 neurons of TβH mutant flies. Starved TβH flies were fed either non-nutritious L-fucose or nutritious sucrose, both sweet sugars that reinforce long-term appetitive memory. **A–C)** All PAM subsets have similar feeding response profiles to fucose (violet) and sucrose (green), but the PAM-γ4 response evoked by fucose decays almost immediately after feeding onset. **D)** No significant differences between sucrose and fucose were observed with respect to the peak feeding response (first 10 s) in PAM-β′2 ($p = 0.87$; two-sample t-test) and PAM-γ5 ($p = 0.51$; two-sample t-test), although sucrose may evoke a higher peak response in PAM-γ4 ($p = 0.051$; two-sample t-test). **E)** Fucose evokes a substantially smaller response in terms of its overall magnitude (area, first 10 s) in PAM-γ4 ($p < 0.05$; two-sample t-test) but not in PAM-β′2 ($p = 0.70$; two-sample t-test) or PAM-γ5 ($p = 0.27$; two-sample t-test). **F)** No significant differences in any PAM subset were observed concerning the baseline post-response (last 15 s, $p > 0.22$ for each subset; two-sample t-test). All data plotted are mean ± SEM. Sugars presented at 1 M concentration (fucose $N = 6$, sucrose $N = 4$).

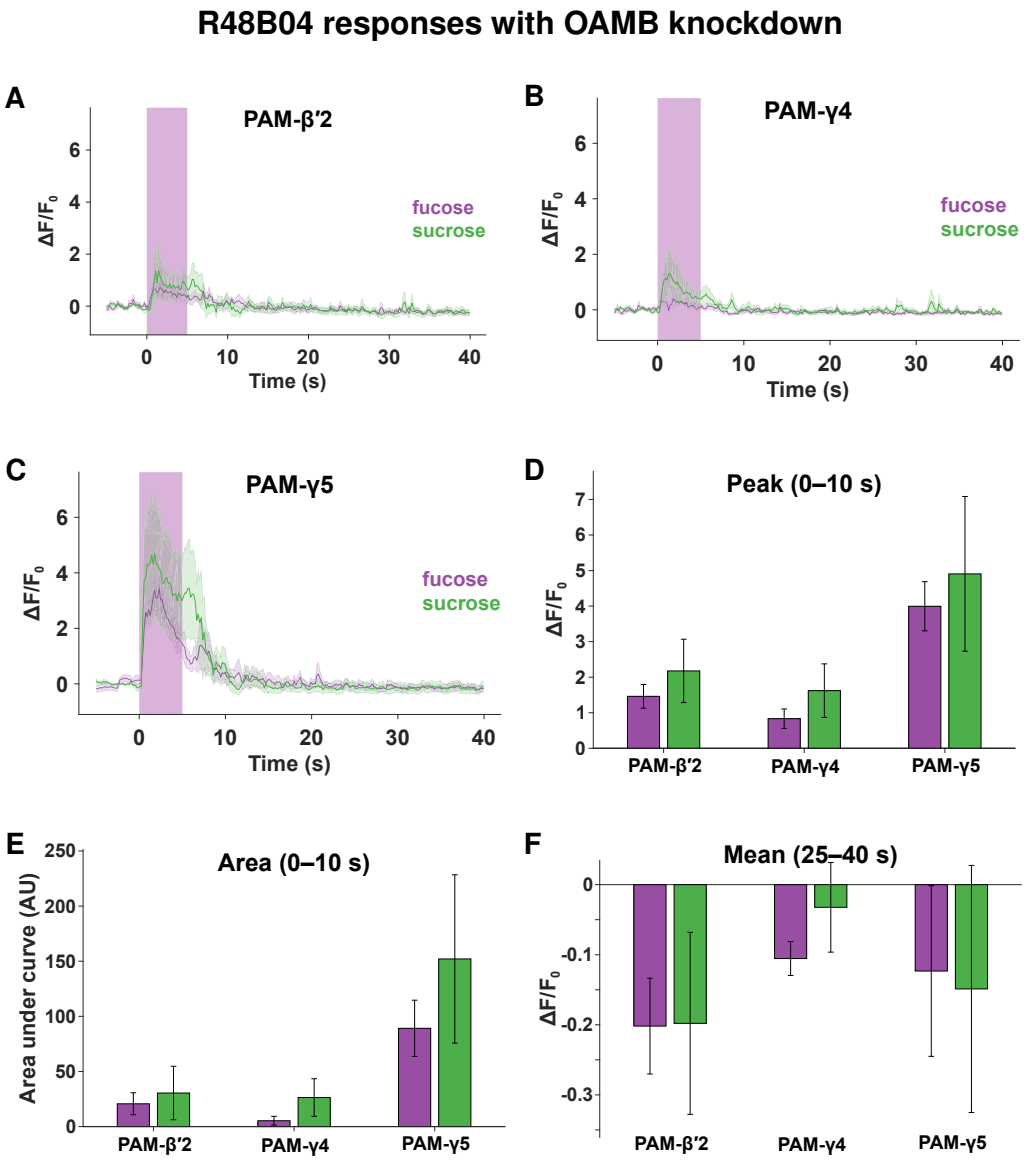

Figure 4.7: Fucose evokes similar responses to sucrose in R48B04 neurons with knocked down OAMB receptors. Flies expressing RNAi against *oamb* in R48B04 neurons were fed either non-nutritious L-fucose or nutritious sucrose. **A–C)** All PAM subsets have similar feeding response profiles to fucose (violet) and sucrose (green). No significant differences were observed between fucose and sucrose for any PAM subset with respect to **D)** the peak feeding response (first 10 s, $p > 0.31$ for each subset; two-sample t-test), **E)** the overall magnitude (area, first 10 s) of the response ($p > 0,22$ for each subset; two-sample t-test), or **F)** the baseline post-response (last 15 s, $p > 0.28$ for each subset; two-sample t-test). All data plotted are mean ± SEM. Sugars presented at 1 M concentration (fucose $N = 6$, sucrose $N = 5$).

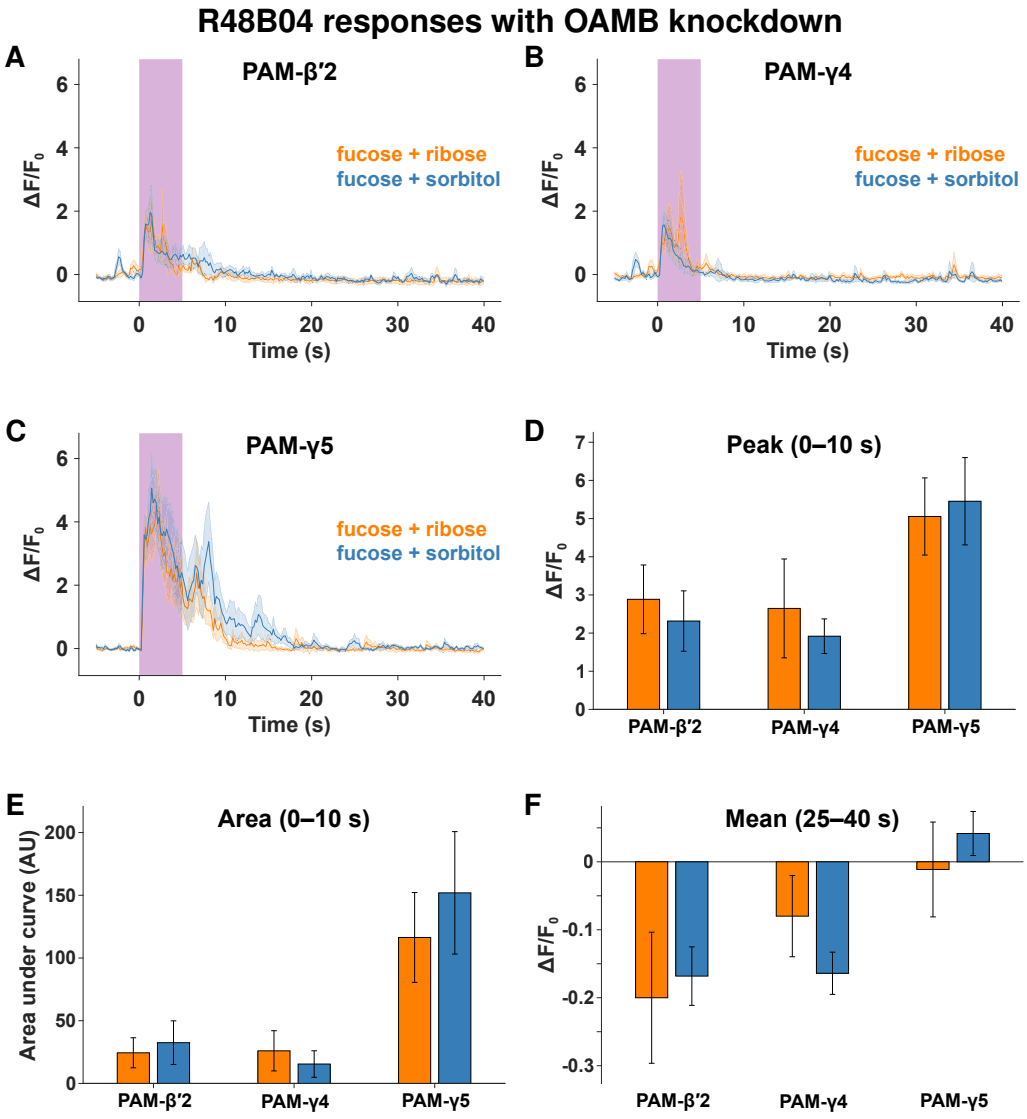

Figure 4.8: Fucose evokes similar responses to sucrose in R48B04 neurons with knocked down OAMB receptors. Flies expressing RNAi against *oamb* in R48B04 neurons were fed one of two compounds: non-nutritious L-fucose plus D-ribose (not nutritious) or D-sorbitol (nutritious). **A–C)** All PAM subsets have similar feeding response profiles to fucose + ribose (orange) and fucose + sorbitol (blue). No significant differences were observed between the droplets for any PAM subset with respect to **D)** the peak feeding response (first 10 s, $p > 0.61$ for each subset; two-sample t-test), **E)** the overall magnitude (area, first 10 s) of the response ($p > 0.57$ for each subset; two-sample t-test), or **F)** the baseline post-response (last 15 s, $p > 0.24$ for each subset; two-sample t-test). All data plotted are mean ± SEM. Compound sugars presented at 1 M concentration (each $N = 5$).

be a result of accumulated tyramine, which may still be able to signal through the OAMB receptor, or octopamine may still provide information about sweet taste to R48B04 neurons through other receptors.

4.2.3 Different sugars evoke similar PAM-α1 responses

Since other PAM subsets have also been implicated in nutrient reinforcement, I also investigated them for nutrient-specific differences during feeding. I first investigated the PAM subsets labelled by R15A04-GAL4 (Figure 3.2A) since it encompasses a large subset of PAM-γ5 neurons, including the 'narrow' ones labelled by R48B04-GAL4.

R15A04 also labels PAM-α1 and PAM-β′1 neurons, which are located more laterally than PAM-γ5. Although I could still image these three subsets in the same plane, their distance from each other meant I could only image one hemisphere at a time with similar magnification (Figure 2.4B). I did not record responses from PAM-β2 neurons, which are also labelled by R15A04, because they were not found in the same imaging plane as the other PAM subsets.

Initially, it was incredibly difficult to localize PAM-α1 neurons due to their very low calcium signal baseline. I overcame the problem by coexpressing the bright red fluorescent protein tdTomato as an anatomical reference in the same neurons. Using tdTomato also provided the coincident benefit of tracking sample plane movement during feeding. Dividing the GCaMP signal with that of tdTomato reliably flattened out fluctuations in the former that were observed during sudden movement. Coexpression of GCaMP and tdTomato is used in all experiments hereafter in this thesis except where otherwise specified.

I presented D-arabinose, sucrose, or water for 5 s to starved flies expressing both GCaMP6f and tdTomato in R15A04 neurons and recorded feeding responses in all three PAM subsets of one hemisphere (Figure 4.9). Whereas feeding evoked responses in all PAM neurons labelled by R48B04, feeding did not evoke responses in all R15A04 PAM subsets.

In PAM-α1 neurons, both sucrose and arabinose evoked feeding responses that were greater than that of water but indistinguishable from each other (Figures 4.9A, 4.9D and 4.9E). Despite its prominent baseline calcium signal, no feeding responses were observed in PAM-β′1, and perhaps even a minor inhibition was evoked (Figure 4.9B). Feeding on arabinose may also have resulted in a lower PAM-β′1 baseline post-response (Figure 4.9F).

All three droplets evoked feeding responses with a similar peak in PAM-γ5 (Figure 4.9C), although the water response may decay earlier (Figure 4.9E). The similarity between both sugar response profiles for PAM-α1 and PAM-γ5 suggests that these neurons either do not encode immediate nutrient reinforcement or that they do so in a manner that is not clear from two-photon calcium imaging alone.

Since the relative size of feeding responses was generally anticorrelated with the size of odour responses in R48B04 neurons (Figures 3.4 and 3.7), I investigated whether R15A04 PAM neurons had similarly anticorrelated responses. Using the same repeated odour presentation protocol as for R48B04 neurons (Section 3.2.4), I presented starved or satiated flies with MCH or OCT alternately five times each and recorded responses in R15A04 neurons (Figure 4.10).

In PAM-α1 neurons, MCH and OCT each evoked a small response during the first presentation, but subsequent odour presentations evoked even smaller responses that did not diminish much further (Figures 4.10A and 4.10B). Intriguingly, odours evoked the most prominent responses in PAM-β′1 neurons (Figures 4.10C and 4.10D). The PAM-β′1 odour response diminished the most between the first and second presentations of each odour but not much more thereafter.

Repeated responses to each odour tended to be larger in starved than dehydrated flies, even though the initial peak response was similar in either state (Figures 4.10G and 4.10H). Therefore, R15A04 odour responses reflect a trend between starved and satiated flies similar to that previously observed for R48B04 neurons (Figure 3.8).

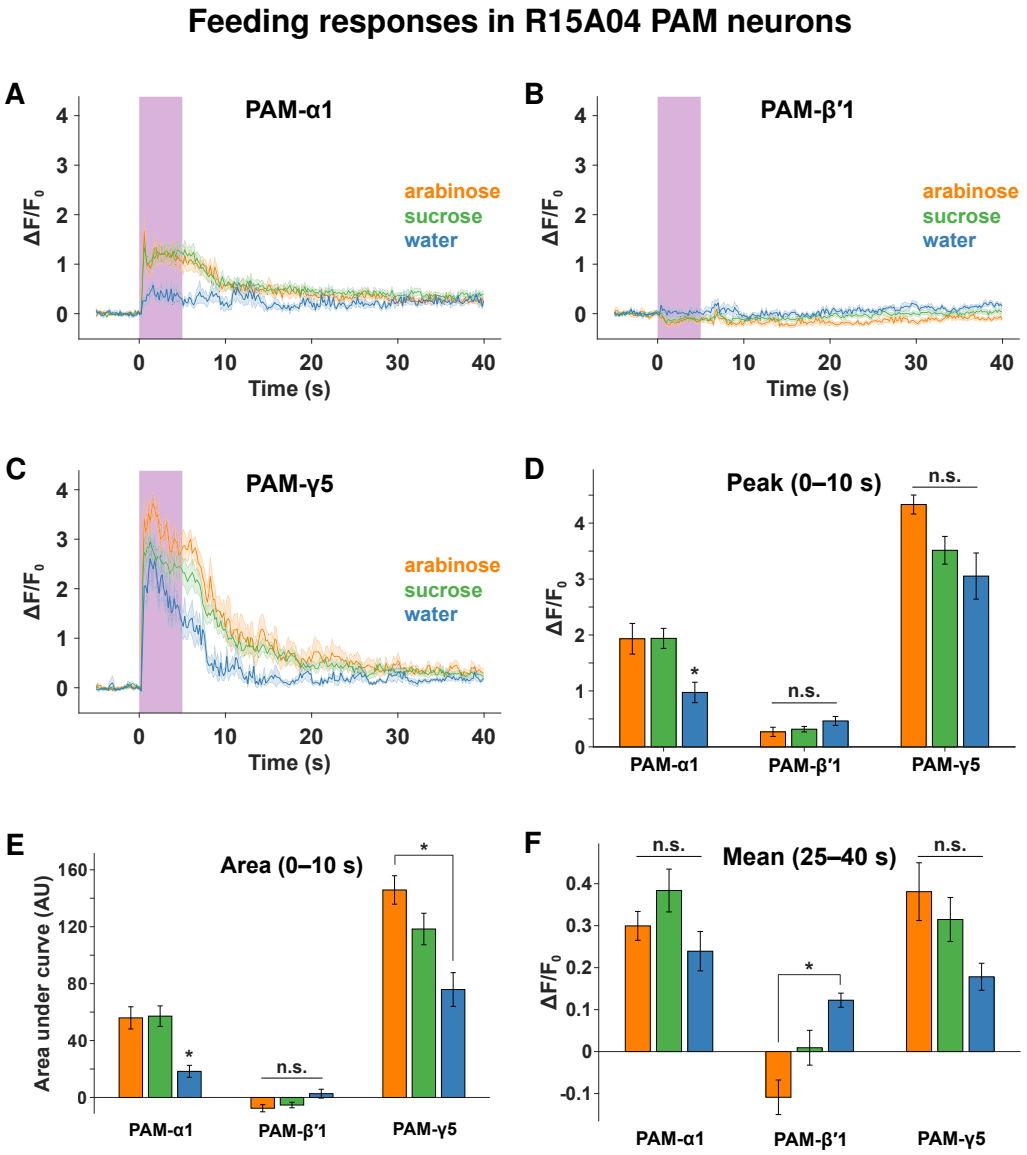

Figure 4.9: Feeding evokes differing responses in the three PAM subsets labelled by R15A04-GAL4. A–C) Ingesting food evokes a calcium response in PAM-α1 and PAM-γ5, but not PAM-β′1, where perhaps minor inhibition might be evoked. **D)** The peak (first 10 s) of the water response in PAM-α1 was substantially lower than for either sugar ($p < 0.05$ compared to the two sugars; ANOVA). Such peak response differences were not observed for PAM-β′1 ($p = 0.24$; ANOVA) or PAM-γ5 ($p = 0.055$; ANOVA). **E)** The overall magnitude (area, first 10 s) of the water response in PAM-α1 was substantially lower than for either sugar ($p < 0.05$ compared to the two sugars; ANOVA). No differences in area between droplets were observed for PAM-β′1 ($p > 0.05$; ANOVA), while arabinose appeared to evoke a greater PAM-γ5 response area than ($p < 0.05$ arabinose versus water; ANOVA followed by *post hoc* Tukey's HSD test). **F)** No substantial differences were observed in the baseline post-response (last 15 s) between droplets for PAM-α1 ($p = 0.22$; ANOVA) or PAM-γ5 ($p = 0.19$; ANOVA) although arabinose appeared to evoke a substantially lower post-response than water in PAM-β′1 ($p < 0.05$ arabinose versus water; ANOVA followed by *post hoc* Tukey's HSD test). All data plotted are mean ± SEM. Sugars presented at 1 M concentration (arabinose $N = 9$, sucrose $N = 22$, water $N = 7$).

Odours evoked the smallest responses in PAM-γ5 neurons and repeated presentations did not evoke decaying responses (Figures 4.10E and 4.10F). Similar odour responses were previously observed for the PAM-γ5 'narrow' subset in R48B04 neurons (Figure 3.8). Again, an off-response was observed for MCH but not OCT, primarily in PAM-β′1 neurons (Figure 4.10C). Taken together, the experiments here suggest that odour response size may indeed be anticorrelated with that of feeding in rewarding PAM neurons.

4.2.4 Feeding evokes similar PAM-γ5b (broad) responses

Having observed that arabinose and sucrose evoked similar responses in PAM-α1 neurons, I decided to investigate the other PAM subset implicated in long-term sucrose memory: the PAM-γ5b (broad) subset [36]. Although PAM-γ5b is already labelled by the R15A04 driver line, I used the intersection of 0104-GAL4 and R48B04-GAL80 to image this subset exclusively in the γ5 zone along with PAM-β′2m (middle) in the same imaging plane (Figures 2.4C and 4.11A).

I presented starved flies with D-arabinose, sucrose, or water for 5 s and recorded feeding responses in these two PAM subsets. All three droplets evoked clear but small responses in both subsets (Figures 4.11B and 4.11C), with that evoked by water tending to decay a little earlier. Both subsets had responses of similar magnitude although PAM-γ5b neurons evoked slightly larger responses overall. Nonetheless, no particularly consistent differences were observed when comparing the peak (first 10 s), overall magnitude (area, first 10 s), or post-baseline (mean, final 15 s) of each response (Figures 4.11D to 4.11F). As for PAM-α1 in R15A04, there is no clear evidence of a nutrient-specific signal from these results.

Since the feeding responses were roughly of similar magnitude for both of these subsets, I then tested whether the odour responses were hence also similar. Using the same repeated odour presentation protocol as for R48B04 and R15A04, I recorded odour-evoked responses in these neurons for starved flies (Figure 4.12). PAM-β′2m had smaller responses (Figures 4.12A and 4.12B) than the other PAM

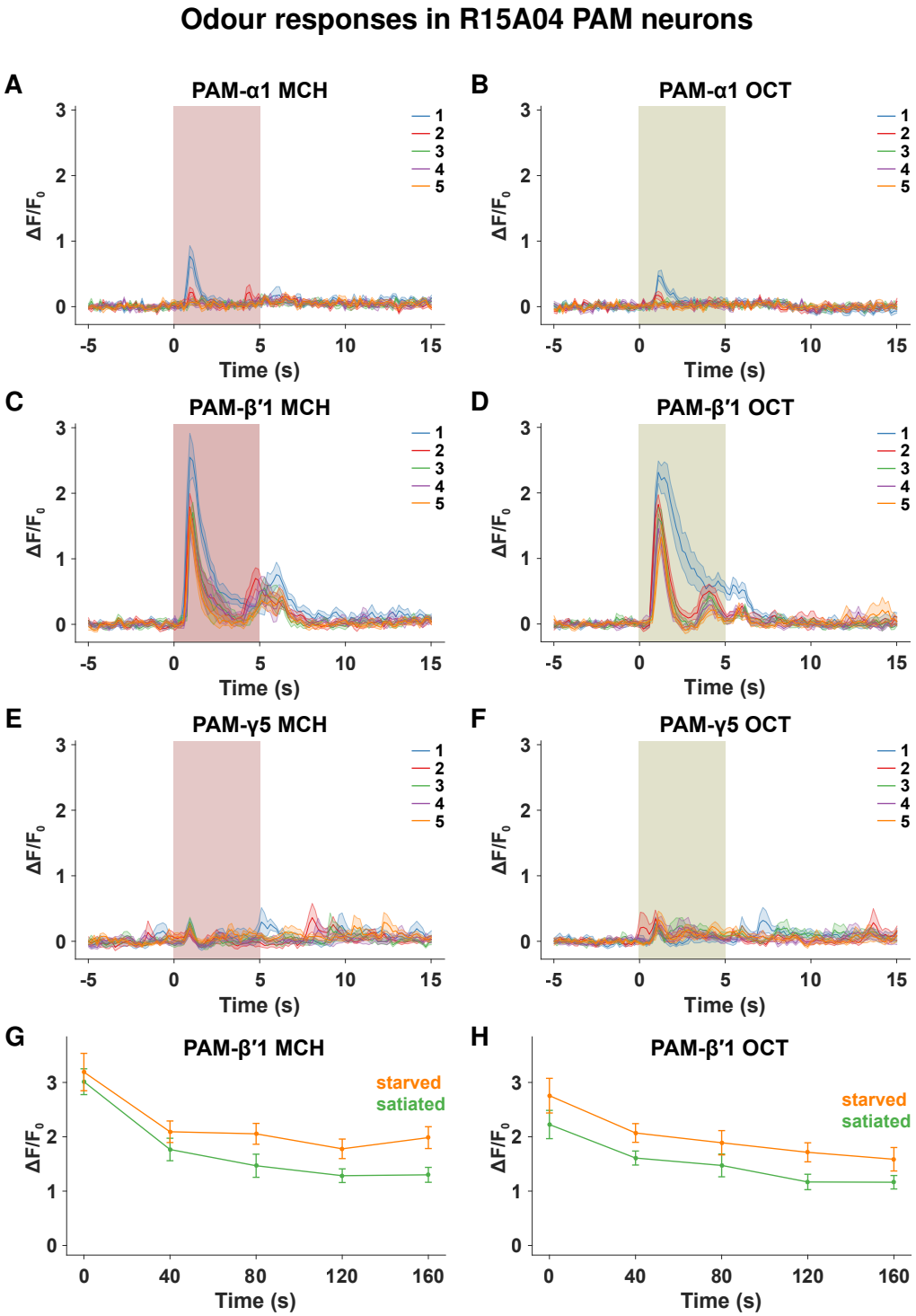

Figure 4.10: Odours evoke different responses in each R15A04 PAM subset. The odours MCH and OCT were alternately presented five times (increasing numbers in legend of each response plot) for 5 s every 20 s to starved flies. **A–B)** Both odours evoke a small PAM-α1 response that diminishes rapidly with repeated presentations. **C–D)** Both odours evoke the largest responses of all three subsets in PAM-β′1. Repeated presentations lead to decreasing but still prominent responses to each odour. **E–F)** The smallest responses are evoked in PAM-γ5, although a peak is still visible and the responses do not diminish further with repeated presentations. **G–H)** Peak PAM-β′1 responses (first 5 s) to MCH and OCT diminish less in starved flies than in satiated flies. All data plotted are mean ± SEM, $N = 7$ each deprivation state.

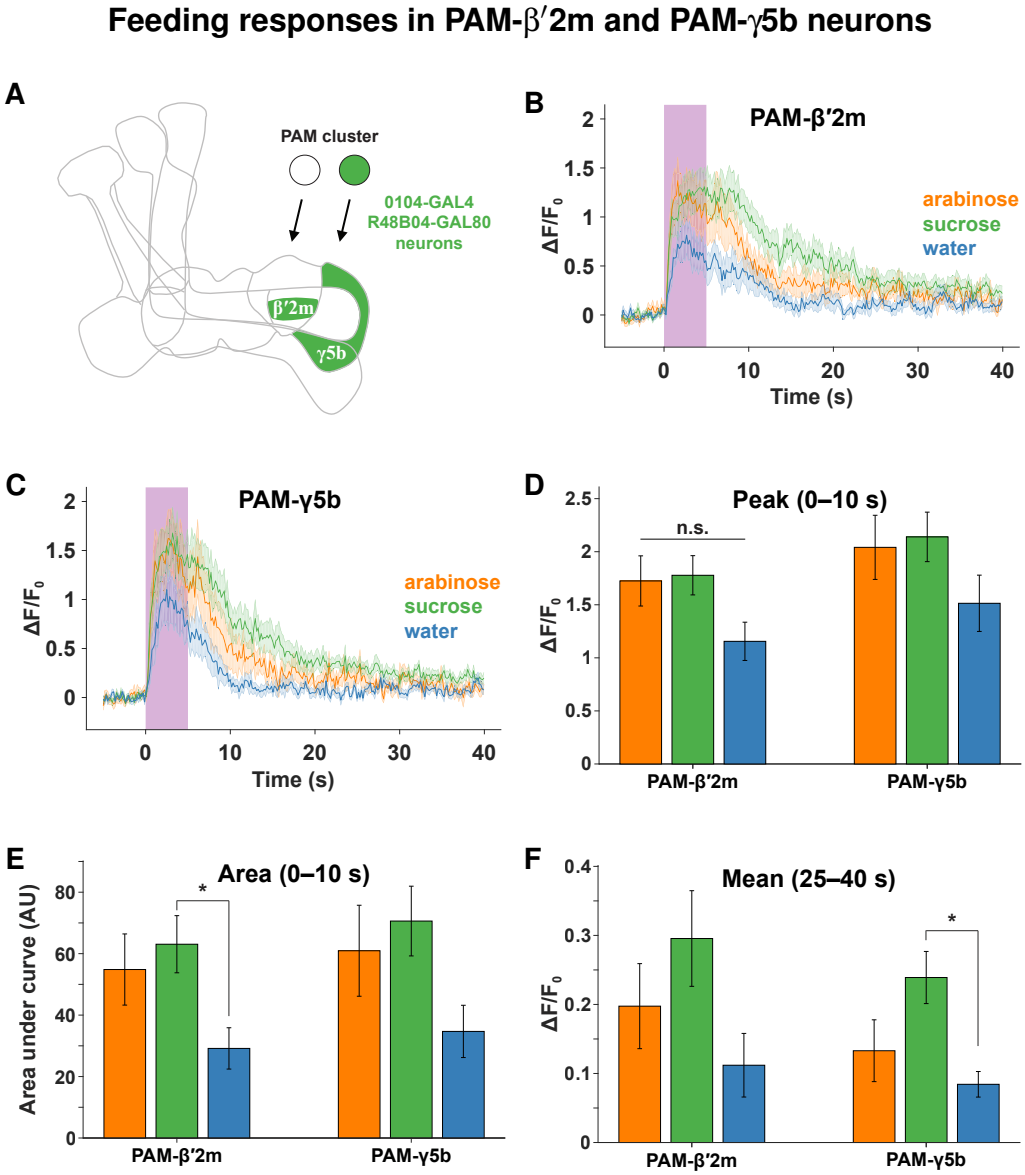

Figure 4.11: Feeding evokes uniform responses in PAM subsets implicated in long-term memory reinforcement. A) The intersection of 0104-GAL4 and R48B04-GAL80 labels PAM-β′2m (middle) and PAM-γ5b (broad) neurons. **B–C)** Feeding evokes a similar calcium response for any droplet in PAM-β′2m and PAM-γ5b, with the sugars tending to evoke a larger response than water. **D)** No significant differences between droplets were observed in each PAM subset with respect to the peak response (first 10 s, $p > 0.05$ for each subset; ANOVA), although there was a trend for both sugar responses to peak more than water. **E)** Sucrose, but not arabinose, evoked a PAM-β′2m response of greater overall magnitude (area, first 10 s) compared to water ($p < 0.05$ sucrose versus water; ANOVA followed by *post hoc* Tukey's HSD test). A similar but not statistically significant trend was evident for PAM-γ5b ($p = 0.07$; ANOVA). **F)** Sucrose, but not arabinose, evoked a greater baseline post-response (mean, final 15 s) in PAM-γ5b compared to water ($p < 0.01$; sucrose versus water; ANOVA followed by *post hoc* Tukey's HSD test). A similar but not statistically significant trend was evident for PAM-β′2m ($p = 0.11$; ANOVA). All data plotted are mean ± SEM. Sugars presented at 1 M concentration (arabinose $N = 8$, sucrose $N = 14$, water $N = 11$).

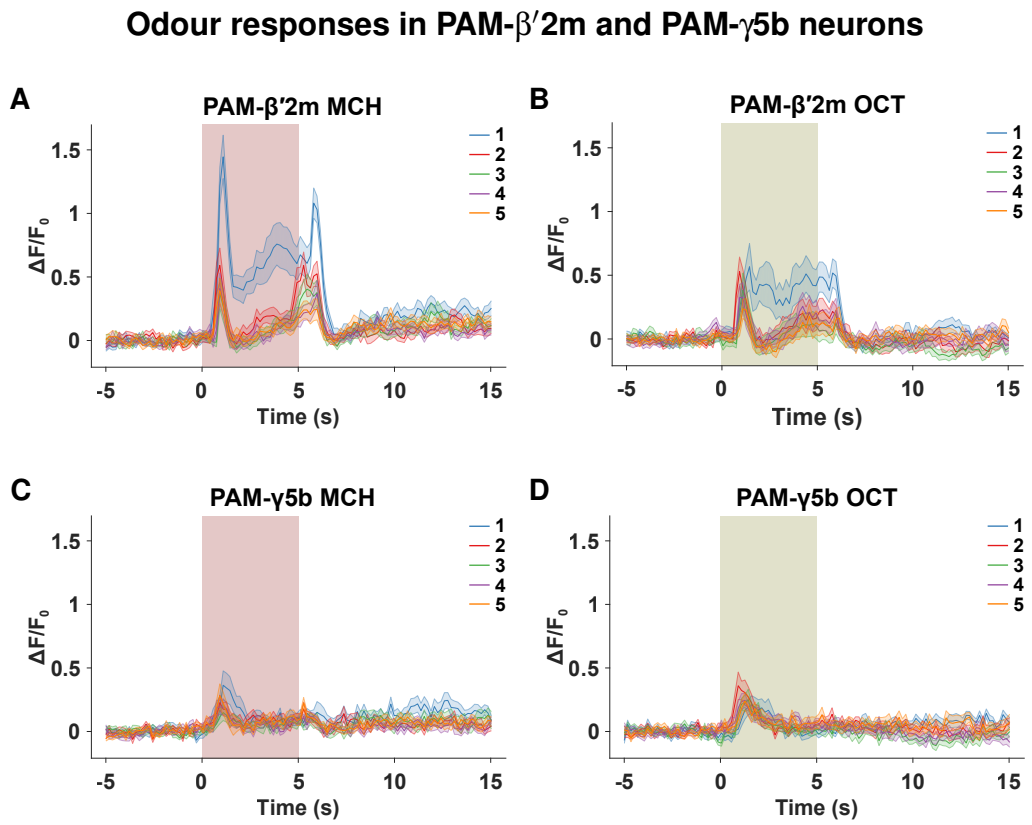

Figure 4.12: Odours evoke larger responses in PAM neurons innervating the β′2 zone. The odours MCH and OCT were alternately presented five times (increasing numbers in legend of each response plot) for 5 s every 20 s to starved flies. **A–B)** Both odours evoke a moderate PAM-β′2m response that diminishes with repeated presentations. **C–D)** Both odours evoke a small response in PAM-γ5b, although a peak is still visible and responses do not diminish further with repeated presentations. All data plotted are mean ± SEM, $N = 15$.

subsets previously imaged in the β′ lobe (Figures 3.7 and 4.10), but these were still more prominent than those observed in PAM-γ5b (Figures 4.12C and 4.12D).

The first response to each odour for PAM-β′2m was more prominent than for the subsequent presentations, which had a similarly smaller response. For PAM-γ5b, the responses to each odour were of similar magnitude regardless of how many times they had been presented before. An off-response peak was again observed for MCH in PAM-β′2 but not PAM-γ5b.

Of all the PAM odour responses surveyed, it can be concluded that those of PAMs projecting to the β′ lobe are most prominent, followed by those projecting to the γ4 zone, and finally those projecting to α1 and γ5, where odour responses are by far the smallest but are nevertheless evoked.

4.2.5 Feeding inhibits and reshapes MP1 oscillations

Having comprehensively surveyed the feeding and odour responses of most PAM neurons thought to be involved in sugar reinforcement, I then focused on MP1 in the PPL1 cluster since it was the only dopaminergic subset previously implicated in the control of appetitive memory expression [33] .

To image MP1, I used c061-GAL4 MB-GAL80 [33] or the MB320C split-GAL4 line [177]. Both labelled MP1 reliably but had a relatively weak expression level, meaning that I could not observe a GCaMP6f signal in starved flies nor could I consistently coexpress tdTomato in these neurons. Instead, I used the brighter and more sensitive GCaMP6s alone despite its slower dynamics, while my agarose preparation (Section 2.5) ensured minimal brain movement during feeding.

Since MP1 projects to the more laterally-oriented $\gamma 1$ zone (Figure 4.13A), I could record responses from only one hemisphere with a similar magnification as for PAM imaging (Figure 2.4D). Despite not coexpressing tdTomato with GCaMP6s, I could localize the weak MP1 baseline signal because its spontaneous oscillations fortuitously provided a regularly brighter fluorescence.

As for the PAM subsets, I presented D-arabinose, sucrose, or water for 5 s to starved flies expressing GCaMP6s in MP1 neurons, but I also recorded MP1 oscillatory activity before and after feeding. Having expected a small excitatory response during feeding [211], I was surprised to observe that feeding on any droplet phasically inhibits MP1 from the moment of ingestion (Figure 4.13B).

I recorded spontaneous oscillations in MP1 before each feed, but also observed that droplet approach in the 10 s before feeding evoked an apparent 'oscillation' of greater root-mean-square (RMS) amplitude compared to the preceding 50 s (Figure 4.13C). The droplet approach peak could reflect vapour sensing, or more speculatively, initial apprehension about a rapidly approaching droplet.

After the immediate inhibition during the 5 s of feeding, MP1 remained inhibited for around 30 s to 60 s before its spontaneous oscillations re-emerged. The mean of the first 60 s post-feeding for any droplet was significantly below the pre-

feeding baseline. For each droplet, the initial lower post-response then increased to a new steady-state (the next 120 s) that was significantly different from both the pre-feeding baseline and the initial post-response (Figure 4.13D).

The oscillations before and after feeding changed depending on the droplet type that was consumed. Only sucrose decreased the relative amplitude of the oscillations that eventually re-emerged post-feeding (Figure 4.13E). Consuming sucrose or arabinose caused oscillations to re-emerge with higher frequency and regularity (Figures 4.13F and 4.13G).

Consuming water also caused inhibition and adjusted the MP1 baseline, but it did not alter the spontaneous oscillations that emerged afterwards. While feeding evoked negative MP1 responses, I observed that presenting the odours MCH and OCT evoked a positive MP1 calcium response (Figure 4.13H), confirming previously published results [61]. Overall, feeding inhibits MP1 oscillations but consuming sugars in particular immediately reshapes them.

4.3 Discussion

4.3.1 Results summary

In R48B04 PAM neurons, the magnitude of feeding responses evoked by the sweet but non-nutritious D-arabinose did not change after supplementing nutritious sugars (Figure 4.3), nor was it any different from that evoked by its similar sweet enantiomer L-arabinose (Figure 4.4), which also reinforces long-term appetitive memory [32]. However, the non-nutritious sugar L-fucose, which is perceived to be sweeter than D-arabinose [31, 32] and also reinforces long-term appetitive memory [32], evoked larger responses that were of similar magnitude to those of sucrose (Figure 4.5). R48B04 feeding-evoked responses thus appear most likely to reflect the immediate palatability of ingested food.

In TβH mutants, PAM-γ4 neurons surprisingly respond less to fucose than to sucrose (Figure 4.6), suggesting that these neurons no longer convey immediate

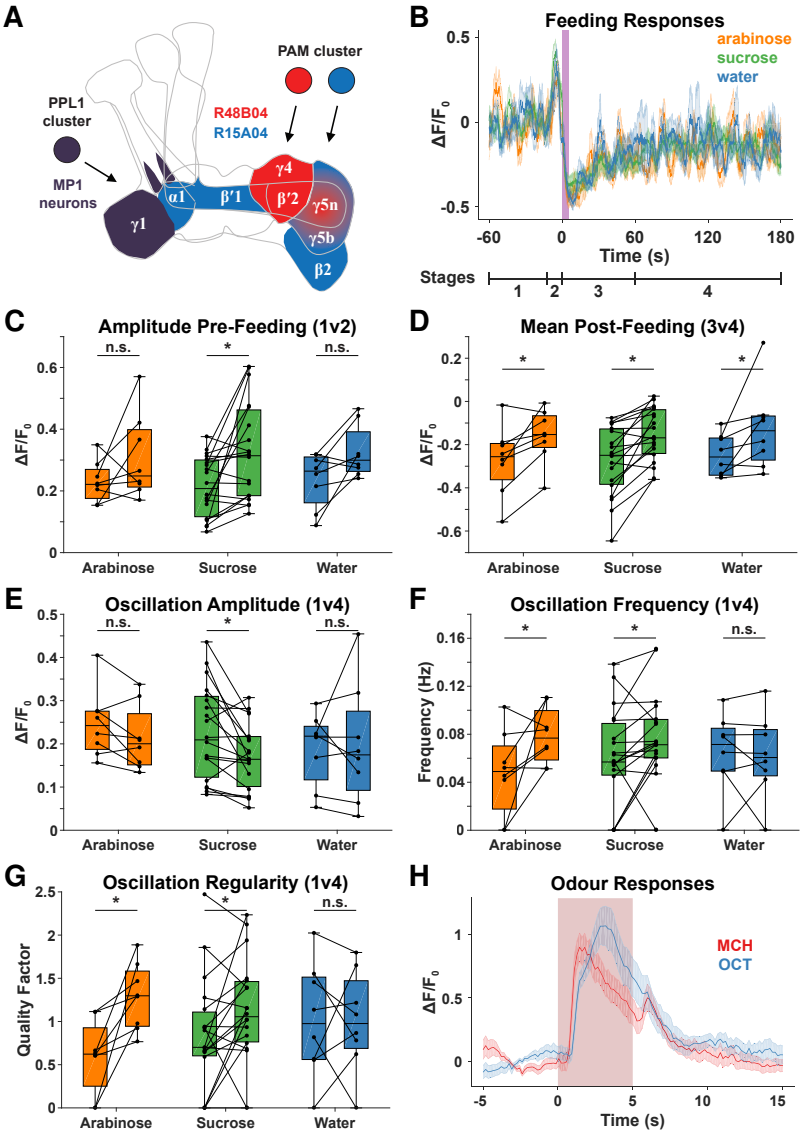

Figure 4.13: Sugar ingestion inhibits MP1 neurons in starved flies and modifies its oscillations. **A)** MP1 projects to the $\gamma 1$ zone and distal α/β peduncle. **B** Feeding inhibits MP1 for up to 60 s, after which its oscillations re-emerge at a lower baseline than before feeding. The response can be compared in four stages: 1) pre-approach (-60 s to -10 s), 2) droplet approach (-10 s to 0 s), 3) initial post-feeding (0 s to 60 s), 4) later post-feeding (60 s to 180 s). **C)** The change in root-mean-squared (RMS) amplitude before feeding. Sucrose ($p < 0.01$) and perhaps water ($p = 0.054$) evoke greater signal amplitude upon droplet approach (arabinose $p = 0.15$, stage 1 versus 2 for each droplet; Wilcoxon's signed-rank test). **D)** The change in mean signal over time post-feeding. All droplets evoke an initial post-feeding response below the pre-approach baseline, which later increases to a new mean that remains below the original ($p < 0.05$, stage 3 versus 4 for each droplet; signed-rank test). **E)** The oscillation RMS amplitude pre-approach compared with later post-feeding. Sucrose decreases oscillations post-feeding ($p < 0.005$, stage 1 versus 2; signed-rank test). Arabinose may have a similar downward trend ($p = 0.11$) but water does not ($p = 0.84$). **F)** The frequency or **G)** regularity (quality factor) of MP1 oscillations pre-approach compared with later post-feeding. Both sugars increase MP1 oscillation frequency and regularity post-feeding ($p < 0.05$, stage 1 versus 4; signed-rank test) but water does not ($p > 0.94$). **H)** The odours MCH and OCT evoke responses of similar magnitude in MP1 neurons. MCH also evokes an off-response similar to that seen for PAM neurons. All curves are mean $\pm$ SEM. All box plots have a median central mark, 25th and 75th percentile box limits; whiskers extend to most extreme data points not considered outliers. Stimuli presented: D-arabinose ($N = 8$), sucrose ($N = 19$), water ($N = 8$); MCH and OCT ($N = 11$).

sweet reinforcement in octopamine-less flies. In contrast, PAM-γ4 neurons responded similarly to both sucrose and fucose (Figure 4.7) or fucose supplemented with nutritious sugars (Figure 4.8) in flies whose octopamine receptor OAMB was knocked down in R48B04 neurons. Therefore, PAM-γ4 neurons may perhaps have an immediate nutrient-evoked response that is normally obscured by octopaminergic input through a different pathway, which would not be consistent with octopamine conveying the sugar signal to PAM neurons.

For the other PAM nutrient reinforcement candidates, only PAM-α1 showed a consistently higher feeding response evoked by sugars compared to water (Figure 4.9). However, there was no difference in the responses evoked between sucrose and D-arabinose that reflected greater nutrient value. Both PAM-β′2m and PAM-γ5b responded similarly to these two sugars and water, albeit with a trend towards a smaller water-evoked response (Figure 4.12). Odour-evoked responses in PAM neurons appear to be most prominent in those that project to the β′ lobes of the mushroom body (Figures 4.10 and 4.12).

Intriguingly, feeding instantaneously inhibited the spontaneous oscillatory calcium activity of punishment MP1 neurons but consuming any sugar increased their oscillation frequency and regularity (Figure 4.13). Only nutritious sucrose appeared to diminish MP1 oscillation amplitude after feeding (Figure 4.13E), suggesting a possible immediate nutrient-dependent signal change. Taken together, the results in this chapter suggest that a nutrient-specific signal may be conveyed in at least PAM-γ4 and MP1 neurons, whereas the inputs to PAM-α1, PAM-β′2m, PAM-γ5b, and R48B04 neurons warrant further investigation.

4.3.2 Comparing and supplementing sugars

The results in the past two chapters have ultimately depended on controlled comparisons between different droplets. It has therefore been assumed that the reinforcement pathways activated by consuming each droplet can be generalized to all droplets of a similar type (Figure 3.3A). Each sugar-responsive gustatory

neuron might express a different combination of gustatory receptors [256], sugars may differentially activate different types of gustatory-receptor-expressing neurons (GRNs) in different locations [257, 258], and the downstream outputs of these neurons to reinforcing neurons (if they exist) may very well be divergent.

Sucrose and D-arabinose are both detected by neurons expressing the Gr64f [32, 259] receptor. However, sucrose also requires the Gr64a receptor [260–262] while D-arabinose possibly requires the Gr61a receptor [32]. Differences in reinforcement could therefore arise from rewarding dopaminergic neurons being connected to some GRNs but not others, or from temporal differences in GRN activity.

The attribution of sweet taste to short-term memory and nutrient value to long-term memory is challenged by the observation that some non-nutritious sugars can reinforce long-term memory (e.g., L-fucose, L-arabinose) [32] whereas others cannot (e.g., D-arabinose) [32]. However, this enabled more specific comparisons between non-nutritious sugars that reinforce different types of memory, such as comparing responses evoked by either arabinose enantiomer (Figure 4.4).

If long-term memory reinforcement depends on particular gustatory-receptor-expressing neurons, then their identity for different sugars appears to be inconsistent [32, 35]. Four neurons expressing the Gr43a receptor in the dorsolateral protocerebrum are thought to function as nutrient sensors of fructose in the haemolymph [77]. These neurons have projections near the dendrites of PAM-α1 neurons but they are not directly connected [35].

Blocking protocerebral Gr43a-expressing neurons during training impairs long-term sucrose memory but not short-term memory for either D-arabinose or sucrose [35]. In contrast, protocerebral Gr43a block does not impair long-term L-arabinose memory; Gr43a-expressing neurons in the distal tarsi are required instead [32]. Surprisingly, D-arabinose evokes larger responses in these tarsal neurons than L-arabinose [32]. One possible explanation is that D-arabinose activates more receptor types in neurons that are primarily sensory. Alternatively, the size

of immediate calcium sugar responses may not be necessarily correlated with resulting memories.

Selecting any sugar as a representative of its particular 'type' is non-trivial. The proboscis extension reflex (PER) assays used to characterize fly responses to different sugars in previous studies [29, 31] are but one way to measure palatability and are a behavioural correlate of sweetness at best. An alternative approach used recently is the two-choice feeding assay [32], which allows perhaps a more hierarchical ranking of different sugars but also involves different decision-making processes. Both approaches have found that L-fucose is preferred over D-arabinose [31, 32] and is presumably sweeter, but such subtlety is lost when binarily categorizing sugars as sweet or non-sweet.

Most studies have compared nutrient value using survival assays, despite some variation in the sugar concentrations used [28–32]. However, survival assays are also behavioural correlates of sweetness and nutrient value because they reflect the acceptability of each sugar for ingestion and the presence of corresponding digestive enzymes respectively [27]. While all studies agree that sucrose can effectively sustain life [28–32], their conclusions for D-arabinose are less consistent.

One study concluded that D-arabinose extends life slightly when provided alone but shortens it when added to sucrose [28], others concluded that it does not extend life any more than water alone [30–32], while yet another concluded that it shortens life even compared to water [29]. On the other hand, two studies found that the nutritious but non-sweet sugar mannose extends life substantially longer than sorbitol [28, 31], yet both are typically classified as non-sweet and nutritious with no further distinction.

The practice of supplementing D-arabinose with sorbitol is intended to overcome the low palatability of the latter alone [17, 29–31, 35, 254]. Nonetheless, one investigation found that repeated training with sorbitol alone could indeed reinforce a long-term memory [30], whereas another found that it could not reinforce

such a memory after 2 min training unless also ingested in sufficient quantities together with D-arabinose [29].

Only one study has generalized beyond the combination of arabinose and sorbitol [31], albeit for sugar preference rather than learning and memory. The rest compare the arabinose-sorbitol combination with the effects of arabinose or sorbitol alone [17, 29, 30, 35, 254], and do not rule out any emergent property that could arise simply from consuming multiple sugars in a meal.

The primary choices of sugars in this chapter (sucrose, D-arabinose, and sorbitol), reflect that most existing behavioural data for learning and memory have used these sugars [17, 29, 30, 35, 254]. With the aforementioned limitations in mind, I extended my comparisons beyond these sugars to provide further insights into R48B04 responses. This step-wise strategy can be similarly applied for any systematic investigation into the reinforcement of different sugar types, whether comparing sweetness (Figures 3.4 and 4.5), nutrient value (Figures 4.3 and 4.5), or the type of memory reinforced (Figure 4.4).

4.3.3 Reward signals in PAM neurons

The experiments of the past two chapters have compared all sugar-water droplets at 1 M, the highest concentration that I found did not leave any droplet on the fly proboscis after feeding ended. Moreover, 1 M is the concentration that elicits saturating responses in gustatory neurons in the suboesophageal zone (SEZ) [263]. Assuming that feeding rate is similar for most sugars consumed within 5 s, comparing different sugars at the same concentration most likely controls for the immediate effect of feeding on haemolymph osmolarity [230, 255].

While most of the experiments presented here have not been previously attempted, the feeding-evoked responses characterized in both R48B04 and R15A04 neurons for starved flies (Figures 3.4, 4.3 to 4.5 and 4.9) are an improvement on those previously published by Yamagata et al. (2015) [35] because they not only compare sugars at the same concentration, but also show the response to water

as a feeding and ingestion control. My inclusion of a water control for R15A04 revealed that PAM-α1 respond more to sugars in particular, an insight missed by the study that implicated PAM-α1 in long-term nutrient memory [35].

Yamagata et al. [35] compared 2 M sucrose with 3 M D-arabinose and attempted to supplement arabinose with 2 M sorbitol for R15A04 imaging. They did not observe any clear difference in response profiles for either PAM subset, except that sucrose evoked larger responses than arabinose in PAM-γ5 for both drivers [35]. However, I only observed such a difference in the PAM-γ5n subset labelled by R48B04 (Figure 3.4). Yamagata et al. [35] only supplemented arabinose with sorbitol for R15A04 imaging, but as I similarly found for R48B04 (Figure 4.3), it did not increase arabinose responses [35].

Apart from octopaminergic neurons in general [17], allatostatin-A-expressing neurons [180], and the possibility of Gr43a-expressing neurons [35], our knowledge of inputs to PAM neurons remains frustratingly limited. However, the recent publication of a complete electron microscopy volume of a whole adult *Drosophila* brain [64] and ongoing efforts that, among other findings, have identified 188 neurons upstream of seven PAM-γ5 neurons (Waddell lab and N. Otto, personal communication), suggest that our understanding of PAM inputs will soon increase substantially.

Many gustatory-receptor-expressing neurons project to the SEZ [264], but it remains unclear how information is then sent from the SEZ to the central brain. Candidate neurons would presumably receive inputs from the SEZ and project to neurons in the protocerebrum. The tracing of neurons upstream of PAM-γ5 suggests that the most promising and specific GAL4 driver lines from the FlyLight collection [199] to test would be R87A01, R88E01, and R88F08 (selected together with N. Otto). Finding such neurons to be involved in taste or nutrient learning would increase our understanding of inputs to rewarding dopaminergic neurons.

Similarly, investigating the inputs to R48B04 neurons further might uncover other octopaminergic subsets or perhaps even the largely unknown role of tyra-

minergic signalling in *Drosophila* [265, 266]. Finally, as discussed in Section 3.3.5, investigating Kenyon cell or possible lateral horn connections to PAM neurons projecting to the mushroom body β' lobe in particular might reveal why the odour-evoked responses in PAM-β'1 and PAM-β'2 are particularly prominent.

4.3.4 Phasic inhibition of MP1 oscillations

MP1 imaging during and after feeding has also been previously attempted, albeit with substantially different approaches. One study [211] recorded MP1 responses evoked by ingesting the insect repellent DEET alone, sugar carrier (3 M xylose and 100 mM sucrose), both together, or water. The study authors reported that all except water evoked small positive responses immediately upon feeding, with no clear differences among them [211].

The MP1 response profiles reported in this study [211] were unusually derived from average traces of seven to seventeen repetitions from only three flies per condition. No ingestion confirmation post-imaging was reported, and there was little mention of MP1 oscillatory activity [211]. While my observation of phasic inhibition during feeding (Figure 4.13B) was therefore unexpected, a similar inhibitory feeding response has recently been observed for PAM-γ3 neurons [180].

It would be informative to repeat my experiments with DEET to determine whether it evokes an excitatory calcium response in MP1 neurons instead. Such a finding would provide evidence for the hypothesis that dopamine neurons can respond oppositely to stimuli of different valence [124, 267], but inverse to that expected for rewarding neurons. The odours MCH and OCT evoke excitatory responses in MP1 neurons (Figure 4.13H) [61], suggesting that the usual role of MP1 during odour presentation is to direct the MBON network towards avoidance [172].

On the other hand, my preliminary attempts to record rewarding R48B04 PAM neurons while delivering electric shock (data not shown) have not revealed shock-evoked inhibition. One limitation is that fly tarsi are left untethered during imag-

ing, increasing movement-induced signals [176]. Perhaps feeding leg-tethered flies DEET while recording PAM neurons would be more useful.

While my observations of MP1 oscillations are broadly consistent with those previously published [81, 129, 210], there are important differences in our analytical approaches. To remove low frequency noise due to sample drift, I applied a high-pass Butterworth filter to the original time-domain signal. In contrast, the approach used in previous investigations [210] smoothed the time-domain signal with a low-pass moving average filter and then applied a similar filter to subsequent frequency-domain data [210].

High-pass filters allow frequencies higher than a designated frequency (in this case 0.01 Hz [81, 129, 210]) to pass through unaffected whereas low-pass filters oppositely allow frequencies lower than the threshold to pass through unaffected. Since the aim is to remove low frequency noise arising from long-term drift, a high-pass Butterworth filter is therefore much more appropriate. Moreover, applying filters multiple times generally increases distortion of the original signal. Therefore, by filtering MP1 signals sparingly and appropriately, I improved the analysis upon which most existing MP1 oscillation data is based [81, 129, 210].

One of these studies [81] observed that MP1 oscillation frequency increases 30 min after feeding nutritious D-glucose compared to non-nutritious L-glucose, but it did not provide a comparison with oscillations pre-feeding as I have. With such a comparison, I did not observe any nutrient-specific frequency increase; rather, the increase was generally sugar-specific (Figure 4.13F).

Previous investigators [81, 129, 210] and I both assigned zero values for the frequency of a particular sample when meaningful oscillations could not be detected. However, previous investigators pooled such samples together with those that oscillated before conducting parametric comparisons [81, 129, 210]. By combining oscillating and non-oscillating samples before comparing oscillations, the average of some treatment groups could be distorted towards zero and may obscure

meaningful oscillation changes. In contrast, my analysis avoided such bias by comparing oscillations within individuals before and after feeding.

The only nutrient-specific change I observed was a decrease in oscillation amplitude after feeding (Figure 4.13E). Although satiated flies have an MP1 signal of greater amplitude compared with starved flies [129], a decrease in the amplitude of oscillations that emerge 30 s to 60 s after nutrient ingestion may be consistent with partial dNPF inhibition of MP1 activity [33].

Depending on its duration, a generally sugar-specific increase in oscillation frequency after brief phasic inhibition (Figure 4.13F) could represent a critical time window in which MP1 neurons represent a sweet reward signal. If total MP1 activity output during the time window is lower than a critical threshold due to nutrition, then reduced MP1 activity may ultimately activate neurons that convey delayed nutrient reinforcement in a manner that reflects meaningful state-dependent valuation. While delayed nutrient reinforcement starts to be conveyed by other neurons, MP1 oscillations would then eventually reach a higher amplitude than during starvation to block similar valuation from taking place in now satiated flies.

Previously published anatomical data [170] suggests that MP1 could be connected to neurons in the α1, β1, or β2 zones of the mushroom body via MVP2. Both PAM-α1 (or PAM-β2) and MBON-α1 are involved in consolidating long-term nutrient memory [179]. Therefore, imaging any of these neurons for longer time periods after feeding or manipulating MP1 activity could be illuminating.

Since both the source and purpose of MP1 oscillatory activity remain unknown, imaging upstream dNPF neurons [33] could reveal whether they too have spontaneous calcium oscillations and whether these change during feeding. Even if dNPF neurons do not also oscillate, they could perhaps have a similar role to hunger-promoting AgRP neurons in mice [268]: both may serve as 'energy calculators' that estimate and broadcast nutritional state to downstream neurons.

4.4 Conclusion

Although the experiments in this chapter have not conclusively identified a rapid nutrient reinforcement signal, they are nevertheless illuminating. Sugar-water feeding evokes different responses among different PAM subsets, suggesting that components of sugar reward may be conveyed specifically to those neurons. In particular, sugars evoke a response in PAM-α1 neurons much more than water does, implying that this subset conveys a sugar-specific signal.

Increasing the nutritious content of the sugar-water droplet does not increase the feeding responses evoked in any rewarding PAM subsets investigated. The magnitude of R48B04 PAM sugar responses in starved flies increases with sugar sweetness, but manipulating its octopaminergic inputs indicates that PAM-γ4 may also convey a nutrient-specific signal. Taken together, such findings suggest that sugar reward responses do not linearly scale with nutrient content.

Feeding rapidly inhibits aversively reinforcing dopaminergic neurons that also control the state-dependent expression of sugar memories. The spontaneous calcium oscillations in MP1 neurons become more frequent after consuming any sugar, and their amplitude appears to be diminished by a possible rapid nutrient signal. The changing oscillatory dynamics observed may play an important role in the consolidation of long-term nutrient memory.

PAM neurons that primarily respond to sugars appear to respond less to odours, suggesting that sugar rewards and odour cues differentially activate dopaminergic neurons. PAM neurons innervating the β' lobe of the mushroom body in particular respond most prominently to odours, whereas PAM neurons innervating the γ5 compartment respond most prominently to sugars.

Nonetheless, with the exception of the odour-specific PAM-β'1, sugars and odours evoke clear on-responses in all PAM subsets investigated. What remains unclear is whether PAM sugar and odour responses change during and after associative learning. The next chapter explores how R48B04 PAM neurons respond to sucrose and odours in different contexts including appetitive conditioning.

Chapter 5

Appetitive conditioning

5.1 Background

5.1.1 The role of dopamine in associative learning

In *Drosophila*, dopaminergic neurons (DANs) are thought to provide the reinforcement signal during olfactory associative learning [17, 34, 127, 130]. Different DAN subsets appear to encode positive or negative valence and release dopamine upon activation by a specific unconditioned stimulus (US) [16, 17, 34, 35, 173, 174, 205]. Each DAN subset projects its axons to distinct compartments of the mushroom body [53, 170], a neuropil formed by the axons of odour-activatable Kenyon cells (KCs) [160, 164, 165]. Each mushroom body compartment is also innervated by the dendrites of distinct mushroom body output neurons (MBONs), the downstream partners of KCs [53, 170].

Dopamine induces second messenger cascades in KCs [269, 270], in which odours also evoke an increase in intracellular calcium [167, 168, 271]. Together, these intracellular changes activate an adenylyl cyclase that is thought to be a coincidence detector [269, 270, 272, 273], leading to a change in the strength of KC-to-MBON synapses [58, 59, 148, 176, 177]. This induced synaptic plasticity between KCs and MBONs is ultimately thought to encode the resulting associative olfactory memory [15, 54, 55, 57, 160, 169, 171, 172, 176, 177, 274–276].

The functional complexity of *Drosophila* DANs is reflected by their many other functions in associative learning. Some DANs can consolidate long-term memory [81, 179] whereas others can integrate deprivation state to control memory formation [35, 36, 205] or expression [33]. DANs are also involved in forgetting [277, 278] as well as memory extinction and reconsolidation [61, 65]. Extensive investigation of just one single DAN, MP1, has implicated it in many different roles for various types of memory (Section 3.1.2) [33, 81, 174, 210, 279].

Some DANs provide teaching signals during associative learning that convey electric shock punishment [174, 175, 280], whereas others provide similar reinforcement for sugar or water reward [17, 34, 205]. Associative learning is also thought to induce plasticity in DANs [127]. During classical conditioning with electric shock, punishment DANs ultimately prolong their response to the odour conditioned stimulus (CS) after it has been paired with the US several times [127].

In mammals, rewarding DANs similarly increase their responses to the CS after repeated rounds of classical conditioning [2, 94]. Moreover, the key difference in our knowledge of DANs between mammals and *Drosophila* is that some mammalian DANs appear to encode reward prediction error (RPE) [2]; that is, their responses reflect the predictability of the rewarding US.

During associative learning, mammalian DANs are first strongly excited by the US, but later responses decrease as the CS increasingly predicts the US [2, 94]. Mammalian DANs no longer respond when the reward is perfectly predicted by the CS, but when the US is predicted but absent, they are phasically inhibited [2, 94]. These findings in mammalian DANs support the RPE hypothesis, which postulates that animals learn the association between the CS and US only when the latter is unpredictable [40].

Whether rewarding DANs in *Drosophila* also encode RPE remains unknown and is the primary focus of this chapter. Conditioning paradigms that have been used to investigate DAN physiology in *Drosophila* are reviewed next.

5.1.2 Previously attempted conditioning protocols

When studying associative learning-induced plasticity in *Drosophila*, perhaps the most straightforward approach is to train flies in a standard behavioural paradigm (e.g., T-maze) and then prepare them for physiological recordings [58, 59, 61]. This is convenient for investigations that compare odour-evoked responses 2 h to 3 h in neurons such as MBONs post-training [58, 59, 61], but such an approach does not provide information about how the neurons of interest respond before and during training within the same individuals.

To investigate whether *Drosophila* DANs encode prediction error, it would be ideal to record their responses during both training and testing. The two published studies that have attempted this to investigate prediction error in *Drosophila* [127, 128] used punishing electric shock as the US. Both studies recorded calcium responses from DANs labelled by the TH-GAL4 driver [281], which predominantly labels punishment DANs in the PPL1 cluster [15, 173].

These studies [127, 128] used training protocols that were forms of forward conditioning, in which the CS onset precedes that of the US and the CS presumably signals that the US will follow. The first study by Riemensperger et al. (2005) [127] used seven rounds of classical delayed conditioning, in which CS presentation (3 s) in each round partially overlapped with the US (2 s) for the final 1 s of the CS. To distinguish between CS and US responses better, the subsequent study by Dylla et al. (2017) [128] used six rounds of trace conditioning, in which each CS presentation (10 s) ended 5 s before the US (four 1.5 s shocks) started.

Despite these differences, both studies concluded that CS-evoked responses in punishment neurons increase after repeated rounds of aversive conditioning [127, 128]. While Riemensperger et al. pooled the activity of different DAN subsets, Dylla et al. found that the extent of this CS response plasticity varied among subsets. Neither study found that responses to the US decreased [127, 128] in a manner expected from similar experiments in mammals that reflect prediction error [2, 94]. Taken together, these studies suggest that although punishment

DANs do not appear to encode prediction error for the US, they may encode the predictive power of the CS nonetheless [127, 128].

While aversive conditioning of tethered flies under the microscope is becoming more prevalent [65, 128, 282], there has also been one recent attempt at appetitive conditioning under the microscope [282], albeit investigating cAMP-dependent plasticity in KCs. This study by Louis et al. (2017) [282] used a simultaneous conditioning protocol in which an odour (the CS^+) was paired together once with 1 M sucrose for 30 s. This was followed by a 30 s break and an unpaired odour (the CS^-) presented for 30 s. The CS^+ or CS^- odour was also presented 5 min before and after conditioning. However, a thin metal wire was used to block the proboscis physically when each fly was not being fed [282], possibly having an unintended aversive effect during certain periods of the protocol.

Critically, none of the studies discussed above tested whether flies actually learnt during these physiological experiments. This is because no reliable behavioural readout from tethered flies has been established for appetitive or aversive conditioning. However, the fly proboscis, which is typically restrained during aversive conditioning and whose movement is an ongoing challenge when recording feeding-evoked responses, could possibly provide such a readout.

The proboscis extension reflex (PER) is observed when tethered flies reflexively extend their proboscis upon sugar being presented to their foreleg tarsi. PER probability can be increased with sugar concentration or decreased by adding bitter substances [283]. Moreover, sugar solutions applied to the legs of satiated flies do not evoke PER as often as they do in starved flies [283], suggesting that deprivation state also controls this apparently reflexive behaviour.

One study [284] showed that PER in tethered flies can be appetitively conditioned using a paradigm established for bees [285, 286]. In this study, Chabaud et al. (2006) [284] used a delayed conditioning protocol in which an odour (10 s) was paired with 0.5 M sucrose applied to the proboscis during the last 5 s of the CS. This was repeated five times with a 15 min interval between trials [284].

Each conditioning round after the first evoked more PER in flies presented with this paired protocol compared with flies presented with an unpaired protocol [284]. However, this memory lasted only as long as the inter-trial interval and was no longer present just 1 h after the final training round [284]. Since this spaced protocol was much longer in total than standard T-maze protocols (75 min compared with 5 min) and 50% mortality was observed within 24 h after training starved flies [284], it is perhaps not representative of typical conditioning paradigms.

5.2 Results

5.2.1 Feeding responses encode salience and value

Most experiments investigating feeding responses in *Drosophila*, including those in the previous two chapters, usually present stimuli for a short controllable duration (e.g. 5 s) and then draw links with behavioural data. In contrast, the typical T-maze appetitive conditioning protocol allows flies to have ad libitum access to food while an odour is presented for 120 s [69]. Therefore, before attempting any conditioning experiment during two-photon imaging, I characterized feeding-evoked responses when sucrose was presented for longer than 5 s.

First, I presented sucrose for 120 s, the longest possible feeding length during a typical T-maze experiment. Since the first feeding bout would last less than 120 s (Figure 3.3B), I would also observe how R48B04 calcium signals change when flies stop and resume feeding. Response profiles to 120 s sucrose presentation (Figure 5.1) appeared surprisingly similar to those of 5 s (Figure 3.4), suggesting that R48B04 neurons primarily respond at the start of feeding.

No changes were observed when a fly broke off contact with the droplet during presentation, but if the fly then resumed feeding, PAM-γ5 responded with a new smaller peak (Figure 5.1C). The PAM-γ5 peak observed was smaller the later during presentation that this took place. In contrast, no changes were observed when a fly stopped feeding but maintained contact with the droplet.

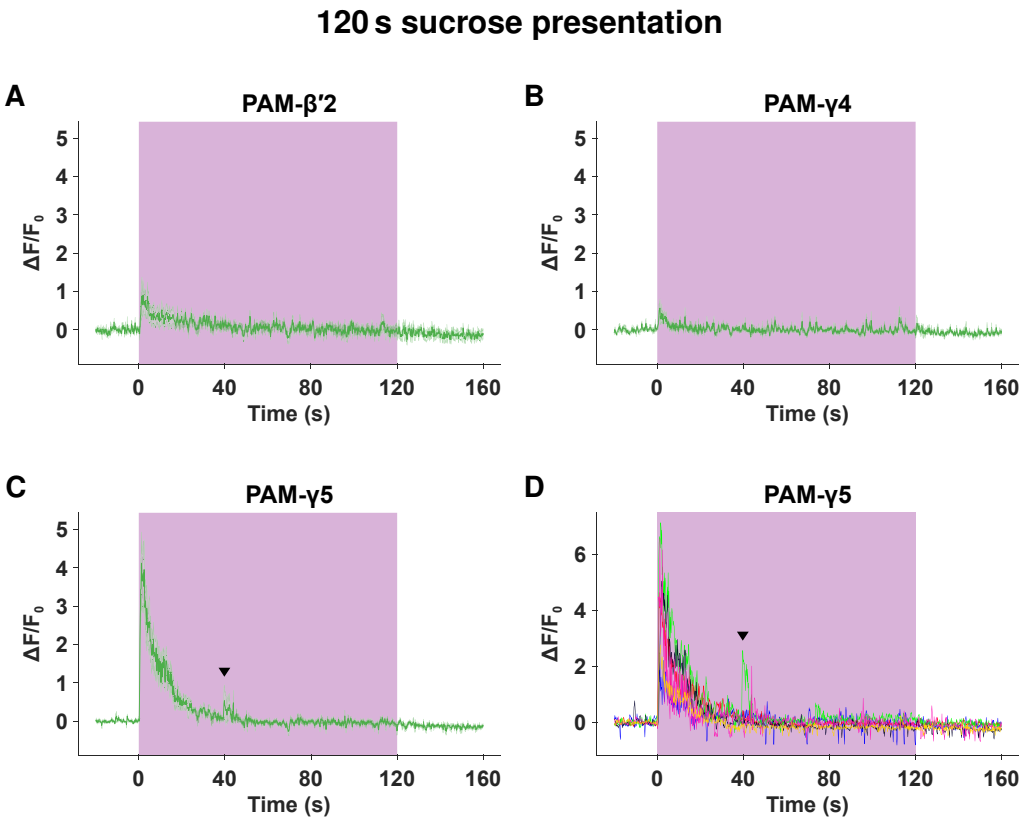

Figure 5.1: Feeding evokes responses primarily upon onset in R48B04 neurons. For this experiment, 1 M sucrose was presented once for 120 s to starved flies. **A–B)** PAM-β′2 and PAM-γ4 primarily respond at the beginning of feeding, regardless of its duration. **C)** PAM-γ5n also primarily responds at the beginning of feeding, but with a longer decay. **D)** Individual responses (plotted on a different scale) show that if droplet contact is broken and re-established, PAM-γ5n responds with a smaller peak at the time of second onset (indicated for one fly by the black arrowhead). All shaded curves plotted are mean ± SEM, $N = 6$.

Taken together with the deprivation state experiments in Chapter 3, PAM-β′2 and PAM-γ4 may signal the value or salience of initial feeding, whereas PAM-γ5 may signal value and salience whenever feeding and droplet contact are renewed.

Since renewing contact with the droplet and feeding led to new PAM-γ5 response peaks, I next investigated how the length of time between each feed influenced the size of R48B04 responses. After all, foraging flies probably do not feed on the same food source for 120 s uninterrupted. First, I presented sucrose for 5 s to starved flies once every 10 min (Figure 5.2). All PAM subsets had similar response profiles for each presentation round (Figures 5.2A to 5.2C) and there was no substantial decay for any subset between the first and final rounds (Fig-

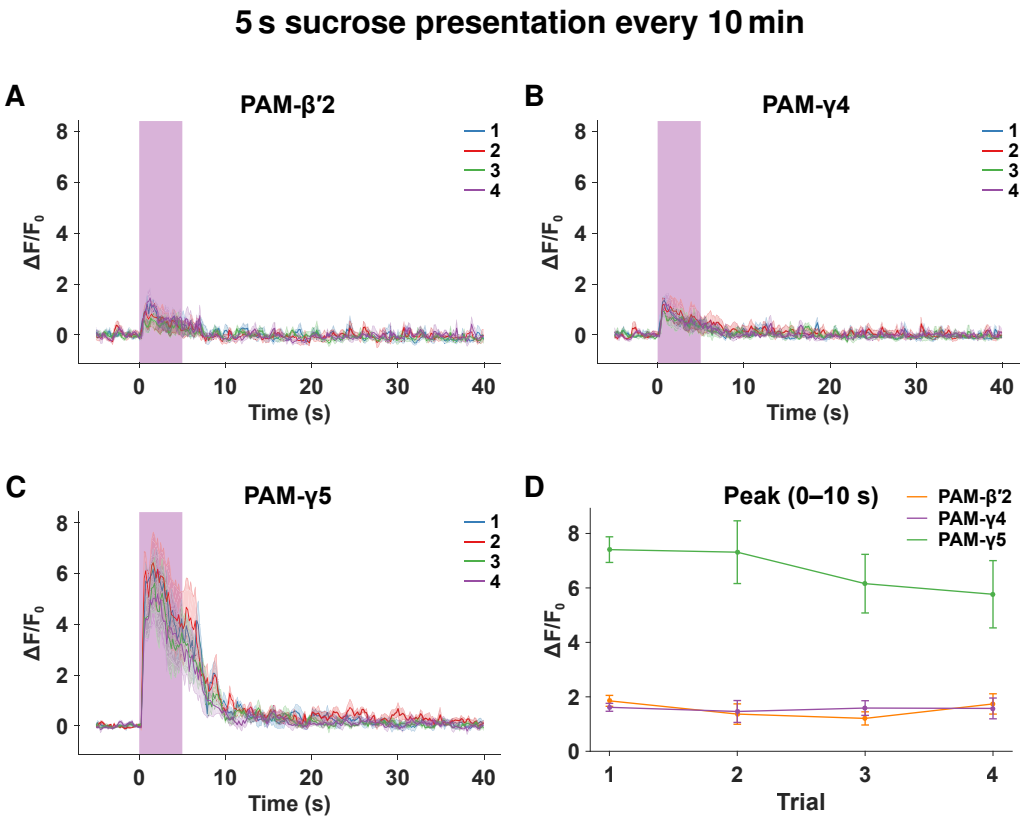

Figure 5.2: Feeding every 10 min evokes responses of similar magnitude in R48B04 neurons. For this experiment, 1 M sucrose was presented for 5 s to starved flies four times, once every 10 min. **A–C)** All PAM subsets response similarly during each presentation (increasing numbers in legend of each response plot). **D)** None of the PAM subsets decay substantially between the first and final presentation in terms of the peak response (maximum, first 10 s). All data mean ± SEM, $N = 5$.

ure 5.2D). When flies eventually rejected the droplet, typically at the fifth or sixth presentation, there was no corresponding feeding response.

Repeated responses of similar magnitude that are time-locked to feeding onset suggest that R48B04 neurons encode value at the salient time of feeding. According to the reward prediction error hypothesis, however, once a fly has experienced the feeding paradigm, future presentations should elicit responses of smaller magnitude because the fly can presumably predict reward from future droplet approaches. Perhaps each round was spaced apart enough and short enough that each feed was perceived to be novel or unexpected.

Next, I reduced the period between feeds to 3 min, which is sometimes used as the time point for immediate appetitive memory testing [17, 36]. Since I previously found that tethered flies typically fed on sweet and nutritious droplets for around

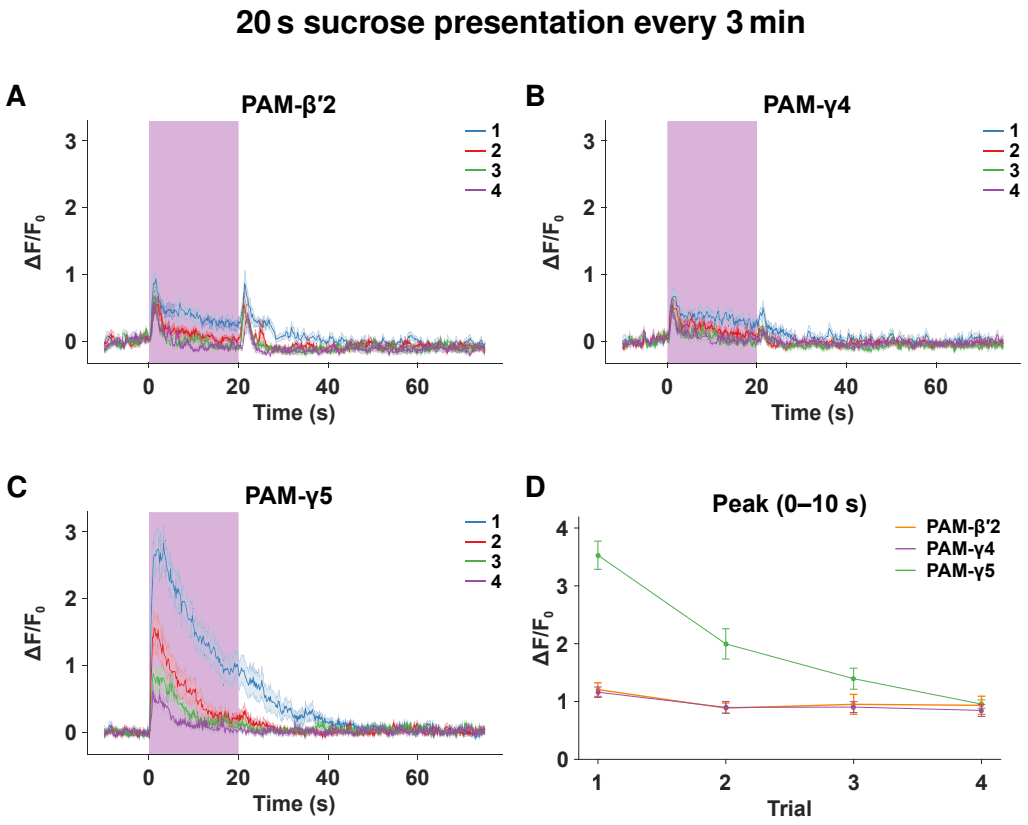

Figure 5.3: Feeding for 20 s every 3 min evokes diminishing responses in R48B04 neurons. For this experiment, 1 M sucrose was presented for 20 s to starved flies four times, once every 3 min. **A–C)** All PAM subsets have decreasing responses with each presentation (increasing numbers in legend of each response plot). Note also the off feeding response in PAM-β′2 and PAM-γ4 neurons. **D)** PAM-γ5 responses decay substantially between the first and final presentation in terms of the peak response (maximum, first 10 s), whereas those of PAM-β′2 and PAM-γ4 diminish primarily in terms of their area (not shown). All data plotted are mean ± SEM, $N = 14$.

20 s (Figure 3.3B), I fed flies for this shorter duration each round. Such a feeding length may also better approximate how long flies actually consume sugar-water during each feeding bout in the T-maze experiments described in Section 3.2.1.

After feeding flies every 3 min for 20 s four times in total (Figure 5.3), I observed diminishing responses in all three PAM subsets (Figures 5.3A to 5.3C), most prominently in PAM-γ5. Although the overall magnitude of each response (area, first 10 s) diminished with each presentation in all subsets, the peak of each response (maximum, first 10 s) only diminished in PAM-γ5 neurons (Figure 5.3D). Therefore, the magnitude of each response reflects prediction in all subsets, whereas the peak of each PAM-γ5 response reflects this as well.

Interestingly, with this protocol I also observed an off-response in PAM-β′2 and PAM-γ4 for 20 s feeds. This suggests that the prominent off-response for the odour MCH previously observed in these two subsets (Figure 3.7) is not necessarily limited to odours or MCH alone.

5.2.2 PAM-γ5 neurons respond to prolonged odours

Since a variation in the feeding protocol revealed a hitherto unseen off-response, I varied odour presentations next with the aim to determine whether the more prominent off-response to MCH previously observed was due to its specific odour identity or because it was presented first.

Since each odour is typically presented for 120 s during training with a T-maze [69], I presented the odours MCH and OCT in either order for 120 s each with a 30 s break in between. After recording R48B04 responses to the prolonged odours, I observed that MCH evokes two odour on-response peaks in PAM-β′2 and PAM-γ4 in the first 10 s irrespective of presentation order, whereas OCT does not (Figures 5.4A to 5.4D). Both odours evoked an odour off-response in these two subsets immediately after they ceased being presented. However, the MCH off-response was present only if MCH was presented first (Figures 5.4A and 5.4C).

Intriguingly, this protocol evoked slightly larger but prolonged PAM-γ5 odour responses throughout their presentation (Figures 5.4E and 5.4F). The elevated calcium signals during odour presentation for all three PAM subsets suggest that perhaps they all respond to odours substantially during appetitive conditioning.

5.2.3 Odours differentially evoke proboscis extension reflexes

The experiment just described was part of a longer recording in which two odours were presented in different sequences to tethered flies during calcium imaging (Figure 5.5A). Each recording consisted of two identical presentation rounds separated by a break of 180 s. Each round presented odours for 120 s each in either order, with a 30 s break between odour presentations.

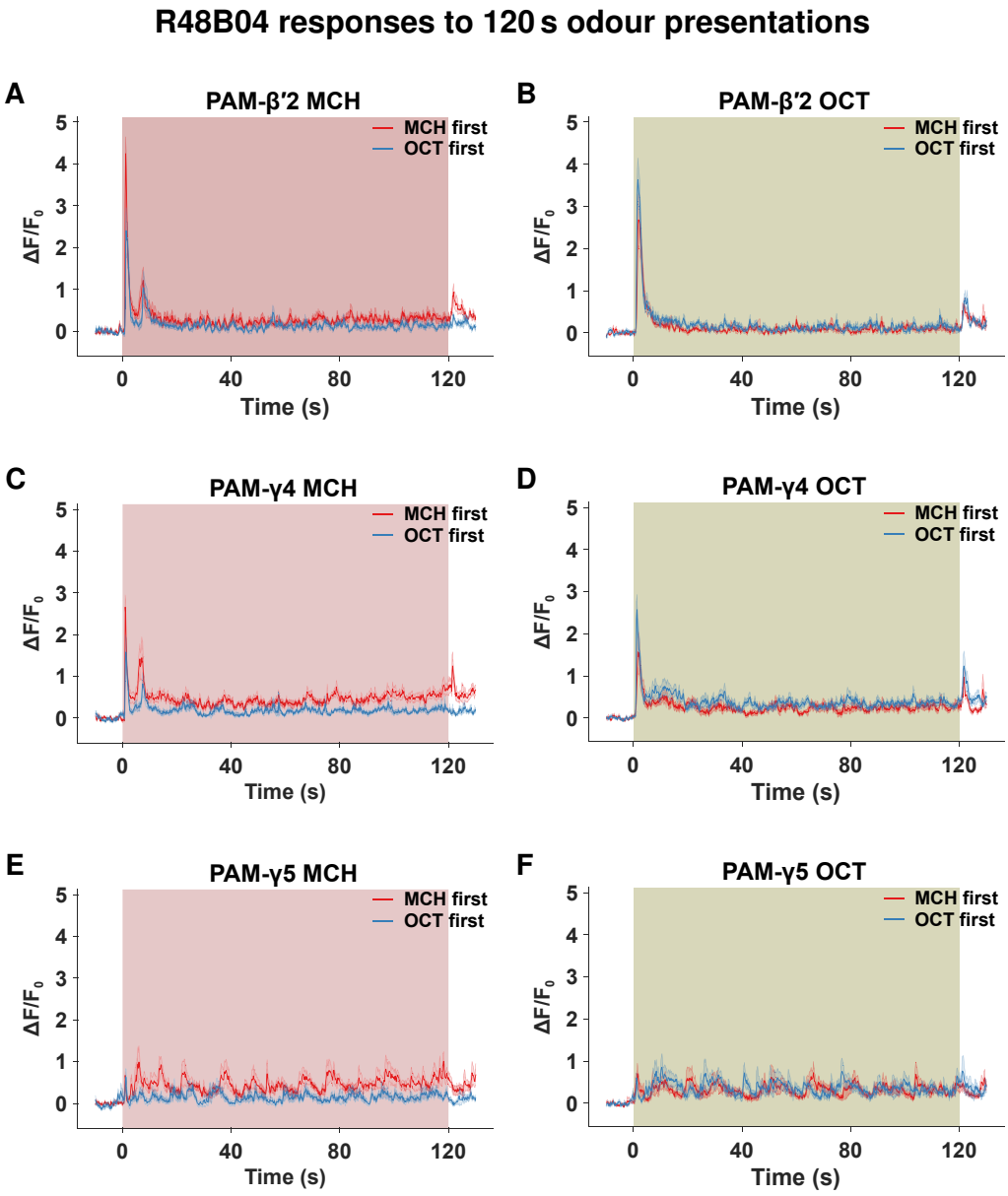

Figure 5.4: 120 s odour presentations evoke prolonged responses in PAM-γ5 neurons. For this comparison, the odours MCH and OCT were presented for 120 s each in either order, indicated as 'MCH first' (red) or 'OCT first' (blue), with a 30 s break between odour presentations. **A–B)** MCH evokes two on-response peaks in PAM-β′2 irrespective of presentation order, whereas OCT does not. Both odours evoke an off-response. **C–D)** PAM-γ4 neurons have similar odour on-response and off-response profiles as PAM-β′2 neurons. However, for both PAM subsets, the off-response for MCH is present only if it is presented first. **E–F)** Both odours evoke an elevated prolonged PAM-γ5 response in addition to the initial small peak. All curves plotted are mean ± SEM; MCH first $N = 10$, OCT first $N = 11$.

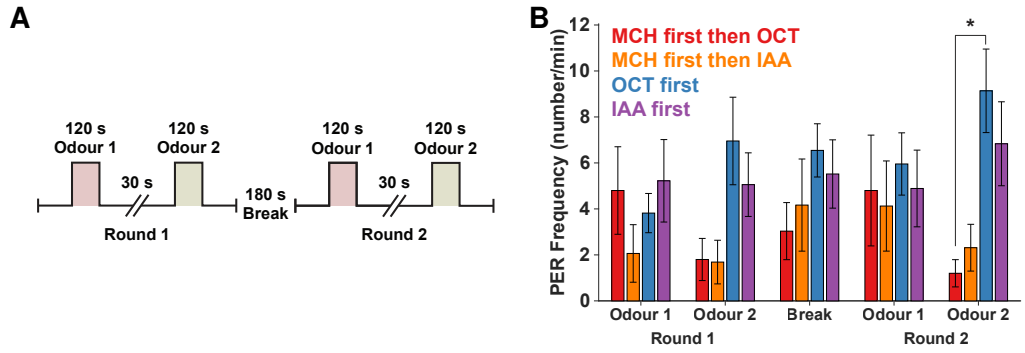

Figure 5.5: Odours evoke different PER frequencies depending on their sequence. A) For this experiment, two identical odour presentation rounds were presented to tethered flies during calcium imaging. Each round consisted of two odours presented in a particular sequence for 120 s each in either order, with a 30 s break between odour presentations. The odour MCH was compared with OCT or IAA. **B)** When MCH is presented first, there is a noticeable trend in which PER frequency reduces towards the odour presented second (either OCT or IAA), with a significant difference observed during the second presentation round (odour 2, MCH first then OCT versus OCT first, $p < 0.005$; ANOVA followed by Tukey's *post hoc* HSD test). All data plotted are mean $\pm$ SEM; $N = 9$–11.

For each fly, I used the feeding camera to record its proboscis extension reflex (PER) behaviour during the presentation of each odour. Since the head and proboscis of the fly are illuminated by the laser during two-photon imaging, I wrote an algorithm that could automatically identify each PER based on light intensity changes recorded by the feeding camera (Figure 2.5).

To determine whether odours differentially evoked PER and if this depended on their sequence, I compared MCH with OCT in either sequence and MCH with another odour, isoamyl acetate (IAA), in either sequence. If odours or their presentation sequence did not differentially evoke PER, then the PER frequency during each round in all four groups should be similar. However, I found that PER frequency appeared to depend on when MCH was presented (Figure 5.5B).

If MCH was presented first, then PER frequency evoked by OCT or IAA afterwards tended to be lower in each presentation round than if MCH was presented second. Indeed, a significant difference was detected between different presentation sequences for the final odour presented. Since all of the odours were presented at the same concentration, these results suggest that MCH induces a PER bias that could confound any behavioural comparisons during imaging.

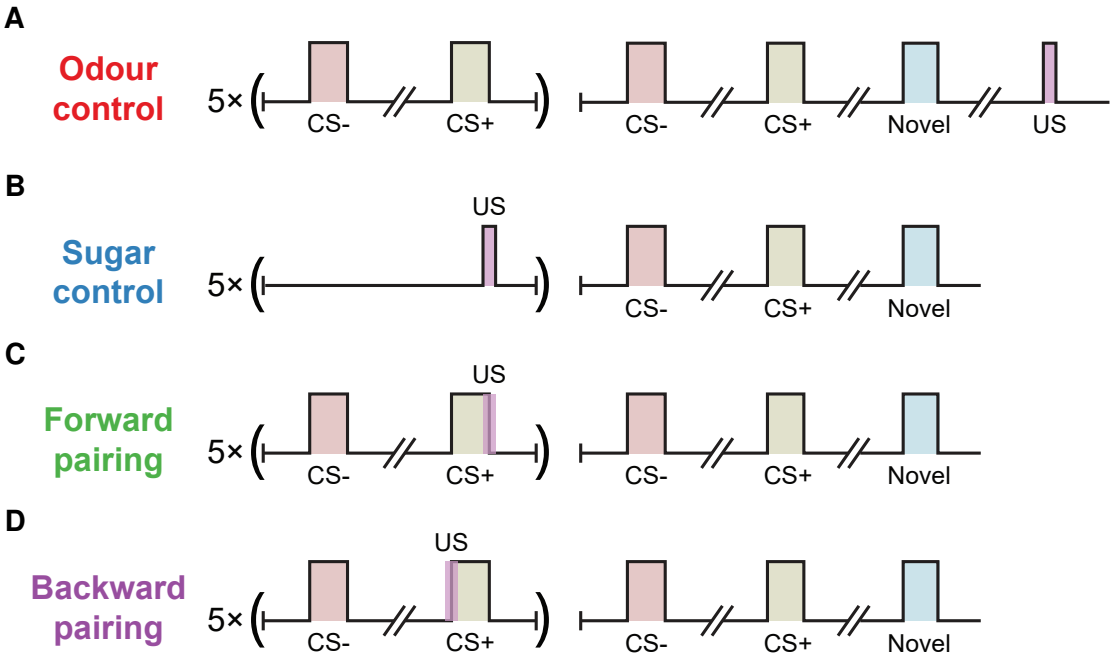

Figure 5.6: The multi-round appetitive conditioning protocol during two-photon imaging. The CS^- odour MCH (dark red), the CS^+ odour OCT (olive), and the novel odour IAA (light blue) were presented for 60 s each time, while the US 1 M sucrose (purple) was presented for 20 s each time. There was a break of 30 s between each stimulus unless otherwise specified in the experimental groups. **A)** The odour control consists of the CS^- and CS^+ odours being presented five times before a final (sixth) round in which each odour is presented, followed by the novel odour and finally the unpaired US. **B)** The sugar control consists of the US sucrose being presented unpaired five times, followed by the final round in which each odour is presented. **C)** The forward pairing group has odours presented at the same time as the odour control and sucrose presented at the same time as the sugar control. Each 20 s US overlaps with the final 10 s of the CS^+ odour. **D)** The backward pairing group has odours presented at the same time as the forward pairing group, but each 20 s US overlaps with the initial 10 s of the CS^+ odour instead.

5.2.4 A multi-round appetitive conditioning protocol

Having characterized feeding and odour responses under conditions similar to those in a T-maze, I then designed an appetitive conditioning protocol for two-photon calcium imaging (Figure 5.6). After trialling many different iterations, I selected a protocol with repeated presentations that could test predictions of the temporal difference model (introduced in Section 1.4). I recorded responses from R48B04 neurons because they are required to reinforce short-term appetitive memory [35, 36] and I could record both training and testing in the same session.

Since I established that the response profiles of MCH and OCT are consistent regardless of presentation order (Figure 5.4), the experiment presented here used MCH as the CS^- odour and OCT as the CS^+ odour. I used sucrose as the US

because it robustly reinforces both short-term and long-term memory in the T-maze (Figure 3.2). For multi-round conditioning under the microscope, I divided flies into four treatment groups, two of which paired the US with the CS^+ odour while the other two were controls.

The odour control (Figure 5.6A) presented the CS^- MCH for 60 s, followed by a 30 s break and then the CS^+ OCT for 60 s. This presentation sequence was repeated five times, with a 30 s break between each round of odour presentations. The US was loaded on the droplet stage but not presented during the five rounds. The sugar control (Figure 5.6B) presented sucrose alone for 20 s once towards the end of each presentation round. No odours were presented during the five rounds.

The forward pairing protocol (Figure 5.6C) presented MCH and OCT at the same time as the odour control and sucrose at the same time as the sugar control. The CS^- MCH was presented for 60 s, followed by a 30 s break, then the CS^+ OCT was presented for 60 s, and sucrose was presented from the last 10 s of the CS^+ until 10 s after CS^+ presentation ended. After such repeated forward pairing, the CS^+ should presumably predict the US.

The backward pairing protocol (Figure 5.6D) presented MCH and OCT at the same time as the odour control but flies received sucrose 10 s before the CS^+ odour and it was withdrawn 10 s after the CS^+ presentation started. After such repeated backward pairing, the CS^+ could possibly come to predict the removal of reward. Alternatively, since the 'CS^-' MCH is actually the odour that precedes reward in the backward pairing group, it may come to predict the US instead.

All four groups received the same odours during the testing round that started 30 s after the final training round. First, the CS^- MCH was presented, then the CS^+ OCT, and finally a novel odour, IAA, was also delivered. Each odour was presented for 60 s with a 30 s break between odours. Critically, the odour control (Figure 5.6A) also received an unpaired US reward 30 s following the testing round. Therefore, I could check that all samples in each group had normal odour

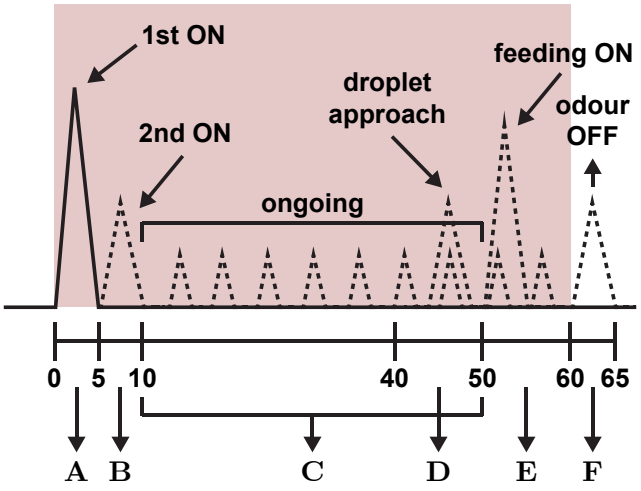

Figure 5.7: The components of a schematic odour response analysed during appetitive conditioning. A schematic 60 s odour response is displayed, with a continuous line indicating the expected on-response and dotted lines other possible responses. For clarity, only the feeding response possible during forward pairing is shown. **A)** The peak (maximum) and magnitude (area under the curve) of the first immediate odour on-response (0–5 s). **B)** The peak and magnitude of a possible second immediate odour on-response (5–10 s). **C)** The mean and RMS (root-mean-squared) amplitude/variation of the ongoing odour response between on-responses or off-responses to odours or sucrose (10–50 s). **D)** The peak and magnitude of possible vapour sensing during droplet stage approach (40–50 s, only for forward pairing). **E)** The peak and magnitude of a possible (predicted) feeding response (50–60 s for forward pairing, −10–0 s for backward). **F)** The peak and magnitude of a possible odour off-response (60–65 s).

or sugar responses; samples could be consistently excluded if they had no calcium responses to either stimulus type.

Each fly was recorded continuously for 20 min, meaning that limiting movement artefacts with an agarose preparation and tracking them with tdTomato coexpression would be critical. Each odour presentation round during training and testing was compared according to response profile components summarized and illustrated in Figure 5.7.

For each odour response parameter compared, I assumed that any clear learning-induced change would reflect a difference between:

- Training and testing for that odour within the same treatment group;
- The CS^- and CS^+ odours for that presentation round (training or testing) within the same treatment group; or
- The odour control and trained group for the same presentation round.

5.2.5 R48B04 neurons primarily signal reward salience

To test whether repeated forward pairing changed R48B04 calcium responses, I compared the CS^- and CS^+ odours of the odour control with those of the forward pairing group for each of the parameters in Figure 5.7 (non-parametric Kruskal-Wallis test followed by Wilcoxon's signed-rank test for relevant values). I first compared the two groups during the first training round (Figure 5.8) and confirmed that there were no differences between the groups for the initial CS^- odour (Figures 5.8A, 5.8C and 5.8E). This observation was expected since there was no difference between the two presentation protocols by this point.

The response profiles of the forward pairing and odour control were also similar for the first CS^+ odour presented until sucrose was delivered to the forward pairing group (Figures 5.8B, 5.8D and 5.8F). During the 20 s of feeding, R48B04 neurons in the forward pairing group displayed sucrose responses in all three subsets that substantially elevated their activity (the two parameters described in Figure 5.7E) compared to the odour control. Therefore, R48B04 neurons signal the value and timing of reward during training.

I then compared the odour control and forward pairing group during the testing (final) round of odour delivery (Figure 5.9). The temporal difference model predicts that the CS^+ cue-evoked response should be greater for the forward pairing group than for the odour control. However, both treatment groups had similar CS^+ odour responses according to the response parameters in Figure 5.7, including the peak CS^+ response in the first 5 s for PAM-$\beta'2$ and PAM-$\gamma4$ ($p > 0.05$; Kruskal-Wallis test).

The one clear effect observed in the forward pairing group was a reduced ongoing PAM-$\gamma5$ response to the CS^+ (the mean in Figure 5.7C) compared to the CS^- (Figure 5.9G). The CS^+ ongoing response was also significantly lower than the CS^+ ongoing response during the initial training round. In contrast, the ongoing responses to both odours during testing for the odour control group were similar (Figure 5.9H). This suggests that R48B04 neurons provide the teaching

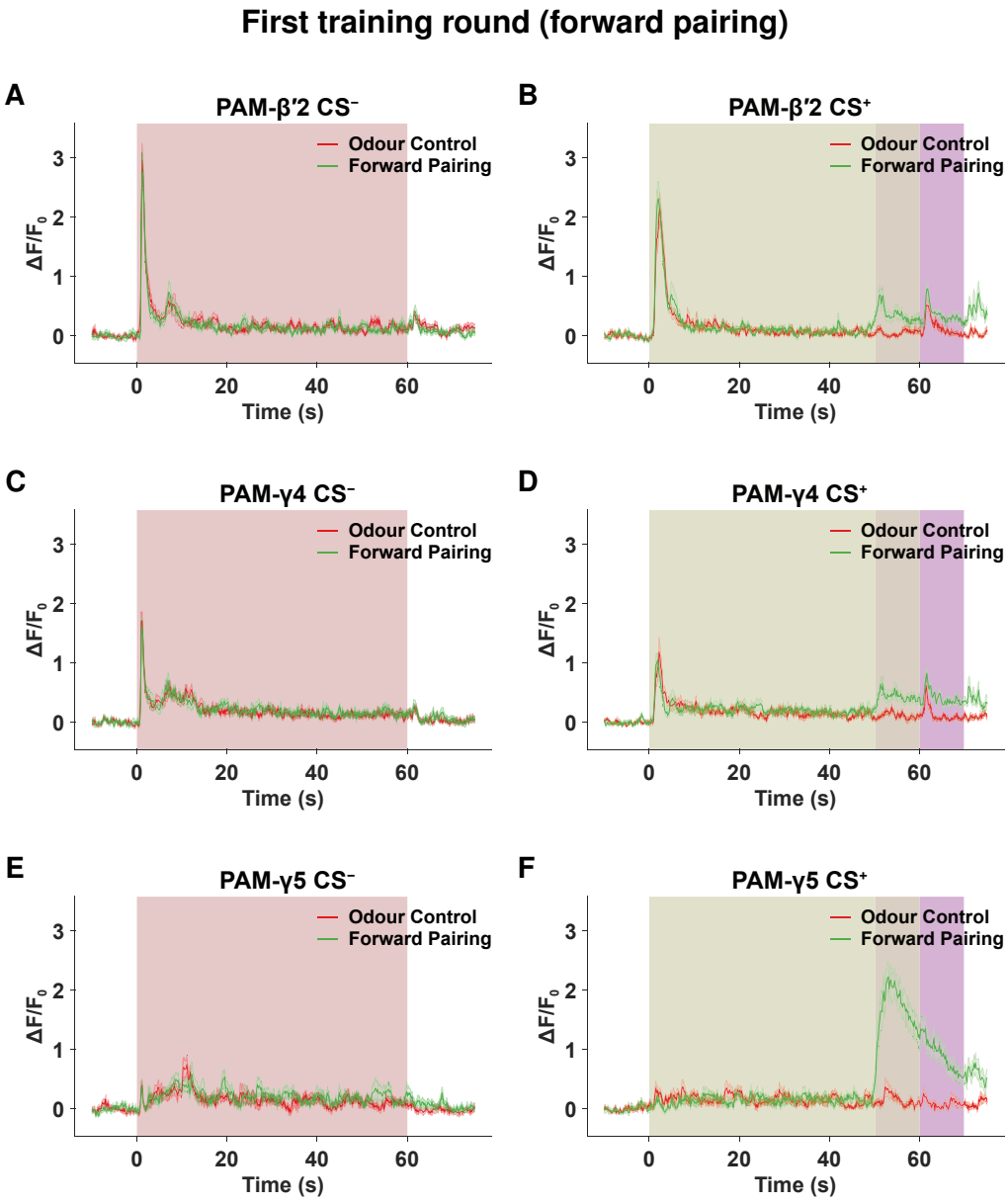

Figure 5.8: The largest difference during the initial forward pairing is the calcium response evoked by sucrose. For both the odour control (red) and forward pairing (green) groups, the first round of training presents the CS^- odour MCH (dark red box) first for 60 s, followed by a 30 s break and then the CS^+ odour OCT (olive box) for 60 s. The forward pairing group also receives the US sucrose (purple box) for 20 s, starting in the final 10 s of the CS^+ (dark olive box). Each row shows a different PAM subset and each column shows responses during either odour. Overall, responses to each odour are similar between groups except for the sucrose response in the forward pairing group. All curves plotted are mean ± SEM; $N = 14$.

signal during training and PAM-γ5 may also convey a greater relative difference between odours after repeated forward pairing.

Next, I compared the backward training group with the odour control, first during the initial round of training and then the final (testing) round. Again, the primary difference during the training round (Figure 5.10) was that evoked by sucrose in the backward pairing group (comparing both response parameters described in Figure 5.7E).

The temporal difference model predicts that after repeated backward pairings, the 'CS$^-$' cue-evoked response should be greater for the backward pairing group than for the odour control. However, both the odour control and the backward pairing group had similar odour responses for most of the response parameters compared (Figure 5.7).

For this comparison, the one clear effect observed in the backward pairing group was a reduced ongoing PAM-γ5 response to the CS$^-$ (the mean in Figure 5.7C) compared to the CS$^+$ (Figure 5.11G). The CS$^-$ ongoing response was also significantly lower than the CS$^-$ ongoing response during the initial training round. In contrast, the ongoing responses to both odours during testing for the odour control group were similar (Figure 5.11H).

To summarize the comparisons above (Figure 5.12), there were two substantial physiological differences between the odour protocol and the pairing protocols. First, sugar presentation during the first training round evokes a substantial response in all R48B04 PAM subsets compared to the odour control and the CS$^-$ odour in either pairing group (Figures 5.12A and 5.12B). Second, during the final (testing) round for either pairing protocol, the ongoing PAM-γ5 response to the odour that predicts reward is depressed relative to the other odour in the paired group, but not compared to the odour control (Figures 5.12C and 5.12D).

These results suggest that the ongoing PAM-γ5 odour response could be conveying a relative comparison between the CS$^+$ and CS$^-$, with a depression towards the odour most likely to be predicting reward. This comparison could be com-

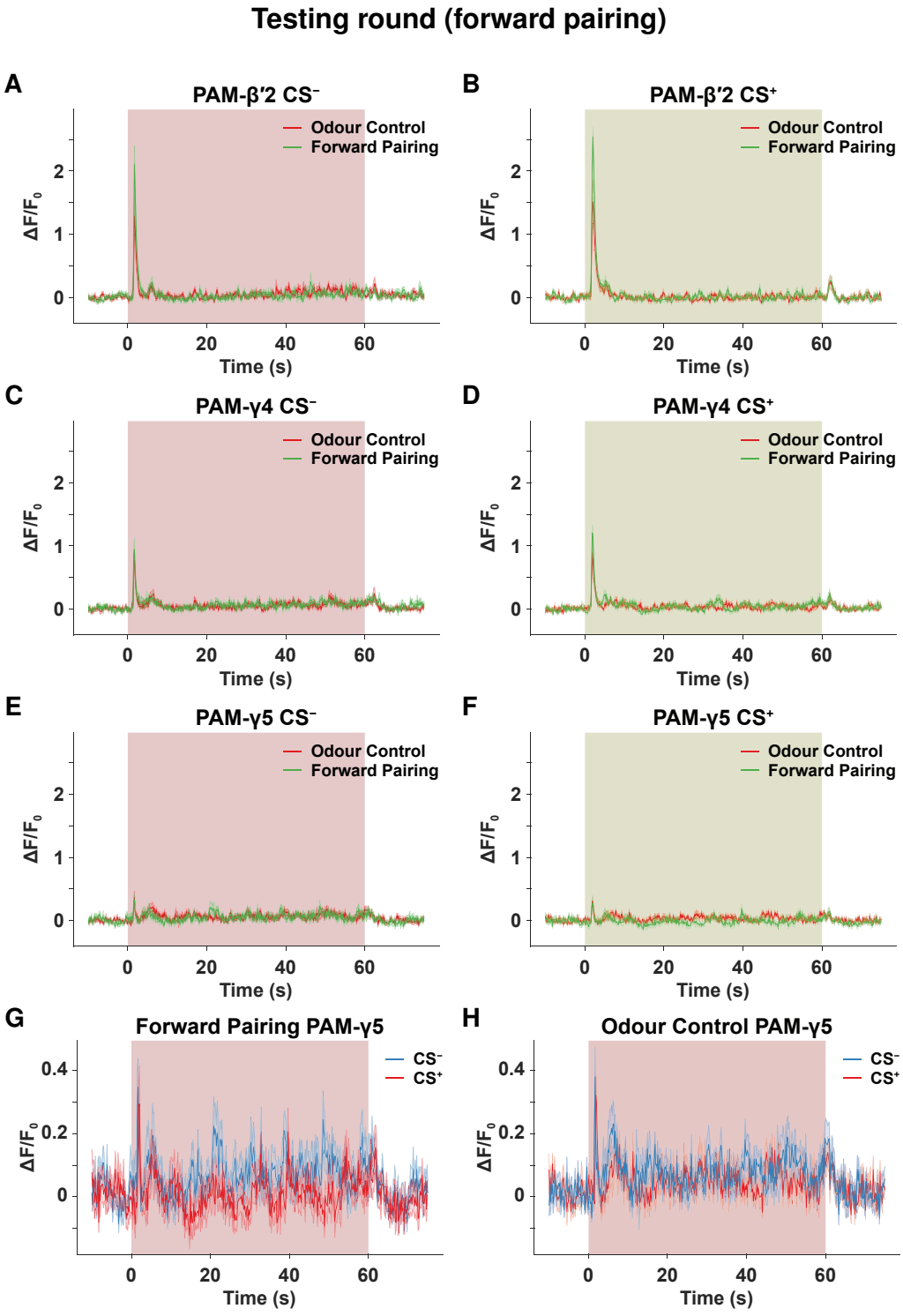

Figure 5.9: Repeated forward pairing induces a relative depression in the ongoing PAM-γ5 response to the CS$^+$ odour. For both the odour control (red) and forward pairing group (green), the final (testing) round presents the CS$^-$ odour MCH (dark red box) first for 60 s, followed by a 30 s break and then the CS$^+$ odour OCT (olive box) for 60 s. Each row shows a different PAM subset and each column shows the response of each group during either odour. Overall, responses to each odour are similar between groups except for **G)** the relative depression in the ongoing CS$^+$ response in PAM-γ5 for the forward pairing group relative to the CS$^-$. **H)** Both odours evoke similar responses in the odour control group. All curves plotted are mean $\pm$ SEM; $N = 14$.

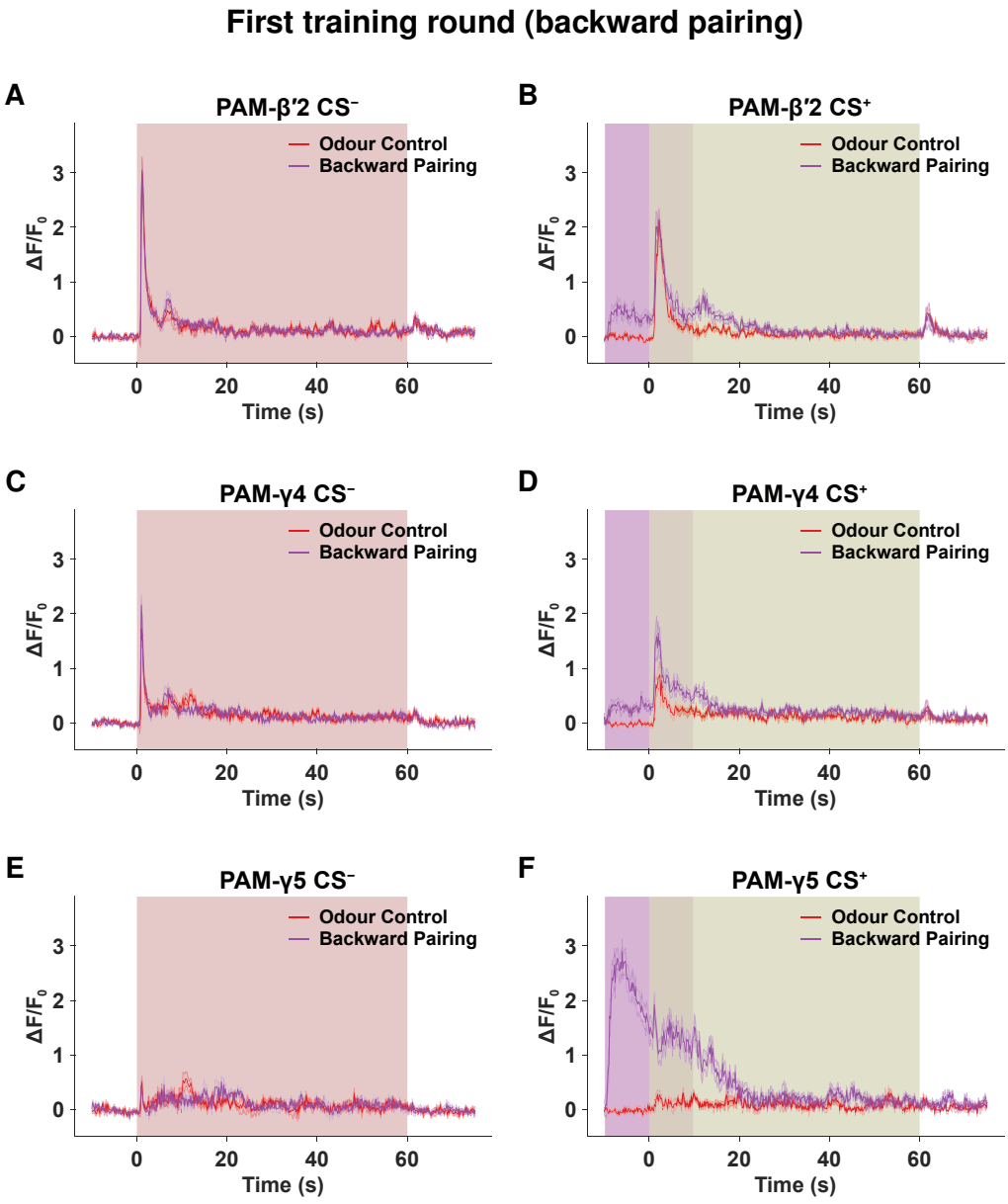

Figure 5.10: The largest difference evoked by backward training is the calcium response evoked by sucrose. For both the odour control (red) and backward pairing group (violet), the first training round presents the CS^- odour MCH (dark red box) first for 60 s, followed by a 30 s break and then the CS^+ odour OCT (olive box) for 60 s. The backward pairing group also receives sucrose (purple box) for 20 s, starting 10 s before the CS^+ and overlapping with it for 10 s (dark olive box). Each row shows a different PAM subset and each column shows the response of each group during either odour. Overall, responses to each odour are similar between groups except for when sucrose is presented to the backward pairing group. All curves are mean ± SEM; $N = 14$.

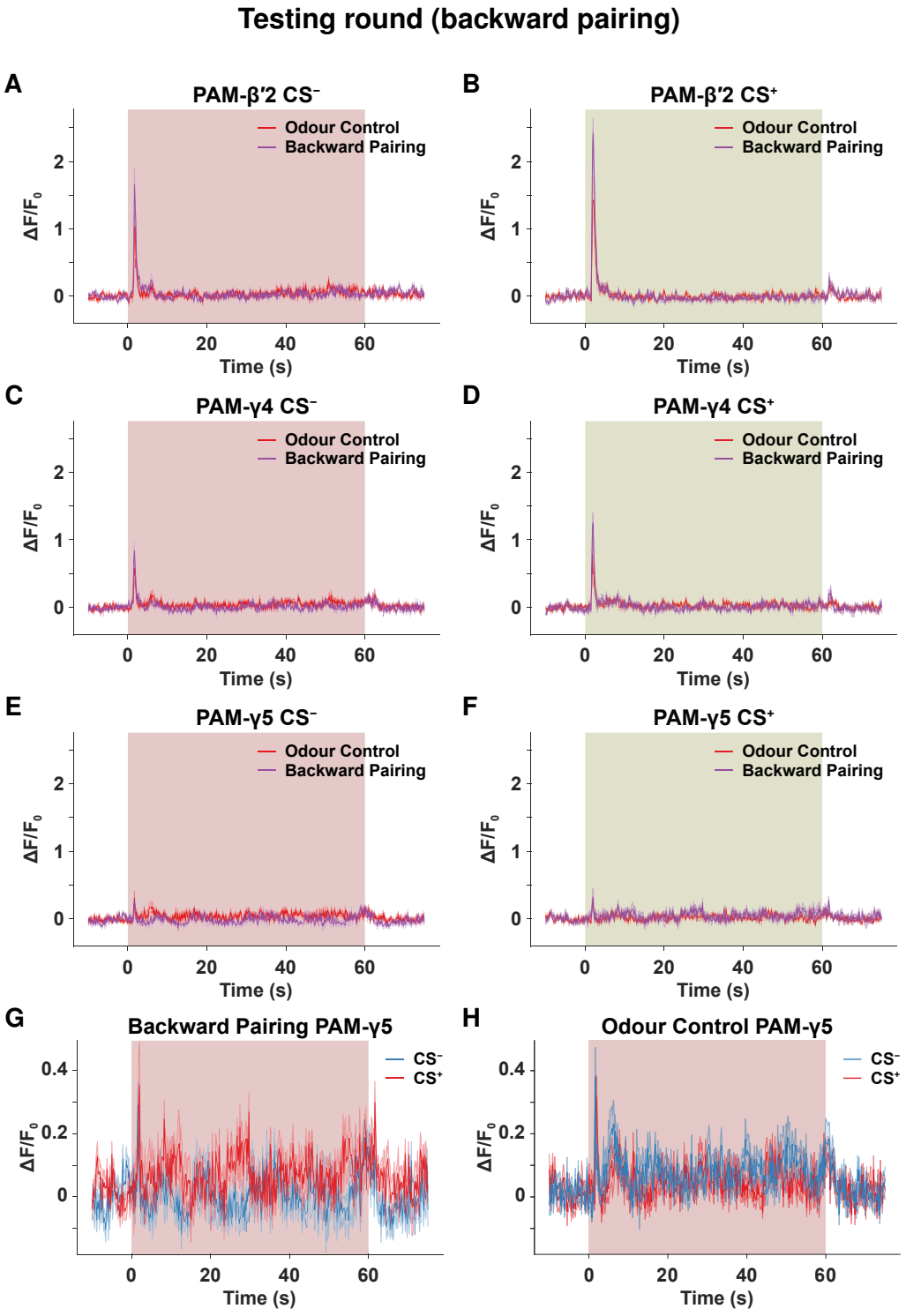

Figure 5.11: Repeated backward pairing induces a relative depression in the ongoing PAM-γ5 response to the CS$^-$ odour. For both the odour control (red) and backward pairing group (violet), the final (testing) round presents the CS$^-$ odour MCH (dark red box) first for 60 s, followed by a 30 s break and then the CS$^+$ odour OCT (olive box) for 60 s. Each row shows a different PAM subset and each column shows the response of each group during either odour. Overall, responses to each odour are similar between groups except for **G)** the relative depression in the ongoing CS$^-$ response in PAM-γ5 for the forward pairing group relative to the CS$^+$. **H)** Both odours evoke similar responses in the odour control group. All curves plotted are mean $\pm$ SEM; $N = 14$.

puted by the PAM neurons themselves or by neurons conveying odour input to them. Otherwise, the results imply that R48B04 neurons primarily deliver a reward teaching signal at the time of feeding. Moreover, it is the coincidence of two calcium signals: the first evoked by the unique response profile to an odour and the second by feeding at a later time that most probably reinforces an association.

A key prediction of the temporal difference model (Section 1.4) is that the increasingly predicted US response diminishes with repeated presentations, whereas the predicting CS response increases over time [2, 94]. Since I paired the CS^+ with the US five times during my protocol (Figure 5.6), I could test this prediction of the model. For each PAM subset, I plotted the peak (maximum, first 5 s) of each CS^+ odour or sucrose feeding response (Figure 5.13). For the CS^+, I compared the forward pairing group with the odour control, and with the sugar control for the US. Any changes observed between these groups should reflect shifts over time due to increasing prediction.

The shift predicted by the temporal difference model suggests an increasing CS^+ response as the US decreases. Although the US diminished with each presentation as expected (Figures 5.13B, 5.13D and 5.13F), especially for PAM-γ5, it diminished similarly for both the sugar control and forward pairing group. In contrast, the CS^+ peak response did not substantially change in any PAM subset for the odour control or the forward pairing group (Figures 5.13A, 5.13C and 5.13E). Taken together with the lack of differences during the testing round, these results suggest that R48B04 neurons do not show acquired predictive capacity after appetitive conditioning as expected from models of reward prediction error.

5.2.6 R48B04 odour responses reflect novelty

Finally, I compared the response profiles of all four treatment groups during their common final (testing) odour presentation round in which MCH, OCT, and the novel odour IAA were presented in sequence to each group (Figure 5.14). This would also show whether prior repeated unpaired feeds affected odour responses.

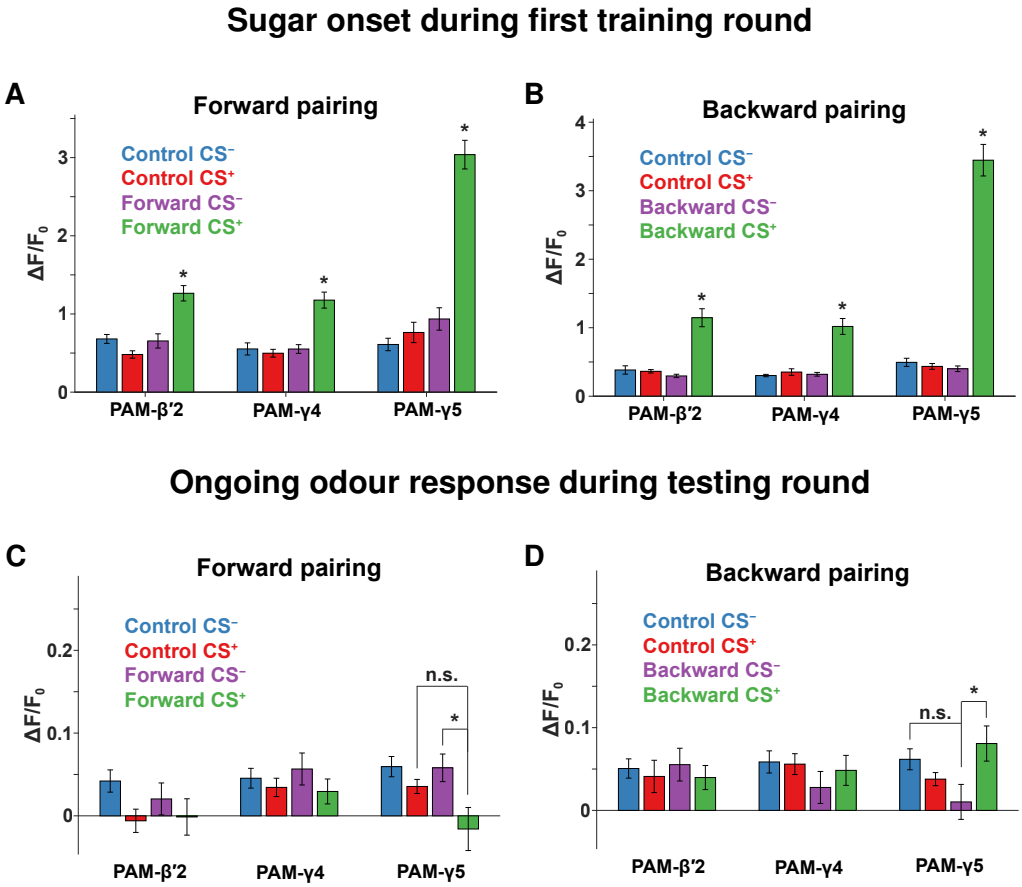

Figure 5.12: Summary of the key differences between calcium signals evoked by the odour control and paired protocols. A–B) For the first training round, both paired protocols have substantially elevated peak responses during sucrose presentation ($p < 0.05$ for each PAM subset, forward/backward CS^+ compared to other odours; Kruskal-Wallis test). Figure 5.7E contains further details about the parameter compared. **C)** For the final (testing) round, the PAM-γ5 mean ongoing response (40 s) is lower for the forward pairing CS^+ than the forward pairing CS^- ($p < 0.05$; Kruskal-Wallis followed by signed-rank test) but not compared to the CS^+ in the control group ($p = 0.16$). No substantial differences in the ongoing odour response between the groups were observed for PAM-β′2 ($p = 0.20$; Kruskal-Wallis test) or PAM-γ4 ($p = 0.57$). **D)** For the final (testing) round, the PAM-γ5 mean ongoing response (40 s) is lower for the backward pairing CS^- than the backward pairing CS^+ ($p < 0.05$; Kruskal-Wallis followed by signed-rank test) but not compared to the CS^- in the control group ($p = 0.08$). No substantial differences in the ongoing odour response between the groups were observed for PAM-β′2 ($p = 0.89$; Kruskal-Wallis test) or PAM-γ4 ($p = 0.53$). Figure 5.7C contains further details about the parameters compared for the testing round. All data plotted are mean ± SEM; $N = 14$.

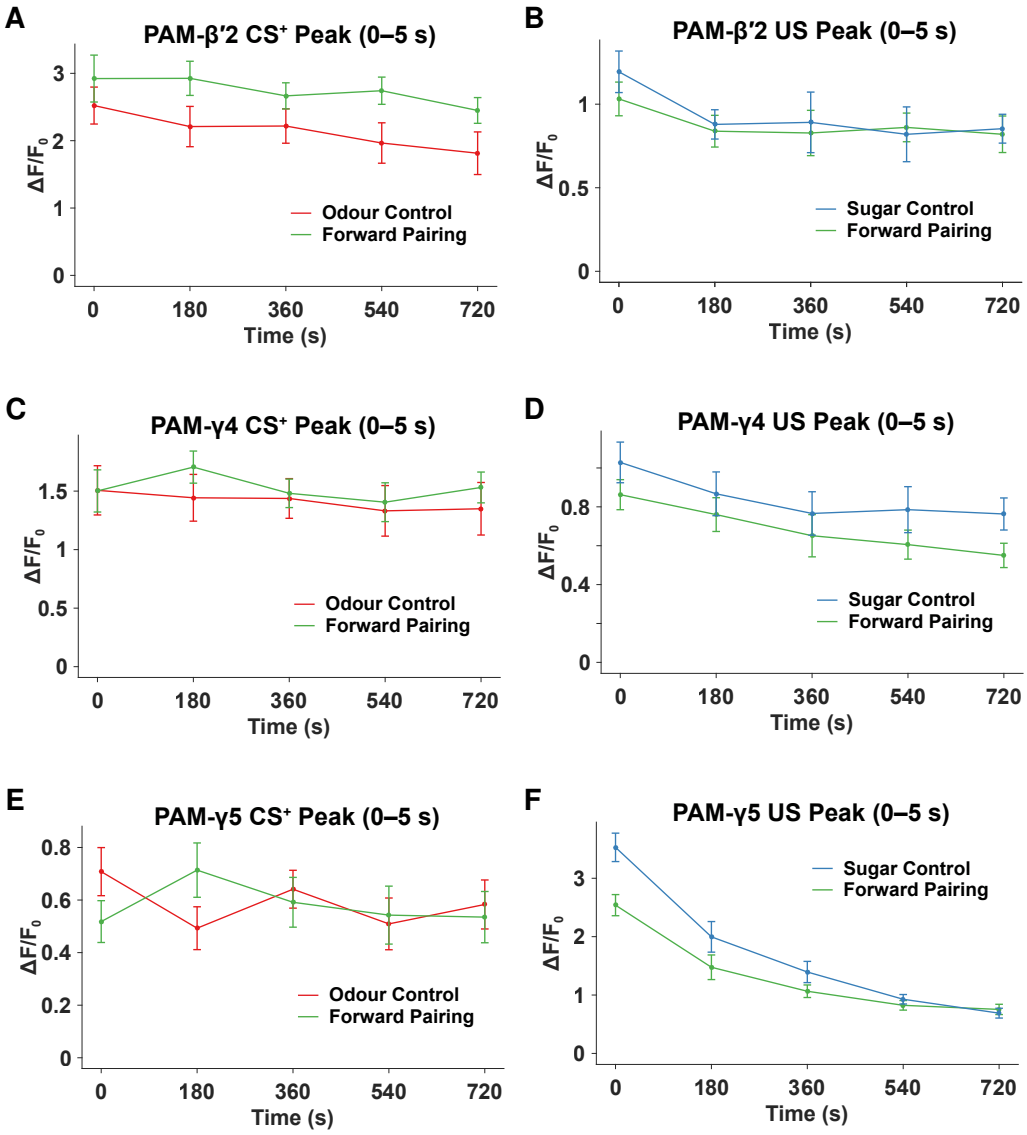

Figure 5.13: R48B04 neurons do not show acquired predictive capacity after appetitive conditioning. A, C, E) The peak (maximum, first 5 s) of the CS^{+} response does not change substantially after repeated pairings in either the odour control (red) or forward pairing (green) groups. **B, D, F)** The peak of the US response decreases substantially after repeated pairings in both the sugar control (blue) or forward pairing (green) groups, particularly in PAM-γ5. All data plotted are mean ± SEM; $N = 14$.

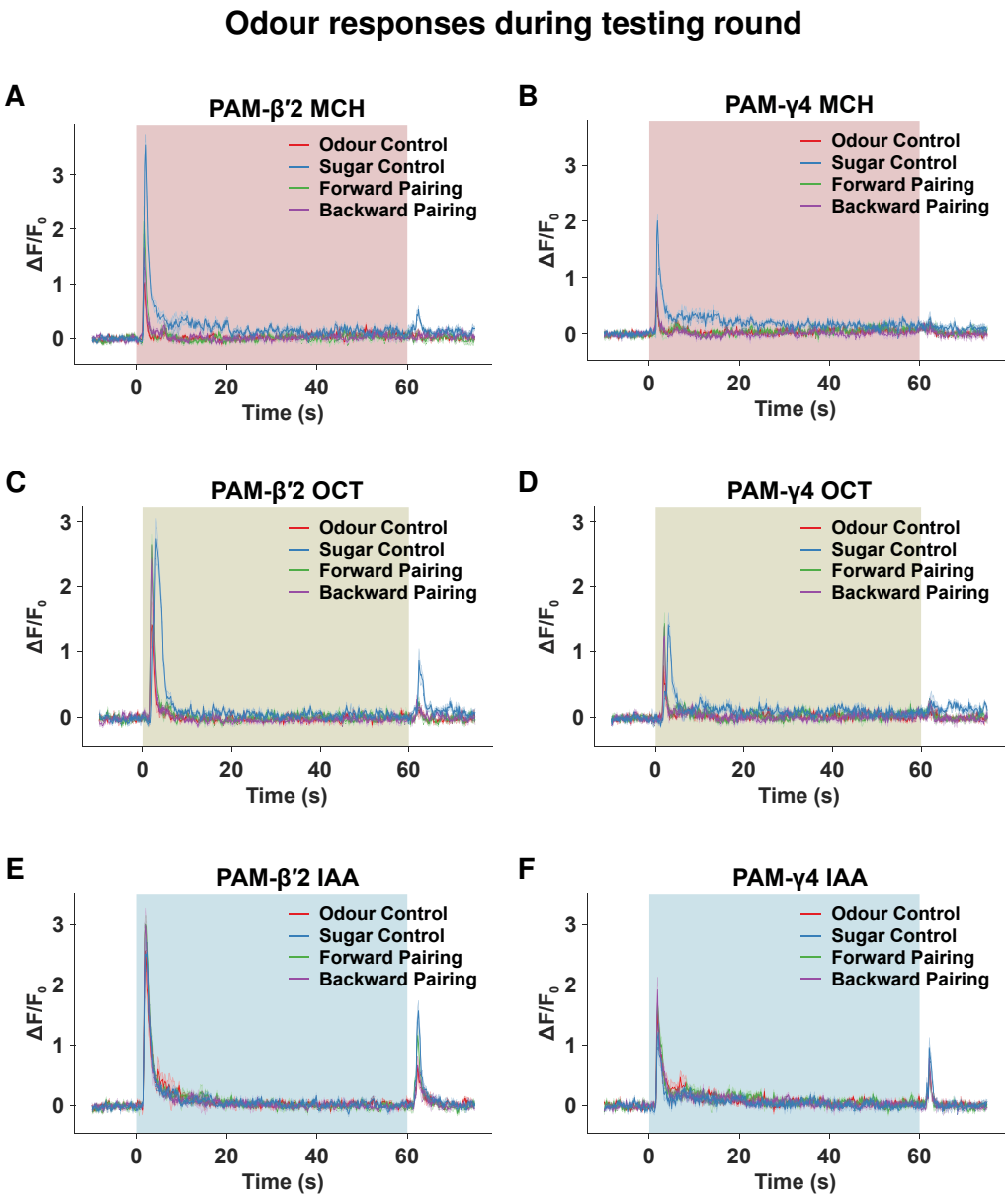

Figure 5.14: R48B04 odour responses reflect novelty. The final presentation round consisting of MCH then OCT then IAA is common to all four treatment groups described in Figure 5.6. While all four groups receive IAA for the first time, only the sugar control group (blue) receives MCH and OCT for the first time during this presentation round whereas the rest receive it for the sixth. **A–B)** MCH evokes PAM-β′2 and PAM-γ4 odour on-responses with the greatest peak and area in the sugar control group that experiences it for the first time. The same applies for the PAM-β′2 odour off-response. **C–D)** OCT evokes odour responses with a similar peak in both groups, but the greatest area in the sugar control group that experiences it for the first time but after MCH has already been presented. The PAM-β′2 odour off-response is similarly larger. **E–F)** IAA evokes similar odour responses in all groups, which all first experience IAA during this presentation. All curves plotted are mean ± SEM; $N = 14$.

The sugar control group that experienced MCH for the first time during the testing round showed odour on-responses in PAM-β′2 and PAM-γ4 with a much higher maximum and area than the other three groups that experienced it for the sixth time (Figures 5.14A and 5.14B). Therefore, the effect of satiety could be immediately ruled out since three groups had this in common.

During the next odour presentation, the sugar control group experienced OCT for the first time but as the second odour following MCH, whereas the other three groups experienced it for the sixth time. The OCT odour on-responses in all groups had a similar height, but the sugar control group had a broader peak with consequently greater area (Figures 5.14C and 5.14D).

The higher response peak to MCH only may convey general novelty to odour presentation, whereas the higher response area and therefore overall magnitude for both odours may convey specific novelty for each odour. IAA, a novel odour for each group, should hence evoke responses of similar height and magnitude in all four groups, even though three of them have already been presented twelve odours. This is indeed the case for all groups (Figures 5.14E and 5.14F), although the sugar control group had a larger odour off-response than two other groups.

Since these effects may be specific to this particular sequence of odours, I also revisited my earlier experiments in which either MCH or OCT was presented first to flies for 120 s (Figure 5.4). When OCT was presented first in those experiments, it also evoked PAM-β′2 and PAM-γ4 responses with a slightly higher peak than when OCT was presented second (Figures 5.4B and 5.4D). Therefore, PAM-β′2 and PAM-γ4 responses appear to convey both general novelty to odour presentation and specific novelty for each new odour regardless of prior experience.

5.2.7 PAM-γ4 neurons may encode prediction error

Although there were hints of possible negative prediction error when reward was omitted in the final round of my repeated appetitive conditioning protocol (Sec-

tion 5.2.5), such prediction errors would be nowhere near the same magnitude as the positive prediction error that results during unexpected sucrose presentation.

Two-photon calcium imaging is generally poor at detecting inhibitory signals and perhaps electrophysiology is better suited for such experiments. Nonetheless, absence of evidence is not evidence of absence. Rather than unexpectedly omitting a reward, I reasoned that a better test of whether R48B04 neurons encode reward prediction error would be unexpectedly presenting a reward instead. The signature of positive prediction error here would be an excitatory response in R48B04 neurons upon receiving sugar reward that is unexpected compared to the reward being preceded by a predictive odour cue.

I used another appetitive conditioning protocol that more closely approximated conditions in the T-maze (120 s of CS^-, then 30 s break, then 120 s of CS^+ with the US presented during the last 90 s, followed by each odour presented again for 120 s each). I omitted the CS^- (MCH) from the testing round and separated flies into two groups: the first (Predicted) group would receive the CS^+ (OCT) for 120 s paired again with the US (sucrose) for the last 90 s, while the second (Surprise) group would only receive the US at the same time as the Predicted group but without the predicting CS^+ odour (Figure 5.15A).

After comparing the second sucrose presentation (either Predicted or Surprising) response profiles, I found that PAM-γ4 neurons had a larger response when the reward was surprising (Figure 5.15C). This was the case for both the peak and area of the response (Figures 5.15E and 5.15F). In contrast, PAM-β'2 and PAM-γ5 responses were similar between both groups (Figures 5.15B and 5.15D). Although further verification is needed, the results here suggest that rewarding dopaminergic neurons in adult *Drosophila* may encode prediction error after all.

5.2.8 Optogenetic stimulation in the T-maze

Finally, I tested whether the two different appetitive conditioning protocols attempted in this chapter could reinforce appetitive approach in the T-maze. How-

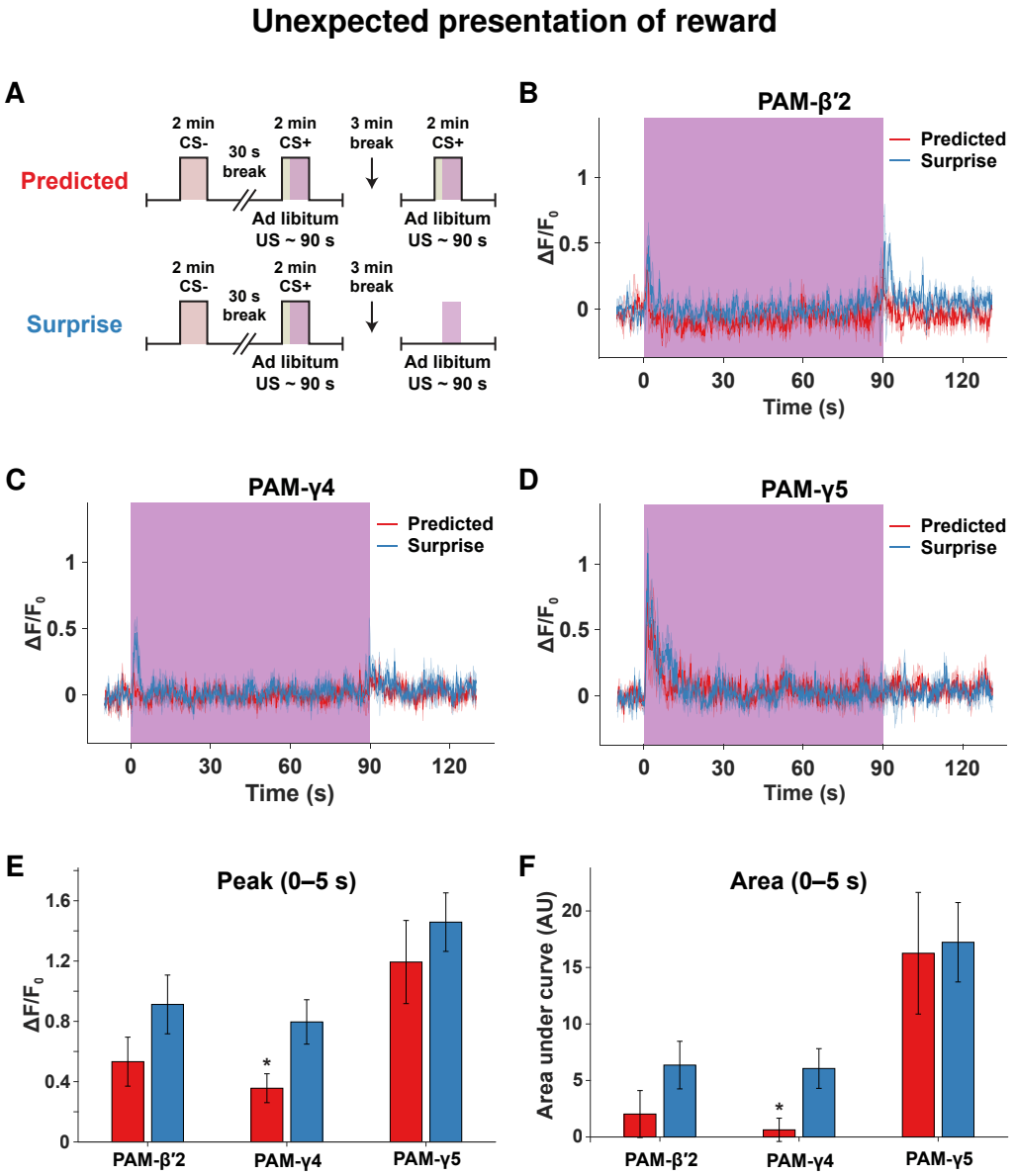

Figure 5.15: PAM-γ4 neurons display positive prediction error during the presentation of unexpected reward. A) All flies in the two treatment groups, Predicted (red) and Surprise (blue), experienced pairing of the US (1 M sucrose) with the CS^+ during training but only the Predicted group experienced this pairing a second time. The Surprise group received the US a second time without the predicting CS^+. **B)** The second presentation of sucrose evoked similar PAM-β′2 responses in both groups. **C)** In PAM-γ4 neurons, the second presentation of sucrose evoked a larger immediate feeding response in the Surprise group. **D)** The second sucrose feed evoked similar PAM-γ5 responses in both groups. **E)** The second sucrose presentation evoked a larger peak response (maximum, first 5 s) in the Surprise group for PAM-γ4 ($p < 0.05$, two-sample t-test) but not PAM-β′2 ($p = 0.16$) or PAM-γ5 ($p = 0.45$). **F)** The second sucrose presentation also evoked a response of greater overall magnitude (area, first 5 s) in the Surprise group for PAM-γ4 ($p < 0.05$, two-sample t-test) but not PAM-β′2 ($p = 0.17$) or PAM-γ5 ($p = 0.88$). All data plotted are mean ± SEM; each group $N = 8$).

ever, in a standard T-maze training paradigm, reward is usually presented simultaneously with the CS^+ odour as dried sucrose paper rolled up into the training tube [69]. To test delayed reward conditioning, I substituted reward with optogenetic stimulation of R48B04 neurons using CsChrimson::mVenus [201] instead.

First, I adapted the four multi-round conditioning protocols described in Figure 5.6 to the T-maze, replacing reward presentation with CsChrimson stimulation (Figure 5.16A). I compared the four protocols with standard pairing, in which the CS^+ odour was paired with R48B04 stimulation for 120 s. However, the forward pairing protocol did not result in approach towards the CS^+ odour after the five training rounds (Figure 5.16C). In contrast, standard pairing resulted in robust approach, replicating previously published experiments using dTrpA1 [35, 36].

Next, I adapted the single delayed (90 s) pairing protocol for the Predicted group in Figure 5.15A, with the difference that the flies had a choice between the CS^+ and CS^- during the second (testing) round (Figure 5.16B). Delayed pairing was compared with the standard pairing and controls in which only odours or 90 s stimulation was provided before testing. Both paired protocols resulted in robust approach compared to the controls (Figure 5.16D).

Taken together, the two experiments suggest that the protocol with 90 s reward presentation more effectively trains flies. Observing the behaviour of the flies during optogenetic stimulation, however, suggested another possible reason. Upon optogenetic stimulation of R48B04-GAL4 neurons, flies rapidly bounce about in the training tube for the first 5 s to 10 s, followed by jitters and general motionlessness for the next 30 s. The flies then recover their movement and jitter about rhythmically for the remainder of the stimulation.

Since R48B04-GAL4 also labels neurons in the ventral nerve cord [199], pulsing red light appears to activate CsChrimson not only in PAM neurons but also in motor neurons outside the reinforcement circuitry. Therefore, optogenetic R48B04 stimulation for only 20 s does not reinforce the CS^+ odour, possibly because motor neuron output appears to dominate the first 40 s of stimulation.

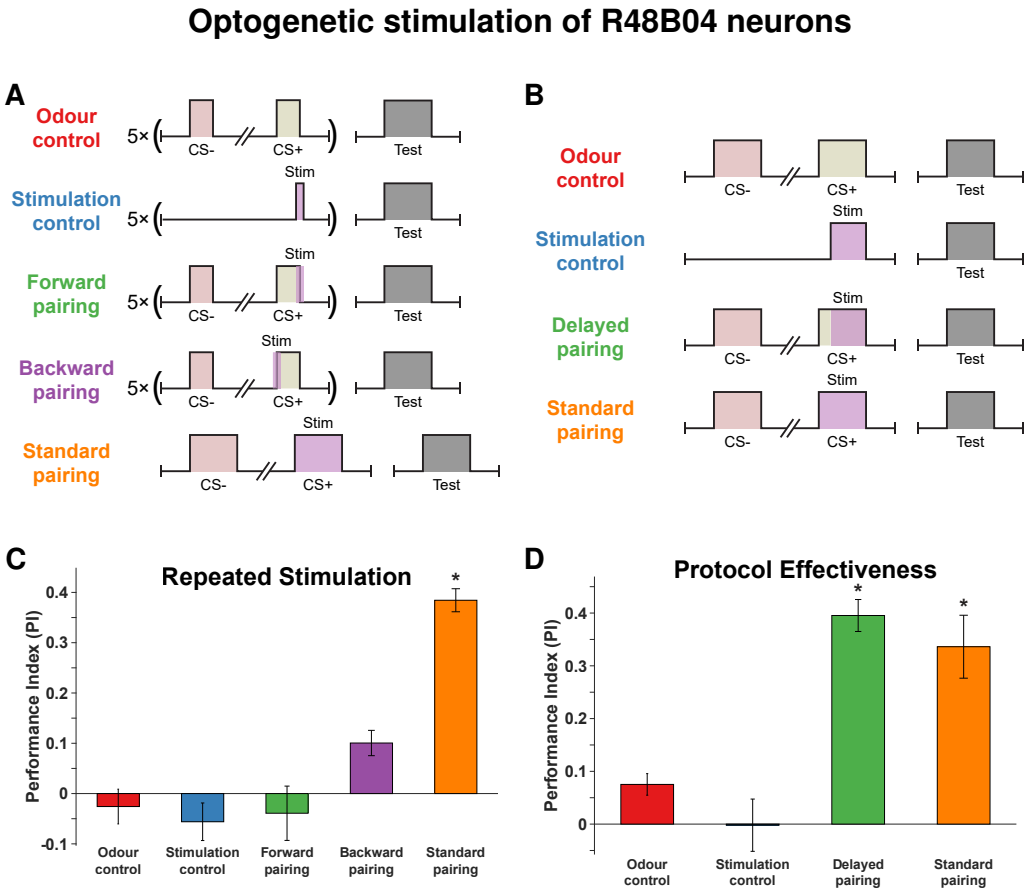

Figure 5.16: Appetitive conditioning in the T-maze with optogenetic substitution of reward. **A)** In the first experiment, the four-multi-round appetitive conditioning protocols described in Figure 5.6 were presented to flies in the T-maze, replacing sucrose presentation with 20 s CsChrimson stimulation (Stim) of R48B04 neurons. The four multi-round protocols were compared with standard pairing, in which odours were presented for 120 s and CsChrimson stimulation was provided for the entire duration of the CS^+ odour. A 2 min testing round (choice between CS^- and CS^+) was provided 30 s after the last training round. **B)** In the second experiment, the same standard pairing protocol was compared with delayed pairing in which flies were presented with the single delayed (90 s) conditioning protocol for the 'expected' treatment group in Figure 5.15A, with the difference that the flies had a choice between the CS^+ and CS^- during the second (testing) round. The two pairing groups were compared to two control groups (odours only or 90 s stimulation only). **C)** For the first experiment, only the standard conditioning protocol (simultaneous 120 s R48B04 stimulation with the CS^+ odour) leads to robust approach behaviour ($p < 0.0001$ compared to all other groups, $N = 3$; ANOVA). The backward pairing protocol may induce less robust approach behaviour ($p = 0.057$ compared to zero; one-sample t-test), whereas the other protocols do not ($p > 0.27$ for each protocol compared to zero; one-sample t-test). **D)** For the second experiment, both paired protocols resulted in robust approach ($p < 0.005$ for each paired protocol compared to the two controls, $N = 5$–7; ANOVA followed by *post hoc* Tukey's HSD test). All data plotted are mean ± SEM.

5.3 Discussion

5.3.1 Results summary

Sugar presentation evokes R48B04 responses primarily upon onset (Figures 5.1 and 5.4), although there are some differences between PAM subsets. The onset of initial feeding evokes a single peak in all PAM subsets irrespective of presentation length, but the response in PAM-γ5 decays the slowest and only this subset responds to renewed droplet contact mid-presentation (Figure 5.1). Since R48B04 neurons also show state-dependent valuation (Chapter 3), PAM-β'2 and PAM-γ4 appear to convey the value or salience of initial feeding, whereas PAM-γ5 conveys the same for each new feeding and droplet contact.

Prolonged odour presentation evokes at least one peak upon onset in all PAM subsets, but this is followed by a possible second prominent peak in PAM-β'2 and PAM-γ4 depending on the odour, or generally elevated activity in PAM-γ5 (Figure 5.4). Therefore, all three PAM subsets respond substantially to odours throughout their presentation. These experiments for both feeding and odours also reveal calcium signal dynamics in PAM neurons that are not apparent from typical protocols presenting stimuli once or for only 5 s (Chapters 3 and 4).

The PAM subsets also respond differently to repeated presentations of stimuli in different contexts. Responses to a 5 s sucrose presentation every 10 min do not decay substantially with repeated presentations for each PAM subset (Figure 5.2), but decay is noticeable if they are spaced apart every 3 min instead (Figure 5.3). Similarly, PAM-β'2 and PAM-γ4 responses to repeated odours spaced 180 s apart (Figure 5.13) do not decay as they do when they are spaced 40 s apart (Figure 3.7). Finally, both of these subsets have odour-evoked responses that reflect general or specific novelty in the height or overall magnitude of their first odour on-response respectively (Figure 5.14).

Calcium imaging throughout a multi-round appetitive conditioning protocol (Figure 5.6) suggests that R48B04 PAM neurons primarily play a role during

training by conveying the reward signal (Figures 5.8 and 5.10). The activity of R48B04 dopamine neurons during this protocol does not correspond with the predictions of the temporal difference model (Figure 5.13). Responses to repeated presentations of the CS^+ do not change for either paired or unpaired odour groups, while responses to repeated presentations of the US similarly decrease in the paired and unpaired feeding groups.

After repeated pairing, the only learning-induced change observed during the unexpected omission of reward (Figures 5.9 and 5.11) was a relative depression in the ongoing PAM-γ5 response to the odour that was most likely to predict the reward (Figure 5.12). Another protocol testing the unexpected presentation of reward, however, suggests that at least PAM-γ4 may encode positive prediction error due to its larger response to unpredicted reward (Figure 5.15).

5.3.2 The origin of PAM responses in different contexts

The experiments in this chapter have revealed much about the calcium dynamics of R48B04 PAM neurons in different contexts. The first is that all of the PAM subsets involved in short-term appetitive memory respond substantially to both odours and reward throughout the duration of their presentation. Current models of associative learning in the mushroom body do not account for DAN responses to odours in general [172, 287], let alone the possibility that they may convey general and specific stimulus novelty.

Odour novelty in the mushroom body has previously been studied by Hattori et al. (2017) [288]. The authors found that MBONs of the $\alpha'3$ compartment respond strongly to the initial presentation of an odour but their responses to subsequent presentations of the same specific odour rapidly diminish due to the odour-evoked activity of the PPL1-$\alpha'3$ DAN [288]. However, Hattori et al. did not investigate the MBONs M4/M6, nor did they seek to distinguish general odour novelty from specific odour novelty. My observation that R48B04 DAN odour responses reflect general and specific odour novelty (Figure 5.14) could be followed up with

shorter and simpler multi-round protocols that present only odours while imaging R48B04 or PPL1-α′3 DANs. For example, the odour control in Figure 5.6A could be compared with a similar protocol without five odour presentation rounds before the final round. It would also be essential to compare different permutations of odours and odour combinations beyond MCH, OCT, and IAA.

Although the experiments in this chapter provide evidence that R48B04 responses reflect odour novelty, R48B04 neurons perhaps also respond to sugar novelty similarly. Repeatedly feeding flies the same sugar or different sugars alternately at different time intervals may be informative. Preliminary evidence for L-fucose presented for 5 s every 10 min (data not shown) suggests that the responses it evokes decay more substantially than sucrose does. Since supplementing fucose with sorbitol leads to similarly decaying responses (data not shown), this may reflect a sucrose-specific effect that requires further investigation.

Given that R48B04 DANs respond substantially less to sucrose in satiated flies than in starved flies, it may seem surprising that sucrose presented every 10 min should not evoke progressively decaying responses with increasing satiety. However, these results instead support the hypothesis that R48B04 DANs are gated by more discrete representations of deprivation state rather than a graded deprivation signal. The upstream neurons that presumably signal deprivation state to these PAM neurons remain unknown.

Although decaying responses to repeated stimuli may reflect negative prediction error or even habituation, it is curious that this takes place on shorter temporal dynamics for odours than for sucrose. At 3 min spacings, responses to both paired and unpaired odours maintain similar magnitude with repeated presentations whereas sucrose responses diminish with each presentation. However, it is worth noting that sucrose was either presented for 5 s every 10 min or for 20 s every 3 min. Differences in feeding length and total feeding time may also influence the rate at which sucrose responses decay. It would be informative to test 20 s feeds every 10 min to determine if a similar decay can be induced.

Different decay dynamics at the very least reflect that odours and sugars are conveyed to R48B04 neurons differently; identifying the possible source of stimulus inputs (neuronal [64] or haemolymph [245]) would be a necessary next step. First, to determine whether sugars reach PAM neurons rapidly, luciferase could be expressed in the PAM neurons of flies that consume food mixed with luciferin [245]. Next, to reveal where sugar or odour signals in DANs come from, recording calcium signals in DAN dendrites or cell bodies instead of the axons during odour or sugar presentation would be insightful.

Since PAM subsets are not anatomically segregated at the dendrites as they are at the axon terminals, GAL4 drivers labelling specific PAM subsets would need to be used. A number of driver lines exclusively labelling a subset of PAM-$\beta'2$ or PAM-$\gamma5$, for example, are already available [170, 289]. KC activity is the most likely origin of odour responses in DANs; optogenetically stimulating KCs under different conditions while recording from DAN axon terminals [289] could test whether KCs are the sole origin of DAN odour responses.

Differing R48B04 decay dynamics could help define a specific time window over which R48B04 DANs can encode prediction error as neurons that reinforce short-term appetitive memory [35, 36]. Alternatively, these differing responses could reflect interactions between associative learning and habituation that have not been explored for DANs in *Drosophila* [290].

Finally, any imaging protocol with more than one droplet presentation introduces unwanted uncertainty for the blue dye feeding verification approach used throughout this thesis. Although the success of the first presentation can be verified using expected calcium responses, with subsequent presentations it becomes less clear whether a fly actually consumes the droplet again. One way to address the problem would be to present another droplet with a different coloured dye for each subsequent presentation.

5.3.3 PAM responses during appetitive conditioning

For appetitive conditioning, the most prominent training-specific response in R48B04 PAM neurons is evoked by sucrose presentation during training. The relative depression in PAM-γ5 ongoing odour responses observed during testing raises the question of whether the underlying process is bidirectional plasticity or plasticity in different places. MBON-γ2α'1 is connected to PAM neurons and drives DAN responses to the CS$^-$ odour [61]. It is possible that MBON-γ2α'1 drives a slight increase in the PAM-γ5 response to the CS$^-$ odour when it does not predict the reward. Moreover, the relative activity changes observed in PAM-γ5 may be consistent with previous findings that odour-evoked responses of MBON-β'2mp are bidirectionally altered in the β'2 compartment after appetitive conditioning [58].

Dopaminergic neurons in mammals often continue responding to food for up to a few hundred training trials before switching to predictive reward cues [291]. Therefore, it is possible that the multi-round appetitive conditioning protocol used in this chapter simply did not have anywhere near enough pairings to evoke a clear reward prediction error in *Drosophila* neurons. The same behavioural and physiological variability observed for mammals during initial training trials could also apply for fruit flies. However, if prevailing reinforcement learning models posit that learning is primarily driven by prediction errors [86] and *Drosophila* can form a robust appetitive memory after a single training trial [25, 26], then it logically follows that some signature of reward prediction error should already be present in *Drosophila* after at least a few training trials.

Although the PAM-γ5 responses observed during the unexpected omission of reward were small and difficult to detect, aversively reinforcing DANs appear to be activated by the lack of expected reward [61]. In the context of unexpected presentation of reward, the positive prediction error observed in PAM-γ4 suggests that DANs in *Drosophila* may be heterogeneous in that some can encode reward prediction errors whereas others have different roles.

To rule out the presence of odour as the cause of a lower sucrose response, follow-up experiments should first test whether the apparent positive prediction error is also present when the CS^- or a novel odour is unexpectedly presented together with the reward. It would also be important to determine whether these observations are generalizable to different combinations of odours and how they compare with two equivalent unpaired sucrose presentations.

Should the next experiments confirm prediction error in PAM neurons, then altering the probability of shorter but more frequent rewards could allow more sophisticated tests of the temporal difference model [85]. Altogether, the experiments in this chapter have revealed the physiology of R48B04 PAM neurons during appetitive conditioning for the very first time, both during the unexpected omission of reward and during the unexpected presentation of reward.

5.3.4 Designing an appetitive conditioning protocol

Investigating the physiology of dopaminergic neurons with two-photon calcium imaging is non-trivial without an established protocol. A simple protocol, for example, would be to pair a 10 s odour with 5 s reward and test for calcium signal changes to the odour 60 s later, but there is little evidence that flies would actually learn in such a paradigm. On the other hand, a tethered fly preparation by definition does not allow flies to move or make choices as they would in a T-maze. Designing an effective appetitive conditioning protocol therefore requires compromise between testing physiological responses of interest and achieving associative learning.

First, I reasoned that a protocol similar to the T-maze would ensure associative learning, yet even such a simple protocol requires many important decisions. Some investigators pre-expose flies to each odour used during training [127, 128, 177, 282]. I opted against pre-exposure because it is not common in standard T-maze behavioural paradigms [66–69]. Consequently, I could only compare the paired CS^+ response during training with an unpaired response during testing,

rather than a hypothetical CS^+ response before training with learning-induced changes after training.

For practical reasons, most appetitive T-maze experiments pair odours with reward simultaneously [66, 69]. However, since R48B04 neurons have distinct calcium responses during both feeding and odour presentation, the calcium responses evoked by simultaneous pairing would be more difficult to interpret. To distinguish between responses evoked by different stimuli, I decided to delay US presentation until the initial CS^+ responses were evoked. Delayed pairing would require odour presentation of at least 20 s before reward, and assumes that there is still a sufficient coincidence of activity simultaneously evoked by both odours and sugars to induce associative learning.

The length of reward presentation is similarly not trivial, because it is not possible to reproduce the random feeding bouts that flies undertake during training in the T-maze. If sugar presentation is too short, then flies could learn to associate the CS^+ with both presentation and withdrawal of reward. Conversely, if presentation is too long, then flies could possibly develop an aversion to continuous droplet contact with the proboscis. It is also unclear whether flies need to feed for a sufficient period of time to make the association, and if so, how this varies between sugar-water droplets and dried sugar.

Deciding when to present each odour also presents problems. During training, it is straightforward to present the CS^- odour then the CS^+ odour paired with reward, although some physiological and behavioural protocols present them in the opposite order. However, during testing, it is not possible to present tethered flies with a meaningful choice between two odours as in the T-maze. Some investigators present only the CS^- or the CS^+ odour during testing [282], but at the cost of doubling the number of samples required for a protocol that may not actually induce associative learning.

In any case, a successful protocol would also need to be duplicated with the odours in reciprocal order to account for any potential odour bias, as is the stan-

dard in T-maze experiments [66, 69]. I initially opted to present the CS^- then the CS^+ during testing in a similar sequential order to training, allowing me to record any learning-induced changes to either odour during training. However, the CS^- also presumably gains some predictive power during training and presenting it again before the CS^+ may unintentionally further reinforce associations between the CS^- and reward.

The ultimate value of an experiment is measured by its controls, and an appetitive conditioning protocol is no exception. The most difficult decisions arose when devising a mock protocol, particularly ensuring that flies in the mock treatment group could provide a valid comparison with the trained group. The obvious approach to present exactly the same protocol and simply omit reward presentation [282] ultimately scuppered most of my protocol iterations. A frequent problem I encountered was that the response to the initial CS^- odour was on average larger in the mock group than in the trained group. Such an observation was unexpected because both protocols would be identical until reward presentation during the initial CS^+. However, not presenting the reward to the mock group at all obscured an important difference in the way I treated both groups.

Impending fly death is foreshadowed by an irreversible rise in intracellular calcium, and starved flies are presumably closer to death than satiated flies. I observed that stimuli presented to such flies before the intracellular rise occurs actually evoke responses at least thrice as large as usual, and primarily to the first presentation of any stimulus type (data not shown). Starved flies that appear to be functioning normally but are actually not far from death also tend not to consume any droplet that is presented to them.

For the experiments in which I observed the initial CS^- discrepancy, flies in the training group were excluded if they were non-responsive to either droplets or odours. In contrast, flies in the mock group were only excluded if they were non-responsive to odours. Since I had not tested whether flies in the mock group actually had a motivation to feed or had normal feeding responses, I possibly

included flies that would otherwise have been excluded had they been in the training group. Such flies presumably had larger odour-evoked calcium responses and skewed the mock group towards having a larger average response to the CS^- than the trained group.

Due to the procedural problem, I had to exclude many of my attempts at appetitive conditioning under the microscope, including those that most closely resembled conditions in the T-maze. In brief, these protocols presented each odour for 120 s with 30 s break in between, feeding during the final 90 s of the initial CS^+, and 120 s between the training and testing round. Such a protocol could be reattempted, provided that flies in the mock group are tested for feeding responses towards the end of each recording. The two conditioning protocols included in this chapter did not have such a CS^- discrepancy because both protocols presented flies in all treatment groups to both odours and sucrose.

The multi-round conditioning protocol (Figure 5.6), although long and arduous for each sample, provided a better test of the temporal difference model than a standard T-maze-like protocol, which only presents the reward once. To keep the recording as short as possible, I presented each odour during each training round for 1 min because flies can still form an appetitive memory after 1 min of training [34]. Moreover, I presented the reward for 20 s at the end of each CS^+ because it was the average first bout length for sweet and nutritious sugars when I tested flies in the feeding assay (Figure 3.3B).

While the multi-round odour control and the sugar control provided insightful comparisons with the forward pairing group, perhaps an unpaired control that presented the CS and US in a pseudorandom sequence (e.g., the unpaired control used by Dylla et al. (2017) [128]) could have been more informative than the backward pairing group. By decoupling the CS and the US, an unpaired control would have illuminated the effect of CS-US pairing in general rather than a presumably less effective form of CS-US pairing.

5.3.5 Linking physiology with behaviour

The experiments using optogenetic substitution of reward in the T-maze (Figures 5.16A and 5.16B) used stimulation parameters (500 Hz for >10 s) that perhaps activate R48B04 neurons substantially more than suggested by the single peaks observed during 120 s odour sampling or sugar consumption under the microscope (Figures 5.1 and 5.4). Although the 120 s standard pairing and 90 s delayed pairing protocols in Figure 5.16B induce robust approach behaviour (Figure 5.16D), follow-up experiments should determine whether activation of R48B04 neurons on a shorter timescale is also sufficient.

When I attempted to test whether the multi-round protocol reinforced approach in the T-maze (Figure 5.16A), however, I encountered the problem whereby R48B04-GAL4 optogenetic stimulation appears to stimulate motor neurons and then evoke general motionlessness for the first 40 s of stimulation. In contrast, such behaviour is not observed when stimulating R58E02-GAL4 (P. Cognigni, personal communication), another driver that labels most PAM neurons including those labelled by R48B04-GAL4. Therefore, a necessary next step would be to block R48B04 expression in the ventral nerve cord using tsh-GAL80 [292] and test whether optogenetic stimulation of R48B04 PAM neurons alone evokes similar behaviour. Alternatively, fewer repeated rounds (for example, three) with longer presentations of each reward could perhaps circumvent the problem.

A key goal of appetitive conditioning under the microscope would be to evoke increased PER to the CS^+ after training. The same memory that induces odour-evoked approach in the T-maze is also assumed to induce increased PER. It would be informative to tether flies and then observe PER frequency while optogenetically manipulating MBONs whose activation or inhibition induces odour-evoked approach or avoidance behaviour. One such MBON candidate would be the MBON M6, whose upstream KCs receive inputs from PAM-$\beta'2$ and PAM-$\gamma5$ [170] and whose blocking converts naive odour avoidance into attraction [172].

The only previous study to attempt appetitive conditioning for PER [284] (but not under the microscope) observed that spontaneous proboscis movements limit the observation of odour responses. Moreover, it noted that the more tethered the flies, the more frequent proboscis PER became [284]. Tethering in general induces stress in flies and may have a non-trivial effect on their learning. To reduce stress significantly, it would be ideal to record from flies that are freely moving [293, 294], although such an approach is not yet a widespread practice. Flies tethered in my setup did indeed show spontaneous PER, but I also observed that different odour sequences could evoke different PER frequencies (Figure 5.5B). My observations suggests that odour-evoked PER responses can nonetheless be observed, even in the presence of spontaneous PER.

The differential PER frequencies evoked by odours suggest that even if training ultimately evoked more PER to the CS^+ during testing than in the mock group, it sometimes would not be different to the PER evoked to the CS^- during testing in the trained group. Consequently, it would fail to meet the second criterion for learning-induced changes that I specified in Section 5.2.4. Lowering and optimizing the concentrations of the odours presented may reduce odour-evoked PER differences and allow learning-induced comparisons.

Although such further optimization may seem somewhat tedious, it would be a small price to pay to link two-photon calcium imaging with behavioural readout in the same individual. A successful protocol could ultimately illuminate the underlying causes of considerable variation in memory expression that arises from individual flies that have the same experience during training.

5.4 Conclusion

The experiments in this chapter have revealed the physiological responses of rewarding dopaminergic neurons during appetitive conditioning in adult *Drosophila*

for the first time. Moreover, they show that R48B04 PAM neurons signal sugar and odour salience differently depending on their frequency and novelty.

R48B04 PAM neurons do not show acquired predictive capacity after appetitive conditioning as expected from current models of reward prediction error. However, PAM-γ4 neurons appear to encode positive prediction error because they are excited by the unexpected presentation of reward. In contrast, the unexpected omission of reward may encode a relative depression in the ongoing CS^+ response in PAM-γ5, although this is difficult to detect with calcium imaging.

Decaying PAM responses to repeated stimuli may reflect negative prediction error or even habituation, but this takes place on shorter temporal dynamics for odours than for sucrose. These different decay dynamics suggest that odours and sugars are conveyed differently to R48B04 PAM neurons. Intriguingly, PAM responses evoked by odours appear to reflect both general and specific novelty. The different response components changed by each kind of novelty can similarly illuminate how dopaminergic neurons encode other types of stimuli.

Together with the results from the previous two chapters, the findings here show that rewarding dopaminergic neurons in *Drosophila* encode not only the salience of sugars and odours, but also their relative novelty, state-dependent value, and positive prediction error.

Chapter 6

Discussion and conclusion

6.1 Experimental limitations

All physiology experiments in this thesis used two-photon *in vivo* calcium imaging [295] to characterize the activity of dopaminergic neurons during feeding or odour presentation. Calcium imaging assumes that action potentials cause changes in intracellular calcium that in turn trigger neurotransmitter release [296, 297]. However, calcium signals are only a reliable indicator of neuronal activity if action potentials are the key source of the changes in calcium signal that are measured, which is not always the case [298–300].

Although genetically encoded calcium indicators such as GCaMP6f [188] have much larger signal-to-noise ratios than the best genetically encoded voltage indicators [301], they are also much slower. Calcium sensors are therefore more suitable for the lower acquisition frame rates that are typically used in two-photon imaging [295, 301], but also more likely to miss temporally important information about neural activity. Moreover, interpreting changes in calcium activity is not necessarily straightforward [302]. Calcium signals are non-linearly related to neuronal activity [303], and fluorescence similarly has a non-linear relationship with intracellular calcium [304]. Therefore, standard calcium imaging analysis that uses a fluorescence change (i.e., $\Delta F/F_0$) to represent neural activity can be misleading for different neurons [302, 305].

One easily observable reason for this possible distortion is the differing calcium baselines between different subsets of neurons. For example, in R48B04 PAM neurons, PAM-β′2 and PAM-γ4 have a much higher baseline calcium signal than PAM-γ5. In R15A04 PAM neurons, the baseline calcium signal for PAM-α1 neurons is very low compared to other PAM subsets. The differing baselines reflect how close neurons are to saturation, but consequently, identical changes in electrical activity may result in different changes in calcium activity [302, 305].

Even if all the assumptions concerning the relationship between calcium signals and action potential indeed hold true for R48B04 PAM neurons, calcium imaging is generally less effective at detecting hyperpolarizations, which do not necessarily change intracellular calcium [251]. Although inhibitory calcium responses can be observed (Figure 4.13) [61, 176, 306, 307], successful imaging also depends substantially upon the calcium baseline of the neurons concerned.

If PAM-γ5 neurons can indeed encode negative prediction error, then the particularly low PAM-γ5 calcium baseline suggests that negative prediction error may not be detectable by calcium imaging. It was challenging to detect slightly elevated PAM-γ5 activity during prolonged odour presentation (Figure 5.4), and it may be too difficult to test inhibitory negative prediction error reliably in PAM subsets with low calcium baselines (Figure 5.12). In contrast, I found it much easier to use calcium imaging to detect excitatory PAM-γ4 responses evoked by unexpected reward presentation (Figure 5.15).

Nonetheless, despite the different calcium baselines of PAM subsets, it appears that equivalent responses approaching saturation can be evoked using odours for PAM-β′2 and PAM-γ4 (Figure 5.4) or sucrose for PAM-γ5 (Figure 5.3). Such observations suggest that each subset responds in a substantially different manner to different stimulus types and that these differences can at least be internally compared. However, within each PAM subset, individual neurons may respond very differently yet be obscured by the strongest responding individual neurons in the group. Imaging the calcium responses of a particular PAM subset labelled

by different GAL4 drivers or GAL4/GAL80 combinations could reveal more heterogeneity in each PAM subset and which lines label the strongest responders.

Although I have thoroughly characterized calcium signals for pooled subsets of DANs, it remains unclear whether DAN responses to sugars and odours trigger dopamine release that activates certain downstream targets but not others. The recent development of $GRAB_{DA}$ sensors [308] provides a genetically-encoded sensor that can specifically detect dopamine on downstream targets of DANs. Expressing $GRAB_{DA}$ sensors on KCs or MBONs downstream of R48B04 neurons during appetitive conditioning protocols under the microscope could reveal the exact timing and targets of the dopamine teaching signal and how it changes once a reward becomes more predictable.

My physiological characterization of reward signals has depended upon each fly consuming a reward with its proboscis while its tarsi remain tethered. However, flies are free to walk during T-maze behavioural assays and can taste sugars using their tarsi. A more representative experience of reward involving both the proboscis and tarsi may lead to more robust learning. Future physiology experiments should characterize tarsal contact responses in DANs and allow flies to touch rewards with both their tarsi and proboscis during appetitive conditioning protocols under the microscope.

6.2 Future experiments

The next experimental steps should focus on reward prediction error, odour novelty, and DAN heterogeneity in particular. First, the experiment testing the unexpected presentation of reward (Figure 5.15) should be repeated with the odours MCH and OCT reversed, along with an odour control group in which the US is presented unexpectedly with the CS^- odour or a novel odour in the final round. Should PAM-γ4 neurons be indeed excited more by the unexpected presentation of reward, then it could be concluded that at least some *Drosophila*

DANs appear to encode reward prediction error. Then the ability of *Drosophila* to exhibit blocking in an appetitive conditioning context should be determined and the requirement for PAM-γ4 tested.

With respect to odour novelty, the next experiment ought to use a shorter and simpler multi-round protocol that presents only odours for 5 s each while imaging R48B04 PAM neurons. The sequence of odours presented in Figure 5.6A could be compared with a similar protocol without five odour presentation rounds before the final round. Should my findings from the multi-round conditioning experiment successfully translate to the simpler protocol, then the experiment should be repeated while blocking the output of KCs or MBONs. It would also be important to determine whether R48B04 odour responses are dendritic or axonal in origin and to record R48B04 calcium responses during repeated optogenetic stimulation of KCs or MBONs.

The next experiment concerning DAN heterogeneity should test whether MP1 neurons are also inhibited when flies consume a droplet containing bitter and aversive DEET. If MP1 neurons appear to bidirectionally signal aversive and rewarding stimuli, then it would be important to determine whether PAM neurons are oppositely inhibited by aversive stimuli. Subsequent experiments could then test PAM and PPL1 cluster interactions by recording calcium signals in PAM neurons while optogenetically stimulating PPL1 neurons and vice versa. Taken together, the experiments suggested here would substantially further our understanding of *Drosophila* DANs beyond the results presented in this thesis.

6.3 Thesis summary

Two-photon *in vivo* calcium imaging was used throughout this thesis to monitor the activity of *Drosophila* dopaminergic neurons during feeding, odour presentation, and appetitive conditioning. The resulting findings have provided the foundations for a much greater understanding of *Drosophila* dopaminergic neuron physiology.

First, deprivation state was found to modulate the sugar-water droplet feeding responses of one subset of dopaminergic neurons. During the consumption of a droplet of sugar-water, PAM-γ5 neurons in starved flies responded primarily to the presence of sugar in the droplet, whereas in dehydrated flies, PAM-γ5 responded primarily to the presence of water. In contrast, sucrose-evoked PAM-γ5 responses in satiated flies were observed to be significantly lower than in either deprivation state, implying a deprivation state-dependent valuation of reward.

Increasing the nutritious content of a sugar-water droplet did not increase the feeding responses of any rewarding PAM dopaminergic neurons investigated throughout this thesis. In contrast, feeding on any droplet rapidly inhibited the calcium oscillations of MP1 dopaminergic neurons in the aversively reinforcing PPL1 cluster. The oscillations that re-emerged after feeding had an increased frequency after a fly consumed sugars specifically and a lower amplitude after consuming nutritious sucrose, suggesting that MP1 neurons may convey different types of information about reward on different timescales.

The calcium responses of PAM dopaminergic neurons labelled by R48B04-GAL4 were also recorded during appetitive conditioning. A multi-round pairing protocol suggested that R48B04 neurons do not show acquired predictive capacity after training as expected from mammalian models of reward prediction error. However, the same protocol surprisingly revealed that PAM-β′2 and PAM-γ4 show calcium response signatures of both general and specific odour novelty. A single-round conditioning protocol also showed that PAM-γ4 neurons appear to be excited by the unexpected presentation of reward.

Taken together, the experiments in this thesis show that rewarding dopaminergic neurons in *Drosophila* convey more than just teaching signals to synapses of the mushroom body. During olfactory associative learning, *Drosophila* dopaminergic neurons respond during the presentation of both cues and rewards, encoding salience, novelty, value, and perhaps even reward prediction error.

Bibliography

[1] Freed, C. R. and Yamamoto, B. K. (1985). Regional brain dopamine metabolism: a marker for the speed, direction, and posture of moving animals. *Science* 229: (4708), 62–65. DOI: 10.1126/science.4012312 (cited on pp. 1, 11).

[2] Schultz, W., Dayan, P., and Montague, P. R. (1997). A neural substrate of prediction and reward. *Science* 275: (5306), 1593–1599. DOI: 10.1126/science.275.5306.1593 (cited on pp. 1, 10, 104, 105, 123).

[3] Salamone, J. D. and Correa, M. (2012). The mysterious motivational functions of mesolimbic dopamine. *Neuron* 76: (3), 470–485. DOI: 10.1016/j.neuron.2012.10.021 (cited on pp. 1, 11).

[4] Schultz, W. (2007). Multiple dopamine functions at different time courses. *Annu. Rev. Neurosci.* 30:1, 259–288. DOI: 10.1146/annurev.neuro.28.061604.135722 (cited on pp. 1, 10, 12).

[5] Berke, J. D. (2018). What does dopamine mean? *Nat. Neurosci.* 21: (6), 787–793. DOI: 10.1038/s41593-018-0152-y (cited on pp. 1, 10–12).

[6] Herculano-Houzel, S. (2007). Encephalization, neuronal excess, and neuronal index in rodents. *Anat. Rec.* 290: (10), 1280–1287. DOI: 10.1002/ar.20598 (cited on p. 1).

[7] Herculano-Houzel, S. (2009). The human brain in numbers: a linearly scaled-up primate brain. *Front. Hum. Neurosci.* 3: 31. DOI: 10.3389/neuro.09.031.2009 (cited on p. 1).

[8] German, D., Schlusselberg, D., and Woodward, D. (1983). Three-dimensional computer reconstruction of midbrain dopaminergic neuronal populations: from mouse to man. *J. Neural Transm.* 57:4, 243–254. DOI: 10.1007/BF01248996 (cited on p. 1).

[9] Nelson, E. L., Liang, C. L., Sinton, C. M., and German, D. C. (1996). Midbrain dopaminergic neurons in the mouse: computer-assisted mapping. *J. Comp. Neurol.* 369: (3), 361–371. DOI: 10.1002/(SICI)1096-9861(19960603)369:3<361::AID-CNE3>3.0.CO;2-3 (cited on p. 1).

[10] Björklund, A. and Dunnett, S. B. (2007). Dopamine neuron systems in the brain: an update. *Trends Neurosci.* 30: (5), 194–202. DOI: 10.1016/j.tins.2007.03.006 (cited on p. 1).

[11] Nässel, D. R. and Elekes, K. (1992). Aminergic neurons in the brain of blowflies and *Drosophila*: dopamine- and tyrosine hydroxylase-immunoreactive neurons and their relationship with putative histaminergic neurons. *Cell Tissue Res.* 267: (1), 147–167. DOI: 10.1007/BF00318701 (cited on pp. 1, 15).

[12] Mao, Z. and Davis, R. L. (2009). Eight different types of dopaminergic neurons innervate the *Drosophila* mushroom body neuropil: anatomical

and physiological heterogeneity. *Front. Neural Circuits* 3: 5. DOI: 10.3389/neuro.04.005.2009 (cited on pp. 1, 15, 37).

[13] Hammer, M. (1993). An identified neuron mediates the unconditioned stimulus in associative olfactory learning in honeybees. *Nature* 366: 59–63. DOI: 10.1038/366059a0 (cited on pp. 1, 4, 38).

[14] Hammer, M and Menzel, R (1998). Multiple sites of associative odor learning as revealed by local brain microinjections of octopamine in honeybees. *Learn. Mem.* 5: (1-2), 146–156. DOI: 10.1101/lm.5.1.146 (cited on pp. 1, 38).

[15] Schwaerzel, M., Monastirioti, M., Scholz, H., Friggi-Grelin, F., Birman, S., and Heisenberg, M. (2003). Dopamine and octopamine differentiate between aversive and appetitive olfactory memories in *Drosophila*. *J. Neurosci.* 23: (33), 10495–10502. DOI: 10.1523/jneurosci.23-33-10495.2003 (cited on pp. 1, 26, 36, 38, 67, 103, 105).

[16] Schroll, C., Riemensperger, T., Bucher, D., Ehmer, J., Völler, T., Erbguth, K., Gerber, B., Hendel, T., Nagel, G., Buchner, E., and Fiala, A. (2006). Light-induced activation of distinct modulatory neurons triggers appetitive or aversive learning in *Drosophila* larvae. *Curr. Biol.* 16: (17), 1741–1747. DOI: 10.1016/j.cub.2006.07.023 (cited on pp. 1, 36, 38, 103).

[17] Burke, C. J., Huetteroth, W., Owald, D., Perisse, E., Krashes, M. J., Das, G., Gohl, D., Silies, M., Certel, S., and Waddell, S. (2012). Layered reward signalling through octopamine and dopamine in *Drosophila*. *Nature* 492:7429, 433–437. DOI: 10.1038/nature11614 (cited on pp. 1, 3, 7, 12, 15, 17, 32, 38, 44, 66–68, 71, 73, 74, 79, 95–97, 103, 104, 109).

[18] Owald, D., Lin, S., and Waddell, S. (2015a). Light, heat, action: neural control of fruit fly behaviour. *Philos. Trans. R. Soc. B.* 370:1677, 20140211. DOI: 10.1098/rstb.2014.0211 (cited on p. 2).

[19] Frankenhuis, W. E., Panchanathan, K., and Barto, A. G. (2018). Enriching behavioral ecology with reinforcement learning methods. *Behav. Processes*. DOI: 10.1016/j.beproc.2018.01.008 (cited on p. 2).

[20] Ashburner, M., Golic, K., and Hawley, R. S. (2005). *Drosophila*: a laboratory handbook. 2nd ed. Cold Spring Harbor Laboratory Press (cited on p. 2).

[21] Rose, M and Charlesworth, B (1980). A test of evolutionary theories of senescence. *Nature* 287: (5778), 141–142. DOI: 10.1038/287141a0 (cited on p. 2).

[22] Schwartz, N. U., Zhong, L., Bellemer, A., and Tracey, W. D. (2012). Egg laying decisions in *Drosophila* are consistent with foraging costs of larval progeny. *PLoS One* 7: (5), e37910. DOI: 10.1371/journal.pone.0037910 (cited on p. 2).

[23] Lihoreau, M., Poissonnier, L.-A., Isabel, G., and Dussutour, A. (2016). *Drosophila* females trade off good nutrition with high quality oviposition sites when choosing foods. *J. Exp. Biol.* DOI: 10.1242/jeb.142257 (cited on p. 2).

[24] Becher, P. G., Flick, G., Rozpędowska, E., Schmidt, A., Hagman, A., Lebreton, S., Larsson, M. C., Hansson, B. S., Piškur, J., Witzgall, P., et al. (2012). Yeast, not fruit volatiles mediate *Drosophila melanogaster* attraction, oviposition and development. *Funct. Ecol.* 26:4, 822–828. DOI: 10.1111/j.1365-2435.2012.02006.x (cited on p. 2).

[25] Krashes, M. J. and Waddell, S. (2008). Rapid consolidation to a radish and protein synthesis-dependent long-term memory after single-session appetitive olfactory conditioning in *Drosophila*. *J. Neurosci.* 28:12, 3103–3113. DOI: 10.1523/jneurosci.5333-07.2008 (cited on pp. 3, 5, 6, 35, 36, 52, 72, 136).

[26] Colomb, J., Kaiser, L., Chabaud, M.-A., and Preat, T. (2009). Parametric and genetic analysis of *Drosophila* appetitive long-term memory and sugar motivation. *Genes Brain Behav.* 8: (4), 407–415. DOI: 10.1111/j.1601-183X.2009.00482.x (cited on pp. 3, 5, 6, 36, 136).

[27] Wigglesworth, V. B. (1949). The utilization of reserve substances in *Drosophila* during flight. *J. Exp. Biol.* 26: (2), 150–63, illust (cited on pp. 3, 6, 7, 65, 95).

[28] Hassett, C. C. (1948). The utilization of sugars and other substances by *Drosophila*. *Biol. Bull.* 95: (1), 114–123. DOI: 10.2307/1538158 (cited on pp. 3, 6, 7, 74, 95).

[29] Burke, C. J. and Waddell, S. (2011). Remembering nutrient quality of sugar in *Drosophila*. *Curr. Biol.* 21:9, 746–750. DOI: 10.1016/j.cub.2011.03.032 (cited on pp. 3, 5–7, 41, 42, 44, 65, 66, 71, 74, 76, 95, 96).

[30] Fujita, M. and Tanimura, T. (2011). *Drosophila* evaluates and learns the nutritional value of sugars. *Curr. Biol.* 21: (9), 751–755. DOI: 10.1016/j.cub.2011.03.058 (cited on pp. 3, 5–7, 74, 95, 96).

[31] Stafford, J. W., Lynd, K. M., Jung, A. Y., and Gordon, M. D. (2012). Integration of taste and calorie sensing in *Drosophila*. *J Neurosci* 32:42, 14767–14774. DOI: 10.1523/jneurosci.1887-12.2012 (cited on pp. 3, 7, 41, 42, 44, 74, 76, 91, 95, 96).

[32] McGinnis, J. P., Jiang, H., Agha, M. A., Perez Sanchez, C., Lange, J. J., Yu, Z., Marion-Poll, F., and Si, K. (2016). Immediate perception of a reward is distinct from the reward's long-term salience. *eLife* 5: DOI: 10.7554/eLife.22283 (cited on pp. 3, 6, 7, 41, 71, 76, 77, 91, 94, 95).

[33] Krashes, M. J., DasGupta, S., Vreede, A., White, B., Armstrong, J. D., and Waddell, S. (2009). A neural circuit mechanism integrating motivational state with memory expression in *Drosophila*. *Cell* 139:2, 416–427. DOI: 10.1016/j.cell.2009.08.035 (cited on pp. 3, 6, 17, 22, 35, 36, 52, 53, 71, 73, 90, 100, 104).

[34] Liu, C., Plaçais, P.-Y., Yamagata, N., Pfeiffer, B. D., Aso, Y., Friedrich, A. B., Siwanowicz, I., Rubin, G. M., Preat, T., and Tanimoto, H. (2012a). A subset of dopamine neurons signals reward for odour memory in *Drosophila*. *Nature* 488:7412, 512–516. DOI: 10.1038/nature11304 (cited on pp. 3, 7, 12, 15, 32, 38, 61, 68, 103, 104, 140).

[35] Yamagata, N., Ichinose, T., Aso, Y., Plaçais, P.-Y., Friedrich, A. B., Sima, R. J., Preat, T., Rubin, G. M., and Tanimoto, H. (2015). Distinct dopamine neurons mediate reward signals for short- and long-term memories. *PNAS* 112:2, 578–583. DOI: 10.1073/pnas.1421930112 (cited on pp. 3, 6, 7, 12, 15, 17, 32, 38–42, 44, 52, 53, 55, 67–71, 73, 74, 94–97, 103, 104, 114, 130, 135).

[36] Huetteroth, W., Perisse, E., Lin, S., Klappenbach, M., Burke, C., and Waddell, S. (2015). Sweet taste and nutrient value subdivide rewarding dopaminergic neurons in *Drosophila*. *Curr. Biol.* 25:6, 751–758. DOI: 10.1016/j.cub.2015.

01.036 (cited on pp. 3, 6, 7, 15, 22, 32, 38–42, 44, 52, 53, 55, 67–71, 73, 79, 86, 104, 109, 114, 130, 135).

[37] Byrne, J. H. and Hawkins, R. D. (2015). Nonassociative learning in invertebrates. *Cold Spring Harb. Perspect. Biol.* 7: (5). DOI: 10.1101/cshperspect.a021675 (cited on p. 3).

[38] Hawkins, R. D. and Byrne, J. H. (2015). Associative learning in invertebrates. *Cold Spring Harb. Perspect. Biol.* 7: (5). DOI: 10.1101/cshperspect.a021709 (cited on pp. 3, 4).

[39] Pavlov, I. and Anrep, G. (1927). Conditioned reflexes: an investigation of the physiological activity of the cerebral cortex. Oxford University Press: Humphrey Milford (cited on p. 4).

[40] Rescorla, R. A. and Wagner Allan, R. (1972). A theory of Pavlovian conditioning: Variations in the effectiveness of reinforcement and nonreinforcement. In: *Classical conditioning II: Current research and theory*. Ed. by A. H. Black and W. F. Prokasy. Appleton-Century-Crofts, 64–99 (cited on pp. 4, 8, 104).

[41] Pearce, J. M. (1987). A model for stimulus generalization in Pavlovian conditioning. *Psychol. Rev.* 94: (1), 61–73. DOI: http://dx.doi.org/10.1037/0033-295X.94.1.61 (cited on p. 4).

[42] Sutton, R. S. and Barto, A. G. (1990). Time-derivative models of Pavlovian reinforcement. In: *Learning and computational neuroscience: Foundations of adaptive networks*. Ed. by M. Gabriel and J. Moore. The MIT Press, 497–537 (cited on p. 4).

[43] Pearce, J. M. (1994). Similarity and discrimination: a selective review and a connectionist model. *Psychol. Rev.* 101:4, 587. DOI: 10.1037/0033-295X.101.4.587 (cited on p. 4).

[44] Hawkins, R. D., Abrams, T. W., Carew, T. J., and Kandel, E. R. (1983). A cellular mechanism of classical conditioning in *Aplysia*: activity-dependent amplification of presynaptic facilitation. *Science* 219: (4583), 400–405. DOI: 10.1126/science.6294833 (cited on p. 4).

[45] Carew, T. J. and Sahley, C. L. (1986). Invertebrate learning and memory: from behavior to molecules. *Annu. Rev. Neurosci.* 9: 435–487. DOI: 10.1146/annurev.ne.09.030186.002251 (cited on p. 4).

[46] Thorndike, E. (1911). Animal intelligence: experimental studies. Animal behavior series. Macmillan (cited on p. 4).

[47] Skinner, B. F. (1950). Are theories of learning necessary? *Psychol. Rev.* 57: (4), 193–216. DOI: http://dx.doi.org/10.1037/h0054367 (cited on p. 4).

[48] Horridge, G. A. (1962). Learning of leg position by headless insects. *Nature* 193: 697–698. DOI: 10.1038/193697a0 (cited on p. 4).

[49] Booker, R and Quinn, W. G. (1981). Conditioning of leg position in normal and mutant *Drosophila*. *PNAS* 78: (6), 3940–3944. DOI: 10.1073/pnas.78.6.3940 (cited on p. 4).

[50] Quinn, W. G., Harris, W. A., and Benzer, S. (1974). Conditioned behavior in *Drosophila melanogaster*. *PNAS* 71:3, 708–712. DOI: 10.1073/pnas.71.3.708 (cited on pp. 4, 5, 22, 26, 49).

[51] Heisenberg, M., Borst, A., Wagner, S., and Byers, D. (1985). *Drosophila* mushroom body mutants are deficient in olfactory learning. *J. Neurogenet.* 2: (1), 1–30. DOI: 10.3109/01677068509100140 (cited on pp. 4, 14, 15).

[52] Waddell, S., Armstrong, J. D., Kitamoto, T., Kaiser, K., and Quinn, W. G. (2000). The amnesiac gene product is expressed in two neurons in the *Drosophila* brain that are critical for memory. *Cell* 103: (5), 805–813. DOI: 10.1016/S0092-8674(00)00183-5 (cited on pp. 4, 72).

[53] Tanaka, N. K., Tanimoto, H., and Ito, K. (2008). Neuronal assemblies of the *Drosophila* mushroom body. *J. Comp. Neurol.* 508: (5), 711–755. DOI: 10.1002/cne.21692 (cited on pp. 4, 36–39, 41, 42, 69, 103).

[54] Séjourné, J., Plaçais, P.-Y., Aso, Y., Siwanowicz, I., Trannoy, S., Thoma, V., Tedjakumala, S. R., Rubin, G. M., Tchénio, P., Ito, K., Isabel, G., Tanimoto, H., et al. (2011). Mushroom body efferent neurons responsible for aversive olfactory memory retrieval in *Drosophila*. *Nat. Neurosci.* 14:7, 903–910. DOI: 10.1038/nn.2846 (cited on pp. 4, 103).

[55] Pai, T.-P., Chen, C.-C., Lin, H.-H., Chin, A.-L., Lai, J. S.-Y., Lee, P.-T., Tully, T., and Chiang, A.-S. (2013). *Drosophila* ORB protein in two mushroom body output neurons is necessary for long-term memory formation. *PNAS* 110: (19), 7898–7903. DOI: 10.1073/pnas.1216336110 (cited on pp. 4, 103).

[56] Plaçais, P.-Y., Trannoy, S., Friedrich, A. B., Tanimoto, H., and Preat, T. (2013). Two pairs of mushroom body efferent neurons are required for appetitive long-term memory retrieval in *Drosophila*. *Cell Rep.* 5: (3), 769–780. DOI: 10.1016/j.celrep.2013.09.032 (cited on p. 4).

[57] Bouzaiane, E., Trannoy, S., Scheunemann, L., Plaçais, P.-Y., and Preat, T. (2015). Two independent mushroom body output circuits retrieve the six discrete components of *Drosophila* aversive memory. *Cell Rep.* 11: (8), 1280–1292. DOI: 10.1016/j.celrep.2015.04.044 (cited on pp. 4, 103).

[58] Owald, D., Felsenberg, J., Talbot, C. B., Das, G., Perisse, E., Huetteroth, W., and Waddell, S. (2015b). Activity of defined mushroom body output neurons underlies learned olfactory behavior in *Drosophila*. *Neuron* 86:2, 417–427. DOI: 10.1016/j.neuron.2015.03.025 (cited on pp. 4, 15, 17, 37, 103, 105, 136).

[59] Perisse, E., Owald, D., Barnstedt, O., Talbot, C. B., Huetteroth, W., and Waddell, S. (2016). Aversive learning and appetitive motivation toggle feed-forward inhibition in the *Drosophila* mushroom body. *Neuron*. DOI: 10.1016/j.neuron.2016.04.034 (cited on pp. 4, 15, 17, 37, 59, 103, 105).

[60] Eichler, K., Li, F., Litwin-Kumar, A., Park, Y., Andrade, I., Schneider-Mizell, C. M., Saumweber, T., Huser, A., Eschbach, C., Gerber, B., et al. (2017). The complete connectome of a learning and memory centre in an insect brain. *Nature* 548:7666, 175. DOI: 10.1038/nature23455 (cited on pp. 4, 17).

[61] Felsenberg, J., Barnstedt, O., Cognigni, P., Lin, S., and Waddell, S. (2017). Re-evaluation of learned information in *Drosophila*. *Nature* 544: (7649), 240–244. DOI: 10.1038/nature21716 (cited on pp. 4, 17, 59, 91, 98, 104, 105, 136, 146).

[62] Takemura, S.-Y., Aso, Y., Hige, T., Wong, A., Lu, Z., Xu, C. S., Rivlin, P. K., Hess, H. F., Zhao, T., Parag, T., Berg, S., Huang, G., et al. (2017). A connectome of a learning and memory center in the adult *Drosophila* brain. *eLife* 6: DOI: 10.7554/eLife.26975 (cited on pp. 4, 12, 17).

[63] Wu, J.-K., Tai, C.-Y., Feng, K.-L., Chen, S.-L., Chen, C.-C., and Chiang, A.-S. (2017). Long-term memory requires sequential protein synthesis in three

subsets of mushroom body output neurons in *Drosophila*. *Sci. Rep.* 7: (1), 7112. DOI: 10.1038/s41598-017-07600-2 (cited on p. 4).

[64] Zheng, Z., Lauritzen, J. S., Perlman, E., Robinson, C. G., Nichols, M., Milkie, D., Torrens, O., Price, J., Fisher, C. B., Sharifi, N., Calle-Schuler, S. A., Kmecova, L., et al. (2018). A complete electron microscopy volume of the brain of adult *Drosophila melanogaster*. *Cell* 174: (3), 730–743.e22. DOI: 10.1016/j.cell.2018.06.019 (cited on pp. 4, 15, 97, 135).

[65] Felsenberg, J., Jacob, P. F., Walker, T., Barnstedt, O., Edmondson-Stait, A. J., Pleijzier, M. W., Otto, N., Schlegel, P., Sharifi, N., Perisse, E., Smith, C. S., Lauritzen, J. S., et al. (2018). Integration of parallel opposing memories underlies memory extinction. *Cell*. DOI: 10.1016/j.cell.2018.08.021 (cited on pp. 4, 37, 104, 106).

[66] Tempel, B. L., Bonini, N., Dawson, D. R., and Quinn, W. G. (1983). Reward learning in normal and mutant *Drosophila*. *PNAS* 80:5, 1482–1486 (cited on pp. 4, 6, 32, 35, 36, 137–139).

[67] Tully, T. and Quinn, W. G. (1985). Classical conditioning and retention in normal and mutant *Drosophila melanogaster*. *J. Comp. Physiol. A* 157:2, 263–277 (cited on pp. 4, 137).

[68] Krashes, M. J. and Waddell, S. (2011a). *Drosophila* aversive olfactory conditioning. *Cold Spring Harb. Protoc.* 2011: (5). DOI: 10.1101/pdb.prot5608 (cited on pp. 4, 137).

[69] Krashes, M. J. and Waddell, S. (2011b). *Drosophila* appetitive olfactory conditioning. *Cold Spring Harb. Protoc.* 2011: (5). DOI: 10.1101/pdb.prot5609 (cited on pp. 4, 107, 111, 130, 137–139).

[70] Vosshall, L. B. (2007). Into the mind of a fly. *Nature* 450:7167, 193–197. DOI: 10.1038/nature06335 (cited on pp. 5, 66).

[71] Chabaud, M.-A., Isabel, G., Kaiser, L., and Preat, T. (2009). Social facilitation of long-lasting memory retrieval in *Drosophila*. *Curr. Biol.* 19: (19), 1654–1659. DOI: 10.1016/j.cub.2009.08.017 (cited on p. 5).

[72] Chabaud, M.-A., Preat, T., and Kaiser, L. (2010). Behavioral characterization of individual olfactory memory retrieval in *Drosophila melanogaster*. *Front. Behav. Neurosci.* 4: 192. DOI: 10.3389/fnbeh.2010.00192 (cited on p. 5).

[73] Lechner, H. A., Squire, L. R., and Byrne, J. H. (1999). 100 years of consolidation—remembering Müller and Pilzecker. *Learn. Mem.* 6: (2), 77–87. DOI: 10.1101/lm.6.2.77 (cited on p. 5).

[74] Folkers, E., Drain, P., and Quinn, W. G. (1993). Radish, a *Drosophila* mutant deficient in consolidated memory. *PNAS* 90: (17), 8123–8127. DOI: 10.1073/pnas.90.17.8123 (cited on pp. 5, 6).

[75] Tully, T., Preat, T., Boynton, S. C., and Del Vecchio, M. (1994). Genetic dissection of consolidated memory in *Drosophila*. *Cell* 79: (1), 35–47. DOI: 10.1016/0092-8674(94)90398-0 (cited on pp. 5, 6).

[76] Quinn, W. G. and Dudai, Y (1976). Memory phases in *Drosophila*. *Nature* 262: (5569), 576–577. DOI: 10.1038/262576a0 (cited on pp. 5, 6).

[77] Miyamoto, T., Slone, J., Song, X., and Amrein, H. (2012). A fructose receptor functions as a nutrient sensor in the *Drosophila* brain. *Cell* 151:5, 1113–1125. DOI: 10.1016/j.cell.2012.10.024 (cited on pp. 6, 66, 94).

[78] Dus, M., Ai, M., and Suh, G. S. B. (2013). Taste-independent nutrient selection is mediated by a brain-specific Na+/solute co-transporter in *Drosophila*. *Nat. Neurosci.* 16:5, 526–528. DOI: 10.1038/nn.3372 (cited on pp. 6, 66).

[79] Musso, P.-Y., Lampin-Saint-Amaux, A., Tchenio, P., and Preat, T. (2017). Ingestion of artificial sweeteners leads to caloric frustration memory in *Drosophila*. *Nat. Commun.* 8:1. DOI: 10.1038/s41467-017-01989-0 (cited on pp. 7, 72).

[80] Qi, W., Yang, Z., Lin, Z., Park, J.-Y., Suh, G. S. B., and Wang, L. (2015). A quantitative feeding assay in adult *Drosophila* reveals rapid modulation of food ingestion by its nutritional value. *Mol. Brain.* 8: 87. DOI: 10.1186/s13041-015-0179-x (cited on pp. 7, 23, 41, 62).

[81] Musso, P.-Y., Tchenio, P., and Preat, T. (2015). Delayed dopamine signaling of energy level builds appetitive long-term memory in *Drosophila*. *Cell Rep.* DOI: 10.1016/j.celrep.2015.01.036 (cited on pp. 7, 37, 69, 71–73, 99, 104).

[82] Perisse, E., Burke, C., Huetteroth, W., and Waddell, S. (2013a). Shocking revelations and saccharin sweetness in the study of *Drosophila* olfactory memory. *Curr. Biol.* 23:17, R752–R763. DOI: 10.1016/j.cub.2013.07.060 (cited on pp. 6, 14, 16).

[83] Bush, R. R. and Mosteller, F. (1951a). A mathematical model for simple learning. *Psychol. Rev.* 58: (5), 313–323. DOI: http://dx.doi.org/10.1037/h0054388 (cited on p. 8).

[84] Bush, R. R. and Mosteller, F. (1951b). A model for stimulus generalization and discrimination. *Psychol. Rev.* 58:6, 413–423. DOI: 10.1037/h0054576 (cited on p. 8).

[85] Glimcher, P. W. (2011). Understanding dopamine and reinforcement learning: the dopamine reward prediction error hypothesis. *PNAS* 108 Suppl 3: 15647–15654. DOI: 10.1073/pnas.1014269108 (cited on pp. 8–10, 137).

[86] Daw, N. and Tobler, P. (2013). Value learning through reinforcement: The basics of dopamine and reinforcement learning. In: *Neuroeconomics: Decision Making and the Brain: Second Edition*. Elsevier Inc., 283–298. DOI: 10.1016/B978-0-12-416008-8.00015-2 (cited on pp. 8, 9, 136).

[87] Sutton, R. S. and Barto, A. G. (1998). Reinforcement learning: an introduction. Adaptive computation and machine learning. London: MIT Press (cited on pp. 8–11, 13, 55).

[88] Kamin, L. J. (1969). Predictability, surprise, attention and conditioning. In: *Punishment and aversive behavior*. Ed. by B. A. Campbell and R. M. Church. Appleton-Century-Crofts, 279–296 (cited on p. 9).

[89] Sutton, R. S. and Barto, A. G. (1981). Toward a modern theory of adaptive networks: expectation and prediction. *Psychol. Rev.* 88: (2), 135–70 (cited on pp. 9–11, 13, 55).

[90] Houk, J., L. Adams, J, and G. Barto, A (1995). A model of how the basal ganglia generate and use neural signals that predict reinforcement. In: *Models of information processing in the basal ganglia*. Vol. Vol. 13. MIT Press, 249–270 (cited on p. 10).

[91] Montague, P. R., Dayan, P, and Sejnowski, T. J. (1996). A framework for mesencephalic dopamine systems based on predictive Hebbian learning. *J.*

Neurosci. 16: (5), 1936–1947. DOI: 10.1523/jneurosci.16-05-01936.1996 (cited on p. 10).

[92] Sharpe, M. J. and Schoenbaum, G. (2018). Evaluation of the hypothesis that phasic dopamine constitutes a cached-value signal. *Neurobiol. Learn. Mem.* 153: (Pt B), 131–136. DOI: 10.1016/j.nlm.2017.12.002 (cited on pp. 10, 12, 13).

[93] Schultz, W. (1986). Responses of midbrain dopamine neurons to behavioral trigger stimuli in the monkey. *J. Neurophysiol.* 56: (5), 1439–1461. DOI: 10.1152/jn.1986.56.5.1439 (cited on p. 10).

[94] Schultz, W., Apicella, P., and Ljungberg, T. (1993). Responses of monkey dopamine neurons to reward and conditioned stimuli during successive steps of learning a delayed response task. *J. Neurosci.* 13: (3), 900–913. DOI: 10.1523/jneurosci.13-03-00900.1993 (cited on pp. 10, 104, 105, 123).

[95] Fiorillo, C. D., Tobler, P. N., and Schultz, W. (2003). Discrete coding of reward probability and uncertainty by dopamine neurons. *Science* 299: (5614), 1898–1902. DOI: 10.1126/science.1077349 (cited on p. 10).

[96] Lak, A., Stauffer, W. R., and Schultz, W. (2014). Dopamine prediction error responses integrate subjective value from different reward dimensions. *PNAS* 111: (6), 2343–2348. DOI: 10.1073/pnas.1321596111 (cited on p. 10).

[97] Stauffer, W. R., Lak, A., and Schultz, W. (2014). Dopamine reward prediction error responses reflect marginal utility. *Curr. Biol.* 24: (21), 2491–2500. DOI: 10.1016/j.cub.2014.08.064 (cited on p. 10).

[98] Bayer, H. M., Lau, B., and Glimcher, P. W. (2007). Statistics of midbrain dopamine neuron spike trains in the awake primate. *J. Neurophysiol.* 98: (3), 1428–1439. DOI: 10.1152/jn.01140.2006 (cited on p. 10).

[99] Cohen, J. Y., Haesler, S., Vong, L., Lowell, B. B., and Uchida, N. (2012). Neuron-type-specific signals for reward and punishment in the ventral tegmental area. *Nature* 482: (7383), 85–88. DOI: 10.1038/nature10754 (cited on p. 10).

[100] Eshel, N., Tian, J., Bukwich, M., and Uchida, N. (2016). Dopamine neurons share common response function for reward prediction error. *Nat. Neurosci.* 19: (3), 479–486. DOI: 10.1038/nn.4239 (cited on pp. 10, 12).

[101] Steinberg, E. E., Keiflin, R., Boivin, J. R., Witten, I. B., Deisseroth, K., and Janak, P. H. (2013). A causal link between prediction errors, dopamine neurons and learning. *Nat. Neurosci.* 16: (7), 966–973. DOI: 10.1038/nn.3413 (cited on p. 10).

[102] Hamid, A. A., Pettibone, J. R., Mabrouk, O. S., Hetrick, V. L., Schmidt, R., Vander Weele, C. M., Kennedy, R. T., Aragona, B. J., and Berke, J. D. (2016). Mesolimbic dopamine signals the value of work. *Nature neuroscience* 19: (1), 117–126. DOI: 10.1038/nn.4173 (cited on pp. 10–12).

[103] Watabe-Uchida, M., Eshel, N., and Uchida, N. (2017). Neural circuitry of reward prediction error. *Annu. Rev. Neurosci.* DOI: 10.1146/annurev-neuro-072116-031109 (cited on p. 10).

[104] Wyvell, C. L. and Berridge, K. C. (2000). Intra-accumbens amphetamine increases the conditioned incentive salience of sucrose reward: enhancement of reward "wanting" without enhanced "liking" or response reinforcement. *J. Neurosci.* 20: (21), 8122–8130. DOI: 10.1523/jneurosci.20-21-08122.2000 (cited on p. 10).

[105] Cagniard, B., Beeler, J. A., Britt, J. P., McGehee, D. S., Marinelli, M., and Zhuang, X. (2006). Dopamine scales performance in the absence of new learning. *Neuron* 51: (5), 541–547. DOI: 10.1016/j.neuron.2006.07.026 (cited on p. 10).

[106] Shiner, T., Seymour, B., Wunderlich, K., Hill, C., Bhatia, K. P., Dayan, P., and Dolan, R. J. (2012). Dopamine and performance in a reinforcement learning task: evidence from Parkinson's disease. *Brain* 135:6, 1871–1883. DOI: 10.1093/brain/aws083 (cited on p. 10).

[107] Leventhal, D. K., Stoetzner, C., Abraham, R., Pettibone, J., DeMarco, K., and Berke, J. D. (2014). Dissociable effects of dopamine on learning and performance within sensorimotor striatum. *Basal ganglia* 4: (2), 43–54. DOI: 10.1016/j.baga.2013.11.001 (cited on p. 10).

[108] Gonon, F., Burie, J. B., Jaber, M., Benoit-Marand, M., Dumartin, B., and Bloch, B. (2000). Geometry and kinetics of dopaminergic transmission in the rat striatum and in mice lacking the dopamine transporter. *Prog. Brain Res.* 125: 291–302. DOI: 10.1016/S0079-6123(00)25018-8 (cited on p. 11).

[109] Aragona, B. J., Cleaveland, N. A., Stuber, G. D., Day, J. J., Carelli, R. M., and Wightman, R. M. (2008). Preferential enhancement of dopamine transmission within the nucleus accumbens shell by cocaine is attributable to a direct increase in phasic dopamine release events. *J. Neurosci.* 28: (35), 8821–8831. DOI: 10.1523/jneurosci.2225-08.2008 (cited on p. 11).

[110] Owesson-White, C. A., Roitman, M. F., Sombers, L. A., Belle, A. M., Keithley, R. B., Peele, J. L., Carelli, R. M., and Wightman, R. M. (2012). Sources contributing to the average extracellular concentration of dopamine in the nucleus accumbens. *J. Neurochem.* 121: (2), 252–262. DOI: 10.1111/j.1471-4159.2012.07677.x (cited on p. 11).

[111] Strecker, R. E., Steinfels, G. F., and Jacobs, B. L. (1983). Dopaminergic unit activity in freely moving cats: lack of relationship to feeding, satiety, and glucose injections. *Brain Res.* 260: (2), 317–321. DOI: 10.1016/0006-8993(83)90688-1 (cited on p. 11).

[112] Cohen, J. Y., Amoroso, M. W., and Uchida, N. (2015). Serotonergic neurons signal reward and punishment on multiple timescales. *eLife* 4: DOI: 10.7554/eLife.06346 (cited on p. 11).

[113] Phillips, P. E. M., Stuber, G. D., Heien, M. L.A. V., Wightman, R. M., and Carelli, R. M. (2003). Subsecond dopamine release promotes cocaine seeking. *Nature* 422: (6932), 614–618. DOI: 10.1038/nature01476 (cited on p. 11).

[114] Wassum, K. M., Ostlund, S. B., and Maidment, N. T. (2012). Phasic mesolimbic dopamine signaling precedes and predicts performance of a self-initiated action sequence task. *Biol. Psychiatry* 71: (10), 846–854. DOI: 10.1016/j.biopsych.2011.12.019 (cited on p. 11).

[115] Howe, M. W., Tierney, P. L., Sandberg, S. G., Phillips, P. E. M., and Graybiel, A. M. (2013). Prolonged dopamine signalling in striatum signals proximity and value of distant rewards. *Nature* 500: (7464), 575–579. DOI: 10.1038/nature12475 (cited on p. 11).

[116] Schultz, W. (1998). Predictive reward signal of dopamine neurons. *J. Neurophysiol.* 80:1, 1–27 (cited on p. 12).

[117] Lammel, S., Hetzel, A., Häckel, O., Jones, I., Liss, B., and Roeper, J. (2008). Unique properties of mesoprefrontal neurons within a dual mesocorticolimbic dopamine system. *Neuron* 57: (5), 760–773. DOI: 10.1016/j.neuron.2008.01.022 (cited on p. 12).

[118] Poulin, J.-F., Zou, J., Drouin-Ouellet, J., Kim, K.-Y. A., Cicchetti, F., and Awatramani, R. B. (2014). Defining midbrain dopaminergic neuron diversity by single-cell gene expression profiling. *Cell Rep.* 9: (3), 930–943. DOI: 10.1016/j.celrep.2014.10.008 (cited on p. 12).

[119] Morales, M. and Margolis, E. B. (2017). Ventral tegmental area: cellular heterogeneity, connectivity and behaviour. *Nat. Rev. Neurosci.* 18: (2), 73–85. DOI: 10.1038/nrn.2016.165 (cited on p. 12).

[120] Matsumoto, M. and Hikosaka, O. (2009). Two types of dopamine neuron distinctly convey positive and negative motivational signals. *Nature* 459: (7248), 837–841. DOI: 10.1038/nature08028 (cited on p. 12).

[121] Menegas, W., Akiti, K., Amo, R., Uchida, N., and Watabe-Uchida, M. (2018). Dopamine neurons projecting to the posterior striatum reinforce avoidance of threatening stimuli. *Nat. Neurosci.* 21: (10), 1421–1430. DOI: 10.1038/s41593-018-0222-1 (cited on p. 12).

[122] Redgrave, P., Prescott, T. J., and Gurney, K. (1999). Is the short-latency dopamine response too short to signal reward error? *Trends Neurosci.* 22: (4), 146–151. DOI: 10.1016/S0166-2236(98)01373-3 (cited on p. 12).

[123] Redgrave, P. and Gurney, K. (2006). The short-latency dopamine signal: a role in discovering novel actions? *Nat. Rev. Neurosci.* 7: (12), 967–975. DOI: 10.1038/nrn2022 (cited on p. 12).

[124] Bromberg-Martin, E. S., Matsumoto, M., and Hikosaka, O. (2010). Dopamine in motivational control: rewarding, aversive, and alerting. *Neuron* 68: (5), 815–834. DOI: 10.1016/j.neuron.2010.11.022 (cited on pp. 12, 98).

[125] Howe, M. W. and Dombeck, D. A. (2016). Rapid signalling in distinct dopaminergic axons during locomotion and reward. *Nature* 535: (7613), 505–510. DOI: 10.1038/nature18942 (cited on p. 12).

[126] Rice, M. E. and Cragg, S. J. (2008). Dopamine spillover after quantal release: rethinking dopamine transmission in the nigrostriatal pathway. *Brain Res. Rev.* 58: (2), 303–313. DOI: 10.1016/j.brainresrev.2008.02.004 (cited on p. 12).

[127] Riemensperger, T., Völler, T., Stock, P., Buchner, E., and Fiala, A. (2005). Punishment prediction by dopaminergic neurons in *Drosophila*. *Curr. Biol.* 15:21, 1953–1960. DOI: 10.1016/j.cub.2005.09.042 (cited on pp. 12, 13, 36, 59, 103–106, 137).

[128] Dylla, K. V., Raiser, G., Galizia, C. G., and Szyszka, P. (2017). Trace conditioning in *Drosophila* induces associative plasticity in mushroom body Kenyon cells and dopaminergic neurons. *Front. Neural Circuits* 11: 42. DOI: 10.3389/fncir.2017.00042 (cited on pp. 12, 13, 105, 106, 137, 140).

[129] Plaçais, P.-Y. and Preat, T. (2013). To favor survival under food shortage, the brain disables costly memory. *Science* 339: (6118), 440–442. DOI: 10.1126/science.1226018 (cited on pp. 12, 36, 71, 99, 100).

[130] Waddell, S. (2013). Reinforcement signalling in *Drosophila*; dopamine does it all after all. *Curr. Opin. Neurobiol.* 23:3, 324–329. DOI: 10.1016/j.conb.2013.01.005 (cited on pp. 12, 103).

[131] Alekseyenko, O. V., Chan, Y.-B., Li, R., and Kravitz, E. A. (2013). Single dopaminergic neurons that modulate aggression in *Drosophila*. *PNAS* 110: (15), 6151–6156. DOI: 10.1073/pnas.1303446110 (cited on p. 13).

[132] Ueno, T., Tomita, J., Tanimoto, H., Endo, K., Ito, K., Kume, S., and Kume, K. (2012). Identification of a dopamine pathway that regulates sleep and arousal in *Drosophila*. *Nat. Neurosci.* 15: (11), 1516–1523. DOI: 10.1038/nn.3238 (cited on p. 13).

[133] Keleman, K., Vrontou, E., Krüttner, S., Yu, J. Y., Kurtovic-Kozaric, A., and Dickson, B. J. (2012). Dopamine neurons modulate pheromone responses in *Drosophila* courtship learning. *Nature* 489: (7414), 145–149. DOI: 10.1038/nature11345 (cited on p. 13).

[134] Kong, E. C., Woo, K., Li, H., Lebestky, T., Mayer, N., Sniffen, M. R., Heberlein, U., Bainton, R. J., Hirsh, J., and Wolf, F. W. (2010). A pair of dopamine neurons target the D1-like dopamine receptor DopR in the central complex to promote ethanol-stimulated locomotion in *Drosophila*. *PLoS ONE* 5: (4), e9954. DOI: 10.1371/journal.pone.0009954 (cited on p. 13).

[135] Liu, Q., Tabuchi, M., Liu, S., Kodama, L., Horiuchi, W., Daniels, J., Chiu, L., Baldoni, D., and Wu, M. N. (2017). Branch-specific plasticity of a bifunctional dopamine circuit encodes protein hunger. *Science* 356: (6337), 534–539. DOI: 10.1126/science.aal3245 (cited on p. 13).

[136] Marella, S., Mann, K., and Scott, K. (2012). Dopaminergic modulation of sucrose acceptance behavior in *Drosophila*. *Neuron* 73: (5), 941–950. DOI: 10.1016/j.neuron.2011.12.032 (cited on p. 13).

[137] Liu, Q., Liu, S., Kodama, L., Driscoll, M. R., and Wu, M. N. (2012b). Two dopaminergic neurons signal to the dorsal fan-shaped body to promote wakefulness in *Drosophila*. *Curr. Biol.* 22: (22), 2114–2123. DOI: 10.1016/j.cub.2012.09.008 (cited on p. 13).

[138] Smith, B. H. and Cobey, S. (1994). The olfactory memory of the honeybee *Apis mellifera*. II. Blocking between odorants in binary mixtures. *J. Exp. Biol.* 195: 91–108 (cited on p. 13).

[139] Gerber, B. and Ullrich, J. (1999). No evidence for olfactory blocking in honeybee classical conditioning. *J. Exp. Biol.* 202 (Pt 13): 1839–1854 (cited on p. 13).

[140] Hosler, J. S. and Smith, B. H. (2000). Blocking and the detection of odor components in blends. *The Journal of experimental biology* 203: (Pt 18), 2797–2806 (cited on p. 13).

[141] Guerrieri, F., Lachnit, H., Gerber, B., and Giurfa, M. (2005). Olfactory blocking and odorant similarity in the honeybee. *Learn. Mem.* 12: (2), 86–95. DOI: 10.1101/lm.79305 (cited on p. 13).

[142] Terao, K., Matsumoto, Y., and Mizunami, M. (2015). Critical evidence for the prediction error theory in associative learning. *Sci. Rep.* 5: 8929. DOI: 10.1038/srep08929 (cited on p. 13).

[143] Brembs, B. and Heisenberg, M. (2001). Conditioning with compound stimuli in *Drosophila melanogaster* in the flight simulator. *J. Exp. Biol.* 204: (Pt 16), 2849–2859 (cited on p. 13).

[144] Brogden, W. J. (1939). Sensory pre-conditioning. *J. Exp. Psychol.* 25:4, 323–332. DOI: 10.1037/h0058944 (cited on p. 13).

[145] Brogden, W. J. (1947). Sensory pre-conditioning of human subjects. *J. Exp. Psychol.* 37: (6), 527–539. DOI: http://dx.doi.org/10.1037/h0058465 (cited on p. 13).

[146] Kenyon, F. C. (1896). The brain of the bee. A preliminary contribution to the morphology of the nervous system of the arthropoda. *J. Comp. Neurol.* 6:3, 133–210. DOI: 10.1002/cne.910060302 (cited on p. 14).

[147] Technau, G. and Heisenberg, M. (1982). Neural reorganization during metamorphosis of the corpora pedunculata in *Drosophila melanogaster*. *Nature* 295: (5848), 405–407. DOI: 10.1038/295405a0 (cited on p. 14).

[148] Barnstedt, O., Owald, D., Felsenberg, J., Brain, R., Moszynski, J.-P., Talbot, C. B., Perrat, P. N., and Waddell, S. (2016). Memory-relevant mushroom body output synapses are cholinergic. *Neuron*. DOI: 10.1016/j.neuron.2016.02.015 (cited on pp. 14, 17, 37, 103).

[149] Laissue, P. P. and Vosshall, L. B. (2008). The olfactory sensory map in *Drosophila*. *Adv. Exp. Med. Biol.* 628: 102–114. DOI: 10.1007/978-0-387-78261-4_7 (cited on p. 14).

[150] Wilson, R. I. and Laurent, G. (2005). Role of GABAergic inhibition in shaping odor-evoked spatiotemporal patterns in the *Drosophila* antennal lobe. *J. Neurosci.* 25: (40), 9069–9079. DOI: 10.1523/jneurosci.2070-05.2005 (cited on p. 14).

[151] Shang, Y., Claridge-Chang, A., Sjulson, L., Pypaert, M., and Miesenböck, G. (2007). Excitatory local circuits and their implications for olfactory processing in the fly antennal lobe. *Cell* 128:3, 601–612. DOI: 10.1016/j.cell.2006.12.034 (cited on pp. 14, 26).

[152] Olsen, S. R., Bhandawat, V., and Wilson, R. I. (2007). Excitatory interactions between olfactory processing channels in the *Drosophila* antennal lobe. *Neuron* 54: (1), 89–103. DOI: 10.1016/j.neuron.2007.03.010 (cited on p. 14).

[153] Olsen, S. R. and Wilson, R. I. (2008). Lateral presynaptic inhibition mediates gain control in an olfactory circuit. *Nature* 452: 956. DOI: 10.1038/nature06864 (cited on p. 14).

[154] Root, C. M., Masuyama, K., Green, D. S., Enell, L. E., Nässel, D. R., Lee, C.-H., and Wang, J. W. (2008). A presynaptic gain control mechanism fine-tunes olfactory behavior. *Neuron* 59: (2), 311–321. DOI: 10.1016/j.neuron.2008.07.003 (cited on p. 14).

[155] Ignell, R., Root, C. M., Birse, R. T., Wang, J. W., Nässel, D. R., and Winther, A. M. E. (2009). Presynaptic peptidergic modulation of olfactory receptor neurons in *Drosophila*. *PNAS* 106: (31), 13070–13075. DOI: 10.1073/pnas.0813004106 (cited on p. 14).

[156] Yaksi, E. and Wilson, R. I. (2010). Electrical coupling between olfactory glomeruli. *Neuron* 67: (6), 1034–1047. DOI: 10.1016/j.neuron.2010.08.041 (cited on p. 14).

[157] Wong, A. M., Wang, J. W., and Axel, R. (2002). Spatial representation of the glomerular map in the *Drosophila* protocerebrum. *Cell* 109: (2), 229–241. DOI: 10.1016/S0092-8674(02)00707-9 (cited on p. 15).

[158] Heimbeck, G., Bugnon, V., Gendre, N., Keller, A., and Stocker, R. F. (2001). A central neural circuit for experience-independent olfactory and courtship

behavior in *Drosophila melanogaster*. *PNAS* 98: (26), 15336–15341. DOI: 10.1073/pnas.011314898 (cited on p. 15).

[159] Jefferis, G. S.X. E., Potter, C. J., Chan, A. M., Marin, E. C., Rohlfing, T., Maurer, C. R., and Luo, L. (2007). Comprehensive maps of *Drosophila* higher olfactory centers: spatially segregated fruit and pheromone representation. *Cell* 128: (6), 1187–1203. DOI: 10.1016/j.cell.2007.01.040 (cited on p. 15).

[160] Heisenberg, M. (2003). Mushroom body memoir: from maps to models. *Nat. Rev. Neurosci.* 4: (4), 266–275. DOI: 10.1038/nrn1074 (cited on pp. 15, 103).

[161] Bräcker, L. B., Siju, K. P., Varela, N., Aso, Y., Zhang, M., Hein, I., Vasconcelos, M. L., and Grunwald Kadow, I. C. (2013). Essential role of the mushroom body in context-dependent CO2 avoidance in *Drosophila*. *Curr. Biol.* 23: (13), 1228–1234. DOI: 10.1016/j.cub.2013.05.029 (cited on p. 15).

[162] Tsao, C.-H., Chen, C.-C., Lin, C.-H., Yang, H.-Y., and Lin, S. (2018). *Drosophila* mushroom bodies integrate hunger and satiety signals to control innate food-seeking behavior. *eLife* 7: DOI: 10.7554/eLife.35264 (cited on pp. 15, 59).

[163] Dolan, M.-J., Belliart-Guérin, G., Bates, A. S., Frechter, S., Lampin-Saint-Amaux, A., Aso, Y., Roberts, R. J. V., Schlegel, P., Wong, A., Hammad, A., Bock, D., Rubin, G. M., et al. (2018). Communication from learned to innate olfactory processing centers is required for memory retrieval in *Drosophila*. *Neuron*. DOI: 10.1016/j.neuron.2018.08.037 (cited on pp. 15, 59).

[164] Turner, G. C., Bazhenov, M., and Laurent, G. (2008). Olfactory representations by *Drosophila* mushroom body neurons. *J. Neurophysiol.* 99:2, 734–746. DOI: 10.1152/jn.01283.2007 (cited on pp. 15, 103).

[165] Murthy, M., Fiete, I., and Laurent, G. (2008). Testing odor response stereotypy in the *Drosophila* mushroom body. *Neuron* 59: (6), 1009–1023. DOI: 10.1016/j.neuron.2008.07.040 (cited on pp. 15, 103).

[166] Caron, S. J. C., Ruta, V., Abbott, L. F., and Axel, R. (2013). Random convergence of olfactory inputs in the *Drosophila* mushroom body. *Nature* 497: (7447), 113–117. DOI: 10.1038/nature12063 (cited on p. 15).

[167] Campbell, R. A. A., Honegger, K. S., Qin, H., Li, W., Demir, E., and Turner, G. C. (2013). Imaging a population code for odor identity in the *Drosophila* mushroom body. *J. Neurosci.* 33: (25), 10568–10581. DOI: 10.1523/jneurosci.0682-12.2013 (cited on pp. 15, 103).

[168] Lin, A. C., Bygrave, A. M., de Calignon, A., Lee, T., and Miesenböck, G. (2014a). Sparse, decorrelated odor coding in the mushroom body enhances learned odor discrimination. *Nat. Neurosci.* 17:4, 559–568. DOI: 10.1038/nn.3660 (cited on pp. 15, 103).

[169] Cognigni, P., Felsenberg, J., and Waddell, S. (2018). Do the right thing: neural network mechanisms of memory formation, expression and update in *Drosophila*. *Curr. Opin. Neurobiol.* 49: 51–58. DOI: 10.1016/j.conb.2017.12.002 (cited on pp. 16, 17, 103).

[170] Aso, Y., Hattori, D., Yu, Y., Johnston, R. M., Iyer, N. A., Ngo, T.-T., Dionne, H., Abbott, L., Axel, R., Tanimoto, H., and Rubin, G. M. (2014a). The neuronal architecture of the mushroom body provides a logic for associative learning.

eLife 3: DOI: 10.7554/eLife.04577 (cited on pp. 15, 22, 37, 69, 100, 103, 135, 141).

[171] Aso, Y., Sitaraman, D., Ichinose, T., Kaun, K. R., Vogt, K., Belliart-Guérin, G., Plaçais, P.-Y., Robie, A. A., Yamagata, N., Schnaitmann, C., Rowell, W. J., Johnston, R. M., et al. (2014b). Mushroom body output neurons encode valence and guide memory-based action selection in *Drosophila*. *eLife* 3: DOI: 10.7554/eLife.04580 (cited on pp. 15, 22, 37, 52, 103).

[172] Owald, D. and Waddell, S. (2015). Olfactory learning skews mushroom body output pathways to steer behavioral choice in *Drosophila*. *Curr. Opin. Neurobiol.* 35: 178–184. DOI: 10.1016/j.conb.2015.10.002 (cited on pp. 15, 17, 37, 98, 103, 133, 141).

[173] Claridge-Chang, A., Roorda, R. D., Vrontou, E., Sjulson, L., Li, H., Hirsh, J., and Miesenböck, G. (2009). Writing memories with light-addressable reinforcement circuitry. *Cell* 139: (2), 405–415. DOI: 10.1016/j.cell.2009.08.034 (cited on pp. 15, 103, 105).

[174] Aso, Y., Siwanowicz, I., Bräcker, L., Ito, K., Kitamoto, T., and Tanimoto, H. (2010). Specific dopaminergic neurons for the formation of labile aversive memory. *Curr. Biol.* 20: (16), 1445–1451. DOI: 10.1016/j.cub.2010.06.048 (cited on pp. 15, 103, 104).

[175] Aso, Y., Herb, A., Ogueta, M., Siwanowicz, I., Templier, T., Friedrich, A. B., Ito, K., Scholz, H., and Tanimoto, H. (2012). Three dopamine pathways induce aversive odor memories with different stability. *PLoS Genet.* 8:7, e1002768. DOI: 10.1371/journal.pgen.1002768 (cited on pp. 15, 36, 104).

[176] Cohn, R., Morantte, I., and Ruta, V. (2015). Coordinated and compartmentalized neuromodulation shapes sensory processing in *Drosophila*. *Cell* 163:7, 1742–1755. DOI: 10.1016/j.cell.2015.11.019 (cited on pp. 17, 44, 60, 61, 99, 103, 146).

[177] Hige, T., Aso, Y., Modi, M. N., Rubin, G. M., and Turner, G. C. (2015a). Heterosynaptic plasticity underlies aversive olfactory learning in *Drosophila*. *Neuron* 88: (5), 985–998. DOI: 10.1016/j.neuron.2015.11.003 (cited on pp. 17, 90, 103, 137).

[178] Cervantes-Sandoval, I., Phan, A., Chakraborty, M., and Davis, R. L. (2017). Reciprocal synapses between mushroom body and dopamine neurons form a positive feedback loop required for learning. *eLife* 6: e23789. DOI: http://dx.doi.org/10.7554/eLife.23789 (cited on pp. 17, 59).

[179] Ichinose, T., Aso, Y., Yamagata, N., Abe, A., Rubin, G. M., and Tanimoto, H. (2015). Reward signal in a recurrent circuit drives appetitive long-term memory formation.i. *eLife* 4: e10719. DOI: http://dx.doi.org/10.7554/eLife.10719 (cited on pp. 17, 53, 67–70, 73, 100, 104).

[180] Yamagata, N., Hiroi, M., Kondo, S., Abe, A., and Tanimoto, H. (2016). Suppression of dopamine neurons mediates reward. *PLoS Biol.* 14: (12), e1002586. DOI: 10.1371/journal.pbio.1002586 (cited on pp. 17, 97, 98).

[181] Berridge, M. J., Lipp, P, and Bootman, M. D. (2000). The versatility and universality of calcium signalling. *Nat. Rev. Mol. Cell Biol.* 1: (1), 11–21. DOI: 10.1038/35036035 (cited on p. 18).

[182] Grienberger, C. and Konnerth, A. (2012). Imaging calcium in neurons. *Neuron* 73: (5), 862–885. DOI: 10.1016/j.neuron.2012.02.011 (cited on pp. 18, 19).

[183] Neher, E. and Sakaba, T. (2008). Multiple roles of calcium ions in the regulation of neurotransmitter release. *Neuron* 59: (6), 861–872. DOI: 10.1016/j.neuron.2008.08.019 (cited on p. 18).

[184] Zucker, R. S. (1999). Calcium- and activity-dependent synaptic plasticity. *Curr. Opin. Neurobiol.* 9:3, 305–313. DOI: 10.1016/s0959-4388(99)80045-2 (cited on p. 18).

[185] Berridge, M. J., Bootman, M. D., and Roderick, H. L. (2003). Calcium signalling: dynamics, homeostasis and remodelling. *Nat. Rev. Mol. Cell Biol.* 4: (7), 517–529. DOI: 10.1038/nrm1155 (cited on p. 18).

[186] Lyons, M. R. and West, A. E. (2011). Mechanisms of specificity in neuronal activity-regulated gene transcription. *Prog. Neurobiol.* 94: (3), 259–295. DOI: 10.1016/j.pneurobio.2011.05.003 (cited on p. 18).

[187] Miyawaki, A., Llopis, J., Heim, R., McCaffery, J. M., Adams, J. A., Ikura, M., and Tsien, R. Y. (1997). Fluorescent indicators for Ca2+ based on green fluorescent proteins and calmodulin. *Nature* 388: (6645), 882–887. DOI: 10.1038/42264 (cited on p. 18).

[188] Chen, T.-W., Wardill, T. J., Sun, Y., Pulver, S. R., Renninger, S. L., Baohan, A., Schreiter, E. R., Kerr, R. A., Orger, M. B., Jayaraman, V., Looger, L. L., Svoboda, K., et al. (2013). Ultrasensitive fluorescent proteins for imaging neuronal activity. *Nature* 499:7458, 295–300. DOI: 10.1038/nature12354 (cited on pp. 18, 22, 145).

[189] Nagai, T., Yamada, S., Tominaga, T., Ichikawa, M., and Miyawaki, A. (2004). Expanded dynamic range of fluorescent indicators for Ca(2+) by circularly permuted yellow fluorescent proteins. *PNAS* 101: (29), 10554–10559. DOI: 10.1073/pnas.0400417101 (cited on p. 18).

[190] Wang, J. W., Wong, A. M., Flores, J., Vosshall, L. B., and Axel, R. (2003). Two-photon calcium imaging reveals an odor-evoked map of activity in the fly brain. *Cell* 112: (2), 271–282 (cited on p. 18).

[191] Conchello, J.-A. and Lichtman, J. W. (2005). Optical sectioning microscopy. *Nat. Methods* 2: (12), 920–931. DOI: 10.1038/nmeth815 (cited on p. 18).

[192] Denk, W., Strickler, J. H., and Webb, W. W. (1990). Two-photon laser scanning fluorescence microscopy. *Science* 248: (4951), 73–76 (cited on p. 19).

[193] Yuste, R. and Denk, W. (1995). Dendritic spines as basic functional units of neuronal integration. *Nature* 375: (6533), 682–684. DOI: 10.1038/375682a0 (cited on p. 19).

[194] Helmchen, F. and Denk, W. (2005). Deep tissue two-photon microscopy. *Nat. Methods* 2: (12), 932–940. DOI: 10.1038/nmeth818 (cited on p. 19).

[195] Svoboda, K. and Yasuda, R. (2006). Principles of two-photon excitation microscopy and its applications to neuroscience. *Neuron* 50: (6), 823–839. DOI: 10.1016/j.neuron.2006.05.019 (cited on p. 19).

[196] Peng, H., Chung, P., Long, F., Qu, L., Jenett, A., Seeds, A. M., Myers, E. W., and Simpson, J. H. (2011). BrainAligner: 3D registration atlases of *Drosophila* brains. *Nat. Methods* 8:6, 493–498. DOI: 10.1038/nmeth.1602 (cited on p. 19).

[197] Gohl, D. M., Silies, M. A., Gao, X. J., Bhalerao, S., Luongo, F. J., Lin, C.-C., Potter, C. J., and Clandinin, T. R. (2011). A versatile in vivo system for directed dissection of gene expression patterns. *Nat. Methods* 8: (3), 231–237. DOI: 10.1038/nmeth.1561 (cited on pp. 22, 68).

[198] Krashes, M. J., Keene, A. C., Leung, B., Armstrong, J. D., and Waddell, S. (2007). Sequential use of mushroom body neuron subsets during Drosophila odor memory processing. *Neuron* 53:1, 103–115. DOI: 10.1016/j.neuron.2006.11.021 (cited on pp. 22, 72).

[199] Jenett, A., Rubin, G. M., Ngo, T.-T. B., Shepherd, D., Murphy, C., Dionne, H., Pfeiffer, B. D., Cavallaro, A., Hall, D., Jeter, J., Iyer, N., Fetter, D., et al. (2012). A GAL4-driver line resource for *Drosophila* neurobiology. *Cell Rep.* 2: (4), 991–1001. DOI: 10.1016/j.celrep.2012.09.011 (cited on pp. 22, 38, 40, 97, 130).

[200] Monastirioti, M., Linn Jr, C., and White, K. (1996). Characterization of *Drosophila* tyramine beta-hydroxylase gene and isolation of mutant flies lacking octopamine. *J. Neurosci.* 16:12, 3900–3911 (cited on pp. 22, 67).

[201] Klapoetke, N. C., Murata, Y., Kim, S. S., Pulver, S. R., Birdsey-Benson, A., Cho, Y. K., Morimoto, T. K., Chuong, A. S., Carpenter, E. J., Tian, Z., Wang, J., Xie, Y., et al. (2014). Independent optical excitation of distinct neural populations. *Nat. Methods* 11: (3), 338–346. DOI: 10.1038/nmeth.2836 (cited on pp. 22, 130).

[202] Dietzl, G., Chen, D., Schnorrer, F., Su, K.-C., Barinova, Y., Fellner, M., Gasser, B., Kinsey, K., Oppel, S., Scheiblauer, S., Couto, A., Marra, V., et al. (2007). A genome-wide transgenic RNAi library for conditional gene inactivation in *Drosophila*. *Nature* 448: (7150), 151–156. DOI: 10.1038/nature05954 (cited on p. 22).

[203] Kitamoto, T. (2001). Conditional modification of behavior in *Drosophila* by targeted expression of a temperature-sensitive shibire allele in defined neurons. *J. Neurobiol.* 47:2, 81–92. DOI: 10.1002/neu.1018 (cited on pp. 22, 38, 67).

[204] Shaner, N. C., Campbell, R. E., Steinbach, P. A., Giepmans, B. N. G., Palmer, A. E., and Tsien, R. Y. (2004). Improved monomeric red, orange and yellow fluorescent proteins derived from *Discosoma* sp. red fluorescent protein. *Nat. Biotechnol.* 22: (12), 1567–1572. DOI: 10.1038/nbt1037 (cited on pp. 22, 60).

[205] Lin, S., Owald, D., Chandra, V., Talbot, C., Huetteroth, W., and Waddell, S. (2014b). Neural correlates of water reward in thirsty *Drosophila*. *Nat. Neurosci.* 17:11, 1536–1542. DOI: 10.1038/nn.3827 (cited on pp. 25, 28, 32, 35, 38–42, 44, 52, 53, 55, 57, 58, 69, 71, 103, 104).

[206] Yoshihara, M. (2012). Simultaneous recording of calcium signals from identified neurons and feeding behavior of *Drosophila melanogaster*. *J. Vis. Exp.* 62. DOI: 10.3791/3625 (cited on pp. 26, 60).

[207] Pologruto, T. A., Sabatini, B. L., and Svoboda, K. (2003). ScanImage: flexible software for operating laser scanning microscopes. *Biomed. Eng. Online* 2: 13. DOI: 10.1186/1475-925X-2-13 (cited on p. 26).

[208] Schindelin, J., Arganda-Carreras, I., Frise, E., Kaynig, V., Longair, M., Pietzsch, T., Preibisch, S., Rueden, C., Saalfeld, S., Schmid, B., Tinevez, J.-Y., White, D. J., et al. (2012). Fiji: an open-source platform for biological-image analysis. *Nat. Methods* 9: (7), 676–682. DOI: 10.1038/nmeth.2019 (cited on p. 28).

[209] Schneider, C. A., Rasband, W. S., and Eliceiri, K. W. (2012). NIH Image to ImageJ: 25 years of image analysis. *Nat. Methods* 9: (7), 671–675. DOI: 10.1038/nmeth.2089 (cited on p. 28).

[210] Plaçais, P.-Y., Trannoy, S., Isabel, G., Aso, Y., Siwanowicz, I., Belliart-Guérin, G., Vernier, P., Birman, S., Tanimoto, H., and Preat, T. (2012). Slow oscillations in two pairs of dopaminergic neurons gate long-term memory formation in *Drosophila*. *Nat. Neurosci.* 15:4, 592–599. DOI: 10.1038/nn.3055 (cited on pp. 31, 36, 37, 61, 72, 99, 104).

[211] Das, G., Klappenbach, M., Vrontou, E., Perisse, E., Clark, C. M., Burke, C. J., and Waddell, S. (2014). *Drosophila* learn opposing components of a compound food stimulus. *Curr. Biol.* 24:15, 1723–1730. DOI: 10.1016/j.cub.2014.05.078 (cited on pp. 32, 36, 37, 52, 67, 68, 90, 98).

[212] Bargmann, C. I. (2012). Beyond the connectome: how neuromodulators shape neural circuits. *BioEssays* 34: (6), 458–465. DOI: 10.1002/bies.201100185 (cited on p. 36).

[213] Marder, E. (2012). Neuromodulation of neuronal circuits: back to the future. *Neuron* 76: (1), 1–11. DOI: 10.1016/j.neuron.2012.09.010 (cited on p. 36).

[214] Taghert, P. H. and Nitabach, M. N. (2012). Peptide neuromodulation in invertebrate model systems. *Neuron* 76: (1), 82–97. DOI: 10.1016/j.neuron.2012.08.035 (cited on p. 36).

[215] Nässel, D. R. and Winther, A. M. E. (2010). *Drosophila* neuropeptides in regulation of physiology and behavior. *Prog. Neurobiol.* 92: (1), 42–104. DOI: 10.1016/j.pneurobio.2010.04.010 (cited on p. 36).

[216] Wu, Q., Wen, T., Lee, G., Park, J. H., Cai, H. N., and Shen, P. (2003). Developmental control of foraging and social behavior by the *Drosophila* neuropeptide Y-like system. *Neuron* 39: (1), 147–161. DOI: 10.1016/S0896-6273(03)00396-9 (cited on p. 36).

[217] Wen, T., Parrish, C. A., Xu, D., Wu, Q., and Shen, P. (2005). *Drosophila* neuropeptide F and its receptor, NPFR1, define a signaling pathway that acutely modulates alcohol sensitivity. *PNAS* 102: (6), 2141–2146. DOI: 10.1073/pnas.0406814102 (cited on p. 36).

[218] Brown, M. R., Crim, J. W., Arata, R. C., Cai, H. N., Chun, C, and Shen, P (1999). Identification of a *Drosophila* brain-gut peptide related to the neuropeptide Y family. *Peptides* 20: (9), 1035–1042. DOI: 10.1016/S0196-9781(99)00097-2 (cited on p. 36).

[219] Saper, C. B., Chou, T. C., and Elmquist, J. K. (2002). The need to feed: homeostatic and hedonic control of eating. *Neuron* 36: (2), 199–211. DOI: 10.1016/S0896-6273(02)00969-8 (cited on p. 36).

[220] Galili, D. S., Dylla, K. V., Lüdke, A., Friedrich, A. B., Yamagata, N., Wong, J. Y. H., Ho, C. H., Szyszka, P., and Tanimoto, H. (2014). Converging circuits mediate temperature and shock aversive olfactory conditioning in Drosophila. *Curr. Biol.* 24:15, 1712–1722. DOI: 10.1016/j.cub.2014.06.062 (cited on p. 36).

[221] Tomchik, S. M. (2013). Dopaminergic neurons encode a distributed, asymmetric representation of temperature in *Drosophila*. *J. Neurosci.* 33: (5), 2166–276a. DOI: 10.1523/jneurosci.3933-12.2013 (cited on p. 37).

[222] Hige, T., Aso, Y., Rubin, G. M., and Turner, G. C. (2015b). Plasticity-driven individualization of olfactory coding in mushroom body output neurons. *Nature* 526: (7572), 258–262. DOI: 10.1038/nature15396 (cited on p. 37).

[223] Albin, S. D., Kaun, K. R., Knapp, J.-M., Chung, P., Heberlein, U., and Simpson, J. H. (2015). A subset of serotonergic neurons evokes hunger in adult *Drosophila*. *Curr. Biol.* 25:18, 2435–2440. DOI: 10.1016/j.cub.2015.08.005 (cited on p. 37).

[224] Han, K. A., Millar, N. S., and Davis, R. L. (1998). A novel octopamine receptor with preferential expression in *Drosophila* mushroom bodies. *J. Neurosci.* 18: (10), 3650–3658. DOI: 10.1523/jneurosci.18-10-03650 (cited on p. 38).

[225] Maqueira, B., Chatwin, H., and Evans, P. D. (2005). Identification and characterization of a novel family of *Drosophila* beta-adrenergic-like octopamine G-protein coupled receptors. *J. Neurochem.* 94: (2), 547–560. DOI: 10.1111/j.1471-4159.2005.03251.x (cited on p. 38).

[226] Kawasaki, F., Hazen, M., and Ordway, R. W. (2000). Fast synaptic fatigue in shibire mutants reveals a rapid requirement for dynamin in synaptic vesicle membrane trafficking. *Nat. Neurosci.* 3: (9), 859–860. DOI: 10.1038/78753 (cited on p. 38).

[227] Shyu, W.-H., Chiu, T.-H., Chiang, M.-H., Cheng, Y.-C., Tsai, Y.-L., Fu, T.-F., Wu, T., and Wu, C.-L. (2017). Neural circuits for long-term water-reward memory processing in thirsty *Drosophila*. *Nat. Commun.* 8: 15230. DOI: 10.1038/ncomms15230 (cited on pp. 38, 39, 53–55).

[228] Nogi, Y. and Fukasawa, T. (1984). Nucleotide sequence of the yeast regulatory gene GAL80. *Nucleic Acids Res.* 12:24, 9287–9298. DOI: 10.1093/nar/12.24.9287 (cited on p. 38).

[229] Lee, T. and Luo, L. (1999). Mosaic analysis with a repressible cell marker for studies of gene function in neuronal morphogenesis. *Neuron* 22: (3), 451–461. DOI: 10.1016/S0896-6273(00)80701-1 (cited on pp. 38, 39).

[230] Jourjine, N., Mullaney, B. C., Mann, K., and Scott, K. (2016). Coupled sensing of hunger and thirst signals balances sugar and water consumption. *Cell*. DOI: 10.1016/j.cell.2016.06.046 (cited on pp. 45, 58, 74, 96).

[231] Kaun, K. R., Azanchi, R., Maung, Z., Hirsh, J., and Heberlein, U. (2011). A *Drosophila* model for alcohol reward. *Nat. Neurosci.* 14: (5), 612–619. DOI: 10.1038/nn.2805 (cited on p. 52).

[232] Ichinose, T. and Tanimoto, H. (2016). Dynamics of memory-guided choice behavior in *Drosophila*. *Proc. Jpn. Acad. Ser. B* 92:8, 346–357. DOI: 10.2183/pjab.92.346 (cited on p. 53).

[233] Aitken, T. J., Greenfield, V. Y., and Wassum, K. M. (2016). Nucleus accumbens core dopamine signaling tracks the need-based motivational value of food-paired cues. *J. Neurochem.* 136: (5), 1026–1036. DOI: 10.1111/jnc.13494 (cited on pp. 54, 55).

[234] Papageorgiou, G. K., Baudonnat, M., Cucca, F., and Walton, M. E. (2016). Mesolimbic dopamine encodes prediction errors in a state-dependent manner. *Cell Rep.* 15:2, 221–228. DOI: 10.1016/j.celrep.2016.03.031 (cited on pp. 54, 55).

[235] Chen, Z., Wang, Q., and Wang, Z. (2010). The amiloride-sensitive epithelial Na+ channel PPK28 is essential for *Drosophila* gustatory water reception.

J. Neurosci. 30: (18), 6247–6252. DOI: 10.1523/jneurosci.0627-10.2010 (cited on p. 57).

[236] Cameron, P., Hiroi, M., Ngai, J., and Scott, K. (2010). The molecular basis for water taste in *Drosophila*. *Nature* 465: (7294), 91–95. DOI: 10.1038/nature09011 (cited on p. 57).

[237] Waterson, M. J., Chung, B. Y., Harvanek, Z. M., Ostojic, I., Alcedo, J., and Pletcher, S. D. (2014). Water sensor ppk28 modulates *Drosophila* lifespan and physiology through AKH signaling. *PNAS* 111: (22), 8137–8142. DOI: 10.1073/pnas.1315461111 (cited on p. 58).

[238] Drobizhev, M., Tillo, S., Makarov, N. S., Hughes, T. E., and Rebane, A. (2009). Absolute two-photon absorption spectra and two-photon brightness of orange and red fluorescent proteins. *J. Phys. Chem. B* 113: (4), 855–859. DOI: 10.1021/jp8087379 (cited on p. 60).

[239] Drobizhev, M., Makarov, N. S., Tillo, S. E., Hughes, T. E., and Rebane, A. (2011). Two-photon absorption properties of fluorescent proteins. *Nat. Methods* 8: (5), 393–399. DOI: 10.1038/nmeth.1596 (cited on p. 60).

[240] Weir, P. T. and Dickinson, M. H. (2015). Functional divisions for visual processing in the central brain of flying *Drosophila*. *PNAS* 112: (40), E5523–E5532. DOI: 10.1073/pnas.1514415112 (cited on p. 60).

[241] Rozin, P. and Kalat, J. W. (1971). Specific hungers and poison avoidance as adaptive specializations of learning. *Psychol. Rev.* 78: (6), 459–486. DOI: http://dx.doi.org/10.1037/h0031878 (cited on p. 65).

[242] Messier, C. and White, N. M. (1984). Contingent and non-contingent actions of sucrose and saccharin reinforcers: effects on taste preference and memory. *Physiol. Behav.* 32: (2), 195–203. DOI: 10.1016/0031-9384(84)90129-X (cited on p. 65).

[243] Harvey, E. N. (1919). Studies on bioluminescence: IX. Chemical nature of Cypridina luciferin and Cypridina luciferase. *J. Gen. Physiol.* 1: (3), 269–293. DOI: 10.1085/jgp.1.3.269 (cited on p. 65).

[244] Brandes, C., Plautz, J. D., Stanewsky, R., Jamison, C. F., Straume, M., Wood, K. V., Kay, S. A., and Hall, J. C. (1996). Novel features of *Drosophila* period transcription revealed by real-time luciferase reporting. *Neuron* 16: (4), 687–692. DOI: 10.1016/S0896-6273(00)80088-4 (cited on p. 66).

[245] Itskov, P. M., Moreira, J.-M., Vinnik, E., Lopes, G., Safarik, S., Dickinson, M. H., and Ribeiro, C. (2014). Automated monitoring and quantitative analysis of feeding behaviour in *Drosophila*. *Nat. Commun.* 5: 4560. DOI: 10.1038/ncomms5560 (cited on pp. 66, 135).

[246] Cole, S. H., Carney, G. E., McClung, C. A., Willard, S. S., Taylor, B. J., and Hirsh, J. (2005). Two functional but noncomplementing *Drosophila* tyrosine decarboxylase genes: distinct roles for neural tyramine and octopamine in female fertility. *J. Biol. Chem.* 280: (15), 14948–14955. DOI: 10.1074/jbc.M414197200 (cited on p. 67).

[247] Das, G., Lin, S., and Waddell, S. (2016). Remembering components of food in *Drosophila*. *Front. Integr. Neurosci.* 10: 4. DOI: 10.3389/fnint.2016.00004 (cited on pp. 67, 69).

[248] Hamada, F. N., Rosenzweig, M., Kang, K., Pulver, S. R., Ghezzi, A., Jegla, T. J., and Garrity, P. A. (2008). An internal thermal sensor controlling

temperature preference in *Drosophila*. *Nature* 454: (7201), 217–220. DOI: 10.1038/nature07001 (cited on pp. 68, 70).

[249] Luan, H., Peabody, N. C., Vinson, C. R., and White, B. H. (2006). Refined spatial manipulation of neuronal function by combinatorial restriction of transgene expression. *Neuron* 52: (3), 425–436. DOI: 10.1016/j.neuron.2006.08.028 (cited on p. 69).

[250] Lee, P.-T., Lin, H.-W., Chang, Y.-H., Fu, T.-F., Dubnau, J., Hirsh, J., Lee, T., and Chiang, A.-S. (2011). Serotonin-mushroom body circuit modulating the formation of anesthesia-resistant memory in *Drosophila*. *PNAS* 108: (33), 13794–13799. DOI: 10.1073/pnas.1019483108 (cited on p. 72).

[251] Haynes, P. R., Christmann, B. L., and Griffith, L. C. (2015). A single pair of neurons links sleep to memory consolidation in *Drosophila melanogaster*. *eLife* 4: DOI: 10.7554/eLife.03868 (cited on pp. 72, 146).

[252] Keene, A. C., Krashes, M. J., Leung, B., Bernard, J. A., and Waddell, S. (2006). Drosophila dorsal paired medial neurons provide a general mechanism for memory consolidation. *Curr. Biol.* 16:15, 1524–1530. DOI: 10.1016/j.cub.2006.06.022 (cited on pp. 72, 73).

[253] Pitman, J. L., Huetteroth, W., Burke, C. J., Krashes, M. J., Lai, S.-L., Lee, T., and Waddell, S. (2011). A pair of inhibitory neurons are required to sustain labile memory in the *Drosophila* mushroom body. *Curr. Biol.* 21: (10), 855–861. DOI: 10.1016/j.cub.2011.03.069 (cited on p. 72).

[254] Cervantes-Sandoval, I. and Davis, R. L. (2012). Distinct traces for appetitive versus aversive olfactory memories in DPM neurons of *Drosophila*. *Curr. Biol.* 22: (13), 1247–1252. DOI: 10.1016/j.cub.2012.05.009 (cited on pp. 72, 74, 95, 96).

[255] Gruber, F., Knapek, S., Fujita, M., Matsuo, K., Bräcker, L., Shinzato, N., Siwanowicz, I., Tanimura, T., and Tanimoto, H. (2013). Suppression of conditioned odor approach by feeding is independent of taste and nutritional value in *Drosophila*. *Curr. Biol.* 23:6, 507–514. DOI: 10.1016/j.cub.2013.02.010 (cited on pp. 74, 96).

[256] Montell, C. (2009). A taste of the *Drosophila* gustatory receptors. *Curr. Opin. Neurobiol.* 19: (4), 345–353. DOI: 10.1016/j.conb.2009.07.001 (cited on p. 94).

[257] Miyamoto, T. and Amrein, H. (2014). Diverse roles for the *Drosophila* fructose sensor Gr43a. *Fly* 8: (1), 19–25. DOI: 10.4161/fly.27241 (cited on p. 94).

[258] Thoma, V., Knapek, S., Arai, S., Hartl, M., Kohsaka, H., Sirigrivatanawong, P., Abe, A., Hashimoto, K., and Tanimoto, H. (2016). Functional dissociation in sweet taste receptor neurons between and within taste organs of *Drosophila*. *Nat. Commun.* 7: 10678. DOI: 10.1038/ncomms10678 (cited on p. 94).

[259] Jiao, Y., Moon, S. J., Wang, X., Ren, Q., and Montell, C. (2008). Gr64f is required in combination with other gustatory receptors for sugar detection in *Drosophila*. *Curr. Biol.* 18: (22), 1797–1801. DOI: 10.1016/j.cub.2008.10.009 (cited on p. 94).

[260] Dahanukar, A., Lei, Y.-T., Kwon, J. Y., and Carlson, J. R. (2007). Two Gr genes underlie sugar reception in *Drosophila*. *Neuron* 56: (3), 503–516. DOI: 10.1016/j.neuron.2007.10.024 (cited on p. 94).

[261] Jiao, Y., Moon, S. J., and Montell, C. (2007). A *Drosophila* gustatory receptor required for the responses to sucrose, glucose, and maltose identified by mRNA tagging. *PNAS* 104: (35), 14110–14115. DOI: 10.1073/pnas.0702421104 (cited on p. 94).

[262] Slone, J., Daniels, J., and Amrein, H. (2007). Sugar receptors in *Drosophila*. *Curr. Biol.* 17: (20), 1809–1816. DOI: 10.1016/j.cub.2007.09.027 (cited on p. 94).

[263] Marella, S., Fischler, W., Kong, P., Asgarian, S., Rueckert, E., and Scott, K. (2006). Imaging taste responses in the fly brain reveals a functional map of taste category and behavior. *Neuron* 49: (2), 285–295. DOI: 10.1016/j.neuron.2005.11.037 (cited on p. 96).

[264] Miyazaki, T. and Ito, K. (2010). Neural architecture of the primary gustatory center of *Drosophila melanogaster* visualized with GAL4 and LexA enhancer-trap systems. *J. Comp. Neurol.* 518: (20), 4147–4181. DOI: 10.1002/cne.22433 (cited on p. 97).

[265] Nagaya, Y., Kutsukake, M., Chigusa, S. I., and Komatsu, A. (2002). A trace amine, tyramine, functions as a neuromodulator in *Drosophila melanogaster*. *Neurosci. Lett.* 329: (3), 324–328. DOI: 10.1016/S0304-3940(02)00596-7 (cited on p. 98).

[266] Saraswati, S., Fox, L. E., Soll, D. R., and Wu, C.-F. (2004). Tyramine and octopamine have opposite effects on the locomotion of *Drosophila* larvae. *J. Neurobiol.* 58: (4), 425–441. DOI: 10.1002/neu.10298 (cited on p. 98).

[267] Matsumoto, H., Tian, J., Uchida, N., and Watabe-Uchida, M. (2016). Midbrain dopamine neurons signal aversion in a reward-context-dependent manner. *eLife* 5: e17328. DOI: 10.7554/eLife.17328 (cited on p. 98).

[268] Beutler, L. R., Chen, Y., Ahn, J. S., Lin, Y.-C., Essner, R. A., and Knight, Z. A. (2017). Dynamics of gut-brain communication underlying hunger. *Neuron* 96: (2), 461–475.e5. DOI: 10.1016/j.neuron.2017.09.043 (cited on p. 100).

[269] Tomchik, S. M. and Davis, R. L. (2009). Dynamics of learning-related cAMP signaling and stimulus integration in the Drosophila olfactory pathway. *Neuron* 64:4, 510–521. DOI: 10.1016/j.neuron.2009.09.029 (cited on p. 103).

[270] Gervasi, N., Tchénio, P., and Preat, T. (2010). PKA dynamics in a Drosophila learning center: coincidence detection by rutabaga adenylyl cyclase and spatial regulation by dunce phosphodiesterase. *Neuron* 65:4, 516–529. DOI: 10.1016/j.neuron.2010.01.014 (cited on p. 103).

[271] Honegger, K. S., Campbell, R. A. A., and Turner, G. C. (2011). Cellular-resolution population imaging reveals robust sparse coding in the *Drosophila* mushroom body. *J. Neurosci.* 31: (33), 11772–11785. DOI: 10.1523/jneurosci.1099-11.2011 (cited on p. 103).

[272] Duerr, J. S. and Quinn, W. G. (1982). Three *Drosophila* mutations that block associative learning also affect habituation and sensitization. *PNAS* 79: (11), 3646–3650. DOI: 10.1073/pnas.79.11.3646 (cited on p. 103).

[273] Dudaí, Y., Uzzan, A., and Zvi, S. (1983). Abnormal activity of adenylate cyclase in the *Drosophila* memory mutant rutabaga. *Neurosci. Lett.* 42: (2), 207–212. DOI: 10.1016/0304-3940(83)90408-1 (cited on p. 103).

[274] Dubnau, J., Grady, L., Kitamoto, T., and Tully, T. (2001). Disruption of neurotransmission in Drosophila mushroom body blocks retrieval but not

acquisition of memory. *Nature* 411: 476. DOI: 10.1038/35078077 (cited on p. 103).

[275] McGuire, S. E., Le, P. T., and Davis, R. L. (2001). The role of *Drosophila* mushroom body signaling in olfactory memory. *Science* 293: (5533), 1330–1333. DOI: 10.1126/science.1062622 (cited on p. 103).

[276] Zhang, S. and Roman, G. (2013). Presynaptic inhibition of gamma lobe neurons is required for olfactory learning in *Drosophila*. *Curr. Biol.* 23: (24), 2519–2527. DOI: 10.1016/j.cub.2013.10.043 (cited on p. 103).

[277] Berry, J. A., Cervantes-Sandoval, I., Nicholas, E. P., and Davis, R. L. (2012). Dopamine is required for learning and forgetting in *Drosophila*. *Neuron* 74:3, 530–542. DOI: 10.1016/j.neuron.2012.04.007 (cited on p. 104).

[278] Berry, J. A., Cervantes-Sandoval, I., Chakraborty, M., and Davis, R. L. (2015). Sleep facilitates memory by blocking dopamine neuron-mediated forgetting. *Cell* 161: (7), 1656–1667. DOI: 10.1016/j.cell.2015.05.027 (cited on p. 104).

[279] Aso, Y. and Rubin, G. M. (2016). Dopaminergic neurons write and update memories with cell-type-specific rules. *eLife* 5: DOI: 10.7554/eLife.16135 (cited on p. 104).

[280] Qin, H., Cressy, M., Li, W., Coravos, J. S., Izzi, S. A., and Dubnau, J. (2012). Gamma neurons mediate dopaminergic input during aversive olfactory memory formation in *Drosophila*. *Curr. Biol.* 22: (7), 608–614. DOI: 10.1016/j.cub.2012.02.014 (cited on p. 104).

[281] Friggi-Grelin, F., Coulom, H., Meller, M., Gomez, D., Hirsh, J., and Birman, S. (2003). Targeted gene expression in *Drosophila* dopaminergic cells using regulatory sequences from tyrosine hydroxylase. *J. Neurobiol.* 54: (4), 618–627. DOI: 10.1002/neu.10185 (cited on p. 105).

[282] Louis, T., Stahl, A., Boto, T., and Tomchik, S. M. (2017). Cyclic AMP-dependent plasticity underlies rapid changes in odor coding associated with reward learning. *PNAS*, 201709037. DOI: 10.1073/pnas.1709037115 (cited on pp. 106, 137–139).

[283] Dethier, V. G. (1976). The hungry fly : a physiological study of the behavior associated with feeding. Cambridge, Mass: Harvard University Press (cited on p. 106).

[284] Chabaud, M.-A., Devaud, J.-M., Pham-Delègue, M.-H., Preat, T., and Kaiser, L. (2006). Olfactory conditioning of proboscis activity in *Drosophila melanogaster*. *J. Comp. Physiol. A* 192: (12), 1335–1348. DOI: 10.1007/s00359-006-0160-3 (cited on pp. 106, 107, 142).

[285] Faber, T, Joerges, J, and Menzel, R (1999). Associative learning modifies neural representations of odors in the insect brain. *Nat. Neurosci.* 2: (1), 74–78. DOI: 10.1038/4576 (cited on p. 106).

[286] Menzel, R. (2001). Searching for the memory trace in a mini-brain, the honeybee. *Learn. Mem.* 8:2, 53–62. DOI: 10.1101/lm.38801 (cited on p. 106).

[287] Busto, G. U., Cervantes-Sandoval, I., and Davis, R. L. (2010). Olfactory learning in *Drosophila*. *Physiology* 25: (6), 338–346. DOI: 10.1152/physiol.00026.2010 (cited on p. 133).

[288] Hattori, D., Aso, Y., Swartz, K. J., Rubin, G. M., Abbott, L., and Axel, R. (2017). Representations of novelty and familiarity in a mushroom body compartment. *Cell*. DOI: 10.1016/j.cell.2017.04.028 (cited on p. 133).

[289] Zhao, X., Lenek, D., Dag, U., Dickson, B. J., and Keleman, K. (2018). Persistent activity in a recurrent circuit underlies courtship memory in Drosophila. *eLife* 7: e31425. DOI: 10.7554/eLife.31425 (cited on p. 135).

[290] Twick, I., Lee, J. A., and Ramaswami, M. (2014). Olfactory habituation in Drosophila - Odor encoding and its plasticity in the antennal lobe. In: *Progress in Brain Research*. Elsevier, 3–38. DOI: 10.1016/b978-0-444-63350-7.00001-2 (cited on p. 135).

[291] Wise, R. A. (2004). Dopamine, learning and motivation. *Nat. Rev. Neurosci.* 5:6, 483–494. DOI: 10.1038/nrn1406 (cited on p. 136).

[292] Clyne, J. D. and Miesenböck, G. (2008). Sex-specific control and tuning of the pattern generator for courtship song in Drosophila. *Cell* 133:2, 354–363. DOI: 10.1016/j.cell.2008.01.050 (cited on p. 141).

[293] Aimon, S., Katsuki, T., Grosenick, L., Broxton, M., Deisseroth, K., Sejnowski, T. J., and Greenspan, R. J. (2017). Fast whole brain imaging in adult Drosophila during response to stimuli and behavior. *bioRxiv*. DOI: 10.1101/033803 (cited on p. 142).

[294] Huang, C., Maxey, J. R., Sinha, S., Savall, J., Gong, Y., and Schnitzer, M. J. (2018). Long-term optical brain imaging in live adult fruit flies. *Nat. Commun.* 9:1, 872. DOI: 10.1038/s41467-018-02873-1 (cited on p. 142).

[295] Stosiek, C., Garaschuk, O., Holthoff, K., and Konnerth, A. (2003). In vivo two-photon calcium imaging of neuronal networks. *PNAS* 100: (12), 7319–7324. DOI: 10.1073/pnas.1232232100 (cited on p. 145).

[296] Fatt, P. and Katz, B. (1952). Spontaneous subthreshold activity at motor nerve endings. *J. Physiol.* 117: (1), 109–128 (cited on p. 145).

[297] Baker, P. F., Hodgkin, A. L., and Ridgway, E. B. (1971). Depolarization and calcium entry in squid giant axons. *J. Physiol.* 218: (3), 709–755 (cited on p. 145).

[298] Helmchen, F., Svoboda, K., Denk, W., and Tank, D. W. (1999). In vivo dendritic calcium dynamics in deep-layer cortical pyramidal neurons. *Nat. Neurosci.* 2: (11), 989–996. DOI: 10.1038/14788 (cited on p. 145).

[299] Charpak, S., Mertz, J., Beaurepaire, E., Moreaux, L., and Delaney, K. (2001). Odor-evoked calcium signals in dendrites of rat mitral cells. *PNAS* 98: (3), 1230–1234. DOI: 10.1073/pnas.021422798 (cited on p. 145).

[300] Yang, H. H., St-Pierre, F., Sun, X., Ding, X., Lin, M. Z., and Clandinin, T. R. (2016). Subcellular imaging of voltage and calcium signals reveals neural processing in vivo. *Cell*. DOI: 10.1016/j.cell.2016.05.031 (cited on p. 145).

[301] Storace, D., Sepehri Rad, M., Kang, B., Cohen, L. B., Hughes, T., and Baker, B. J. (2016). Toward better genetically encoded sensors of membrane potential. *Trends Neurosci.* 39: (5), 277–289. DOI: 10.1016/j.tins.2016.02.005 (cited on p. 145).

[302] Peron, S., Chen, T.-W., and Svoboda, K. (2015). Comprehensive imaging of cortical networks. *Curr. Opin. Neurobiol.* 32: 115–123. DOI: 10.1016/j.conb.2015.03.016 (cited on pp. 145, 146).

[303] Scheuss, V., Yasuda, R., Sobczyk, A., and Svoboda, K. (2006). Nonlinear [Ca2+] signaling in dendrites and spines caused by activity-dependent depression of Ca2+ extrusion. *J. Neurosci.* 26: (31), 8183–8194. DOI: 10.1523/jneurosci.1962-06.2006 (cited on p. 145).

[304] Akerboom, J., Chen, T.-W., Wardill, T. J., Tian, L., Marvin, J. S., Mutlu, S., CalderÃşn, N. C., Esposti, F., Borghuis, B. G., Sun, X. R., Gordus, A., Orger, M. B., et al. (2012). Optimization of a GCaMP calcium indicator for neural activity imaging. *J. Neurosci.* 32: (40), 13819–13840. DOI: 10.1523/jneurosci.2601-12.2012 (cited on p. 145).

[305] Nauhaus, I., Nielsen, K. J., and Callaway, E. M. (2012). Nonlinearity of two-photon Ca2+ imaging yields distorted measurements of tuning for V1 neuronal populations. *J. Neurophysiol.* 107: (3), 923–936. DOI: 10.1152/jn.00725.2011 (cited on pp. 145, 146).

[306] Cayre, M, Buckingham, S. D., Yagodin, S, and Sattelle, D. B. (1999). Cultured insect mushroom body neurons express functional receptors for acetylcholine, GABA, glutamate, octopamine, and dopamine. *J. Neurophysiol.* 81: (1), 1–14. DOI: 10.1152/jn.1999.81.1.1 (cited on p. 146).

[307] Perisse, E., Yin, Y., Lin, A. C., Lin, S., Huetteroth, W., and Waddell, S. (2013b). Different kenyon cell populations drive learned approach and avoidance in *Drosophila*. *Neuron* 79: (5), 945–956. DOI: 10.1016/j.neuron.2013.07.045 (cited on p. 146).

[308] Sun, F., Zeng, J., Jing, M., Zhou, J., Feng, J., Owen, S. F., Luo, Y., Li, F., Wang, H., Yamaguchi, T., Yong, Z., Gao, Y., et al. (2018). A genetically encoded fluorescent sensor enables rapid and specific detection of dopamine in flies, fish, and mice. *Cell* 174: (2), 481–496.e19. DOI: 10.1016/j.cell.2018.06.042 (cited on p. 147).